

Copyright
by
Miqueias P. Brikalski
2022

**The Thesis Committee for Miqueias P. Brikalski
Certifies that this is the approved version of the following Thesis:**

**Impact of Angularity, Particle Size and Particle Size Distribution on the
Stiffness of the Soil-Geosynthetic Composite**

**APPROVED BY
SUPERVISING COMMITTEE:**

Jorge G. Zornberg, Supervisor

Chadi El Mohtar

**Impact of Angularity, Particle Size and Particle Size Distribution on the
Stiffness of the Soil-Geosynthetic Composite**

by

Miqueias P. Brikalski

Thesis

Presented to the Faculty of the Graduate School of

The University of Texas at Austin

in Partial Fulfillment

of the Requirements

for the Degree of

Master of Science in Engineering

The University of Texas at Austin

December 2022

Dedication

To my parents, Pedro and Luiza, my sisters, Miriam, Marcela and Rute and my nephew,
Jonathan, and my niece, Alice.

Acknowledgements

I would like to express my gratitude to many people for their support during my time as a master's student at the University of Texas.

I will always be grateful to Dr. Jorge Zornberg for his guidance, encouragement, and patience. I have benefited greatly from his knowledge and wisdom both in his roles as professor and research advisor.

The people in our research group are truly resourceful, and I am grateful for their help and valuable insights. My special thanks to Yagizer Yalcin for his insights and guidance in the many conversations we had about topics covered in this study. Also, grateful to Mahfooz Alam and Gerardo Trevino for their help in running many tests.

The Geotech Faculty have taught me more than I thought I could learn about geotechnical engineering. I owe my gratitude to Drs. Robert Gilbert and Krishna Kumar for their wonderful lectures. I am especially grateful to Dr. Rathje, who allowed me to work as a teaching assistant, and Dr. Chadi El Mohtar, who was part of my thesis committee.

I also want to acknowledge my professors at Santa Catarina State University. Particularly Larissa Tabalipa and Dr. Edgar Odebrecht, who planted on my mind the seed of interest in geotechnical engineering, and Andreza Kalbusch, who provided me with the first opportunity to do research.

Finally, I thank my family and friends for their love, support, and encouragement. Among my friends in Austin, I must mention Bradley Bzdyra, Timothy Wang, Terry Dykstra, Filipe de Moraes, the Holts, and the Olaskys for their immeasurable support.

Abstract

Impact of Angularity, Particle Size and Particle Size Distribution on the Stiffness of the Soil-Geosynthetic Composite

Miqueias P. Brikalski, MSE

The University of Texas at Austin, 2022

Supervisor: Jorge G. Zornberg

Comparatively small strains are mobilized when the geosynthetic is used for its stiffening function, as is the case in the stabilization of road bases. The objective is to control the deformation in the soil-geosynthetic composite. Fundamental to accomplishing that is the increased stiffness resulting from the soil-geosynthetic interaction. The soil-geosynthetic composite (SGC) model combines the tensile properties of the geosynthetic with the shear strength properties of the soil-geosynthetic interface, under low strain conditions, into a single parameter, the stiffness of the soil-geosynthetic composite (K_{SGC}). This study evaluated the impact of aggregate angularity, particle size, and particle size distribution on the K_{SGC} involving geogrids and geotextiles using the small-scale soil-geosynthetic interaction (SGI) test. The results indicate that aggregate angularity and particle size distribution impact the K_{SGC} , increasing its value for both geosynthetic types. The increase was more significant in the case of geotextiles than in the case of geogrids. The magnitude of the increase was found to also be affected by the tensile modulus of the

geosynthetic (J). The impact of particle size on K_{SGC} was observed to be very small for both geosynthetic types. When evaluating the suitability of aggregates involved in this study to be used as a reference when testing geotextiles, it was found that aggregate angularity facilitates the assessment of geotextile performance.

Table of Contents

List of Tables	xvi
List of Figures	xviii
Chapter 1: Introduction	1
1.1 Research Motivation	1
1.2 Research Objectives	3
1.3 Thesis outline	3
Chapter 2: Background information	4
2.1 Overview	4
2.2 Soil-Geosynthetic Composite (SGC) model	5
Chapter 3: Small scale soil-geosynthetic interaction test	9
3.1 Test setup	9
3.1.1 Small SGI box	11
3.1.2 Load cell and Load frame	11
3.1.3 LVDT	11
3.1.4 Linear potentiometers	12
3.1.3 Confining Pressure Application and Pressure Gauges	13
3.1.4 Image processing	13
3.3 Testing Procedure	14
3.3.1 Sample preparation	14
3.2.2 Test-specific correction procedure for each LP	17
3.2.3 Soil-geosynthetic interaction test	18
3.4 Interpretation of the data	19

3.5 Outlier analysis	23
Chapter 4: Materials and testing program.....	26
4.1 Geosynthetics used in the testing program	26
4.1.1 Typical image analysis results from a test involving GG1	27
4.1.2 Typical image analysis results from a test involving GT1	28
4.2. Aggregate identification and index properties.....	30
4.2.1 Background for the well graded aggregate	31
4.2.2 Determination of equivalent unit weight	33
4.3 Outline of the SGI testing campaign.....	35
Chapter 5: SGI Test results	38
5.1 Geogrids.....	38
5.1.1 Tests conducted with Geosynthetic GG1	38
5.1.1.1 Tests involving GG1 and Round SAggr2	38
5.1.1.2 Tests involving GG1 and Angular SAggr2.....	41
5.1.1.3 Tests involving GG1 and Angular SAggr3.....	43
5.1.1.4 Tests involving GG1 and Angular WG	45
5.1.1.5 Tests involving GG1 and 50-50 SAggr2	47
5.1.2 Tests conducted with Geosynthetic GG2.....	49
5.1.2.1 Tests involving GG2 and Round SAggr2	49
5.1.2.2 Tests involving GG2 and Angular SAggr2.....	51
5.2 Geotextiles	53
5.2.1 Tests conducted with Geosynthetic GT1	53
5.2.1.1 Tests involving GT1 and Round SAggr2.....	53

5.2.1.2 Tests involving GT1 and Angular SAggr2	56
5.2.1.3 Tests involving GT1 and Angular SAggr3	58
5.2.1.4 Tests involving GT1 and Angular WG	60
5.2.1.5 Tests involving GT1 and 50-50 SAggr2	62
5.2.1.5 Tests involving GT1 and Monterey Sand	64
5.2.2 Tests conducted with Geosynthetic GT2	66
5.2.2.1 Tests involving GT2 and Round SAggr2	66
5.2.2.2 Tests involving GT2 and Angular SAggr2	68
Chapter 6: Evaluation of the impact of backfill and geosynthetic properties on K_{SGC}	70
6.1 Geogrids: Effect of Relevant Variables on K_{SGC}	70
6.1.1 Effect of aggregate angularity	70
6.1.2 Effect of particle size and particle size distribution	71
6.1.3 Effect of geogrid characteristics	73
6.2 Geotextiles: Effect of Relevant Variables on K_{SGC}	74
6.2.1 Effect of aggregate angularity	74
6.2.2 Effect of particle size and particle size distribution	76
6.2.2 Effect of geotextile characteristics	77
6.3 Effect of particle size distribution on the unit tension curve	78
Chapter 7: Conclusion	83
7.1 General conclusions	83
7.2 Impact of angularity of aggregates on K_{SGC} involving geogrids	84
7.3 impact of aggregates angularity on K_{SGC} involving geotextiles	85
7.4 Effect of particle size and particle size distribution on K_{SGC} involving geogrids	86

7.5 Effect of particle size and particle size distribution on K_{SGC} for geotextiles.....	86
7.6 Identification of aggregates for use as reference when testing geotextiles.....	87
7.7 Recommendations for future studies	88
Appendix A: Extensive list of test results obtained in this study	90
A.1 Configuration involving GG1 and Round SAggr2	91
A.1.1 Test 1	91
A.1.2 Test 2	93
A.1.3 Test 3	95
A.1.4 Test 4	97
A.1.5 Test 5	99
A.1.6 Summary of results from configuration involving GG1 and Round SAggr2	101
A.2 Configuration involving GG1 and Angular SAggr2.....	102
A.2.1 Test 1	102
A.2.2 Test 2	104
A.2.3 Test 3	106
A.2.4 Test 4	108
A.2.5 Test 5	110
A.2.6 Summary of results from configuration involving GG1 and Angular SAggr2	112
A.3 Configuration involving GG1 and Angular SAggr3.....	113
A.3.1 Test 1	113
A.3.2 Test 2	115
A.3.3 Test 3	117

A.3.4 Test 4.....	119
A.3.5 Test 5.....	121
A.3.6 Summary of results from configuration involving GG1 and Angular SAggr3	123
A.4 Configuration involving GG1 and Angular WG	124
A.4.1 Test 1.....	124
A.4.2 Test 2.....	126
A.4.3 Test 3.....	128
A.4.4 Test 4.....	130
A.4.5 Test 5.....	132
A.4.6 Summary of results from configuration involving GG1 and Angular SAggr3	134
A.5 Configuration involving GG1 and 50-50 SAggr2	135
A.5.1 Test 1.....	135
A.5.2 Test 2.....	137
A.5.3 Test 3.....	139
A.5.4 Test 4.....	141
A.5.5 Test 5.....	143
A.5.6 Summary of results from configuration involving GG1 and 50-50 SAggr2	145
A.6 Configuration involving GG2 and Round SAggr2	146
A.6.1 Test 1.....	146
A.6.2 Test 2.....	148
A.6.3 Test 3.....	150
A.6.4 Test 4.....	152

A.6.5 Test 5	154
A.6.6 Summary of results from configuration involving GG2 and Round SAggr2	156
A.7 Configuration involving GG2 and Angular SAggr2.....	157
A.7.1 Test 1	157
A.7.2 Test 2	159
A.7.3 Test 3	161
A.7.4 Test 4	163
A.7.5 Test 5	165
A.7.6 Summary of results from configuration involving GG2 and Angular SAggr2	167
A.8 Configuration involving GT1 and Round SAggr2.....	168
A.8.1 Test 1	168
A.8.2 Test 2	170
A.8.3 Test 3	172
A.8.4 Test 4	174
A.8.5 Test 5	176
A.8.6 Summary of results from configuration involving GT1 and Round SAggr2	178
A.9 Configuration involving GT1 and Angular SAggr2	179
A.9.1 Test 1	179
A.9.2 Test 2	181
A.9.3 Test 3	183
A.9.4 Test 4	185
A.9.5 Test 5	187

A.9.6 Summary of results from configuration involving GT1 and Angular SAggr2	189
A.10 Configuration involving GT1 and Angular SAggr3	190
A.10.1 Test 1	190
A.10.2 Test 2	192
A.10.3 Test 3	194
A.10.4 Test 4	196
A.10.5 Test 5	198
A.10.6 Summary of results from configuration involving GT1 and Angular SAggr3	200
A.11 Configuration involving GT1 and Angular WG	201
A.11.1 Test 1	201
A.11.2 Test 2	202
A.11.3 Test 3	204
A.11.4 Test 4	206
A.11.5 Test 5	208
A.11.6 Summary of results from configuration involving GT1 and Angular WG	210
A.12 Configuration involving GT1 and 50-50 SAggr2	211
A.12.1 Test 1	211
A.12.2 Test 2	213
A.12.3 Test 3	215
A.12.4 Test 4	217
A.12.5 Test 5	219

A.12.6 Summary of results from configuration involving GT1 and 50-50 SAggr2	221
A.13 Configuration involving GT1 and Monterey Sand	222
A.13.1 Test 1	222
A.13.2 Test 2	224
A.13.3 Test 3	226
A.13.4 Summary of results from configuration involving GT1 and Monterey Sand	228
A.14 Configuration involving GT2 and Round SAggr2	229
A.14.1 Test 1	229
A.14.2 Test 2	231
A.14.3 Test 3	233
A.14.4 Test 4	235
A.14.5 Test 5	237
A.14.6 Summary of results from configuration involving GT2 and Round SAggr2	239
A.15 Configuration involving GT2 and Angular SAggr2	240
A.15.1 Test 1	240
A.15.2 Test 2	242
A.15.3 Test 3	244
A.15.4 Test 4	246
A.15.5 Test 5	248
References	249

List of Tables

Table 4.1 - Main characteristics of the four geosynthetics used in this study	27
Table 4.2 - Index properties of the six aggregates used in this study	31
Table 4.3 - Target unit weight of each aggregate used in this study	35
Table 4.4 - List of all the test configurations used in this study	36
Table 5.2 - Final K_{SGC} and pullout capacity resulting from 5 tests done with GG1 tested with Angular SAggr2.....	42
Table 5.3 - Final K_{SGC} and pullout capacity resulting from test results for GG1 tested with Angular SAggr3.....	44
Table 5.4 - Final K_{SGC} and pullout capacity resulting from test results for GG1 tested with well graded aggregate.	46
Table 5.5 - Final K_{SGC} and pullout capacity resulting from test results for GG1 tested with the 50-50 SAggr2.....	48
Table 5.6 - Final K_{SGC} and maximum pullout capacity for GG2 tested 5 times with Round SAggr2.	50
Table 5.7 - Final K_{SGC} and pullout capacity from 5 tests run with GG2 and Angular SAggr2.	52
Table 5.8 - Average K_{SGC} and maximum pullout capacity for GT1 tested with Round SAggr2 5 times.	55
Table 5.9 - Average K_{SGC} and pullout capacity for 5 tests done with GT1 and Angular SAggr2.	57
Table 5.10 - Average K_{SGC} and average pullout capacity from 5 tests done with GT1 and Angular SAggr3.	59

Table 11 - Average K_{SGC} and average pullout capacity from 5 tests done with GT1 and Angular SAggr3.	61
Table 5.12 - Average K_{SGC} and average pullout capacity from 5 tests done with GT1 and 50-50 SAggr2.	63
Table 5.13 - Average K_{SGC} and average pullout capacity from 5 tests done with GT1 and Monterey Sand.	65
Table 5.14 - Average K_{SGC} and maximum pullout capacity for GT2 tested with Round SAggr2 5 times.	67
Table 5.15 - Average K_{SGC} and maximum pullout capacity from 5 tests with GT2 with Angular SAggr2 5 times.	69
Table 6.1 - Results of tests involving geogrids to evaluate the impact of angularity on K_{SGC}	70
Table 6.2 - Results from test involving geogrids for evaluation of the impact of particle size and particle size distribution on K_{SGC}	72
Table 6.3 - Test results to evaluate the effect of geogrid characteristics on K_{SGC}	73
Table 6.4 - Results from tests involving geotextiles to evaluate the impact of aggregate angularity on K_{SGC}	74
Table 6.5 - Results from tests involving geotextiles to evaluate the impact of particle size and particle size distribution on K_{SGC}	76
Table 6.6 - Test results to evaluate the impact of geotextile stiffness on K_{SGC}	77

List of Figures

Figure 2.1 - Constitutive model: a) unit tension-strain linear relationship; b) shear stress-displacement rigid-perfectly plastic response (Zornberg, Roodi &Gupta, 2017).	6
Figure 2.2 – Active length and the progression of the mobilized zone (Zornberg, Roodi &Gupta, 2017).....	7
Figure 3.1 - Complete setup for the Small SGI test.	9
Figure 3.2 - Side view of loading system, with details about its several components.....	10
Figure 3.3 - LVDT used to check the displacement rate of the loading frame.....	12
Figure 3.4 - Close view of one of the LPs used to measure displacement during the SGI test.....	12
Figure 3.5 - Views of the SGI box lid: (a) view of the air bladder; (b) view of the digital and analog pressure gauge.	13
Figure 3.6 - Disposition of the markers on the unconfined portion of the geosynthetic. ..	14
Figure 3.7 - Telltale attachment: (a) geogrids, (b) geotextiles.....	15
Figure 3.8 - Top view of the box after the first two layers and the geosynthetic are placed.	16
Figure 3.9 - LP reading versus imposed displacement obtained from test-specific correction	18
Figure 3.10 – Example of a frontal unit tension versus time plot.....	19
Figure 3.11 – Typical time history of the displacement readings at the five telltale locations.	20
Figure 3.12 - Typical unit tension at telltale location vs displacement plot.	21

Figure 3.13 - Example of the linear portion of the unit tension squared versus displacement plot.	22
Figure 3.14 - Example of a plot of deviation from a line versus displacement for the LPs closer to the center.	23
Figure 4.1 – Geosynthetics used in the testing program: a) Geogrid 01 (GG 01); b) Geogrid 02 (GG02); c) Geotextile 01 (GT01); d) Geotextile 02 (GT02).	26
Figure 4.2 - Typical frontal unit tension-unconfined axial strain data for GG1 based on image analysis results.	28
Figure 4.3 - Typical frontal unit tension-unconfined axial strain data for GT1 based on image analysis results.	29
Figure 4.4 – Particle size distribution of SAggr2, SAggr3 and Monterey Sand.	31
Figure 4.5 - Funk and Dinger particle size distribution curve used to generate the Angular WG aggregate.	33
Table 5 - Correspondence between test configurations and their goals.	37
Figure 5.1 - Representative result of GG1 with Round SAggr2: a) Load vs Time, b) Displacement vs Time, c) Unit tension vs displacement and d) Linear portion of the Unit tension squared vs displacement.	39
Table 5.1 - Final K_{SGC} and pullout unit tension for GG01 tested with Round SAggr2 5 times.	40
Figure 5.2 - Representative result of GG1 with Angular SAggr2: a) Load vs Time, b) Displacement vs Time, c) Unit tension vs displacement and d) Linear portion of the Unit tension squared vs displacement.	41
Figure 5.3 - Representative result of GG1 with Angular SAggr3: a) Load vs Time, b) Displacement vs Time, c) Unit tension vs displacement and d) Linear portion of the Unit tension squared vs displacement.	43

Figure 5.4 - Representative result of GG1 with Angular WG: a) Load vs Time, b) Displacement vs Time, c) Unit tension vs displacement and d) Linear portion of the Unit tension squared vs displacement.	45
Figure 5.5 - Representative result of GG1 with 50-50 SAggr2: a) Load vs Time, b) Displacement vs Time, c) Unit tension vs displacement and d) Linear portion of the Unit tension squared vs displacement.	47
Figure 5.6 - Representative result of GG2 with Round SAggr2: a) Load vs Time, b) Displacement vs Time, c) Unit tension vs displacement and d) Linear portion of the Unit tension squared vs displacement.	49
Figure 5.7 - Representative result of GG2 with Angular SAggr2: a) Load vs Time, b) Displacement vs Time, c) Unit tension vs displacement and d) Linear portion of the Unit tension squared vs displacement.	51
Figure 5.8 - Representative result of GT01 with Round SAggr2: a) Load vs Time, b) Displacement vs Time, c) Unit tension vs displacement and d) Linear portion of the Unit tension squared vs displacement.	54
Figure 5.9 - Representative result of GT1 with Angular SAggr2: a) Load vs Time, b) Displacement vs Time, c) Unit tension vs displacement and d) Linear portion of the Unit tension squared vs displacement.	56
Figure 5.10 - Representative result of GT1 with Angular SAggr3: a) Load vs Time, b) Displacement vs Time, c) Unit tension vs displacement and d) Linear portion of the Unit tension squared vs displacement.	58
Figure 5.11 - Representative result of GT1 with Angular WG: a) Load vs Time, b) Displacement vs Time, c) Unit tension vs displacement and d) Linear portion of the Unit tension squared vs displacement.	60

Figure 5.12 - Representative result of GT1 with 50-50: a) Load vs Time, b) Displacement vs Time, c) Unit tension vs displacement and d) Linear portion of the Unit tension squared vs displacement.	62
Figure 5.13 - Representative result of GS01 with Monterey Sand: a) Load vs Time, b) Displacement vs Time, c) Unit tension vs displacement and d) Linear portion of the Unit tension squared vs displacement.	64
Figure 5.14 - Representative result of GT2 with Round SAggr2: a) Load vs Time, b) Displacement vs Time, c) Unit tension vs displacement and d) Linear portion of the Unit tension squared vs displacement.	66
Figure 5.15 - Representative result of GT2 with Angular SAggr2: a) Load vs Time, b) Displacement vs Time, c) Unit tension vs displacement and d) Linear portion of the Unit tension squared vs displacement.	68
Figure 6.1 - Comparison of the time history of frontal unit tension obtained from tests using Round SAggr2 and Angular SAggr2, both with GG1.	79
Figure 6.2 - Frontal unit tension time history for two tests involving the GG1: one test using Angular SAggr2 (a) and another test using Angular WG (b).	80
Figure 6.3 - Frontal unit tension time history comparison, from two tests involving GT1: one test using Round SAggr2 (a) and another test using Angular SAggr2 (b).	81
Figure 6.4 – Frontal unit tension time history from two tests involving GT1, conducted using a uniform (a) and well-graded (b) aggregate.	82
Figure A.1 – Results from the first test of configuration involving GG1 and Round SAggr2	91
Figure A.2 - Results from the second test of configuration involving GG1 and Round SAggr2	93

Figure A.3 - Results from the third test of configuration involving GG1 and Round	
SAggr2	95
Figure A.4 - Results from the fourth test of configuration involving GG1 and Round	
SAggr2	97
Figure A.5 - Results from fifth test of configuration involving GG1 and Round	
SAggr2	99
Figure A.6 - Results from the first test of configuration involving GG1 and Angular	
SAggr2	102
Figure A.7 - Results from the second test of configuration involving GG1 and	
Angular SAggr2	104
Figure A.8 - Results from the third test of configuration involving GG1 and Angular	
SAggr2	106
Figure A.9 - Results from the fourth test of configuration involving GG1 and Angular	
SAggr2	108
Figure A.10 - Results from the fifth test of configuration involving GG1 and Angular	
SAggr2	110
Figure A.11 - Results from the first test of configuration involving GG1 and Angular	
SAgg3	113
Figure A.12 - Results from the second test of configuration involving GG1 and	
Angular SAgg3	115
Figure A.13 - Results from the third test of configuration involving GG1 and Angular	
SAgg3	117
Figure A.14 - Results from the fourth test of configuration involving GG1 and	
Angular SAgg3	119

Figure 15 - Results from the fourth test of configuration involving GG1 and Angular	
SAgg3	121
Figure A.16 - Results from the first test of configuration involving GG1 and Angular	
WG.....	124
Figure A.17 - Results from the second test of configuration involving GG1 and	
Angular WG.....	126
Figure A.18 - Results from the third test of configuration involving GG1 and Angular	
WG.....	128
Figure A.19 - Results from the fourth test of configuration involving GG1 and	
Angular WG.....	130
Figure A.20 - Results from the fifth test of configuration involving GG1 and Angular	
WG.....	132
Figure A.21 - Results from the first test of configuration involving GG1 and 50-50	
SAggr2	135
Figure A.22 - Results from the second test of configuration involving GG1 and 50-50	
SAggr2	137
Figure A.23 - Results from the third test of configuration involving GG1 and 50-50	
SAggr2	139
Figure A.24 - Results from the fourth test of configuration involving GG1 and 50-50	
SAggr2	141
Figure A.25 - Results from the fifth test of configuration involving GG1 and 50-50	
SAggr2	143
Figure A.26 - Results from the first test of configuration involving GG2 and Round	
SAggr2	146

Figure A.27 - Results from the second test of configuration involving GG2 and Round SAggr2	148
Figure A.28 - Results from the third test of configuration involving GG2 and Round SAggr2	150
Figure 29 - Results from the fourth test of configuration involving GG2 and Round SAggr2	152
Figure A.30 - Results from the fifth test of configuration involving GG2 and Round SAggr2	154
Figure A.31 - Results from the first test of configuration involving GG2 and Angular SAggr2	157
Figure A.32 - Results from the second test of configuration involving GG2 and Angular SAggr2	159
Figure A.33 - Results from the third test of configuration involving GG2 and Angular SAggr2	161
Figure A.34 - Results from the fourth test of configuration involving GG2 and Angular SAggr2	163
Figure A.35 - Results from the fifth test of configuration involving GG2 and Angular SAggr2	165
Figure A.36 - Results from the first test of configuration involving GT1 and Round SAggr2	168
Figure A.37 - Results from the second test of configuration involving GT1 and Round SAggr2	170
Figure A.38 - Results from the third test of configuration involving GT1 and Round SAggr2	172

Figure A.39 - Results from the fourth test of configuration involving GT1 and Round	
SAggr2	174
Figure A.40 - Results from the fifth test of configuration involving GT1 and Round	
SAggr2	176
Figure A.41 - Results from the first test of configuration involving GT1 and Angular	
SAggr2	179
Figure A.42 - Results from the second test of configuration involving GT1 and	
Angular SAggr2	181
Figure A.43 - Results from the third test of configuration involving GT1 and Angular	
SAggr2	183
Figure 44 - Results from the fourth test of configuration involving GT1 and Angular	
SAggr2	185
Figure A.45 - Results from the fifth test of configuration involving GT1 and Angular	
SAggr2	187
Figure A.46 - Results from the first test of configuration involving GT1 and Angular	
SAggr3	190
Figure A.47 - Results from the second test of configuration involving GT1 and	
Angular SAggr3	192
Figure A.48 - Results from the third test of configuration involving GT1 and Angular	
SAggr3	194
Figure A.49 - Results from the fourth test of configuration involving GT1 and	
Angular SAggr3	196
Figure A.50 - Results from the fifth test of configuration involving GT1 and Angular	
SAggr3	198

Figure A.51 - Results from the first test of configuration involving GT1 and Angular WG.....	201
Figure A.52 - Results from the second test of configuration involving GT1 and Angular WG.....	202
Figure A.53 - Results from the third test of configuration involving GT1 and Angular WG.....	204
Figure A.54 - Results from the fourth test of configuration involving GT1 and Angular WG.....	206
Figure A.55 - Results from the fifth test of configuration involving GT1 and Angular WG.....	208
Figure A.56 - Results from the first test of configuration involving GT1 and 50-50 SAggr2	211
Figure A.57 - Results from the second test of configuration involving GT1 and 50-50 SAggr2	213
Figure A.58 - Results from the third test of configuration involving GT1 and 50-50 SAggr2	215
Figure A.59 - Results from the fourth test of configuration involving GT1 and 50-50 SAggr2	217
Figure A.60 - Results from the fifth test of configuration involving GT1 and 50-50 SAggr2	219
Figure A.61 - Results from the first test of configuration involving GT1 and Monterey Sand.....	222
Figure A.62 - Results from the first test of configuration involving GT1 and Monterey Sand.....	224

Figure A.63 - Results from the third test of configuration involving GT1 and Monterey Sand	226
Figure A.64 - Results from the first test of configuration involving GT2 and Round SAggr2	229
Figure A.65 - Results from the second test of configuration involving GT2 and Round SAggr2	231
Figure A.66 - Results from the third test of configuration involving GT2 and Round SAggr2	233
Figure A.67 - Results from the fourth test of configuration involving GT2 and Round SAggr2	235
Figure A.68 - Results from the fourth test of configuration involving GT2 and Round SAggr2	237
Figure A.69 - Results from the first test of configuration involving GT2 and Angular SAggr2	240
Figure A.70 - Results from the second test of configuration involving GT2 and Angular SAggr2	242
Figure A.71 - Results from the third test of configuration involving GT2 and Angular SAggr2	244
Figure A.72 - Results from the fourth test of configuration involving GT2 and Angular SAggr2	246
Figure A.73 - Results from the fifth test of configuration involving GT2 and Angular SAggr2	248

Chapter 1: Introduction

1.1 RESEARCH MOTIVATION

Over the past several decades, geosynthetics have been used in several types of geotechnical engineering applications to fulfill functions such as separation, filtration, barrier, drainage, protection, reinforcement, and stiffening. Two of these functions involve mechanical improvements: (a) the reinforcement function, which relies on maximum strength and therefore, utilizes parameters determined under failure conditions, and (b) the stiffening function, which aims to improve the deformability and attain specific serviceability criteria related to maintain low strain conditions.

Common examples of applications in which geosynthetics are used as reinforcement are retaining structures, such as mechanically stabilized earth (MSE) walls, stabilized slopes, and stabilized roads founded on soft subgrades. On the other hand, common uses in which geosynthetic are used to fulfill a stiffening function include the stabilization of unbound aggregates in road bases, ballast in railways, and load-carrying platforms. In the applications involving use of geosynthetics to fulfill a stiffening function in road bases, the mechanism involved is lateral restraint, which consists of minimizing the time-dependent displacement of the base material.

A number of tests to determine the mechanical properties of the different types of geosynthetics are available. The most common tests are those that involve testing the geosynthetic in unconfined condition. Less common are tests that evaluate the combined behavior of the geosynthetic and the soil, among which the pullout test is a good example. The focus of pullout test, however, is on the failure state in which large displacements take place and the pullout strength is measured.

The soil-geosynthetic composite (SGC) model on the other hand, was developed with the purpose of combining the tensile properties of the geosynthetic with the shear strength properties of the soil-geosynthetic interface into a single parameter, identified as the stiffness of the soil-geosynthetic composite (K_{SGC}) (Zornberg, Roodi and Gupta, 2017).

To experimentally measure the K_{SGC} , a large-scale pullout apparatus was initially used. However, such setup required a large amount of soil as well as a considerable effort and time for sample preparation. Consequently, and in order to facilitate practical adoption of the new test, a smaller version of the test involving a large-scale setup, called small soil-geosynthetic interaction (SGI) test, was developed in order to facilitate the practical application of the parameter.

However, until now, small SGI tests have been primarily performed using a single (reference) aggregate, which is a uniformly graded, round gravel (Roodi, 2016; Roodi et al., 2018; Peve, 2020). The characteristics of such reference aggregate had been selected to facilitate repeatability of the test and minimize issues related to particle breakage and moisture.

On the other hand, the use of different aggregates can provide understanding on the impact of aggregate characteristics, such as angularity and particle size distribution, which may affect the soil-geosynthetic interaction and ultimately the stiffening capability of the material. Moreover, the majority of SGI tests conducted so far has involved use of geogrids (Roodi, 2016; Roodi et al., 2018; Peve, 2020)., and preliminary evaluations have indicated that the current reference aggregate may not allow proper ranking of different types of geotextiles. Therefore, it would be useful to explore the use of other reference aggregates that may result in suitable K_{SGC} values to rank multiple types of geosynthetics, including geotextiles. Consequently, this study evaluates, using the small soil-geosynthetic interaction (SGI) test, the impact of aggregate angularity, particle size and particle size

distribution on the soil-geosynthetic composite stiffness (K_{SGC}) for geosynthetics such as geogrids and geotextiles.

1.2 RESEARCH OBJECTIVES

The following are the objectives of this study:

- Evaluate the impact of angularity on the soil-geosynthetic composite stiffness (K_{SGC}) for geogrids and geotextiles.
- Evaluate the impact of particle size distribution on the soil-geosynthetic composite stiffness (K_{SGC}) for geogrids and geotextiles.
- Evaluate the impact of particle size on the soil-geosynthetic composite stiffness (K_{SGC}) for geogrids and geotextiles.
- Identify an aggregate that may be considered as reference to facilitate ranking of different geotextiles according to their K_{SGC} value.

1.3 THESIS OUTLINE

Following this introductory chapter, the background information for the soil geosynthetic interaction (SGI) test is presented in Chapter 2. The procedure and setup for small SGI test, as well as the collection and interpretation of the data, are discussed in Chapter 3. The different aggregates and geosynthetics used in this study are described in Chapter 4, which also outlines the testing program conducted in this investigation. In Chapter 5, the test results of the experimental testing program are described for each combination of aggregate and geosynthetic. Chapter 6 provides further discussion of the results, especially on the comparison of test results obtained for different combinations of geosynthetics and aggregates. Finally, Chapter 7 presents the conclusions of the study and provides suggestions for further research.

Chapter 2: Background information

2.1 OVERVIEW

Geosynthetics have been successfully used in roadways applications to fulfill many functions, among them being functions such as separation, filtration, barrier, drainage, protection, reinforcement, and stiffening. A good understanding of the last two functions, which involve the enhancement of mechanical properties, is relevant in the context of road base stabilization.

When a geosynthetic is used for its reinforcement function, the goal is to increase the bearing capacity of the soils. This case involves the mobilization of comparatively high geosynthetic strains. Consequently, a fundamental design property for this function is the geosynthetic tensile strength. On the other hand, when the geosynthetic is used for its stiffening function, the objective is to control the deformation in the soil-geosynthetic composite. To achieve that, comparatively small geosynthetic strains are mobilized. Therefore, key design properties to accomplish this function are related to quantifying the increased stiffness resulting from the soil-geosynthetic interaction under small strains (Zornberg, 2017).

When used for base stabilization, the function of the geosynthetic being tapped into is stiffening. In this case, control of deformation in the soil-geosynthetic composite is required, as the rutting depth must be kept low. When used for subgrade stabilization, the mobilized function of the geosynthetic is reinforcement since the desired effect is the increase in bearing capacity, which requires not only adequate stiffness but also proper tensile strength. Sometimes a single geosynthetic may be used for more than one application. A geosynthetic placed between the base and the subgrade is an example of a case in which a single geosynthetic is used in more than one application. This is because,

in this case, the geosynthetic will not only increase the subgrade load-carrying capacity (reinforcement) but will also control the lateral displacement of the base material (stiffening).

Properties of the geosynthetic in isolation, such as tensile strength and stiffness, flexural rigidity, geogrid junction strength, and rib strength, are comparatively easy to obtain. Tests to determine such properties are available and have been performed for several decades. However, the properties of the geosynthetic in isolation may not directly correlate to its performance in road stabilization. For instance, no direct relationship was found between roadway performance and tensile strength at 5% strain (Giroud & Han, 2006).

2.2 SOIL-GEOSYNTHETIC COMPOSITE (SGC) MODEL

The soil-geosynthetic composite (SGC) model is an analytical model developed at the University of Texas at Austin, with the purpose of combining the tensile properties of the geosynthetic and the shear strength properties of the soil-geosynthetic interface into a single parameter, identified as the stiffness of the soil-geosynthetic composite (K_{SGC}) (Gupta 2009; Zornberg, Roodi & Gupta, 2017).

The model under consideration involves assuming two constitutive relationships. The first is regarding the geosynthetic under confinement, which relates the geosynthetic unit tension (T) to the corresponding tensile strain (ϵ). The confined geosynthetic stiffness (J_c) is the slope of the relationship. The second constitutive relationship relates the shear stress (τ) to the relative displacement between the soil and the geosynthetic (u). A rigid-perfectly plastic response is assumed, with a yield shear stress referred to as τ_y (Roodi, 2016). Figure 2.1 illustrates both constitutive relationships.

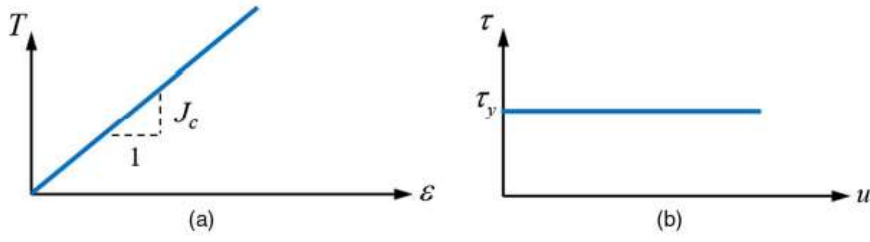


Figure 2.1 - Constitutive model: a) unit tension-strain linear relationship; b) shear stress-displacement rigid-perfectly plastic response (Zornberg, Roodi & Gupta, 2017).

The solution of the governing differential equation of the model, resulting from considering the local force equilibrium of a differential control segment of the geosynthetic, yields the following unit tension squared- displacement:

$$T(x)^2 = (4J_c\tau_y).u(x) \quad \text{Eq. 2.1}$$

The relationship shown in Equation 2.1 includes both the confined stiffness of the geosynthetic and the yield shear stress of the soil-geosynthetic composite (Zornberg, Roodi & Gupta, 2017). As a result, all the terms multiplying $u(x)$ can be reduced to a single constant, which is a key parameter suitable for the characterization of the soil-geosynthetic interaction. This parameter is defined as the “Stiffness of Soil-geosynthetic Composite” or K_{SGC} :

$$K_{SGC} = 4J_c\tau_y \quad \text{Eq. 2.2}$$

Among the outcomes of the model is the prediction of an active length. For a given load, a portion of the soil-geosynthetic interface has reached full mobilization of the interface shear strength, while the interface shear strength has not yet been mobilized along the rest of the interface (i.e., has zero shear stress). An increase in frontal loading causes the front of the mobilized zone to move forward, leading to a corresponding increase in the active length. Such progression of the mobilized zone is illustrated by Figure 2.2.

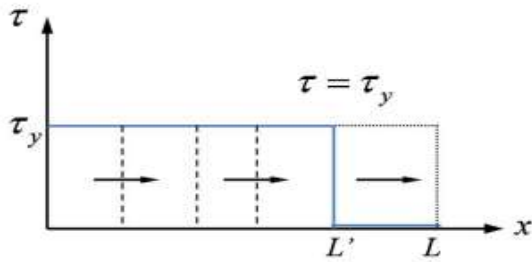


Figure 2.2 – Active length and the progression of the mobilized zone (Zornberg, Roodi & Gupta, 2017).

A Soil-Geosynthetic Interaction (SGI) test was developed in order to reproduce the SGC model in laboratory settings. Initially, the same apparatus conventionally used for a large pullout test was adopted (Gupta, 2009). That involved the placement of a large volume of aggregate and required a substantial amount of compaction.

A small-scale soil geosynthetic interaction test involving a considerably smaller setup was subsequently adopted to make the execution of the test simpler and faster. The use of a smaller box resulted in a reduction in the amount of aggregate used: the volume of soil needed to fill the smaller box is only 5% of the volume of aggregate needed to fill the large pullout box. Because a smaller box is used, the tests done with the new apparatus are called “small SGI tests”.

Roodi (2016) conducted an extensive testing program to establish the validity of the results obtained with the small-scale SGI test and to correlate the small-scale and large-scale results. Among the several findings of that study is that the linearity and uniqueness of the T^2 vs. u data are valid for the small-scale test. Moreover, tests conducted on five geosynthetic products using both the small- and large-scale resulted in the same ranking of the geosynthetics. Thus, confirming the suitability of the small-scale test for comparison among different geosynthetic products.

A comprehensive soil-geosynthetic interaction testing program conducted by Roodi et al. (2018) established the final testing configuration to be used for TxDOT specifications in the selection of geosynthetics for stabilized roadways. The testing program involved the use of three soil types (one sand and two gravels), three normal pressures (1, 3, and 5 psi), and two testing directions (machine and cross-machine direction).

The testing procedure finally adopted involved using No. 8-Truncated backfill (SAggr2) as reference aggregate. The confining pressure adopted for reference testing is 3 psi. Such confining pressure was adopted for two main reasons: it is reasonably similar to the permanent normal stress applied to geosynthetic in a geosynthetic-stabilized roadway, and it results in distinctive K_{SGC} values for several geosynthetic products. A gravel aggregate was considered to better represent the interaction between a flexible base and geosynthetics, and a uniform particle size distribution is expected to be easy to reproduce. Finally, the cross-machine direction was adopted, as it is the direction in which the geosynthetic is loaded by the traffic in roadways applications.

Chapter 3: Small scale soil-geosynthetic interaction test

3.1 TEST SETUP

A view of the entire soil-geosynthetic interaction setup is shown in Figure 3.1. The small-scale soil-geosynthetic interaction equipment incorporates several elements of the traditional pullout equipment, as described in ASTM D6706-01(07) (2007). There are, however, two differences that should be highlighted. First, as mentioned in Chapter 2, the soil volume used in the small-scale box is only 5 % of the soil volume used in the large-scale pullout setup built with the minimum dimensions. In addition, in the small-scale interaction test device, the geosynthetic specimen is pulled in the vertical direction. This setup allows the soil-geosynthetic interaction test to be performed with load frames that are commonly used for wide-width tensile strength tests of geosynthetics, as specified by ASTM D4595-11 (2011) and ASTM D6637/D6637M-15 (2015).



Figure 3.1 - Complete setup for the Small SGI test.

The roller grip used to pull the geosynthetic specimen vertically out of the box is attached to the load cell by a universal joint. The moving head of the load frame has the load cell attached to it. The displacement rate of the load frame was set to 1 mm/minute for all tests done in this study. To ensure the right displacement rate is being applied, an LVDT is used. A schematic view of the test setup is shown in Figure 3.2 (Zornberg et al., 2013).

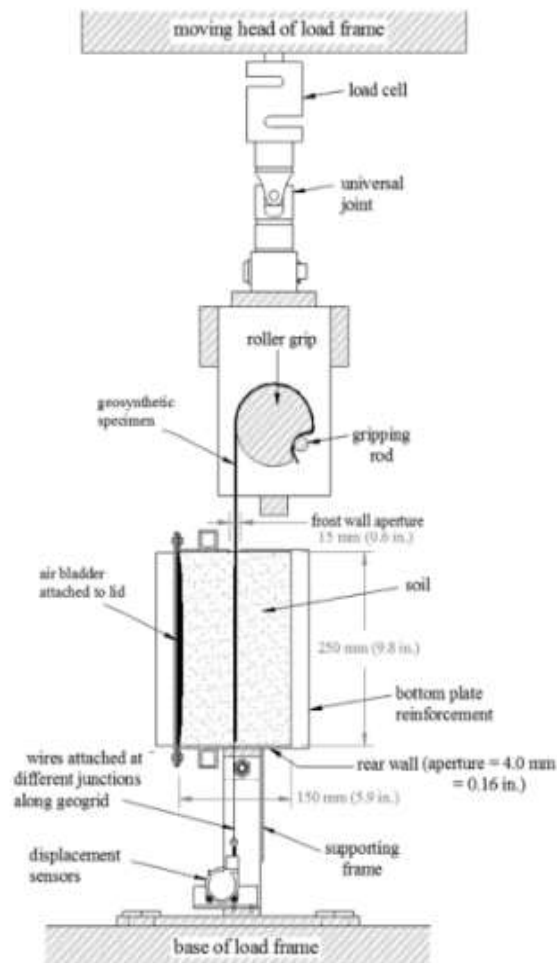


Figure 3.2 - Side view of loading system, with details about its several components.

3.1.1 Small SGI box

The small SGI box is made of steel and its inner dimensions are 300 mm (11.8 in.) in width, 250 mm (9.8 in.) in length, and 150 mm (5.9 in.) in height. The front wall has a horizontally rectangular opening with height of 25 mm (1 in.) in the middle, extending through the entire width of the box. While the back wall has a horizontal opening of 4 mm (0.16 in.) in the middle.

3.1.2 Load cell and Load frame

The frontal load is measured by a 5000 lbf. S-shape load cell, manufactured by Omega Engineering (SN 1457992). The load frame used for the soil-geosynthetic interaction test was manufactured by Satec Systems Inc. (SN 60CG-1009)

3.1.3 LVDT

The LVDT shown in Figure 3.3 and used to check the displacement rate was manufactured by Omega Engineering (model LD620-75). The LVDT is attached to the static part of the loading frame by a small grip.



Figure 3.3 - LVDT used to check the displacement rate of the loading frame.

3.1.4 Linear potentiometers

To measure the displacement at the five points across the geosynthetic specimen, five linear potentiometers (LPs), as the one shown in Figure 3.4, are used. Such LPs have a measuring range of 71.1 mm (2.8 in).



Figure 3.4 - Close view of one of the LPs used to measure displacement during the SGI test.

3.1.3 Confining Pressure Application and Pressure Gauges

The apparatus used to apply and measure the confining pressure is shown in Figure 3.5. The confining pressure is applied through a rubber bladder attached the lid of the SGI box. A piece of non-woven geotextile is situated between the top layers of the soil backfill and the air bladder to prevent puncture of the bladder by the aggregate.



Figure 3.5 - Views of the SGI box lid: (a) view of the air bladder; (b) view of the digital and analog pressure gauge.

3.1.4 Image processing

A camera, mounted on a frame as shown in Figure 3.1, takes a picture every five seconds, while the geosynthetic is being pulled vertically. A shutter speed of 1/40 seconds, an aperture of 4.0, and an ISO value of 1250 have been used.

The markers disposed in three rows on the unconfined portion of the geosynthetic, as shown in Figure 3.6, are used to determine the strain and the unconfined stiffness of the geosynthetic.



Figure 3.6 - Disposition of the markers on the unconfined portion of the geosynthetic.

3.3 TESTING PROCEDURE

3.3.1 Sample preparation

The first step in the sample preparation involves cutting the geosynthetic specimen. Geogrids are usually cut with scissors, while geotextiles are cut with a hot knife. The width of the geosynthetic specimen is targeted to 280 mm while the length of the specimen is about 900 mm.

The telltale attachment locations are shown in Figure 3.7. A hole is drilled at the attachment location to attach the telltales to the geogrid. The wire goes through the hole and is bended at the back of the geogrid specimen. A similar procedure is used for geotextiles, with two differences: it is not necessary to drill the specimen, and glue is placed on the front and the back of the specimen at the telltale locations. The pictures in Figure 3.7 also show the brass tubes extending through the entire length of the wires inside the box. The goal of the brass tubes, which were incorporated to the testing procedure by Peve (2020), is to prevent friction between the aggregate and the wires, which could negatively impact the displacement measurements.

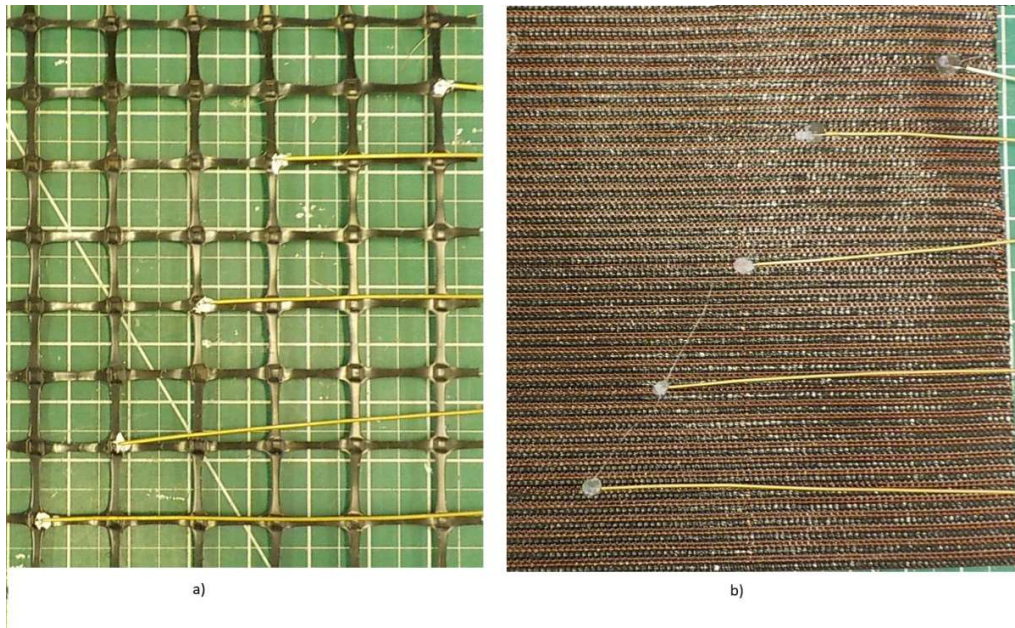


Figure 3.7 - Telltale attachment: (a) geogrids, (b) geotextiles.

Before placing the aggregate inside the box, the weight of the empty box, as well as its lid and the geosynthetic specimen, is measured. The placement of the aggregate inside the box is completed in four layers, with the geosynthetic specimen placed between the second and the third layer. The target thickness for each of the first two layers is 37.5 ± 1.0 mm, while the target thickness for each of the last is 35.0 ± 1.0 mm. Analysis of the effect of unit weight on K_{SGC} have shown that the ± 1.0 mm of acceptable variability in layer thickness has an almost negligible impact on K_{SGC} (Peve, 2020)

The aggregate weight for each layer is determined based on the target unit weight for that aggregate. Such target unit weight is achieved by compacting the layer until the target right is reached. The compaction of each layer is done by placing a wooden plate (with length and width of approximately 285 and 230 mm, respectively, and thickness of 10 mm) on top of the layer and manually hitting the plate with a rubber hammer. The

procedure to determine the target unit weight for each aggregate is presented with details in Section 4.2.2.

After the first layer has been placed and compacted, the surface of the aggregate is scratched, and the placement and compaction of the second layer takes place. After compaction of the second layer, the geosynthetic specimen is placed and two measurements are made: the distance from the end of the specimen to the end of the box as well as the length of the specimen inside the box. Usually, the length of the specimen inside the box is 240 mm. A top view of the box after a geogrid specimen has been placed is shown in Figure 3.8.

Next, aggregate layers three and four are placed and compacted similarly to layers one and two. Finally, a piece of non-woven geotextile is placed on top of the fourth layer, followed by the box lid. The goal of the non-woven geotextile is to protect the air bladder attached to the lid from being punctured by the aggregate. The weight of the box is then measured again.



Figure 3.8 - Top view of the box after the first two layers and the geosynthetic are placed.

Once the preparation of the soil-geosynthetic specimen in the box is completed, confining pressure is applied, and the box is turned vertically and attached to the bottom grip of the load frame. Following that is the attachment of the unconfined portion of the geosynthetic specimen to the roller grip. A 15 lb/ft torque is applied to the screws connecting the rod to the roller grip. The telltale wires are then attached to the corresponding LPs.

3.2.2 Test-specific correction procedure for each LP

Once the different components of the set up are in place, a test-specific correction is performed (Peve, 2020). The test-specific correction consists of imposing 1.6 mm of displacement to all five LPs, by eight steps of 0.2 mm each, and recording the response of each LP. That is followed by the removal of the imposed displacement, which is also done in steps of 0.2 mm. As a result, 16 data points are obtained for each LP. A linear regression is then applied to the displacement imposed versus displacement measured data, and the slope obtained for each LP is the correction coefficient of that LP.

The objective of such correction is to minimize the effects of experimental particularities. Experimental particularities that may change from test to test are: (1) attachment of still wires to geogrid, (2) the condition of the steel wires (straight, inclined or bent), (3) the characteristics of the wires to LPs attachment, and (4) the response of the data acquisition system for the specific conditions (environmental and electrical) at the time a test is performed (Peve, 2020). For the vast majority, the values of correction coefficients obtained are within the range of 0.9-1.1.

Typical results obtained from the test-specific correction procedure for one of the LPs are shown in Figure 3.9. In this case, the LP readings are 0.967 times the imposed

displacement. Therefore, the data obtained from that LP during the test must be multiplied by 1.034 (1 divided by 0.967).

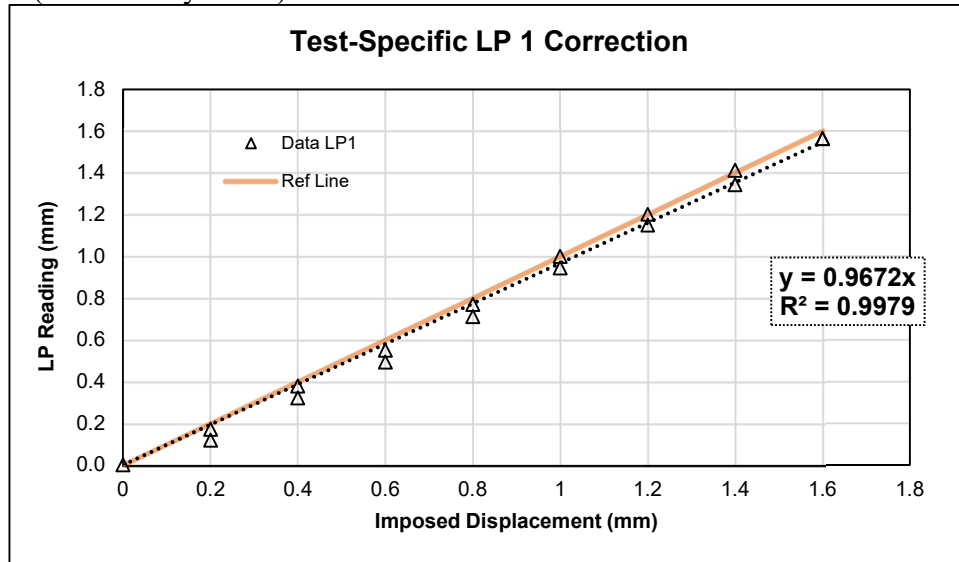


Figure 3.9 - LP reading versus imposed displacement obtained from test-specific correction

3.2.3 Soil-geosynthetic interaction test

After the test-specific correction procedure is complete, a seating load withing 25 to 30 pounds is applied in order to remove possible slacks on the grip attachments and wrinkles on the geosynthetic specimen. Once the seating load is applied, the soil-geosynthetic interaction itself starts. The moving head of the load frame imposes a displacement rate of 1 mm/min. Data collection from the 5 LPs, the load cell, and the LVDT happens every 0.2 seconds, while a picture of the unconfined portion of the geosynthetic is taken every 5 seconds. More details on the instrumentation and data collection are presented next, in Section 3.3.

3.4 INTERPRETATION OF THE DATA

All the data is collected with a frequency of 5 Hz. A moving average filter applied to a window of 50 data points is considered an efficient method of removing noise from the data collected during the SGI test.

The load is measured in pounds and converted to kN after the filter is applied. It is then divided by the width of the geosynthetic specimen (distance between the two uttermost lateral ribs in the case of geogrids) to obtain the frontal unit tension ($T_0(t)$). A typical frontal unit tension time history is shown in Figure 3.10. The pullout capacity, which is the peak frontal unit tension of a given test can be obtained from this plot.

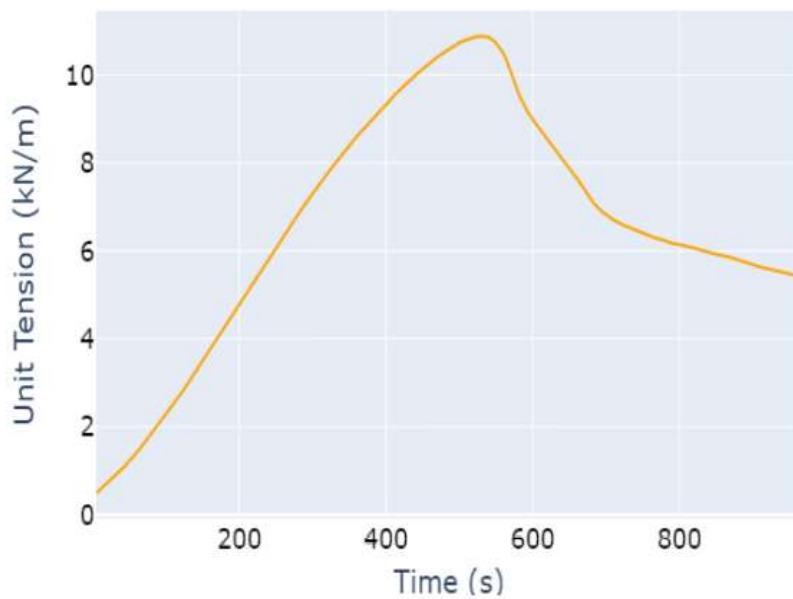


Figure 3.10 – Example of a frontal unit tension versus time plot.

The displacement at five telltale locations (u_i) is obtained multiplying the data from each linear potentiometer (LP) by the correction factor obtained by the test-specific correction procedure, as described in section 3.2.2. After the filter is applied, the displacement time history is used to obtain the triggering time (t_i) of each LP. The criteria

to determine when an LP has been triggered is the measured displacement surpassing a value of 0.02 mm, which was adopted to avoid misinterpreting the noise present in the data recorded by the LPs as being actual telltale displacement (Roodi et al., 2018). Figure 3.11 shows an example of time history of the displacement readings.

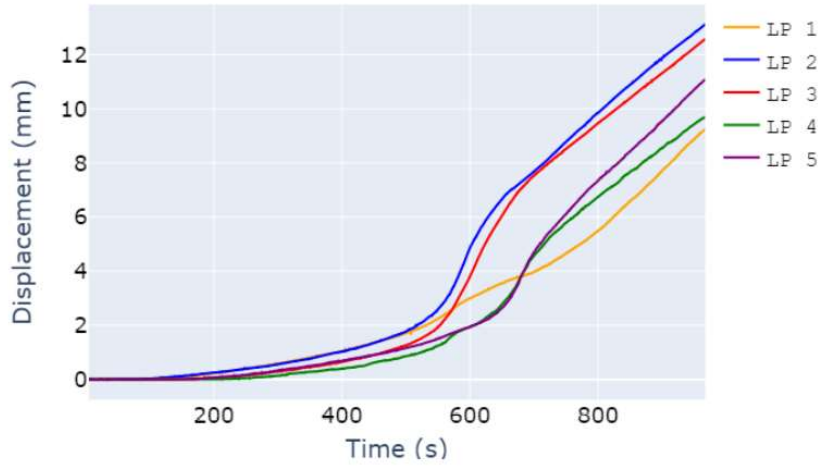


Figure 3.11 – Typical time history of the displacement readings at the five telltale locations.

Once the triggering time of a given LP is known, the frontal load being applied when each LP was triggered can be determined ($T_{0i}(t_i)$). The unit tension in one of the five telltale locations at a given moment can be calculated as the frontal unit tension minus the frontal unit tension measured when that LP was triggered ($T_i(t) = T_0(t) - T_{0i}(t_i)$). Thus, a plot of the unit tension at the telltale location versus displacement is obtained by combining the displacement and unit tension time history, as the example shown in Figure 3.12.

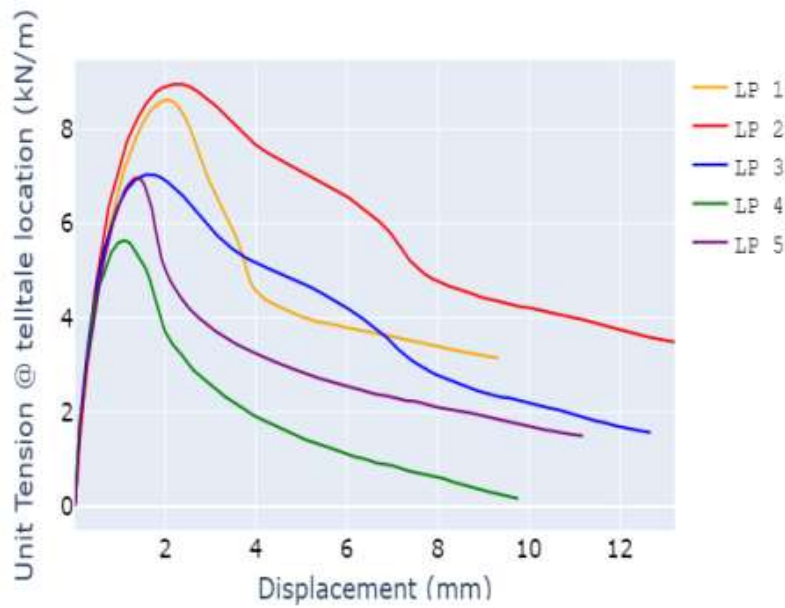


Figure 3.12 - Typical unit tension at telltale location vs displacement plot.

The initial portion of the unit tension squared versus displacement data is expected to be linear. Data between 0.1 and 1.0 mm displacement is used to fit the linear regression model. The lower limit (0.1 mm) of this range of displacement was adopted, so that displacements following initial adjustment of the geosynthetic were not included in the calculations to obtain the K_{SGC} ; the reason for the upper limit (1.0 mm) is to ensure that the data used is within the linear portion of the unit tension squared-displacement relationship (Roodi et al., 2018). The slope of the line obtained from the model is the K_{SGC} for a given telltale location. Figure 3.13 shows the example of a unit tension squared versus displacement plot for LPs 2, 3, and 4, zoomed in the displacement ranging from 0.1 to 1.0 mm. LPs 1 and 5 are not used for K_{SGC} calculation due to boundary effects since the first is very close to the frontal opening of the box, and the second is very close to the back opening.

The current SGI procedure described here, is based on what was documented by Roodi et al. (2018) and incorporate several changes proposed by Peve (2020).

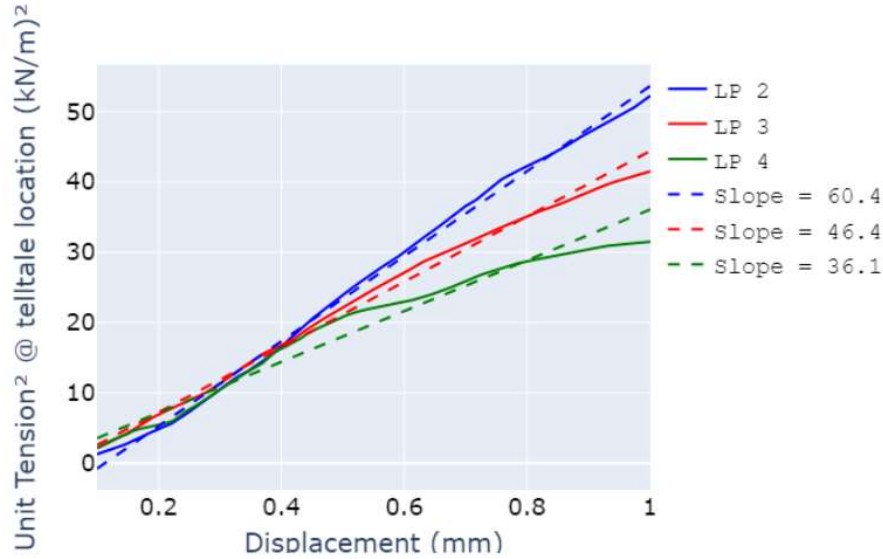


Figure 3.13 - Example of the linear portion of the unit tension squared versus displacement plot.

The statistical analysis for detection of outlier is described next. After that analysis is done on the test level, the K_{SGC} at telltale location ($K_{SGC,i}$) versus distance from the front of the box (l_i) data is used to fit a liner function - $K_{SGC}(l)$. Finally, the final K_{SGC} value is obtained right at the center of the geosynthetic specimen, through Equation 3.1 using the length of the specimen divided by two as the input.

$$K_{SGC,final} = K_{SGC}\left(\frac{L}{2}\right) \quad \text{Eq. 3.1}$$

3.5 OUTLIER ANALYSIS

In order to facilitate the generation of consistent data, outlier analysis is applied at three levels: 1) the linearity of each LP data for the expected linear range (0.1 to 1.0 mm); 2) consistency among the LPs data for a given test; 3) consistency among the final K_{SGC} from each test with a given configuration.

The linearity evaluation is done by calculating the deviation from a line of the linear portion of the unit tension squared. The deviation from a line is the difference between the value of unit tension squared given by the linear model and the value of unit tension squared based on the test data. The criterion expressed in Equation 3.1 is then applied to the standard deviation of the difference between the two values of unit tension. An example is shown in Figure 3.14 of the resulting deviation from a line for LPs 2, 3, and 4.

$$\sigma \leq 1.5$$

$$\text{Eq. 3.2}$$

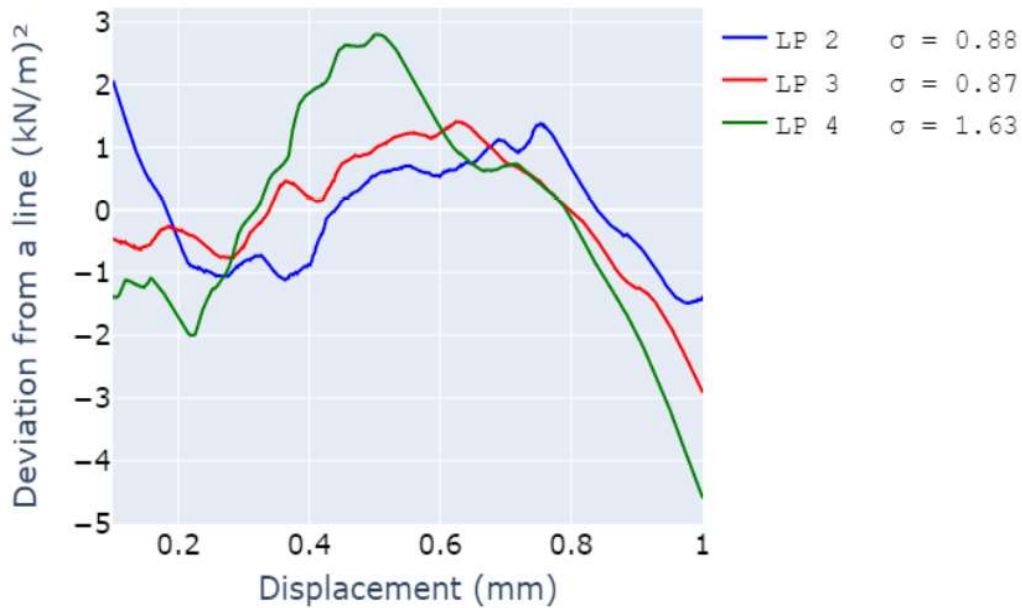


Figure 3.14 - Example of a plot of deviation from a line versus displacement for the 3 LPs closer to the center.

The second level of analysis consists of finding the K_{SGC} value among the three LPs with the highest sum of differences from the other two K_{SGC} values, then determining if the smallest of the two differences is 25% higher or lower than the average of the other two K_{SGC} values. If the K_{SGC} values from the three LPs are arranged as follows:

x_0	x_1	x_2	x_3	x_4
$K_{sgc-LP\ 4}$	$K_{sgc-LP\ 2}$	$K_{sgc-LP\ 3}$	$K_{sgc-LP\ 4}$	$K_{sgc-LP\ 2}$

then the K_{SGC} with the highest sum of differences can be determined using Equation 3.3.

$$n = i(MAX_{i=1}^{i=3}[|x_i - x_{i-1}| + |x_i - x_{i+1}|]) \quad \text{Eq. 3.3}$$

Then the outlier criteria can be applied as in Equation 3.4.

$$\frac{MIN(|x_n - x_{n-1}|; |x_n - x_{n+1}|)}{AVG(x_{n+1}; x_{n-1})} \leq 0.25 \quad \text{Eq. 3.4}$$

The analysis on the test configuration level is done using the median and the concept of MAD - Median of all the Absolute Differences (between the sample values and the sample median). A method of outlier detection that used the median is preferred for relatively small sample sizes, because it eliminates the effect that outliers have on the average and standard deviation (Rousseeuw & Hubert, 2011).

For pullout capacity, the criteria expressed in Equation 3.5 is used, while for the K_{SGC} value, the criteria used is the one expressed in Equation 3.6.

$$\frac{|P_{max,i} - median(P_{max,n})|}{MAD} \leq 2.5 \quad \text{Eq. 3.5}$$

$$\frac{|K_{SGC,i} - median(K_{SGC,n})|}{MAD} \leq 2.0 \quad \text{Eq. 3.6}$$

Chapter 4: Materials and testing program

4.1 GEOSYNTHETICS USED IN THE TESTING PROGRAM

Four commercially available geosynthetics were used in the testing program, two geogrids and two geosynthetics. A picture of each of the four geosynthetics is shown in Figure 4.1.

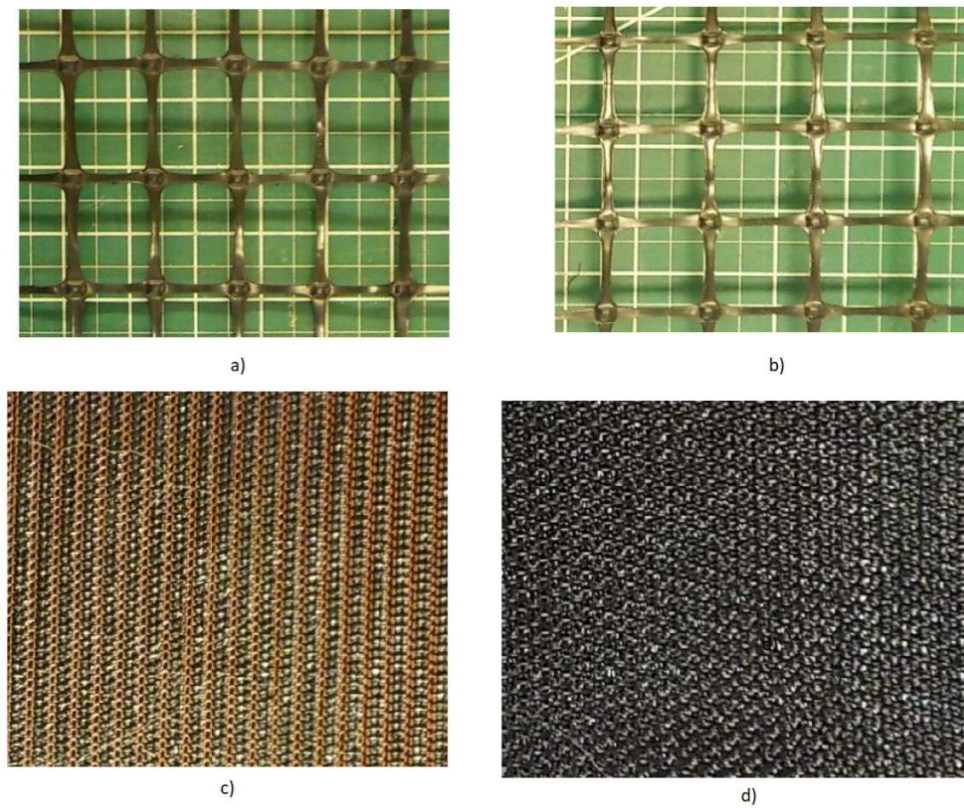


Figure 4.1 – Geosynthetics used in the testing program: a) Geogrid 01 (GG 01); b) Geogrid 02 (GG02); c) Geotextile 01 (GT01); d) Geotextile 02 (GT02).

The first geogrid product is a polypropylene biaxial geogrid manufactured by Tensar Co. as BX1100, referred to as GG1 in this study. The second geogrid, GG2, is a

polypropylene biaxial geogrid distributed by Hanes Geo Components. The two geotextile products are manufactured by Tencate Mirafi as RS380i and HP570, referred to as GT1 and GT2, respectively.

At 2% strain, GG2 has a higher tensile modulus (370 kN/m) than GG1 (330 kN/m). For the same strain level, the tensile modulus of GT2 (965 kN/m) is higher than that of GT1 (745 kN/m). More details about the mechanical properties of the geosynthetics are presented in table 4.1.

Table 4.1 - Main characteristics of the four geosynthetics used in this study

Geosynthetic	GG1	GG2	GT1	GT2
Tensile Modulus @ 2% strain (CD)	330 kN/m	370 kN/m	745 kN/m	965 kN/m 5
Tensile Modulus @ 5% strain (CD)	268 kN/m	299 kN/m	658 kN/m	760 kN/m
Ultimate Tensile Strength (CD)	19 kN/m	20 kN/m	Not specified	70 kN/m
Polymer Composition	Polypropylene	Polypropylene	Polypropylene	Polypropylene
Aperture Dimensions (MD x CD)	25 x 33 mm	33 x 33 mm	--	--
Minimum Rib Thickness (MD – CD)	0.76 – 0.76 mm	1.3 – 0.7 mm	--	--

4.1.1 Typical image analysis results from a test involving GG1

Typical frontal unit tension-unconfined axial strain data from image analysis, obtained from an SGI test performed using GG1, is plotted in Figure 4.2. Data from the two extreme ribs are not considered.

The average frontal unit tension that resulted in 2% strain at each rib is 475 lbs/ft (6.93 kN/m), equivalent to a tensile modulus of 346 kN/m. Roodi (2016), when evaluating

the repeatability of wide width tensile test results from the University of Texas geosynthetic laboratory database, identified a coefficient of variability of 6% (at 2% strain) and 18% (at 1% strain). Therefore, the tensile modulus obtained from image analysis data is deemed to be in good agreement with the tensile modulus, from the product specification sheet, shown in table 4.1.

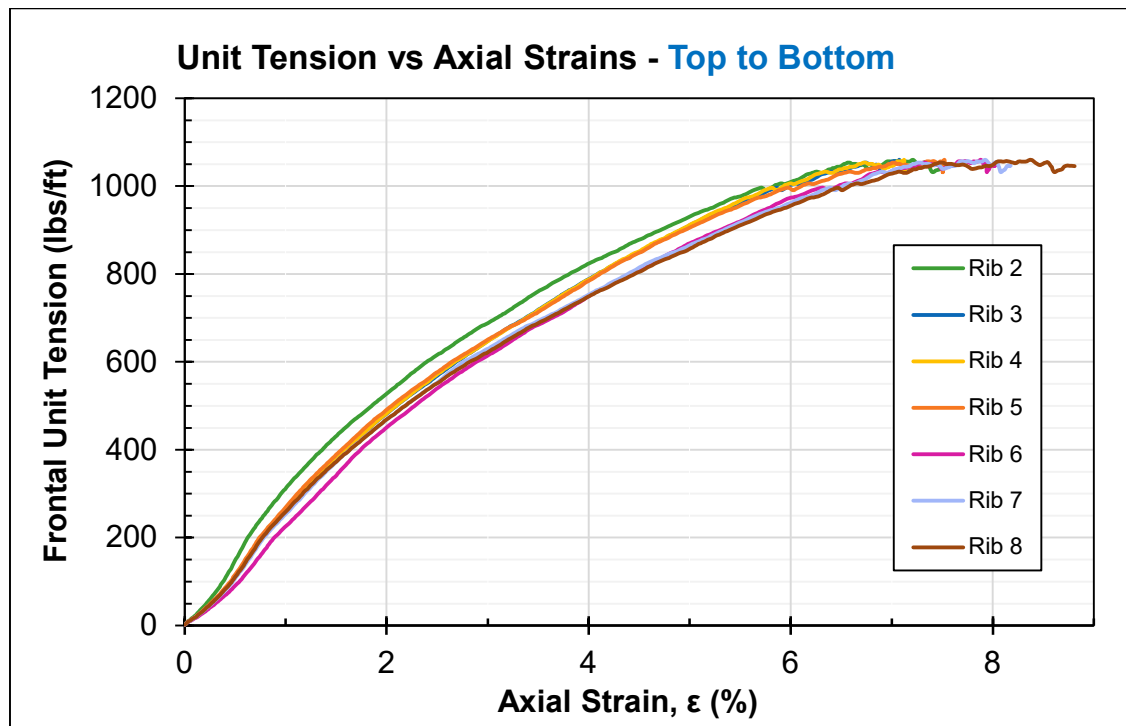


Figure 4.2 - Typical frontal unit tension-unconfined axial strain data for GG1 based on image analysis results.

4.1.2 Typical image analysis results from a test involving GT1

Typical frontal unit tension-unconfined axial strain data from image analysis, obtained from an SGI test performed using GT1, is plotted in Figure 4.2. Each of the “ribs” corresponds to a column of markers and the data was obtained using the displacements

observed for the top and bottom marker of each column. Data from the two uttermost “ribs” are not considered.

The average frontal unit tension when the strain observed on each “rib” reaches 1% is 7.1 kN/m (484 lbs/ft), resulting in a tensile modulus of 710 kN/m at 1% strain. This value cannot be directly compared with the tensile modulus of GT2 shown in Table 4.1, because the strain levels are different. Nonetheless, if the strains are still in the elastic zone, the tensile modulus at 1 and 2% strain would be expected to be within a similar range.

The data in Figure 4.3 also shows that relaxation occurs as the frontal unit tension is passed its peak value. In other words, once pullout failure happens, there is a reduction in frontal unit tension and a corresponding strain relaxation in the geotextile.

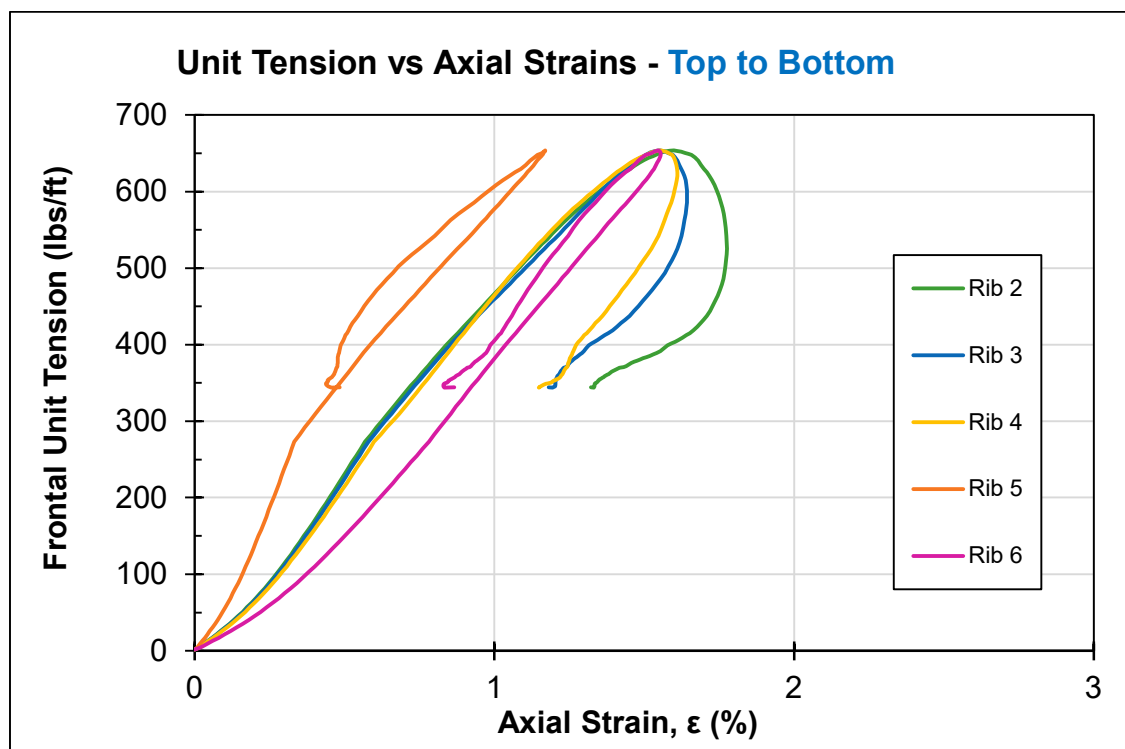


Figure 4.3 - Typical frontal unit tension-unconfined axial strain data for GT1 based on image analysis results.

4.2. AGGREGATE IDENTIFICATION AND INDEX PROPERTIES

A total of 5 aggregates were used in the testing program, and their index properties are listed in Table 4.2. The first aggregate is uniform and composed of round gravel, referred to in this study as Round SAggr2. According to the Unified Soil Classification System (USCS)(ASTM D2487-17), Round SAggr2 classifies as a poorly graded gravel (GP). This aggregate has been used for years as the reference aggregate for SGI tests (Roodi et al., 2018).

The second aggregate, referred to as Angular SAggr2, has the same classification and, in fact, the same particle size distribution. However, Angular SAggr2 is obtained from crushed stone, so it is an angular aggregate. Both aggregates have all particles passing 6.5 mm sieve size and retained by 4.75 sieve size.

The third aggregate, Angular SAggr3, is also uniform and classifies as gravelly sand because its particle size ranges from 4.75 to 2.36 mm.

Finally, the fourth aggregate is classified as GW and referred to in this study as Angular WG. It was carefully crafted to be well graded and to have no fines (no particles passing sieve #200). Further discussion of the particle size distribution of this material is presented in section 4.2.1.

The fifth aggregate, 50-50 SAggr2, is a combination of Round SAggr2 and Angular SAggr2. Therefore, it has the same particle size distribution, with 50% (in terms of weight) of the round and 50% of the angular aggregate. A similar combination was used a study that evaluated the impact of the angularity of the aggregate on shear strength (Tutumluer & Pan, 2008).

Finally, the sixth aggregate, known as Monterey Sand #30, is a poorly graded sand (SP) according to the Unified Soil Classification System (USCS). The particle size distributions for all six aggregates are shown in Figure 4.4.

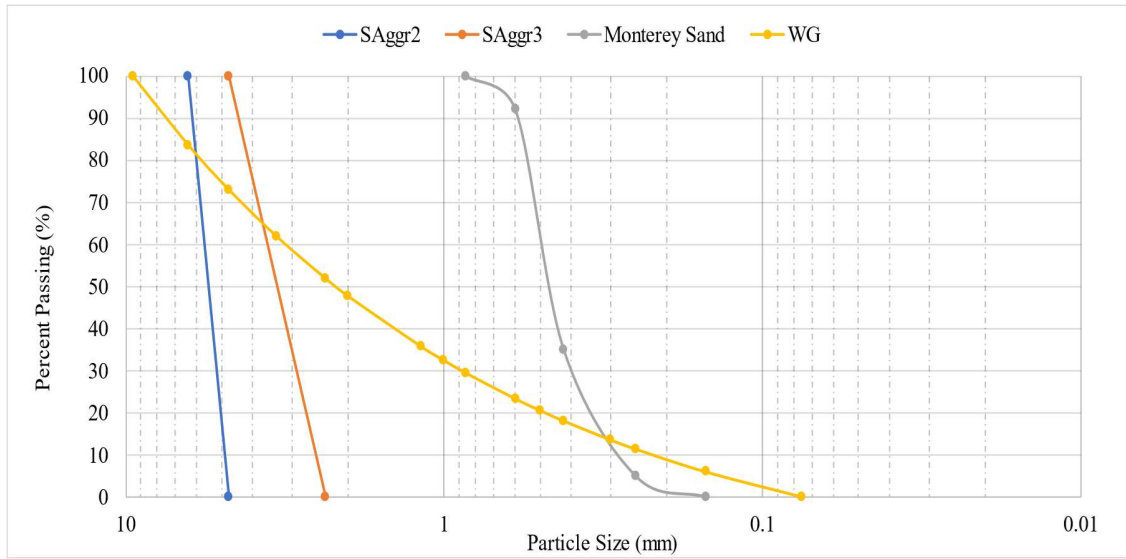


Figure 4.4 – Particle size distribution of SAggr2, SAggr3 and Monterey Sand.

Table 4.2 - Index properties of the six aggregates used in this study

Aggregate	Soil Classification	Particle Size Distribution				
		D10 (mm)	D30 (mm)	D60 (mm)	Cu	Cc
Round SAggr2	GP	5.60	5.60	5.60	1.0	1.0
Angular SAggr2	GP	5.60	5.60	5.60	1.0	1.0
Angular SAggr3	SP	3.60	3.60	3.60	1.0	1.0
Angular WG	GW	0.22	0.88	3.36	14.2	1.1
50-50 SAggr2	GP	5.60	5.60	5.60	1.0	1.0
Monterey Sand #30	SP	0.28	0.41	0.50	1.8	1.2

4.2.1 Background for the well graded aggregate

Many studies have been conducted to develop particle packing models and find the optimum packing of aggregates. That is, find the ratio of each particle size that would lead

to the highest density. Fuller and Thompson (1907) were among the pioneers in trying to determine the optimum packing of particles. An empirical relationship was developed by Fuller and Thompson and later expressed by Talbot and Richart (1929) in the form of Equation 4.1:

$$p = \left(\frac{d}{D}\right)^m \quad \text{Eq. 4.1}$$

where p is the percentage passing a given sieve, d is the size of that sieve, D is the maximum particle size, and m is a variable parameter that assumes the value of 0.45 for optimum packing. However, such a model does not limit the smallest particle size, implicitly assuming infinitesimal particles can fill the voids, which is not realistic.

That led Funk and Dinger (1994) to develop a model that includes the smallest particle size as a parameter and can be expressed by Equation 4.2.

$$p = \frac{d^n - d_s^n}{d_l^n - d_s^n} \quad \text{Eq. 4.2}$$

where p is the percentage passing a given sieve, m is the size of the sieve, d_s is the smallest particle size, d_l is the largest particle size, and n is a variable parameter that is made equal to 0.365 for optimum packing.

The theoretical particle size distribution curve of the well-graded aggregate was obtained from Equation 2, with d_s equal 0.075 mm, to avoid having fines. d_l was set equal to 9.5 mm, which comes from the necessity to limit the maximum particle size to half of the size of the frontal opening of the box. To obtain a well-graded aggregate, it was necessary to first sieve the source material (commercially available as a base course) using eight sieves of standard sizes (3/8", 1/4", #4, #8, #30, #50, #100, and #200) (ASTM E11-20). Once the amount of material of each sieve size required to achieve the desired particle size distribution was determined, based on the Funk and Dinger particle size distribution,

the different particle sizes were combined again. Thus, resulting in an aggregate, the Angular WG, with the same particle size distribution as the theoretical particle size distribution shown in Figure 4.5.

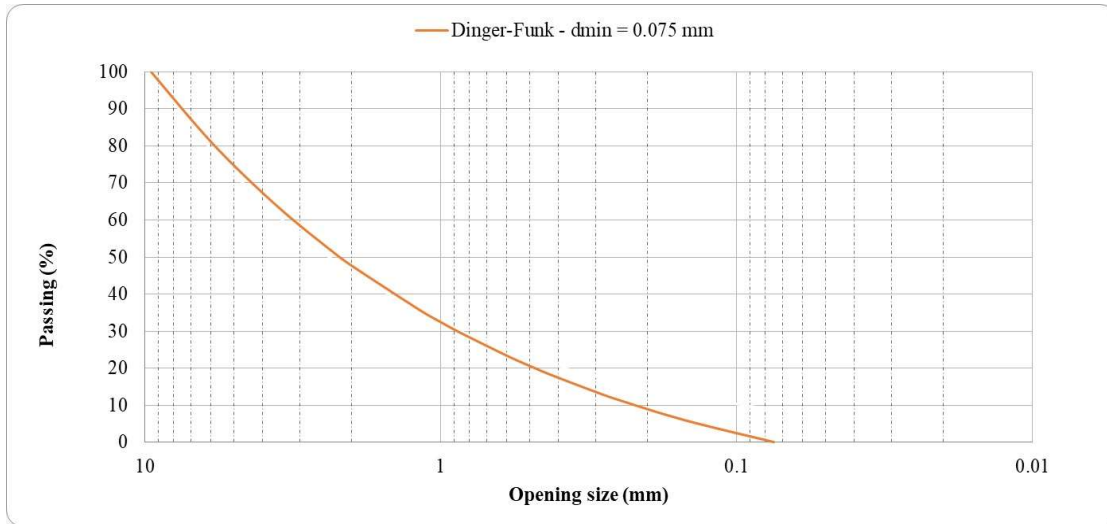


Figure 4.5 - Funk and Dinger particle size distribution curve used to generate the Angular WG aggregate.

4.2.2 Determination of equivalent unit weight

Equivalent unit weight in the context of this study can be defined as the unit weight obtained with the same compaction effort. For instance, two aggregates have equivalent unit weights if the unit weight of each aggregate was obtained with the same compaction effort. A simple test was developed, referred to as Equivalent Density Compaction Test, to determine the equivalent unit weight of the materials used in this study, using Round SAggr2 as the reference since this is one of the aggregates used the most in past studies involving the SGI test. A description of the testing procedure is done next.

The apparatus necessary for the Equivalent Density Compaction Test includes the small SGI box, the wooden plate (both described in section 3.2.1), and a standard proctor hammer. The amount of aggregate used is 4 kg.

The aggregate is placed inside the box using a funnel to allow it to start in a very loose state. The wooden plate is laid over the aggregate layer, and the proctor hammer goes on top of the wooden plate. Then 100 blows are applied, and the unit weight is measured at specific numbers of blows (0, 1, 2, 3, 4, 6, 10, 20, 30, 40, 50, 70, 100 blows). The unit weight is measured indirectly by measuring the height of the layer of aggregate.

Three trials repeat the same procedure, and the data is plotted as exemplified in Figure 4.6. A final unit weight versus number of blows curve is obtained by fitting the data. A logarithmic equation was found to fit best the data obtained for such a test.

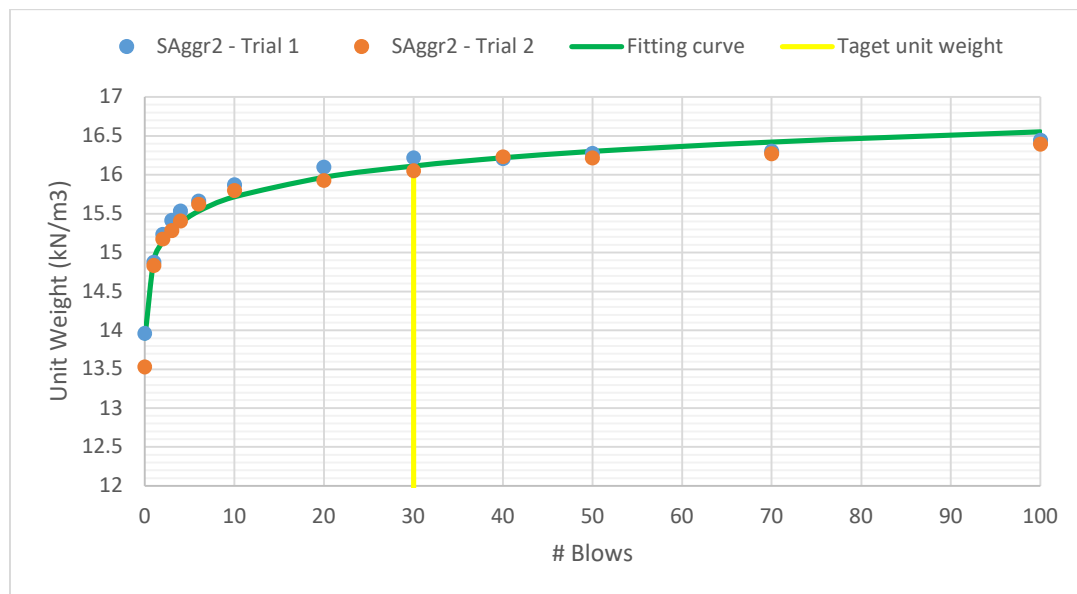


Figure 4.6 – Example of the data obtained with the Equivalent Density Compaction Test.

The reference aggregate was tested first, and it was found that 30 blows were necessary to achieve the target unit weight (16.12. kN/m³). The target unit weight of the reference aggregate was based on the unit weight used in past SGI tests involving this aggregate. The equivalent unit weight of all five other aggregates was determined with this test, having 30 blows as the compaction effort that gives the unit weight to be used as the target for the SGI test. The resulting unit weights are shown in Table 4.3.

Table 4.3 - Target unit weight of each aggregate used in this study

Aggregate	Target unit weight (kN/m³)
Round SAggr2	16.12
Angular SAggr2	16.11
Angular SAggr3	16.53
Angular WG	20.10
50-50 SAggr2	16.27
Monterey Sand	16.74

4.3 OUTLINE OF THE SGI TESTING CAMPAIGN

Fifteen configurations, involving different combinations of geosynthetics and aggregates, were used in this study to evaluate the impact of aggregate and geosynthetic properties on K_{SGC} . Table 4.3 shows the geosynthetic, the aggregate, and the number of tests for each configuration. The term configuration here refers to the combination of one geosynthetic and one aggregate used in each SGI test.

Table 4.4 - List of all the test configurations used in this study

Configuration #	Aggregate	Geosynthetic	# of tests
1	Round SAggr2	GT1	5
2		GT2	5
3		GG1	5
4		GG2	5
5	Angular SAggr2	GT1	5
6		GT2	5
7		GG1	5
8		GG2	5
9	50-50 SAggr2	GT1	5
10		GG1	5
11	Angular SAggr3	GT1	5
12		GG1	5
13	Angular WG	GT1	5
14		GG1	5
15	Monterey Sand	GT1	5

The different configurations were adopted to isolate a single parameter and change just that parameter when comparing the results obtained from one configuration to another. For instance, configurations 1, 5, and 9 have the same geosynthetic (GG1) and particle size distribution (SAggr2). The only parameter that changes from one configuration to another is the angularity of the aggregate. This is also the case for configurations 2 and 6 (using GG2), as well as configurations 3, 7, and 11 (using GT1) and configurations 4 and 8 (using GT2). Therefore, the goal of adopting the configurations mentioned above was to evaluate the effect of angularity on the K_{SGC} .

The correspondence between the configurations and the goal of each one is done in Table 4.5. The test results from each configuration are presented in Chapter 5 and further discussed in Chapter 6.

Table 5 - Correspondence between test configurations and their goals

Goal	Configurations
Evaluate the effect of angularity on geotextiles	1, 5 and 9 (GT1); 2 and 6 (GT2)
Evaluate the effect of angularity on geogrids	3, 7 and 10 (GG1); 4 and 8 (GG2)
Evaluate the effect of particle size on geotextiles	5, 11 and 15 (GT1)
Evaluate the effect of particle size on geogrids	7 and 12 (GG1)
Evaluate the effect of particle size distribution on geotextiles	5, 13 and 15 (GT1)
Evaluate the effect of particle size distribution on geogrids	7 and 14 (GG1)

Chapter 5: SGI Test results

This chapter describes the results obtained from tests conducted in the different testing series laid out in Chapter 4. Further discussion and comparisons are provided in Chapter 6.

5.1 GEOGRIDS

This section presents the test results from the configurations involving the use of geogrids. First the test results for GG1 are presented, followed by the test results for GG2

5.1.1 Tests conducted with Geosynthetic GG1

Geosynthetic GG1 was tested with 5 different aggregates: Round SAggr2, Angular SAggr2, Angular SAggr3, Angular WG, and 50-50 SAggr2. The test results with each aggregate are presented separately in the subsections that follow.

5.1.1.1 Tests involving GG1 and Round SAggr2

The results of a representative test for GG1 with Round SAggr2 are shown in Figure 5.1. This configuration was used as reference in the evaluation of the impact of angularity of the K_{SGC} for geogrids.

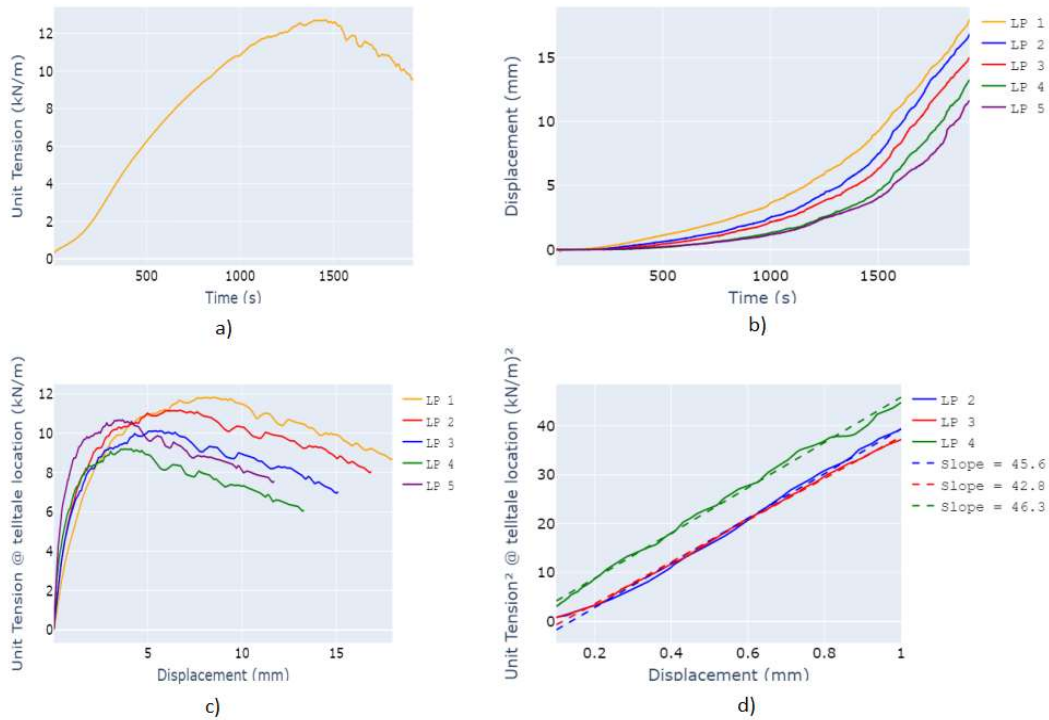


Figure 5.1 - Representative result of GG1 with Round SAggr2: a) Load vs Time, b) Displacement vs Time, c) Unit tension vs displacement and d) Linear portion of the Unit tension squared vs displacement.

Figure 5.1(a) shows the frontal unit tension versus time data. The tension increases gradually in the first stage of the test and then starts to decrease shortly after the unit tension reaches its peak. Figure 5.1(b) displays the displacement versus time data. It is relevant to note that all five points are initially static and are triggered as the loading front progresses. The unit tension at telltale location-displacement data, obtained by combining the frontal unit tension and the displacement time histories, is shown in Figure 5.1(c). which shows the unit tension at telltale location versus displacement. Figure 5.1(d) shows the unit tension squared versus displacement data ranging from 0.1 to 1.0 mm, only for LPs 2, 3, and 4. The line resulting from the linear regression model used to fit the unit tension squared-displacement data is also displayed in Figure 5.1(d). According to the model, the

K_{SGC} at each point being tracked is the slope of the line. A detailed discussion of how the raw data obtained from an SGI is processed was provided in Chapter 3, which also describes the statistical analyses adopted to detect outliers.

Based on the regression model, the K_{SGC} for LP2, LP3, and LP4 were respectively 45.4, 42.7, and 46.5 (kN/m)²/mm. Therefore, the final K_{SGC} for this test is 44.7 (kN/m)²/mm. The pullout capacity, obtained from the frontal unit tension time history shown in Figure 5.1(a), was 12.7 kN/m for this test. Table 5.1 shows this configuration's final K_{SGC} and unit tension for the five tests.

Table 5.1 - Final K_{SGC} and pullout unit tension for GG01 tested with Round SAggr2 5 times.

Test #	K_{SGC} (kN/m) ² /mm	Pmax (kN/m)	Outlier
1	44.7	12.7	False
2	40.3	12.5	False
3	40.1	12.2	False
4	NA	4.2	True
5	50.0	9.0	True
Average	41.7	12.5	-
Coefficient of Variation	5.1%	1.7%	

For Test #4, all LPs resulted in outlier values of K_{SGC} based on the criteria discussed in chapter 3. The unit tension value resulting from Test #5 is also an outlier. Consequently, both tests are not considered when calculating the average K_{SGC} and pullout unit tension for this configuration, resulting in an average K_{SGC} of 41.7 (kN/m)²/mm and an average pullout unit tension equal to 12.5 kN/m.

5.1.1.2 Tests involving GG1 and Angular SAggr2

Representative results from a test done with GG1 and Angular SAggr2 are displayed in Figure 5.2. This configuration was used to evaluate the impact of the aggregate angularity on the K_{SGC} of geogrids. It was also used as reference for the evaluation of the impact of particle size and particle size distribution on the K_{SGC} of geogrids.

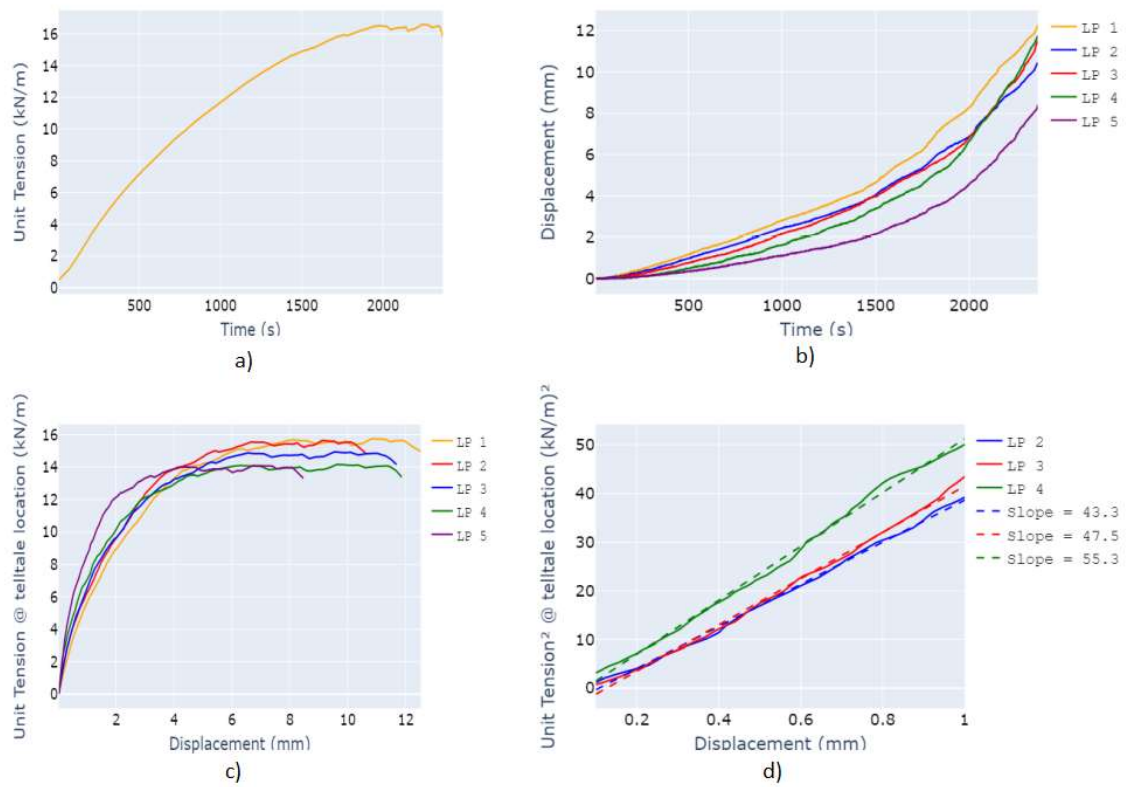


Figure 5.2 - Representative result of GG1 with Angular SAggr2: a) Load vs Time, b) Displacement vs Time, c) Unit tension vs displacement and d) Linear portion of the Unit tension squared vs displacement.

The K_{SGC} values obtained from this test were reasonably consistent, with 43.3, 47.5, and 55.3 (kN/m)²/mm for LPs 3, 4, and 5, respectively. Thus, resulting in a K_{SGC} value of 48.3 (kN/m)²/mm for this test, while the pullout unit tension was 16.6 kN/m. Table 5.2

shows the final K_{SGC} and pullout unit tension for the five tests done with GG2 and Angular Saggr2.

Table 5.2 - Final K_{SGC} and pullout capacity resulting from 5 tests done with GG1 tested with Angular SAggr2.

Test #	K_{SGC} (kN/m) ² /mm	Pmax (kN/m)	Outlier
1	NA	17.1	True
2	50.6	16.6	False
3	63.4	16.8	False
4	48.3	16.6	False
5	61.3	17.9	True
Average	54.1	16.7	-
Coefficient of Variation	12.3%	0.6%	

The K_{SGC} values for all three LPs from Test #1 were outliers (based on the linearity criteria), so it was impossible to calculate the final K_{SGC} for that test. Also, the pullout unit tension for Test #5 was an outlier. As a result, the average K_{SGC} for this configuration was 54.1 (kN/m)²/mm, while the average pullout unit tension was 16.6 kN/m. These results show a clear improvement compared to those obtained when GG2 was tested with Round SAggr2.

5.1.1.3 Tests involving GG1 and Angular SAggr3

Figure 5.3 shows results from a representative test done with GG1 and Angular SAggr3, which is uniform but with smaller particle sizes than the Angular SAggr2. This configuration was used to evaluate the impact of particle size on K_{SGC} of geogrids.

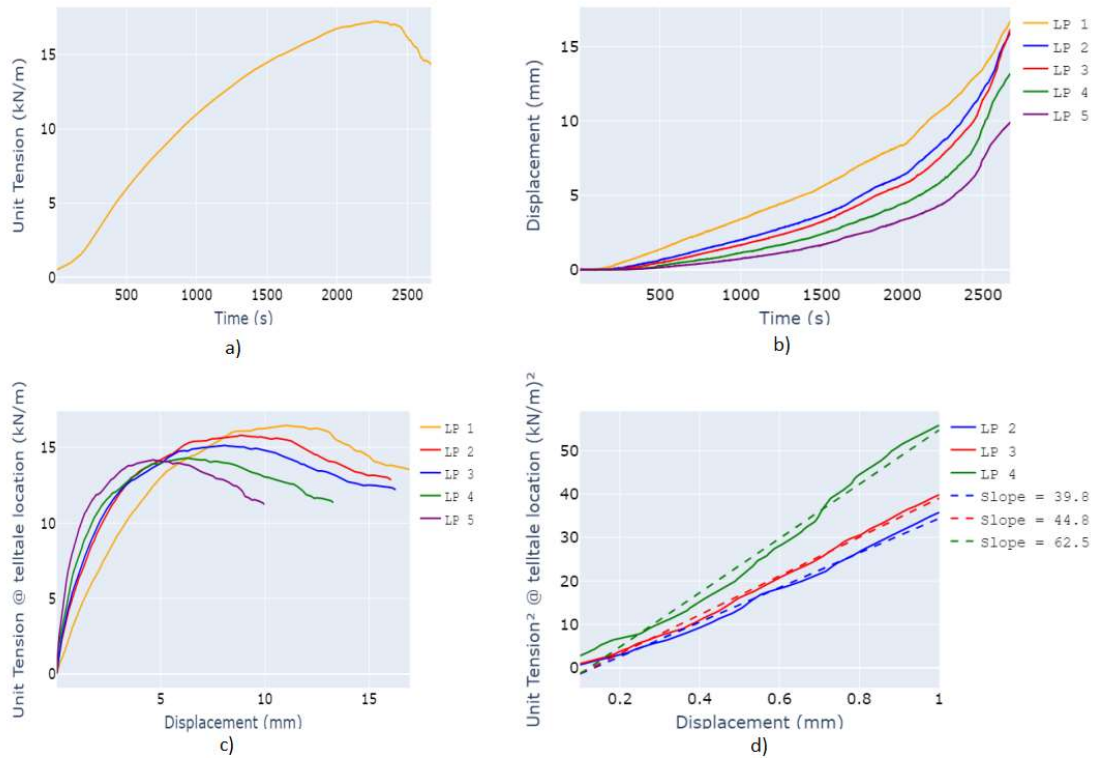


Figure 5.3 - Representative result of GG1 with Angular SAggr3: a) Load vs Time, b) Displacement vs Time, c) Unit tension vs displacement and d) Linear portion of the Unit tension squared vs displacement.

Relatively large displacements are usually required to achieve pullout failure when testing geogrids. An example of such behavior is evident in the unit tension at telltale location-displacement plot shown in Figure 5.4(c).

From linear regression applied to the unit tension squared-displacement data shown in Figure 5.3(d), the K_{SGC} values were obtained, with LPs 2, 3, and 4 resulting in 39.8, 44.8,

and 62.5 (kN/m)²/mm, respectively. The K_{SGC} value from LP 4 was found to be an outlier. Therefore, the resulting K_{SGC} for this test was 45.8 (kN/m)²/mm, and the pullout unit tension was 17.3 kN/m. The resulting K_{SGC} and pullout unit tension from 5 tests done with GG1 and Angular SAggr3 are displayed in Table 5.3. The resulting K_{SGC} and pullout capacity from 5 tests done with GG1 and Angular SAggr3 are displayed in Table 5.3.

Table 5.3 - Final K_{SGC} and pullout capacity resulting from test results for GG1 tested with Angular SAggr3.

Test #	Final K_{SGC} (kN/m) ² /mm	Pmax (kN/m)	Outlier
1	45.8	17.3	False
2	65.4	15.7	False
4	44.5	15.7	False
4	NA	17.2	False
5	72.8	18.7	False
Average	57.1	16.8	-
Coefficient of Variation	21.4%	7.5%	

The results from Test #4 were not considered when calculating the average K_{SGC} and pullout unit tension because all 3 LPs resulted in outlier K_{SGC} values for this test. As a result, the average K_{SGC} for this configuration was 57.1 (kN/m)²/mm, while the average pullout unit tension was found to be 16.8 kN/m. There is a slight decrease in the resulting K_{SGC} when these results are compared to those obtained with Angular SAggr2.

5.1.1.4 Tests involving GG1 and Angular WG

Figure 5.4 shows the results of a representative test done with GT1 and the well-graded aggregate. This configuration was used to evaluate the impact of particle size distribution on K_{SGC} for geogrids.

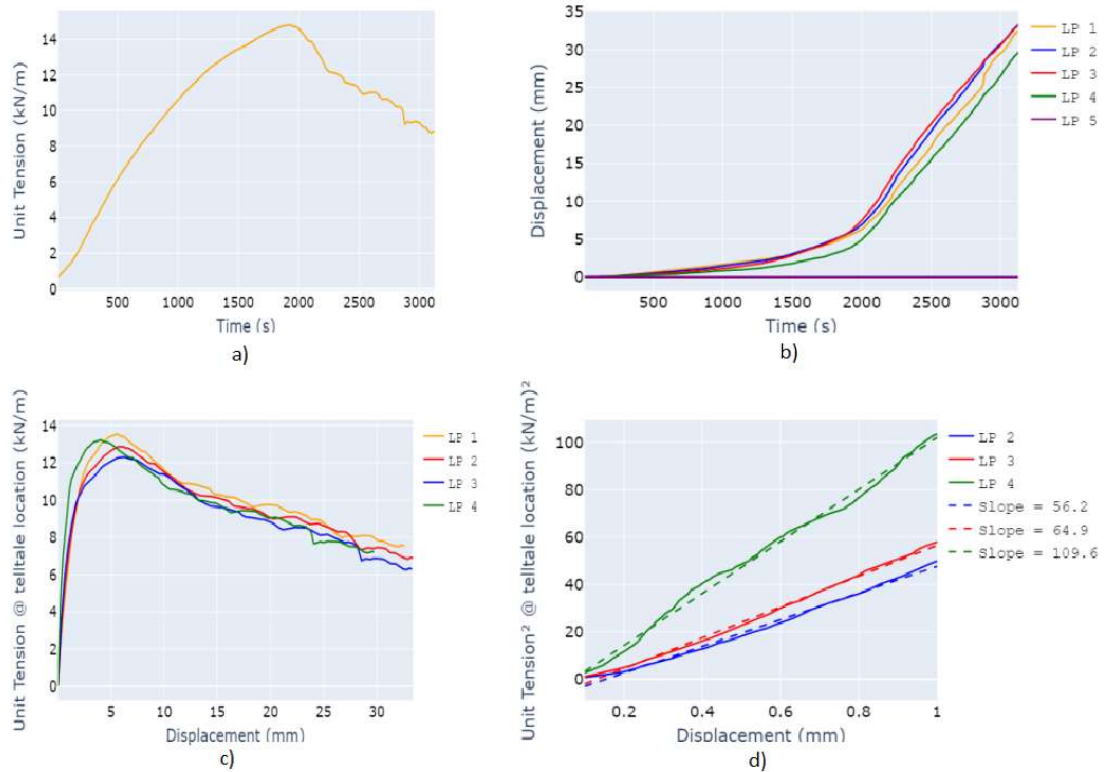


Figure 5.4 - Representative result of GG1 with Angular WG: a) Load vs Time, b) Displacement vs Time, c) Unit tension vs displacement and d) Linear portion of the Unit tension squared vs displacement.

The K_{SGC} values were obtained from the unit tension squared- displacement data shown in Figure 5.4(d). LPs 2, 3, and 4 resulted in K_{SGC} values of 56.2, 64.9, and 109.6 (kN/m)²/mm. LP4 was found to be an outlier, resulting in a final K_{SGC} value of 64.6 (kN/m)²/mm. The pullout capacity obtained for this test was 14.8 kN/m. Table 5.4 shows

the final K_{SGC} values and pullout capacity for the five tests done with GG1 and the well-graded aggregate.

Table 5.4 - Final K_{SGC} and pullout capacity resulting from test results for GG1 tested with well graded aggregate.

Test #	K_{SGC} (kN/m) ² /mm	Pmax (kN/m)	Outlier
1	69.7	14.8	False
2	58.0	15.2	True
3	NA	17.0	True
4	NA	17.4	True
5	64.6	14.8	False
Average	67.2	14.8	-
Coefficient of Variation	3.8%	0.2%	

For Test #3 and Test #4, none of the 3 LPs attended to the linearity criteria, so it was impossible to calculate the final K_{SGC} value for those tests. Test #2 was also considered an outlier due to its pullout capacity value. Therefore, the resulting average K_{SGC} was 67.2 (kN/m)²/mm, with an average pullout capacity of 14.8 kN/m.

These results, when compared to those obtained with the Angular SAggr2, suggest that the impact of particle size distribution on K_{SGC} for geogrids is small, with a slight increase in K_{SGC} and a slight reduction in the pullout capacity.

5.1.1.5 Tests involving GG1 and 50-50 SAggr2

The results shown in Figure 5.5. are from representative test done with GG1 and 50-50 SAggr2, which is a combination of Round SAggr2 and Angular SAggr2. This configuration was used to evaluate the impact of the angularity of the aggregate on K_{SGC} for geogrids.

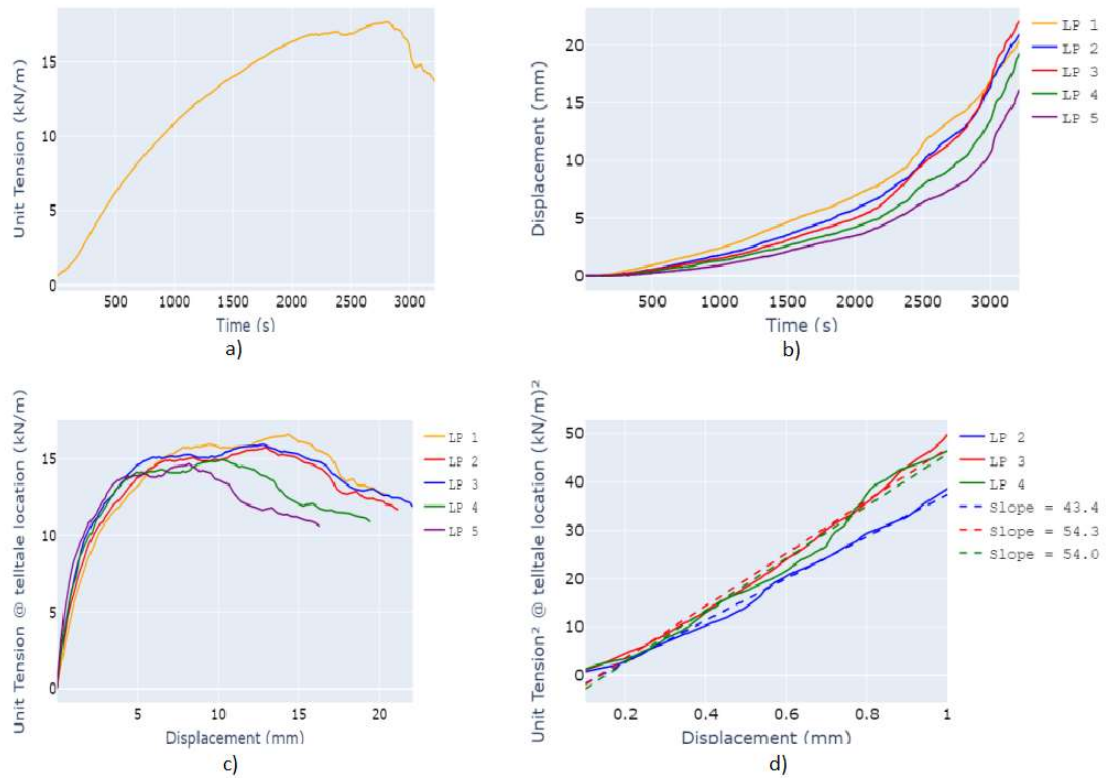


Figure 5.5 - Representative result of GG1 with 50-50 SAggr2: a) Load vs Time, b) Displacement vs Time, c) Unit tension vs displacement and d) Linear portion of the Unit tension squared vs displacement.

As is usual when testing geogrids, relatively large displacements were necessary to reach the pullout capacity in this test. The K_{SGC} values obtained from the unit tension squared versus displacement were 43.2, 54.6, and 54.1 for LPs 2, 3, and 4, respectively. The value from LP 4 was found to be an outlier based on the linearity criteria, leading to a

final K_{SGC} value of 54.9 (kN/m)²/mm and a pullout capacity of 17.7 kN/m. Table 5.5 shows the final K_{SGC} values and the pullout capacity for the five tests done with GG1 and 50-50 SAggr2.

Table 5.5 - Final K_{SGC} and pullout capacity resulting from test results for GG1 tested with the 50-50 SAggr2.

Test #	Final K_{SGC} (kN/m) ² /mm	Pmax (kN/m)	Outlier
1	40.4	17.9	False
2	54.9	17.7	False
3	62.0	18.5	False
4	46.1	16.0	False
5	36.9	15.8	False
Average	48.1	17.2	-
Coefficient of Variation	19.2%	6.3%	

None of the tests were found to be outliers. Thus, resulting in an average K_{SGC} of 48.1 (kN/m)²/mm and an average pullout capacity was 17.2 kN/m.

5.1.2 Tests conducted with Geosynthetic GG2

Two aggregates were used to test geosynthetic GG2: Round SAggr2 and Angular SAggr2. The test results for GG2 obtained with these aggregates are presented next.

5.1.2.1 Tests involving GG2 and Round SAggr2

The test results for GG2 tested with Round SAggr2 is shown in Figure 5.6. This configuration was used as a reference when evaluating the impact of the angularity of the aggregate on K_{SGC} for geogrids.

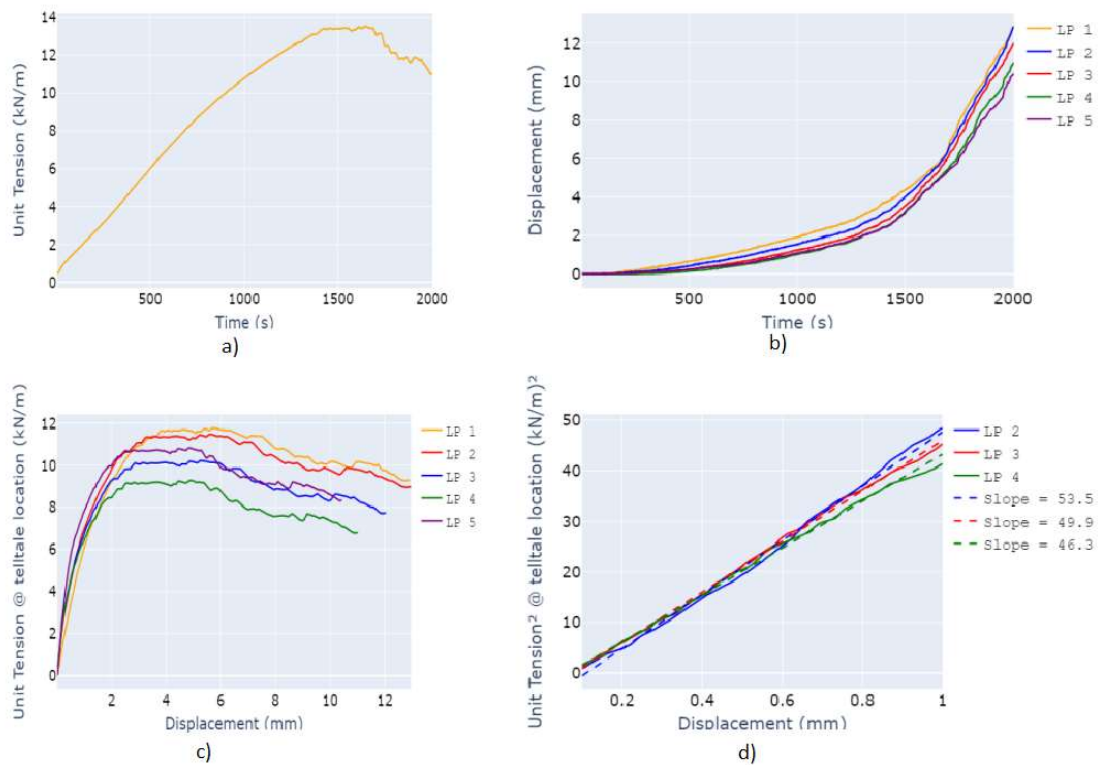


Figure 5.6 - Representative result of GG2 with Round SAggr2: a) Load vs Time, b) Displacement vs Time, c) Unit tension vs displacement and d) Linear portion of the Unit tension squared vs displacement.

The unit tension squared versus displacement (d) highlights great consistency between the three points tracked, resulting in very similar slopes. From the linear regression, the K_{SGC} obtained for LPs 2, 3, and 4 were respectively 53.5, 49.9, and 46.3 (kN/m)²/mm, resulting in a final K_{SGC} value of 49.9 (kN/m)²/mm. The pullout capacity obtained was 13.5 kN/m. The final K_{SGC} value and the pullout capacity for the five tests done with GG2 and Round SAggr2 are displayed in Table 5.6.

Table 5.6 - Final K_{SGC} and maximum pullout capacity for GG2 tested 5 times with Round SAggr2.

Test #	Final K_{SGC} (kN/m) ² /mm	Pmax (kN/m)	Outlier
1	52.2	12.9	False
2	53.7	13.5	False
3	63.1	13.3	True
4	52.2	9.7	True
5	70.7	11.0	True
Average	52.9	13.2	-
Coefficient of Variation	1.4%	2.3%	

Tests #3 and #5 were considered outliers based on their K_{SGC} values, whereas test #4 was because of its pullout capacity value. The average K_{SGC} was 52.9 (kN/m)²/mm, and the average pullout capacity was 13.2 kN/m. Both are higher than those obtained for GG1.

5.1.2.2 Tests involving GG2 and Angular SAggr2

Figure 5.7 shows the results from a test done with GG2 and Angular SAggr2. This configuration was used to evaluate the impact of the angularity of the aggregate on K_{SGC} of geogrids.

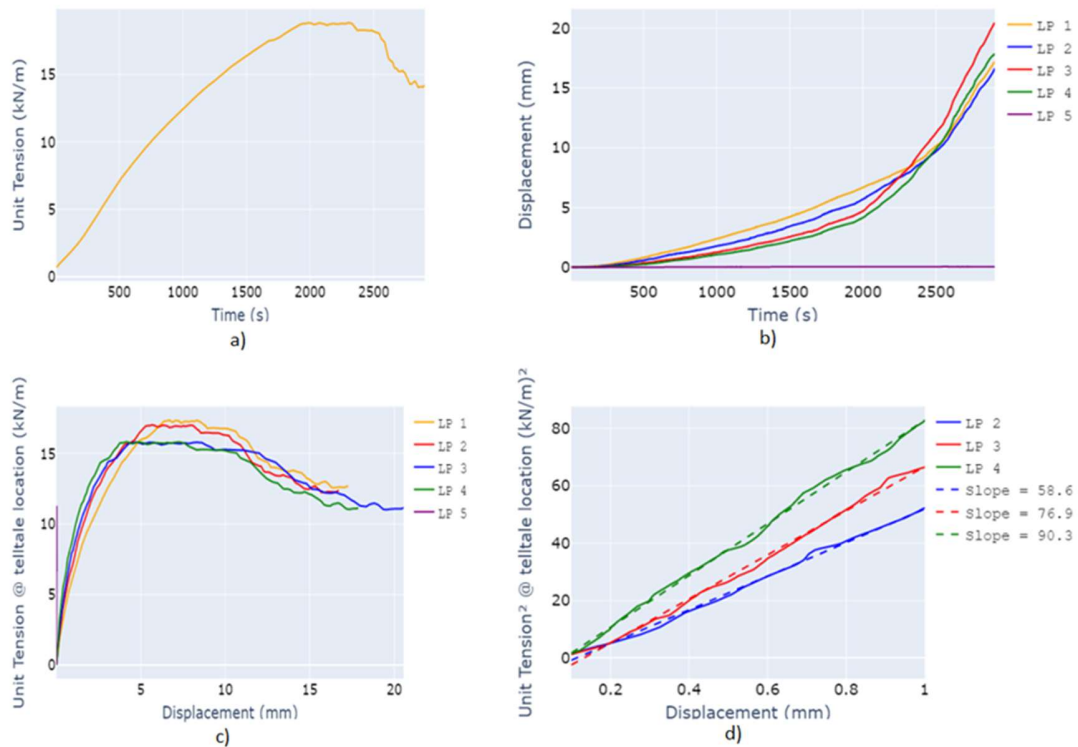


Figure 5.7 - Representative result of GG2 with Angular SAggr2: a) Load vs Time, b) Displacement vs Time, c) Unit tension vs displacement and d) Linear portion of the Unit tension squared vs displacement.

LPs 2, 3, and 4 resulted in K_{SGC} values of 58.6, 76.9, and 90.3 (kN/m)/mm, respectively, resulting in a final K_{SGC} value of 75.7 (kN/m)²/mm. The pullout capacity obtained was 18.8 kN/m. The final K_{SGC} value and the pullout tension for the five tests done with GG2 and Angular SAggr2 are shown in Table 5.7.

Table 5.7 - Final K_{SGC} and pullout capacity from 5 tests run with GG2 and Angular SAggr2.

Test #	Final K_{SGC} (kN/m) ² /mm	Pmax (kN/m)	Outlier
1	73.56	26.6	True
2	90.7	17.1	True
3	75.7	18.8	False
4	NA	18.6	True
5	NA	16.4	True
Average	75.7	18.8	-
Coefficient of Variation	-	-	

None of the LPs from Test #4 and Test #5 attended the linearity criteria. Test #1 had an outlier pullout capacity, while test #2 had an outlier K_{SGC} value. Thus, leaving only Test #3. Thus, resulting in a K_{SGC} of 75.7 (kN/m)²/mm and a pullout capacity of 18.8 kN/m for this configuration.

5.2 GEOTEXTILES

In this section, test results from the configurations involving the use of geotextiles are presented. First the results obtained for GT1 are covered, followed by the results obtained for GT2.

5.2.1 Tests conducted with Geosynthetic GT1

Geosynthetic GT1 was tested with 6 aggregates: Round SAggr2, Angular SAggr2, Angular SAggr3, Angular WG, 50-50 SAggr2, and Monterey Sand. The test results obtained for each aggregate are presented in the following subsections.

5.2.1.1 Tests involving GT1 and Round SAggr2

The results of a representative test for GT1 with Round SAggr2 are shown in Figure 5.8. This configuration was used as a reference in the evaluation of the impact of the angularity of the aggregate on K_{SGC} for geotextiles.

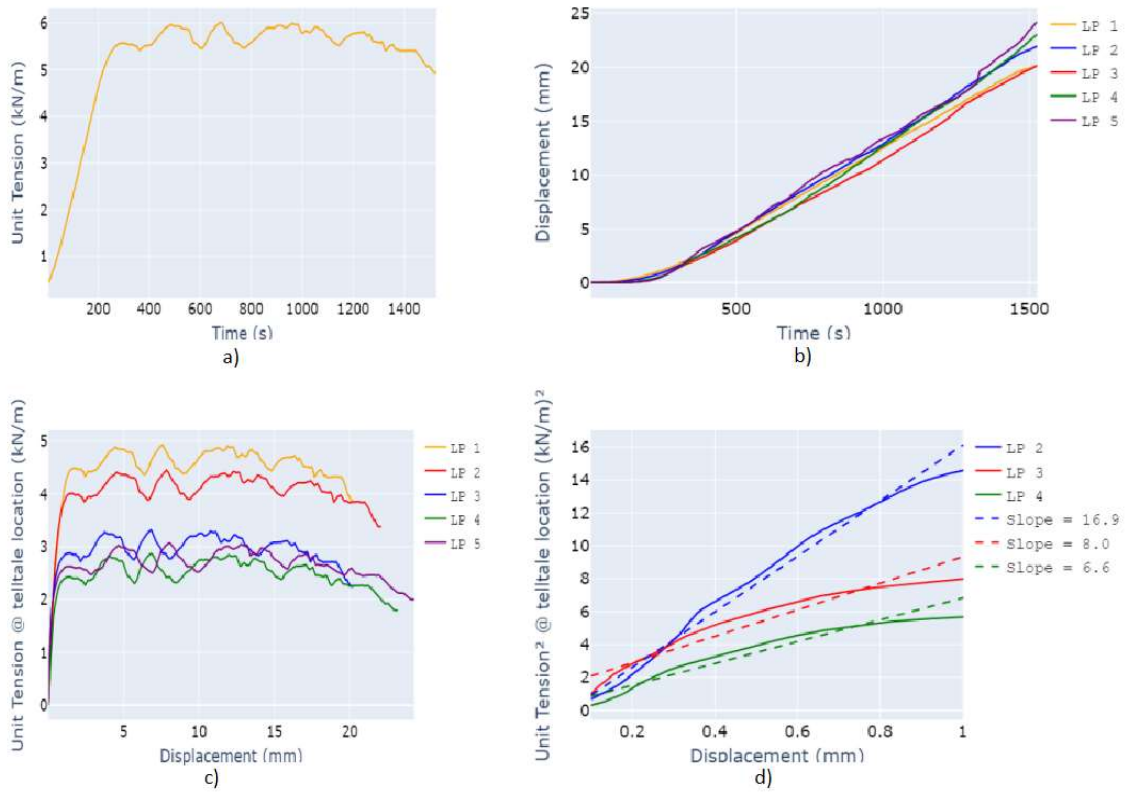


Figure 5.8 - Representative result of GT01 with Round SAggr2: a) Load vs Time, b) Displacement vs Time, c) Unit tension vs displacement and d) Linear portion of the Unit tension squared vs displacement.

As evident in the frontal unit tension time history displayed in Figure 5.8(a), the tension increases rapidly in the first stage of the test, and then it varies within a range where the maximum load is reached. Usually, lower displacements are required to reach pullout failure when testing geotextiles than when testing geogrids.

Based on the regression model of the unit tension squared versus displacement data, the K_{SGC} for LP1, LP2, and LP3 were respectively 17.0, 8.0, and 7.0 (kN/m)²/mm. LP3 is an outlier. Therefore, the final K_{SGC} for this test is 7.4 (kN/m)²/mm. The pullout capacity

obtained from the frontal unit tension versus time graph (Figure 5.8 a) was 6.0 kN/m. Table 5.8 shows the final K_{SGC} and pullout capacity for the five tests with this configuration.

Table 5.8 - Average K_{SGC} and maximum pullout capacity for GT1 tested with Round SAggr2 5 times.

Test #	Final K_{SGC} (kN/m) ² /mm	Pmax (kN/m)	Outlier
1	7.4	6.0	False
2	6.0	6.1	False
3	6.8	5.7	True
4	8.3	6.2	False
5	8.8	6.5	True
Average	7.3	6.1	-
Coefficient of Variation	13.1%	1.0%	

The K_{SGC} values from Test #3 Test #5 are outliers based on the criteria for pullout capacity, as discussed in Chapter 3. Consequently, they are not considered when calculating the average K_{SGC} and pullout unit tension for this configuration. Thus, resulting in an average K_{SGC} value of 7.3 (kN/m)²/mm and an average unit tension equal to 6.1 kN/m.

5.2.1.2 Tests involving GT1 and Angular SAggr2

The results of a test done with GT1 and the angular aggregate (Angular SAggr2) are shown in Figure 5.9. This configuration was used to evaluate the impact of the angularity of the aggregate on K_{SGC} of geotextiles.

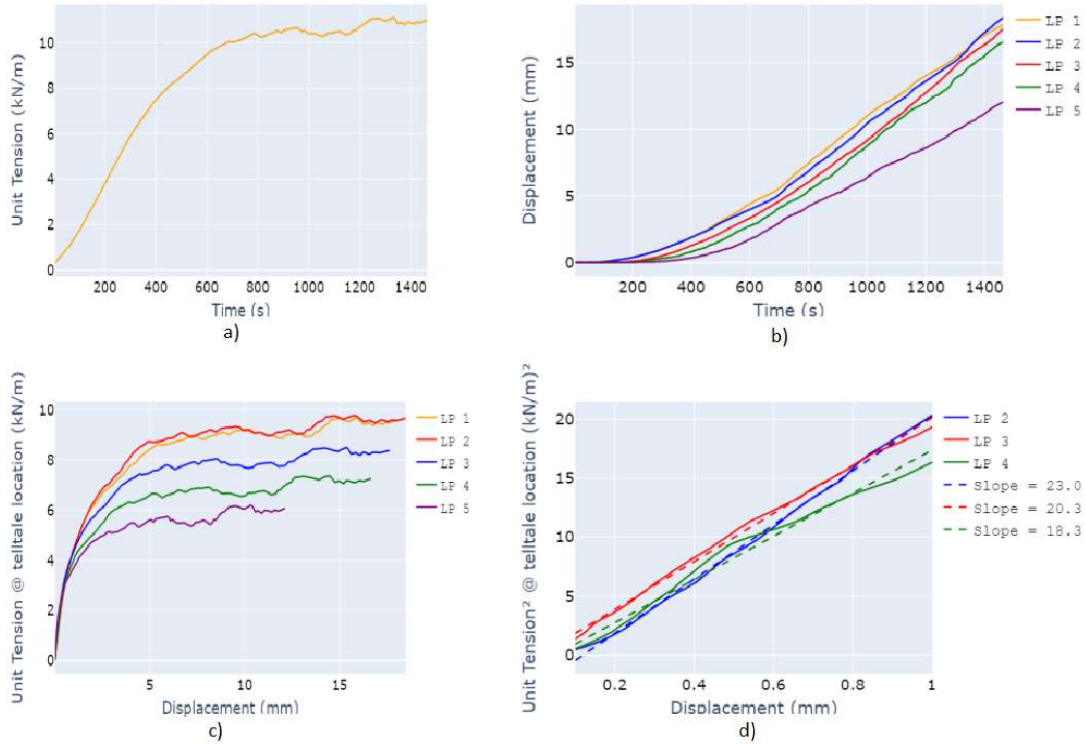


Figure 5.9 - Representative result of GT1 with Angular SAggr2: a) Load vs Time, b) Displacement vs Time, c) Unit tension vs displacement and d) Linear portion of the Unit tension squared vs displacement.

The frontal unit tension time history, displayed in Figure 5.9(a), shows a slightly different behavior than what was observed when this geotextile was tested with the round aggregate, since the load increases over a more extended period. On the other hand, similarly to the results obtained with the round aggregate, the unit tension reaches a plateau and remains within a range for a prolonged period.

The following K_{SGC} values were obtained for LPs 2, 3, and 4, respectively: 23.0, 20.3, and 18.3 (kN/m)²/mm, which resulted in a final K_{SGC} of 20.6 (kN/m)²/mm for this test. The pullout capacity for this test was 11.1 kN/m. The final K_{SGC} value and the pullout capacity for the 5 tests done with GT1 and Angular SAggr2 are displayed in Table 5.9.

Table 5.9 - Average K_{SGC} and pullout capacity for 5 tests done with GT1 and Angular SAggr2.

Test #	Final K_{SGC} (kN/m) ² /mm	Pmax (kN/m)	Outlier
1	18.5	9.9	False
2	22.7	11.1	False
3	20.6	11.1	False
4	21.7	9.9	False
5	23.5	9.5	False
Average	23.0	10.3	-
Coefficient of Variation	13.4%	6.5%	

The average K_{SGC} is 23.0 (kN/m)²/mm, and the average pullout capacity is 10.3 kN/m for this configuration. These results show a considerable improvement in the K_{SGC} and pullout capacity of GT1 compared to those obtained using Round SAggr2.

5.2.1.3 Tests involving GT1 and Angular SAggr3

Figure 5.10 shows the results of a representative test done with GT1 and Angular SAggr3, a uniform aggregate with a smaller particle size than Angular SAggr2. This configuration was used to evaluate the impact of particle size on K_{SGC} of geotextiles.

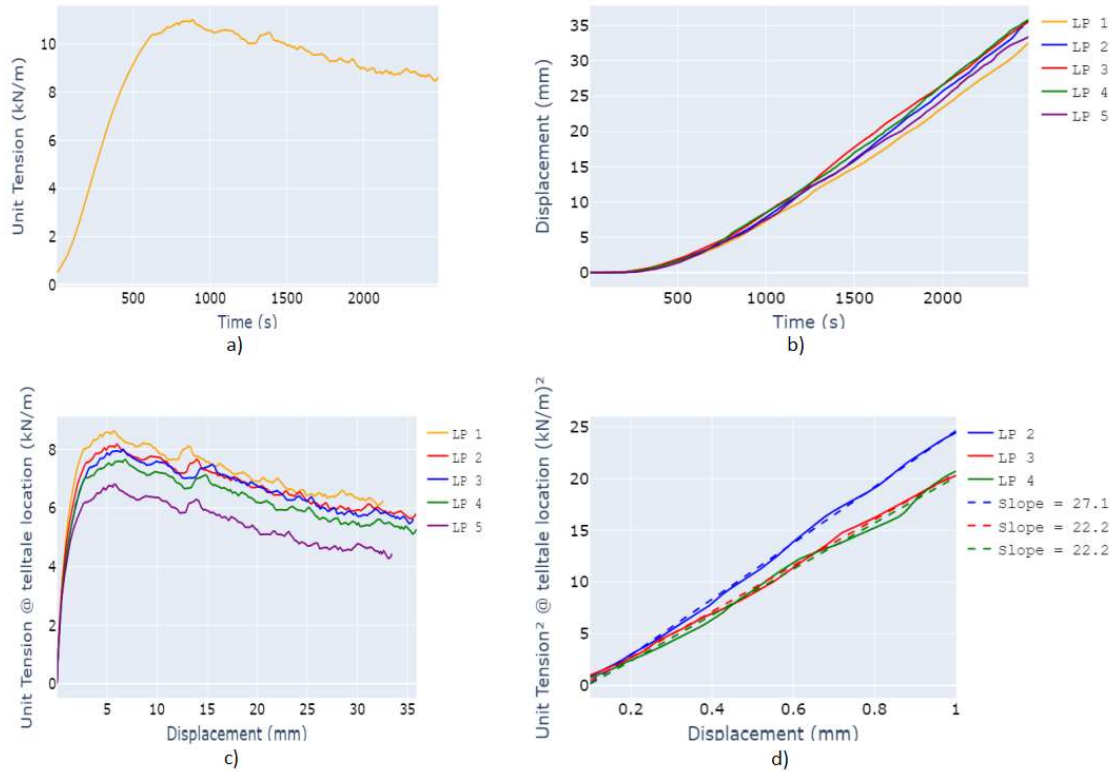


Figure 5.10 - Representative result of GT1 with Angular SAggr3: a) Load vs Time, b) Displacement vs Time, c) Unit tension vs displacement and d) Linear portion of the Unit tension squared vs displacement.

The frontal unit tension-time data, displayed in Figure 5.10(a) shows a typical behavior for geotextiles, with the load increasing sharply in the first stages of the test. In this case, however, there is a clear peak in frontal unit tension.

The K_{SGC} values obtained from linear regression applied to unit tension squared-displacement data, shown in Figure 5.10(d), were 27.1, 22.2, and 22.2 (kN/m)²/mm, for

LPs 2, 3 and 4, respectively, resulting in a final K_{SGC} value of 22.9 (kN/m)²/mm. The pullout capacity for this test was 11.0 kN/m. Table 5.10 shows the final K_{SGC} values and pullout capacity for the five tests done with GT1 and Angular SAggr3.

Table 5.10 - Average K_{SGC} and average pullout capacity from 5 tests done with GT1 and Angular SAggr3.

Test #	Final K_{SGC} (kN/m) ² /mm	Pmax (kN/m)	Outlier
1	22.0	7.7	True
2	22.9	11.0	False
3	32.9	11.9	False
4	13.7	11.0	False
5	63.9	11.9	True
Average	23.0	11.3	-
Coefficient of Variation	35.2%	3.7%	

For the calculation of average K_{SGC} and pullout capacity, Test #5 was not considered due to its K_{SGC} value being an outlier. Neither was test #1, but in this case, due to its pullout capacity. The resulting average K_{SGC} was 23.4 (kN/m)²/mm, while the average pullout capacity was 11.3 kN/m. The difference from the results obtained for GT1 with the Angular SAggr2 is small.

5.2.1.4 Tests involving GT1 and Angular WG

The results from a representative test done with GT1 and the well-graded aggregate are shown in Figure 5.11. This configuration was used to evaluate the impact of particle size distribution on the K_{SGC} value.

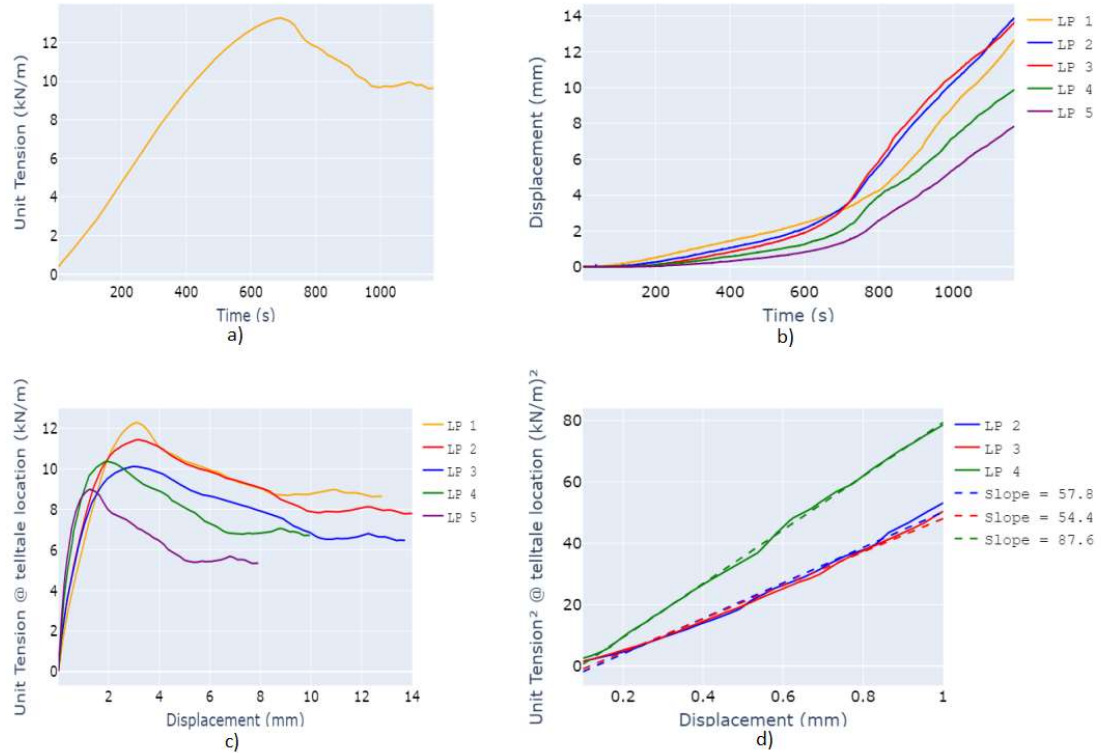


Figure 5.11 - Representative result of GT1 with Angular WG: a) Load vs Time, b) Displacement vs Time, c) Unit tension vs displacement and d) Linear portion of the Unit tension squared vs displacement.

Similar to the previous configuration, the frontal unit tension time history, displayed in Figure 5.11(a), shows a peak strength. It is worth noting that the peak in frontal unit tension coincides with the acute change in the slope of the displacement time history shown in Figure 5.11 (b). These results also show that relatively low displacements are required to reach pullout failure.

The K_{SGC} values, obtained from the unit tension squared versus displacement data, were 57.8, 54.4, and 87.6 (kN/m)²/mm. The latter value was found to be an outlier, resulting in a final K_{SGC} of 54.4 (kN/m)²/mm. The pullout capacity obtained was 13.3 kN/m. Table 5.11 shows the results for this and the other four tests done with this configuration.

Table 11 - Average K_{SGC} and average pullout capacity from 5 tests done with GT1 and Angular SAggr3.

Test #	Final K_{SGC} (kN/m) ² /mm	Pmax (kN/m)	Outlier
1	20.3	9.6	True
2	94.7	14.1	True
3	50.5	12.0	False
4	54.4	13.3	False
5	48.5	12.5	False
Average	49.5	12.7	-
Coefficient of Variation	7.3%	3.6%	

Tests #1 and #2 were not considered in the final calculation because their resulting K_{SGC} values were deemed outliers. Consequently, the average K_{SGC} for this configuration was 49.5 (kN/m)²/mm, whereas the average pullout capacity was 12.7 kN/m. Compared to the results obtained using the Angular SAggr2, it is evident that the use of the well-graded aggregate resulted in a significant improvement, especially regarding the K_{SGC} values.

5.2.1.5 Tests involving GT1 and 50-50 Saggr2

Figure 5.12 shows results from a representative test done with GT1 and 50-50 SAggr2, an aggregate composed of 50% of Angular SAggr2 and 50% of Round SAggr2. This configuration was used to evaluate the impact of aggregate angularity on K_{SGC} for geotextiles.

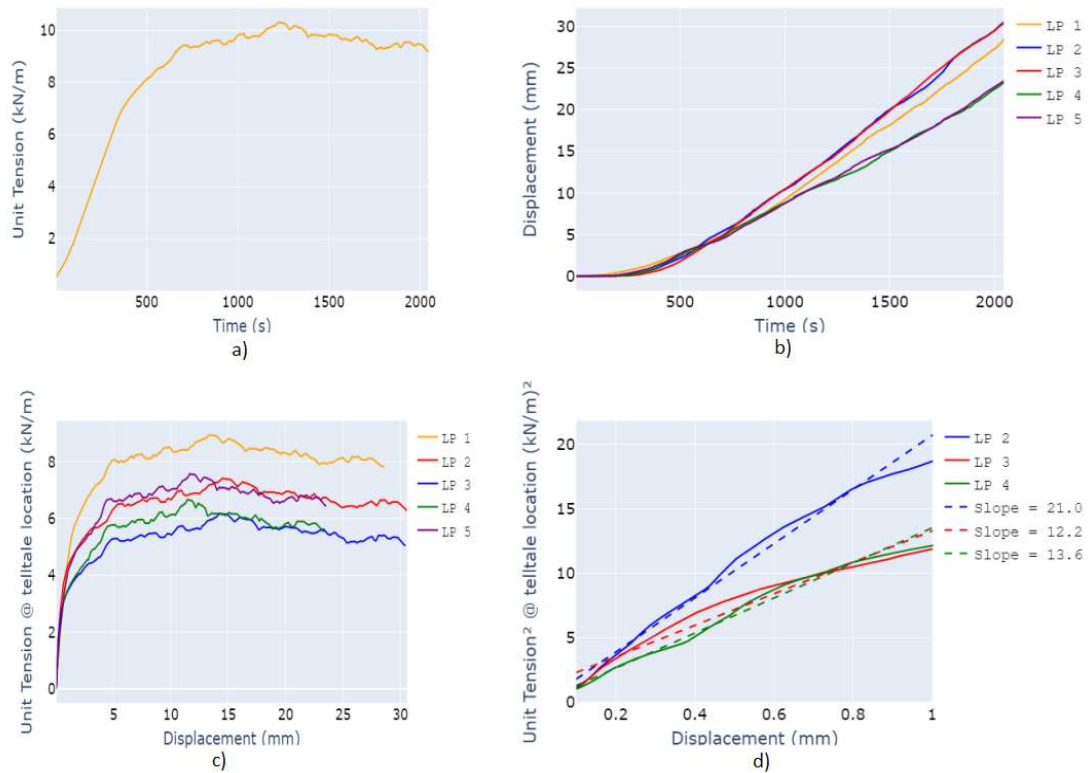


Figure 5.12 - Representative result of GT1 with 50-50: a) Load vs Time, b) Displacement vs Time, c) Unit tension vs displacement and d) Linear portion of the Unit tension squared vs displacement.

Similar to the previous configurations, low displacements were required to achieve pullout failure in this test. Here, however, the frontal unit tension-time data, displayed in Figure 5.12(a) does not show a clear peak.

The K_{SGC} values were obtained, through line regression, from the unit tension square-displacement shown in Figure 5.12(d). The K_{SGC} values for LPs 2, 3, and 4 were 28.1, 11.2, and 12.8 (kN/m)²/mm. The value for LP 2 was found to be an outlier, resulting in a final K_{SGC} of 11.2 (kN/m)²/mm. The pullout capacity obtained for this test was 9.7 kN/m. Table 5.12 shows the results from five tests done with this configuration.

Table 5.12 - Average K_{SGC} and average pullout capacity from 5 tests done with GT1 and 50-50 SAggr2.

Test #	Final K_{SGC} (kN/m) ² /mm	Pmax (kN/m)	Outlier
1	13.0	10.3	True
2	8.1	9.6	False
3	11.2	9.7	False
4	17.0	8.7	True
5	8.3	9.6	False
Average	9.2	9.6	-
Coefficient of Variation	15.2%	0.6%	

The pullout capacity values from Test # 1 and Test #4 were found to be outliers. Therefore, the average K_{SGC} obtained with the remaining three tests was 9.2 (kN/m)²/mm, and the pullout capacity was 9.6 kN/m.

These results are closer to those obtained with Round SAggr2 than those obtained with Angular SAggr2. Nonetheless, there was a good improvement in K_{SGC} compared to the Round SAggr2 results.

5.2.1.5 Tests involving GT1 and Monterey Sand

Figure 5.13 shows the results from a representative test done with GT1 and Monterey Sand. This configuration was used to evaluate the impact of particle size and particle size distribution on K_{SGC} of geotextiles.

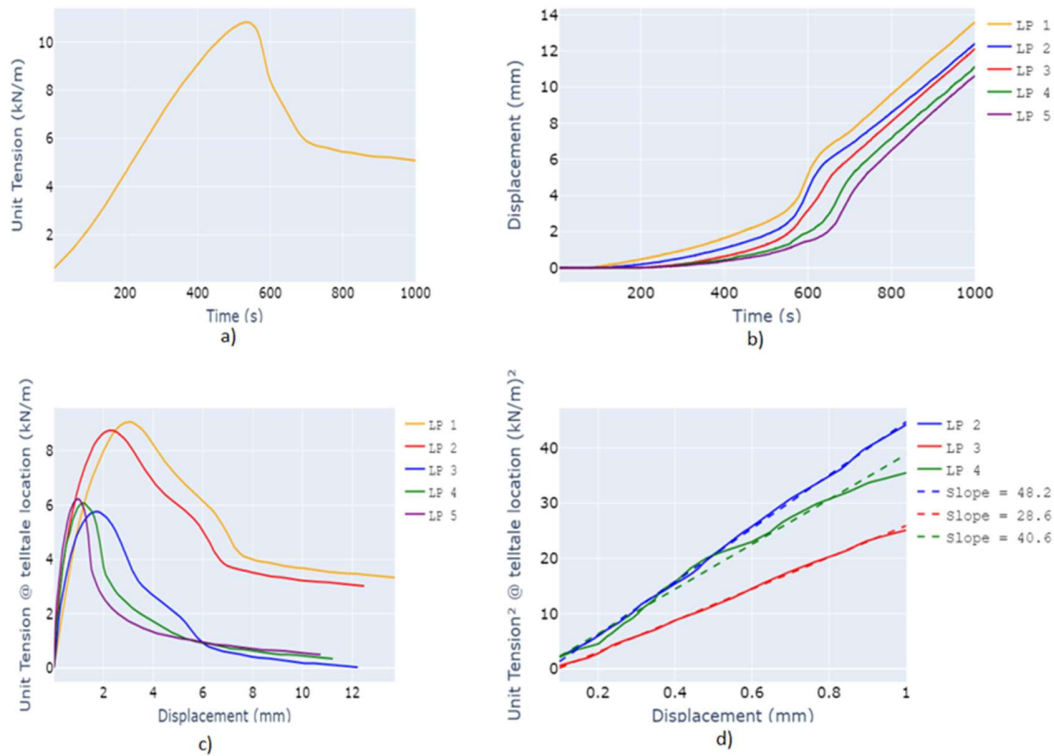


Figure 5.13 - Representative result of GS01 with Monterey Sand: a) Load vs Time, b) Displacement vs Time, c) Unit tension vs displacement and d) Linear portion of the Unit tension squared vs displacement.

One of the outstanding characteristics of the tests with Monterey Sand is the shape of the unit tension-time curve shown in Figure 5.13(a). It is also interesting to notice that the changes in the slope of the displacement-time curve, shown on Figure 5.13(b), match the points where the frontal unit tension reaches its peak and residual strengths.

The K_{SGC} values for the three LPs were obtained from the unit tension squared-displacement data plotted in Figure 5.13(d). The resulting K_{SGC} values for LP 1, 2, and 3 were 48.2, 28.6, and 40.6 (kN/m)²/mm. The value from LP2 was found to be an outlier, resulting in a K_{SGC} value of 44.6 (kN/m)²/mm for this test. The pullout capacity obtained was 10.8 kN/m. Table 5.13 shows the results from five tests done GT1 with Monterey Sand.

Table 5.13 - Average K_{SGC} and average pullout capacity from 5 tests done with GT1 and Monterey Sand.

Test #	K_{SGC} (kN/m) ² /mm	Pmax (kN/m)	Outlier
1	44.6	10.8	False
2	43.8	10.0	True
3	46.4	10.9	False
4			
5			
Average	45.5	10.9	-
Coefficient of Variation	2.0%	0.3%	

Test #2 was found to be an outlier based on the pullout capacity criteria. As a result, the average K_{SGC} for this configuration was 45.5 (kN/m)²/mm, while the average pullout capacity was 10.9 kN/m.

5.2.2 Tests conducted with Geosynthetic GT2

Geosynthetic GT2 was tested with two aggregates: Round SAggr2 and Angular SAggr2. The results from the tests done with each aggregate are presented in the next two subsections.

5.2.2.1 Tests involving GT2 and Round SAggr2

Figure 5.14 shows the test results for GT2 with Round SAggr2. This configuration was used as a reference in the evaluation of the impact of the angularity of the aggregate on K_{SGC} of geotextiles.

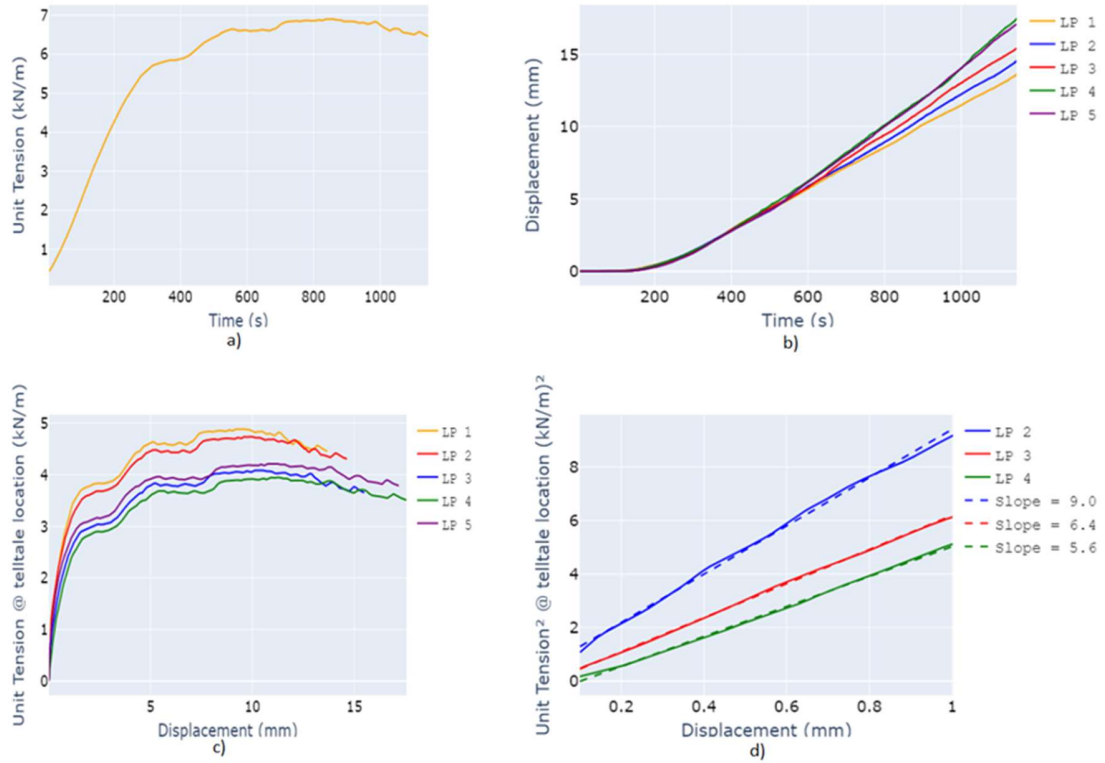


Figure 5.14 - Representative result of GT2 with Round SAggr2: a) Load vs Time, b) Displacement vs Time, c) Unit tension vs displacement and d) Linear portion of the Unit tension squared vs displacement.

The regression model applied to the unit tension squared-displacement data, shown in Figure 5.14(d), resulted in K_{SGC} values of 9.0, 6.4, and 5.6 (kN/m)²/mm for LPs 2, 3, and 4, respectively. The K_{SGC} value for LP1 was found to be an outlier. Therefore, the final K_{SGC} for this test was 6.6 (kN/m)²/mm. A pullout capacity of 6.9 kN/m was obtained. Table 5.14 shows each test's average K_{SGC} and pullout capacity.

Table 5.14 - Average K_{SGC} and maximum pullout capacity for GT2 tested with Round SAggr2 5 times.

Test #	Final K_{SGC} (kN/m) ² /mm	Pmax (kN/m)	Outlier
1	6.2	6.3	False
2	5.9	4.1	True
3	6.6	6.9	False
4	3.2	6.3	True
5	6.5	6.8	False
Average	6.4	6.7	-
Coefficient of Variation	2.6%	4.4%	

The K_{SGC} value from Test #4 was found to be an outlier, as was the pullout capacity from Test #2. Therefore, results from tests 2 and 4 are not considered when calculating the average K_{SGC} (6.4 (kN/m)²/mm) and the average pullout capacity (6.7 kN/m). These results are far from those obtained for GT1 tested with Round SAggr2.

5.2.2.2 Tests involving GT2 and Angular SAggr2

Figure 5.15 shows the results of a test for GT2 with Angular SAggr2. This configuration was used to evaluate the impact of the angularity of the aggregate on K_{SGC} of geotextiles.

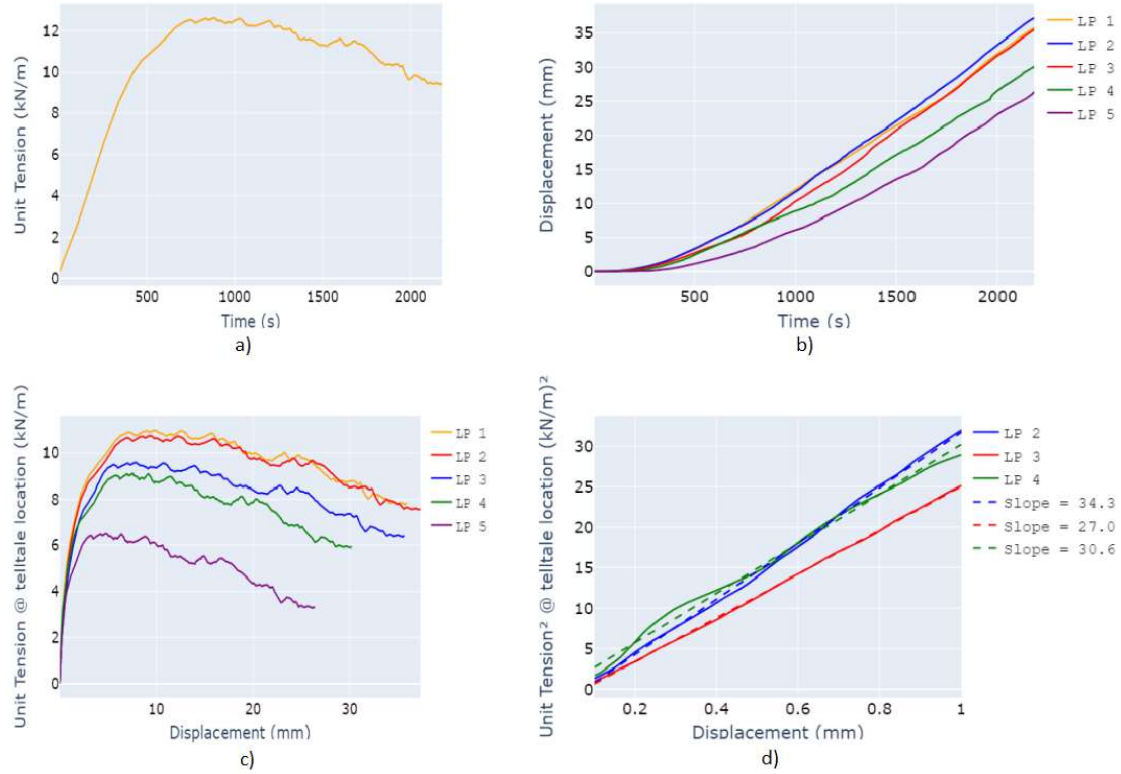


Figure 5.15 - Representative result of GT2 with Angular SAggr2: a) Load vs Time, b) Displacement vs Time, c) Unit tension vs displacement and d) Linear portion of the Unit tension squared vs displacement.

The frontal unit tension time history, displayed in Figure 5.15(a), shows a slight difference compared to the results obtained with Round SAggr2: in this case, there is a clear peak in the unit tension.

The linear portion of the unit tension squared-displacement data, displayed in Figure 5.15(d), shows good consistency among the three LPs. The resulting K_{SGC} values

were 34.3, 27.0, and 30.6 (kN/m)²/mm for LPs 2, 3, and 4, respectively, resulting in a final K_{SGC} value of 26.2 (kN/m)²/mm. The pullout capacity was 12.6 kN/m. Table 5.15 shows the final K_{SGC} and pullout capacity for the five tests done with this configuration.

Table 5.15 - Average K_{SGC} and maximum pullout capacity from 5 tests with GT2 with Angular SAggr2 5 times.

Test #	Final K_{SGC} (kN/m) ² /mm	Pmax (kN/m)	Outlier
1	14.5	12.3	False
2	30.9	13.0	False
3	31.8	13.4	False
4	26.2	12.6	False
5	22.9	12.9	False
Average	25.3	12.6	-
Coefficient of Variation	24.8%	2.2%	

The average K_{SGC} for this configuration was 25.3 (kN/m)²/mm, while the average pullout capacity was 12.7 (kN/m). These results show a significant improvement compared to the results obtained with Round SAggr2.

Chapter 6: Evaluation of the impact of backfill and geosynthetic properties on K_{SGC}

This chapter presents an evaluation of the test results generated in this investigation, building on the results described in Chapter 5. The first section of this chapter focuses on the results of tests involving geogrids. The section includes three subsections, discussing the impact of the angularity of the aggregate, the impact of particle size and particle size distribution, and the impact of mechanical properties of geotextiles on the K_{SGC} . The second section focuses on the evaluation of the same parameters but considering the results of tests involving geotextiles. Finally, the third section focus on the impact of particle size distribution and aggregate angularity on the unit tension versus time curve.

6.1 GEOGRIDS: EFFECT OF RELEVANT VARIABLES ON K_{SGC}

6.1.1 Effect of aggregate angularity

Two geogrids, GG1 and GG2, were used to evaluate the impact of the aggregate angularity on K_{SGC} . For this evaluation, two aggregates were used for both geogrids: a round aggregate (Round SAggr2), adopted as the reference aggregate, and an angular aggregate (Angular SAggr2). In addition, an “intermediary” aggregate (50-50 SAggr2) was also used when testing GG1. In all tests evaluated in this case, the same particle size, particle size distribution, and compaction effort were adopted, making angularity the only changing factor in the three configurations.

Table 6.1 shows the compilation of results from the tests used in this evaluation.

Table 6.1 - Results of tests involving geogrids to evaluate the impact of angularity on K_{SGC} .

Geogrid	Aggregate	K_{SGC} ((kN/m) ² /mm)	Change in relation to Baseline (%)	Pmax (kN/m)	Change in relation to Baseline (%)
GG1	Round SAggr2	41.7	Baseline	12.5	Baseline
	50-50 SAggr2	48.1	15	17.2	38
	Angular SAggr2	54.1	30	16.7	34
GG2	Round SAggr2	52.9	Baseline	13.2	Baseline
	Angular SAggr2	75.6	43	18.8	38

As indicated by the results indicated in Table 6.1 regarding the impact of aggregate angularity on K_{SGC} for tests involving GG1, using 50-50 SAggr2 resulted in about half (15%) of the improvement obtained when using Angular SAggr2 (30%). In terms of pullout capacity (Pmax), on the other hand, the improvement is essentially the same (34 versus 38%), with the improvement obtained with 50-50 SAggr2 being slightly better.

For tests involving GG2, the results in Table 6.1 indicate that using SAggr2 resulted in an improvement of 43% in K_{SGC} value and 38% in pullout capacity.

These results suggest that aggregate angularity has a considerable impact on the magnitude of K_{SGC} when using geogrids. The improvement in K_{SGC} observed in the results of tests involving GG2 was more significant than the improvement observed when testing GG1. Consequently, the actual magnitude of the increase in K_{SGC} due to angularity of the aggregate is affected by the characteristics of the geogrid.

6.1.2 Effect of particle size and particle size distribution

Table 6.2 shows the compilation of results from the tests done to evaluate the impact of particle size and particle size distribution on the K_{SGC} of tests involving geogrids. Comparison of the results of tests conducted using Angular SAggr2 and Saggr3 allow

assessing the effect of particle size, while comparison of the results of tests conducted using Angular SAggr2 and WG allow assessing the impact of particle size distribution on the K_{SGC} for geogrids. Angular SAggr2 was adopted as the reference aggregate for both cases.

Table 6.2 - Results from test involving geogrids for evaluation of the impact of particle size and particle size distribution on K_{SGC} .

Geogrid	Aggregate	K_{SGC} ((kN/m) ² /mm)	Change in relation to baseline (%)	Pmax (kN/m)	Change in relation to baseline (%)
GG1	Angular SAggr2	54.1	Baseline	16.7	Baseline
	Angular SAggr3	57.1	6%	16.8	1%
	Angular WG	67.2	24%	14.8	-11%

Use of an aggregate having a smaller average particle size than the reference aggregate resulted in a comparatively small increase in both K_{SGC} (6%) and pullout capacity (1%). Such results suggest that particle size does not significantly impact the K_{SGC} of tests involving geogrids.

Using the well-graded aggregate resulted in an improvement of 24% in K_{SGC} . On the other hand, a decrease of 11% in pullout capacity was obtained. These results suggest that the impact of the particle size distribution on the K_{SGC} of tests involving geogrids is slightly higher than the impact of particle size but still quite small. The results also suggest that obtaining a higher K_{SGC} does not necessarily imply that a higher pullout capacity will be achieved.

6.1.3 Effect of geogrid characteristics

The results from tests involving GG1 and GG2, but using the same aggregate, are used to evaluate the impact of geogrid properties on K_{SGC} . Table 6.3 shows the results for GG1 and GG2 from tests done with Round SAggr2 and from tests done with Angular SAggr2.

Table 6.3 - Test results to evaluate the effect of geogrid characteristics on K_{SGC} .

Aggregate	Geogrid	K_{SGC} ((kN/m) ² /mm)	Change in relation to baseline (%)	Pmax (kN/m)	Change in relation to baseline (%)
Round SAggr2	GG1	41.7	Baseline	12.5	Baseline
	GG2	52.9	27	13.2	6
Angular SAggr2	GG1	54.1	Baseline	16.7	Baseline
	GG2	75.6	40	18.8	12

Both geogrids have relatively similar aperture size and rib thickness (a detailed description of the geogrid properties is presented in Chapter 4). Therefore, when both geogrids are tested with the same aggregate, the difference in K_{SGC} should be mainly attributed to the difference in tensile modulus. For instance, as indicated by the results shown in Table 6.3, when Round SAggr2 was used, GG2 had a K_{SGC} 27% higher than GG1 and a pullout capacity 6% higher. For tests using Angular SAggr2, GG2 had a K_{SGC} 40% higher than GG1 and a pullout capacity 12% higher. These results suggest that geogrid tensile modulus has a significant impact on the K_{SGC} of geogrids.

6.2 GEOTEXTILES: EFFECT OF RELEVANT VARIABLES ON K_{SGC}

This section discusses the impact of properties of the backfill materials and properties of geosynthetics on the K_{SGC} of tests involving geotextiles.

6.2.1 Effect of aggregate angularity

Table 6.4 shows the results from tests done to evaluate the impact of angularity on K_{SGC} for geotextiles. This evaluation is based on tests involving two geotextiles, GT1 and GT2. As in the case of geogrids, for this evaluation, two aggregates are used for both geogrids: a round aggregate (Round SAggr2), adopted as the reference aggregate, and an angular aggregate (Angular SAggr2). In addition, an “intermediary” aggregate (50-50 SAggr2) was also used when testing GG1. Angularity is the only changing factor in the three configurations, since the same particle size, particle size distribution, and compaction effort were adopted in all tests evaluated in this case.

As the results for tests involving GT1 shown in Table 6.4 indicate, using the “intermediary” aggregate resulted in a noticeable improvement in the K_{SGC} (25%). However, such improvement can be considered small when compared to the improvement obtained with the use of the angular aggregate (Angular SAggr2), which resulted in an increase of 215% in the K_{SGC} . In terms of pullout capacity, there is only a small difference between 50-50 SAggr2 (increase of 57%) and Angular SAggr2 (increase of 69%).

Table 6.4 - Results from tests involving geotextiles to evaluate the impact of aggregate angularity on K_{SGC} .

Geogrid	Aggregate	K_{SGC} ((kN/m) ² /mm)	Change in relation to baseline (%)	Pmax (kN/m)	Change in relation to baseline (%)
GT1	Round SAggr2	7.3	Baseline	6.1	Baseline
	50-50 SAggr2	9.2	25	9.6	57
	Angular SAggr2	23.0	215	10.3	69
GT2	Round SAggr2	6.4	Baseline	6.7	Baseline
	Angular SAggr2	25.3	295	12.6	88

The results in Table 6.4 involving GT2 indicate that using the angular aggregate resulted in an increase of 296% in K_{SGC} and an increase of 88% in pullout capacity.

Such a significant increases in K_{SGC} suggest that the angularity of the aggregate has a significant impact on the magnitude of K_{SGC} when using geotextiles. The improvement in K_{SGC} due to aggregate angularity observed for testes involving GT2 was higher than the improvement observed when considering tests involving GT1. Hence, these results also indicate that the magnitude of the impact on K_{SGC} due to aggregate angularity is affected by geotextile properties.

In addition, the range of K_{SGC} values is wider when using Angular SAggr2, suggesting that the use of the angular aggregate makes it easier to assess the impact of the geosynthetic characteristics on K_{SGC} . On the other hand, the round aggregate resulted in relatively narrow range of K_{SGC} values. In other words, these results indicate that Round SAggr2 may not be a suitable aggregate to differentiate the performance of geotextiles. In particular, Angular SAggr2 is more suitable than Round SAggr2 for use as the reference aggregate when testing geotextile.

6.2.2 Effect of particle size and particle size distribution

Table 6.5 shows the compilation of results from the tests done to evaluate the impact of particle size and particle size distribution on the K_{SGC} for tests involving geotextiles. Comparison of the results of tests conducted using Angular SAggr2 and Saggr3 allow assessing the effect of particle size, while comparison of the results of tests conducted using Angular SAggr2 and WG allow assessing the impact of particle size distribution on the K_{SGC} for geogrids. Angular SAggr2 was adopted as the reference aggregate for both cases.

Table 6.5 - Results from tests involving geotextiles to evaluate the impact of particle size and particle size distribution on K_{SGC} .

Geogrid	Aggregate	K_{SGC} ((kN/m) ² /mm)	Change in relation to Baseline (%)	Pmax (kN/m)	Change in relation to Baseline (%)
GT1	Angular SAggr2	23.0	Baseline	10.3	Baseline
	Angular SAggr3	23.0	0	11.3	10
	Angular WG	49.5	115	12.7	23
	Monterey Sand	45.5	98	10.9	6

The results in Table 6.5 indicate that the use of an aggregate with smaller average particle size than the reference aggregate did not have a noticeable impact on K_{SGC} and had just a small impact on the pullout capacity (increase of 10%). These results suggest that particle size has a significantly small impact on the K_{SGC} of tests involving geotextiles.

On the other hand, the use of the well-graded aggregate had a significant impact on the K_{SGC} (an increase of 115%) and a considerable impact on the of the pullout capacity

(an increase of). These results suggest that the impact of particle size distribution is much more important for the K_{SGC} of tests involving geotextiles than it is for those involving geogrids.

Similarly, the results in Table 6.5 indicate that the use of Monterey Sand resulted in a relevant improvement of the K_{SGC} value, with an increase of 98%. The impact on pullout capacity was minor, with only an increase of 6%. The results with Angular WG and Monterey Sand in combination may suggest that the main factor improving the K_{SGC} in these cases is the presence of finer but still in the sand-size range particles.

6.2.2 Effect of geotextile characteristics

Tests conducted with the two geotextile evaluated in this study, using the same aggregate can be used to evaluate the effect of geotextile stiffness on the K_{SGC} . Table 6.6 compares the results of tests for GT1 and GT2 done with Round SAggr2 and then results of tests for GT1 and GT2 with Angular SAggr2.

The results with Round SAggr2 shown in Table 6.6 were somewhat unexpected, indicating that the geotextile with higher stiffness has a 12% lower K_{SGC} . It suggests, however, that Round SAggr2 might not be suitable as a reference when testing geotextiles.

When the angular aggregate was used, the results in Table 6.6 indicate that GT2 had a K_{SGC} 10% higher than GT1, with is in agreement with the fact that that GT2 has higher tensile modulus than GT1 (745 and 965 kN/m, respectively, at 2% strain). This may suggest that Angular SAggr2 is a more suitable option for use as reference aggregate when testing geotextiles.

Table 6.6 - Test results to evaluate the impact of geotextile stiffness on K_{SGC} .

Aggregate	Geogrid	K_{SGC} ((kN/m) ² /mm)	Change in relation to Baseline (%)	Pmax (kN/m)	Change in relation to Baseline (%)
Round SAggr2	GT1	7.3	Baseline	6.1	Baseline
	GT2	6.4	-12	6.7	10
Angular SAggr2	GT1	23.0	Baseline	10.3	Baseline
	GT2	25.3	10	12.6	22

6.3 EFFECT OF PARTICLE SIZE DISTRIBUTION ON THE UNIT TENSION CURVE

Figure 6.1 shows the time history of frontal unit tension for two tests conducted using GG1: one done with Round Saggr2, shown in Figure 6.1(a), and one done with Angular SAggr2, Figure 6.1(b). These graphs illustrate that, in spite of making the interface connection stronger (i.e., increasing the pullout capacity, and the displacements required to achieve that pullout capacity) the use of an angular aggregate does not affect the shape of the displacement-time curve from tests using geogrids in a noticeable way.

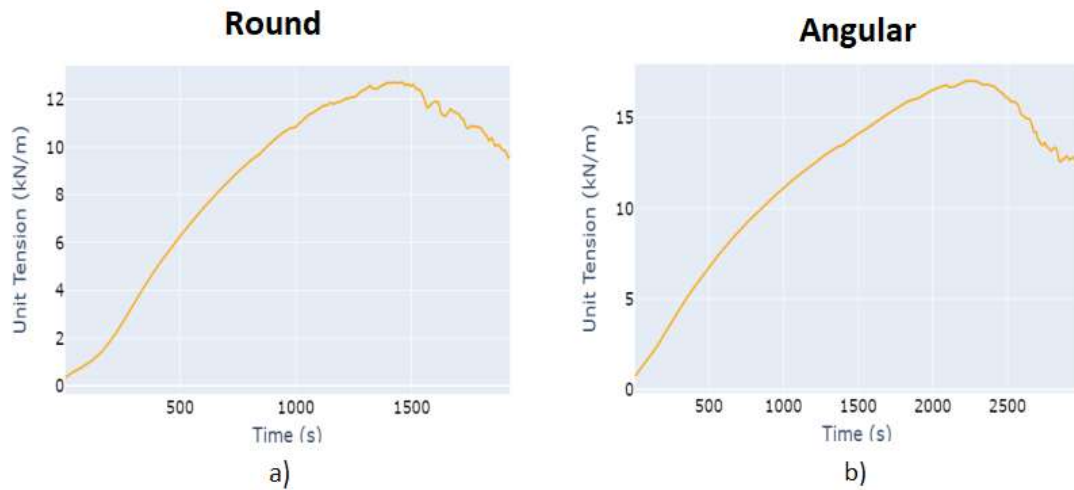


Figure 6.1 - Comparison of the time history of frontal unit tension obtained from tests using Round SAggr2 and Angular SAggr2, both with GG1.

Figure 6.2 shows the time history of frontal unit tension from two tests involving geogrid GG1, one test conducted using Angular SAggr2 (Figure 6.2(a)), which is a uniform aggregate, and another test conducted using Angular WG (Figure 6.2(b)), which is a well-graded aggregate. The results shown in these graphs suggest that particle size distribution does not influence the shape of the unit tension versus time curve. In both cases the curve resembles the behavior that is typical of interface tests (e.g. in a direct shear test), showing a peak and a post peak shear strength loss leading to a residual value.

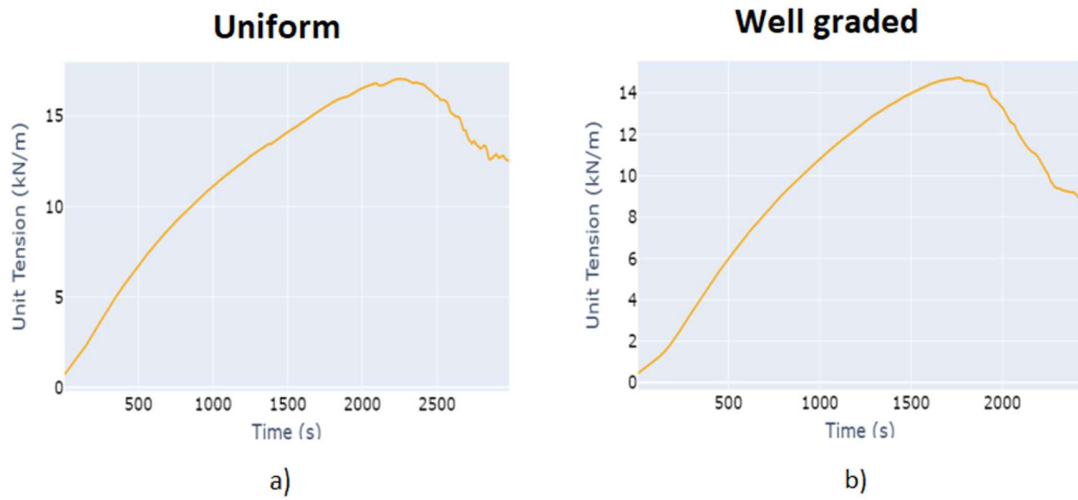


Figure 6.2 - Frontal unit tension time history for two tests involving the GG1: one test using Angular SAggr2 (a) and another test using Angular WG (b).

The frontal unit tension-time data from two tests involving the geotextile GT1 is plotted in Figure 6.3. One test was conducted using Angular SAggr2 (Figure 6.3(a)), which is a uniform aggregate, while the other test was conducted using Angular WG (Figure 6.3(a)), which is a well-graded aggregate. These results suggest that aggregate angularity does not significantly affect the shape of the frontal unit tension-time curve.

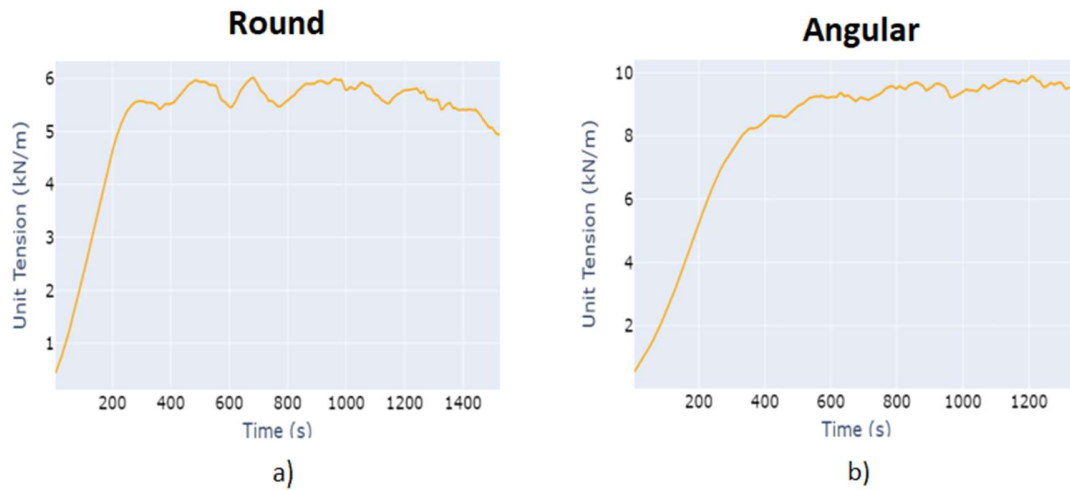


Figure 6.3 - Frontal unit tension time history comparison, from two tests involving GT1: one test using Round SAggr2 (a) and another test using Angular SAggr2 (b).

Figure 6.4 shows the comparison of the frontal unit tension-time data from two tests involving geotextile GT1, one test conducted using Angular SAggr2 (Figure 6.4(a)) and another test conducted using Angular WG (Figure 6.4(b)). Unlike in the previous cases, in this case the particle size distribution clearly affects the shape of the unit tension-time curve. Using the well-graded material results in the curve showing a peak and a post peak shear strength loss leading to a residual value., with may suggest an important change in the mechanism causing pullout failure at the soil-geosynthetic interface.

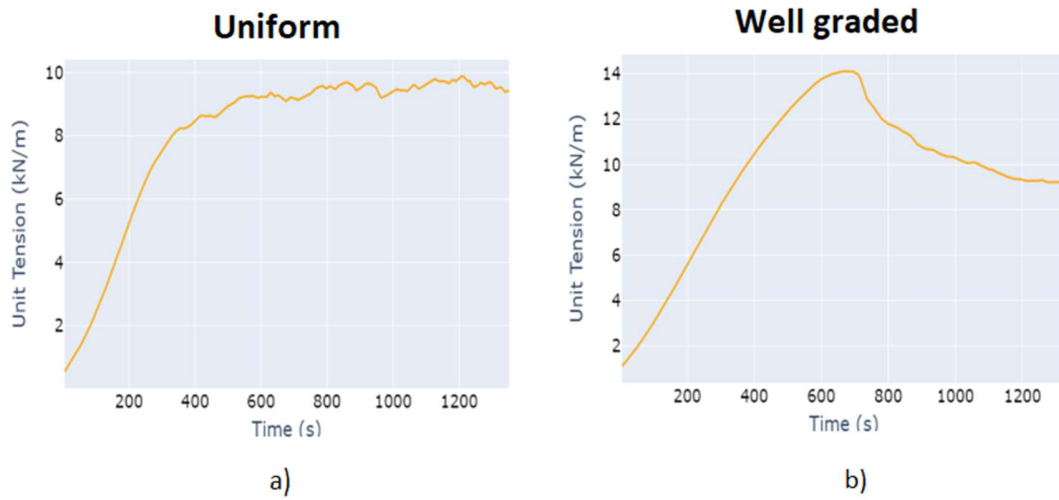


Figure 6.4 – Frontal unit tension time history from two tests involving GT1, conducted using a uniform (a) and well-graded (b) aggregate.

This section focused especially on the results obtained at large displacements, and consequently, under failure and post-failure conditions. It is important to notice however, that the small-scale SGI test was conceived to primarily analyze the small displacement response of the soil geosynthetic composite.

Chapter 7: Conclusion

The main objective of this study was to evaluate the impact that variables related to the shape, distribution, and size of aggregate particle have on the stiffness of the soil geosynthetic composite, K_{SGC} , for both geogrids and geotextiles

7.1 GENERAL CONCLUSIONS

The following are overall conclusions of this study:

- The aggregate angularity was found to impact more significantly the K_{SGC} results obtained when testing geotextiles than when testing geogrids.
- The tensile modulus of geogrids was observed to influence the magnitude of the impact of aggregate angularity on K_{SGC}
- The results obtained on this study suggest that the impact of particle size on K_{SGC} almost negligible for geogrids and geotextiles
- The impact of particle size distribution on K_{SGC} of geotextiles was found to be significant, but its impact was comparatively minor on the K_{SG} of geogrids.
- The impact of particle size distribution was also observed in the shape of the frontal load-time curve. Specifically, use of well graded materials was found to result in a peak unit tension followed by a post-peak tension loss. The impact on the load-displacement curve was also observed when using Monterey Sand as backfill.

7.2 IMPACT OF ANGULARITY OF AGGREGATES ON K_{SGC} INVOLVING GEOGRIDS

The following specific conclusions were obtained regarding the impact of aggregate angularity on K_{SGC} when using geogrids:

- The angularity of aggregates was found to affect the value of K_{SGC} of tests involving geogrids. For the materials used in this study, the average K_{SGC} value for GG1 went from 41.7 (kN/m)²/mm, when using the reference aggregate, to 54.1 (kN/m)²/mm when using the angular aggregate, an increase of 30%.
- Consistent with the expected impact at failure, the angularity of aggregates was found to also affect the magnitude of the pullout resistance. For example, for the materials evaluated in this study, the pullout resistance of geogrid GG1 increased by using the angular aggregate, with the average pullout capacity increasing by 33% (from 12.5 to 16.7 kN/m).
- The increase in K_{SGC} due to angularity was found to also be affected by the tensile modulus of the geogrids. For example, GG2, being very similar to GG1 in all its characteristics but for its tensile modulus (which is higher than that of GG1), showed an improvement on the average K_{SGC} that was even more significant than that seen for GG1, increasing from 52.9 to 75.6 (kN/m)²/mm, (an increase of 43%).
- The tensile modulus of geogrids was also found to affect the increase in pullout resistance of geogrids caused by the angularity of the aggregate. Specifically, the increase in the average pullout resistance for geogrid GG2 was 51% (from 13.2 to 18.8 kN/m) when the angular aggregate was used.

7.3 IMPACT OF AGGREGATES ANGULARITY ON K_{SGC} INVOLVING GEOTEXTILES

The following specific conclusions were obtained regarding the impact of aggregate angularity on K_{SGC} when using geotextiles:

- The angularity of aggregates was found to have a significant impact on the K_{SGC} of tests involving geotextiles. For example, using the angular aggregate instead of the round as the backfill resulted on an increase of 215% (from 7.3 to 23.0 (kN/m)²/mm) in the average K_{SGC} for GT1.
- Likewise, the pullout resistance of geotextiles was found to also be affected by the angularity of aggregates. For instance, the pullout capacity changed from 6.1 to 10.3 kN/m, an increase of 69%, when the angular aggregate was used.
- The increase on the average K_{SGC} due to the angularity of the aggregate was found to be affected by the tensile modulus of geotextiles. That was more clearly observed when using an angular aggregate to assess the K_{SGC} of GT2, which resulted in an increase of 295% (from 6.4 to 25.3 (kN/m)²/mm), a value that is significantly higher than the increase caused on the K_{SGC} of GT1.
- The tensile modulus of geotextiles affected the increase in pullout resistance caused by the angularity of the aggregate as well. That was shown by the increase of 88% (from 6.7 to 12.6 kN/m) in pullout capacity for geogrid GT2, which was larger than the increase seen for GT1.

7.4 EFFECT OF PARTICLE SIZE AND PARTICLE SIZE DISTRIBUTION ON K_{SGC} INVOLVING GEOGRIDS

The following specific conclusions were obtained regarding the impact of particle size and particle size distribution on K_{SGC} when using geogrids:

- The reduction in particle size led to comparatively small increase in K_{SGC} of geogrids. Specifically, for the materials used in this study, an increase of K_{SGC} of 6% was observed for GG1 when using Angular SAggr3 instead of Angular SAggr2 (from 54.1 to 57.1 (kN/m)²/mm) .
- The effect of decreasing the particle size on pullout resistance was found not to be particularly significant. For the specific materials being evaluated, a change of only 1% in the pullout capacity was observed.
- The use of a well graded aggregate resulted in an appreciable increase in the K_{SGC} of geogrids. For instance, the K_{SGC} of GG1 changed from 54.1 to 67.2, a 24% increase, when the well graded aggregate replaced the uniform aggregate used as a reference for this evaluation.
- The effect of particle size distribution was found not to impact positively the pullout resistance of geogrids. For example, there was reduction of 11% on the pullout capacity of GG1 when the well graded aggregate was used instead of the uniform.

7.5 EFFECT OF PARTICLE SIZE AND PARTICLE SIZE DISTRIBUTION ON K_{SGC} FOR GEOTEXTILES

The following specific conclusions were obtained regarding the impact of particle size and particle size distribution on K_{SGC} when using geotextiles:

- The reduction in particle size did not show a noticeable effect on the K_{SGC} of geotextiles. For instance, when the aggregate with smaller particle size (Angular SAggr3) was used, the K_{SGC} of GT1 had a value of 23.0 (kN/m)²/mm, which is equal to K_{SGC} value obtained when using the reference aggregate (Angular SAggr2).
- The effect of reduction in particle size on pullout resistance of geotextiles was also found to be quite small. Specifically in the case of the materials being evaluated, there was an increase of 10% in pullout resistance.
- On the other hand, particle size distribution had a great impact in the K_{SGC} of geotextiles. For example, when the well graded aggregate (Angular WG) was used instead of the reference aggregate (Angular SAggr2), there was a 115% increase in K_{SGC} of GT1 (from 23.0 to 49.5 (kN/m)²/mm)
- In comparison, effect of particle size distribution on the pullout capacity was somewhat small. which increased 23%.

7.6 IDENTIFICATION OF AGGREGATES FOR USE AS REFERENCE WHEN TESTING GEOTEXTILES

One of the goals of this study was to identify aggregates that would be deemed appropriate for use as reference when testing geotextiles. Accordingly, the K_{SGC} results obtained using the different aggregates that were tested with both geotextiles, GT1 and GT2 were evaluated to assess if they allow a cleared differentiation between the two geogrids, based on K_{SGC} values. The following conclusions can be drawn from these evaluations:

- Round SAggr2 was found not to provide a clear differentiation between the two geotextiles in terms of K_{SGC} . There was difference of only 11% between the K_{SGC} of the two geotextiles, with GT1 having a higher K_{SGC} than GT2, which was unexpected, due to its tensile modulus being lower.
- Angular SAggr2 was found to be a more suitable selection because its use results in K_{SGC} values that allow a more consistent evaluation of the mechanical properties of the geotextiles. Specifically, GT2 had a K_{SGC} 10% higher than GT1, which is in accordance with the fact that GT2 has a higher tensile modulus.
- The use of Monterey Sand as well as of Angular WG resulted in K_{SGC} values much higher than those obtained with Round SAggr2 and Angular SAggr2. Since Monterey Sand is easier to handle than Angular WG and can be more easily obtained, it may also be a suitable aggregate to be used as a reference when testing geotextiles.

7.7 RECOMMENDATIONS FOR FUTURE STUDIES

Future work would be valuable in order to address the following:

- the effect on K_{SGC} of the changes in particle size distribution and angularity that result from particle breakage during the testing procedure. The evaluation could encompass quantifying the change in particle size distribution during testing stages of both (1) compaction and (2) pullout for a single test.
- change in angularity caused by surface grading during compaction and during pullout for a single test, and the cumulative change after several tests in particle size distribution and angularity. Alternative methods of

achieving the target unit weight that eliminated particle breakage would significantly contribute to increased repeatability of the testing procedure.

- further investigation of the impact of particle size distribution on K_{SGC} . The fact that a well graded aggregate, containing several particle sizes ranging from gravel to sand, and a poorly graded sand resulted in similar K_{SGC} of geotextiles may suggest that the impact on K_{SGC} seen when the well graded aggregate was used may be attributed to the presence of sand-size particles and not necessarily to the fact that the aggregate is well graded.
- The effect of surface texture of geotextile on K_{SGC} . While this property was not explored in this study, it seems reasonable to think that it effects the soil-geosynthetic interaction in a significant manner.

Appendix A: Extensive list of test results obtained in this study

This appendix lists the results from all SGI tests done in this study. For each test, the following graphs are shown: (a) time history of frontal unit tension data, (b) time history of displacement data, (c) unit tension at telltale location-displacement data, (d) linear portion of the unit tension squared-displacement data, (e) deviation from a line of the unit tension squared-displacement data. The triggering times for all five LPs and the outlier analysis for the three middle LPs are also presented.

The tests are grouped by configuration and after all the test for a given configuration are covered a final summary for that configuration is laid out.

A.1 CONFIGURATION INVOLVING GG1 AND ROUND SAGGR2

A.1.1 Test 1

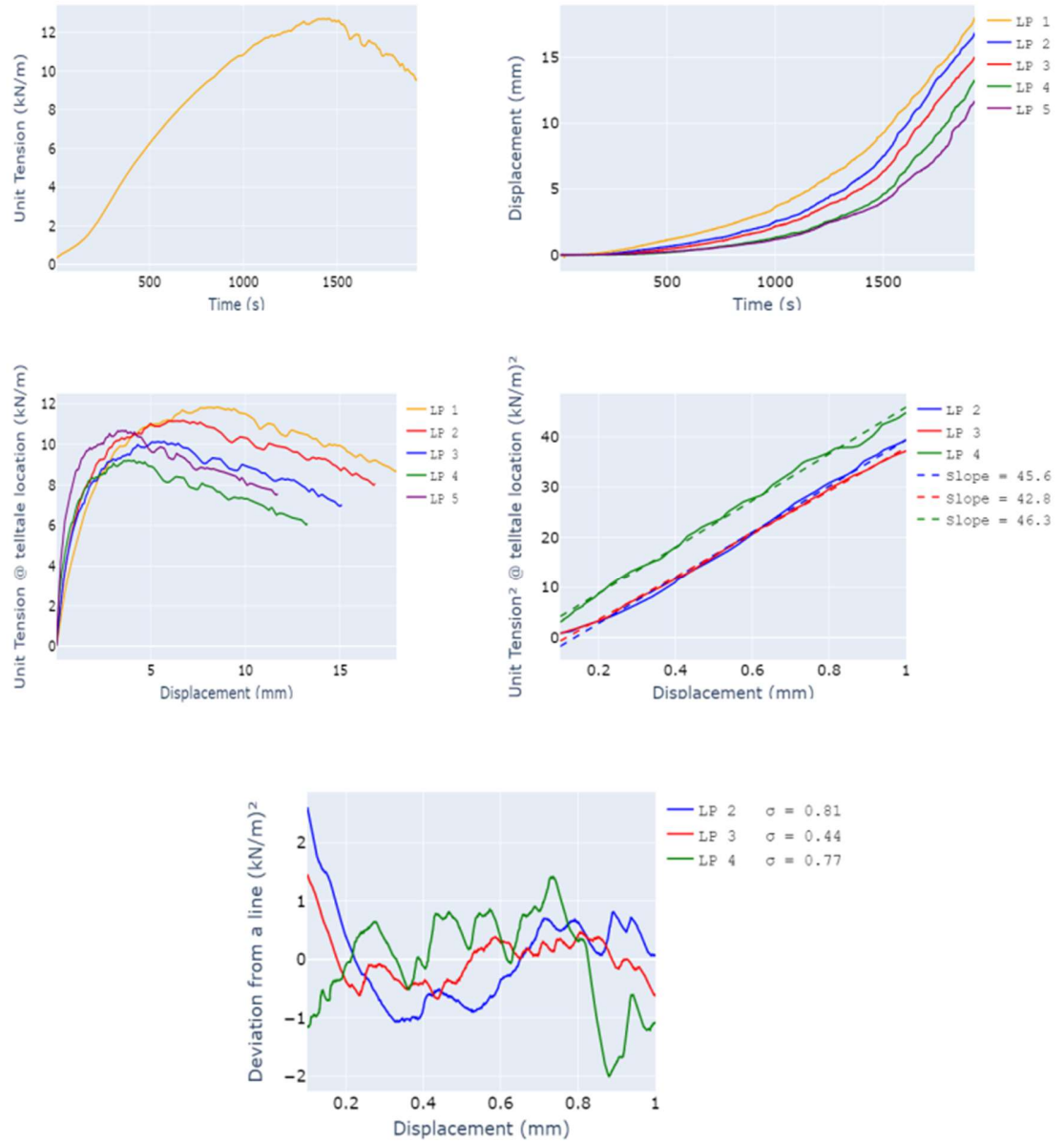


Figure A.1 – Results from the first test of configuration involving GG1 and Round SAGgr2

LP 1: Trigger Time (sec): 95.8 - T0 (kN/m): 0.88
LP 2: Trigger Time (sec): 172.8 - T0 (kN/m): 1.54
LP 3: Trigger Time (sec): 249.2 - T0 (kN/m): 2.58
LP 4: Trigger Time (sec): 305.0 - T0 (kN/m): 3.5
LP 5: Trigger Time (sec): 211.4 - T0 (kN/m): 2.03

Deviation from a line:

LP 2 - sd = 0.81 (kN/m)² - Outlier: False
LP 3 - sd = 0.44 (kN/m)² - Outlier: False
LP 4 - sd = 0.77 (kN/m)² - Outlier: False

K_{SGC} values:

LP2: 45.6 ((kN/m)²/mm) - Outlier = False
LP3: 42.8 ((kN/m)²/mm) - Outlier = False
LP4: 46.3 ((kN/m)²/mm) - Outlier = False

Final results:

$K_{SGC} = 44.66$ ((kN/m)²/mm) - Pmax = 12.72 kN/m

A.1.2 Test 2

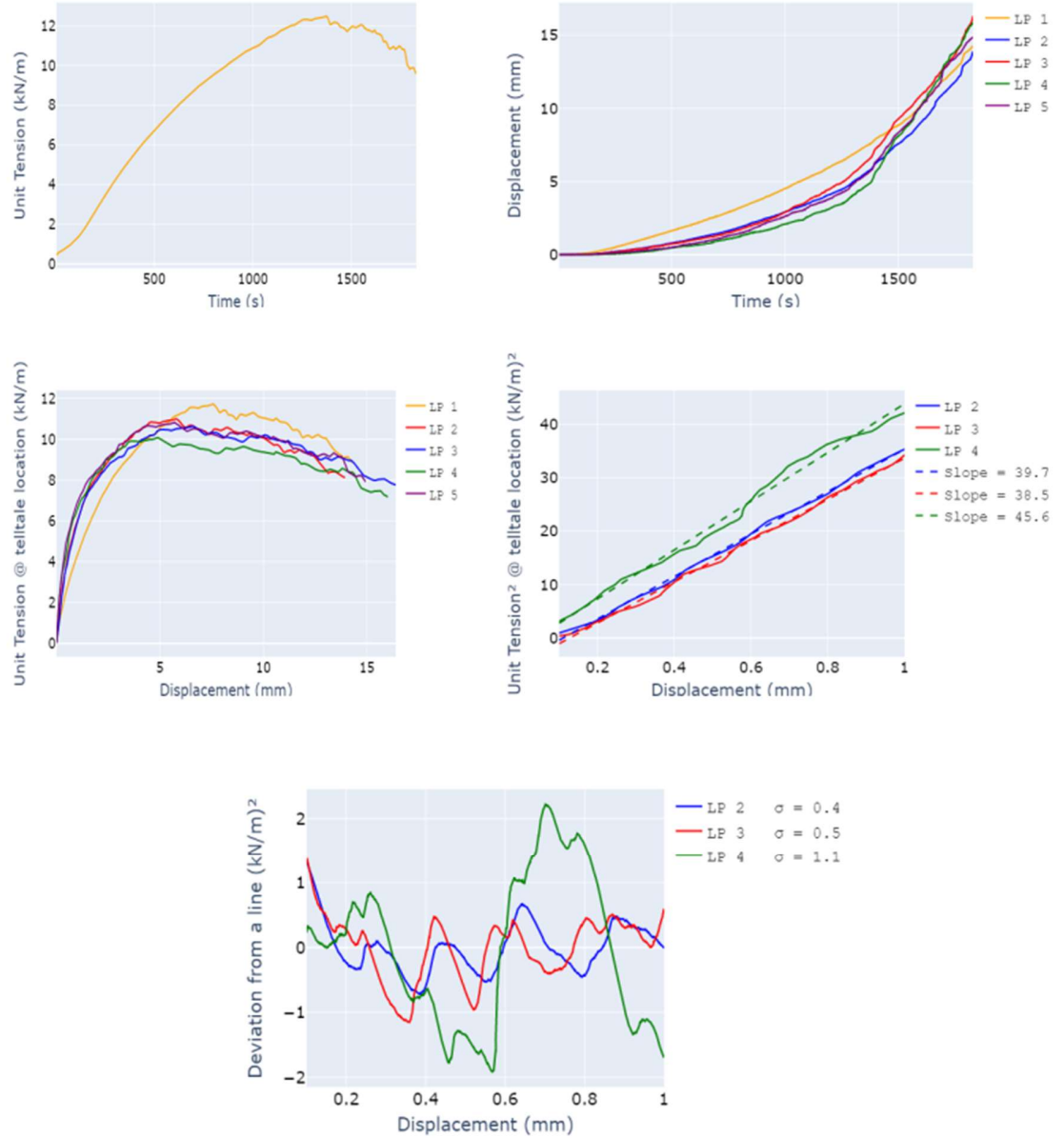


Figure A.2 - Results from the second test of configuration involving GG1 and Round SAggr2

LP 1: Trigger Time (sec): 45.0 - T0 (kN/m): 0.74
LP 2: Trigger Time (sec): 125.0 - T0 (kN/m): 1.47
LP 3: Trigger Time (sec): 150.4 - T0 (kN/m): 1.83
LP 4: Trigger Time (sec): 186.2 - T0 (kN/m): 2.4
LP 5: Trigger Time (sec): 138.2 - T0 (kN/m): 1.65

Deviation from a line:

LP 2 - $sd = 0.4 \text{ (kN/m)}^2$ - Outlier: False
LP 3 - $sd = 0.5 \text{ (kN/m)}^2$ - Outlier: False
LP 4 - $sd = 1.1 \text{ (kN/m)}^2$ - Outlier: False

K_{SGC} values:

LP2: $39.7 \text{ ((kN/m)}^2\text{/mm)}$ - Outlier = False
LP3: $38.5 \text{ ((kN/m)}^2\text{/mm)}$ - Outlier = False
LP4: $45.6 \text{ ((kN/m)}^2\text{/mm)}$ - Outlier = False

Final results:

$K_{SGC} = 40.3 \text{ ((kN/m)}^2\text{/mm)}$ - $P_{max} = 12.5 \text{ (kN/m)}$

A.1.3 Test 3

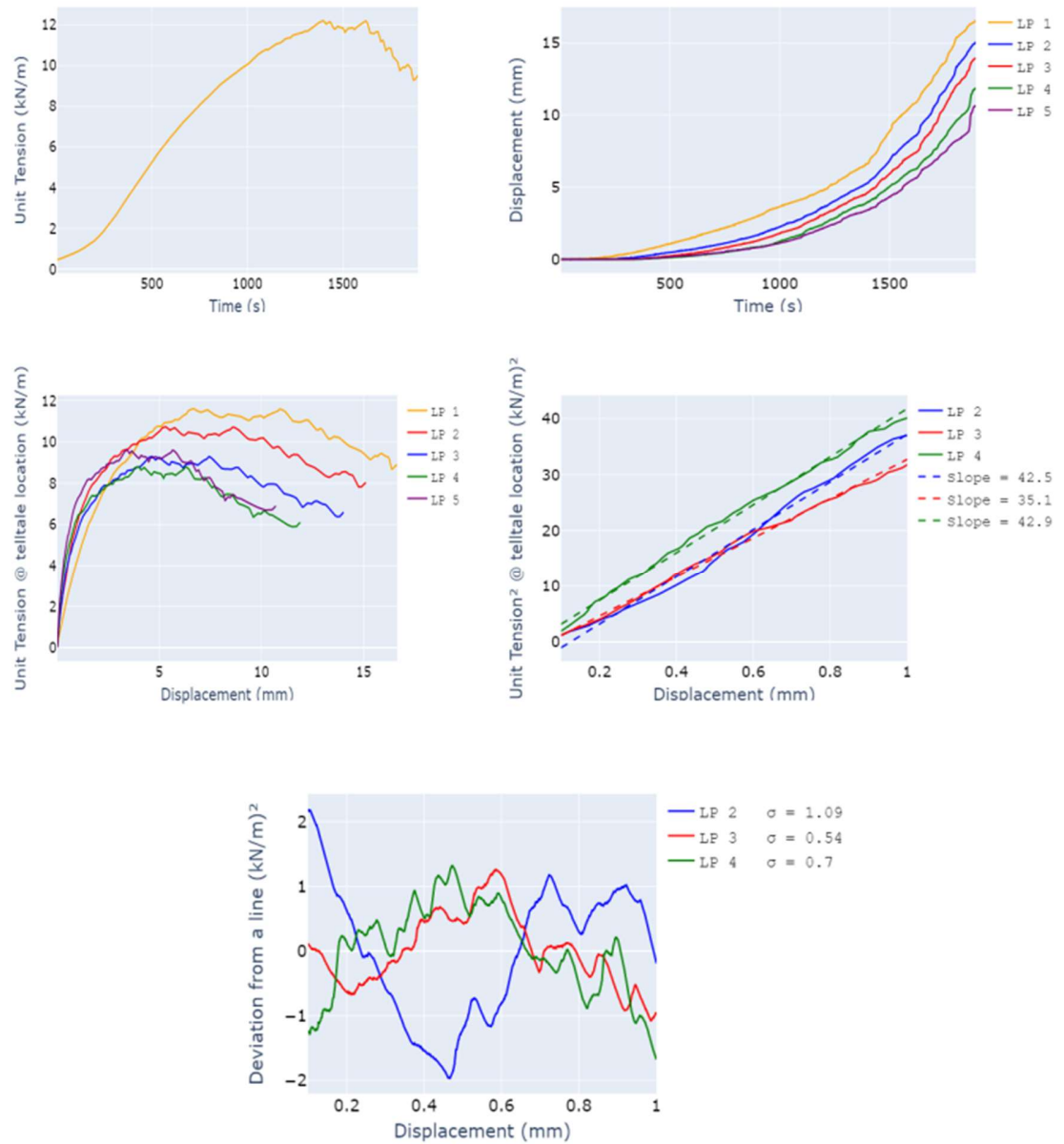


Figure A.3 - Results from the third test of configuration involving GG1 and Round SAggr2

LP 1: Trigger Time (sec): 49.2 - T0 (kN/m): 0.6

LP 2: Trigger Time (sec): 208.8 - T0 (kN/m): 1.5

LP 3: Trigger Time (sec): 330.8 - T0 (kN/m): 2.9

LP 4: Trigger Time (sec): 364.0 - T0 (kN/m): 3.4

LP 5: Trigger Time (sec): 308.2 - T0 (kN/m): 2.6

Deviation from a line:

LP 2 - sd = 1.1 (kN/m)² - Outlier: False

LP 3 - sd = 0.5 (kN/m)² - Outlier: False

LP 4 - sd = 0.7 (kN/m)² - Outlier: False

K_{SGC} values:

LP2: 42.5 ((kN/m)²/mm) - Outlier = False

LP3: 35.1 ((kN/m)²/mm) - Outlier = False

LP4: 42.9 ((kN/m)²/mm) - Outlier = False

Final results:

$K_{SGC} = 40.1$ ((kN/m)²/mm) - Pmax = 12.2 (kN/m)

A.1.4 Test 4

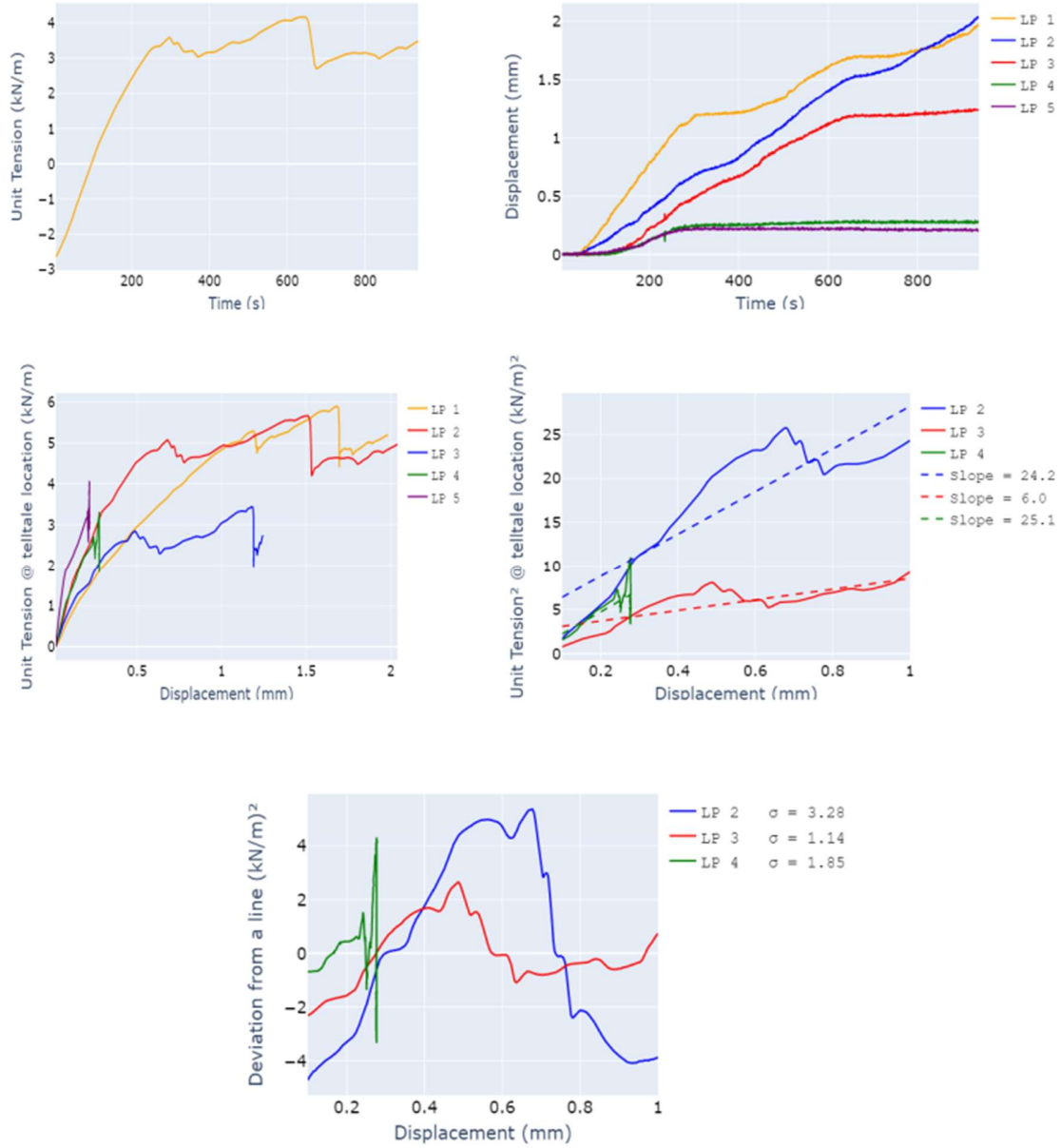


Figure A.4 - Results from the fourth test of configuration involving GG1 and Round SAggr2

LP 1: Trigger Time (sec): 42.0 - T0 (kN/m): -1.7

LP 2: Trigger Time (sec): 49.0 - T0 (kN/m): -1.5

LP 3: Trigger Time (sec): 121.6 - T0 (kN/m): 0.7

LP 4: Trigger Time (sec): 126.6 - T0 (kN/m): 0.9

LP 5: Trigger Time (sec): 99.8 - T0 (kN/m): 0.1

Deviation from a line:

LP 2 - $sd = 3.28 \text{ (kN/m)}^2$ - Outlier: True

LP 3 - $sd = 1.14 \text{ (kN/m)}^2$ - Outlier: False

LP 4 - $sd = 1.85 \text{ (kN/m)}^2$ - Outlier: True

K_{SGC} values:

LP2: $24.2 \text{ ((kN/m)}^2 \text{ /mm)}$ - Outlier = False

LP3: $6.0 \text{ ((kN/m)}^2 \text{ /mm)}$ - Outlier = True

LP4: $25.1 \text{ ((kN/m)}^2 \text{ /mm)}$ - Outlier = False

Final results:

$K_{SGC} = \text{N/A}$ - $P_{\max} = 4.18 \text{ (kN/m)}$

A.1.5 Test 5

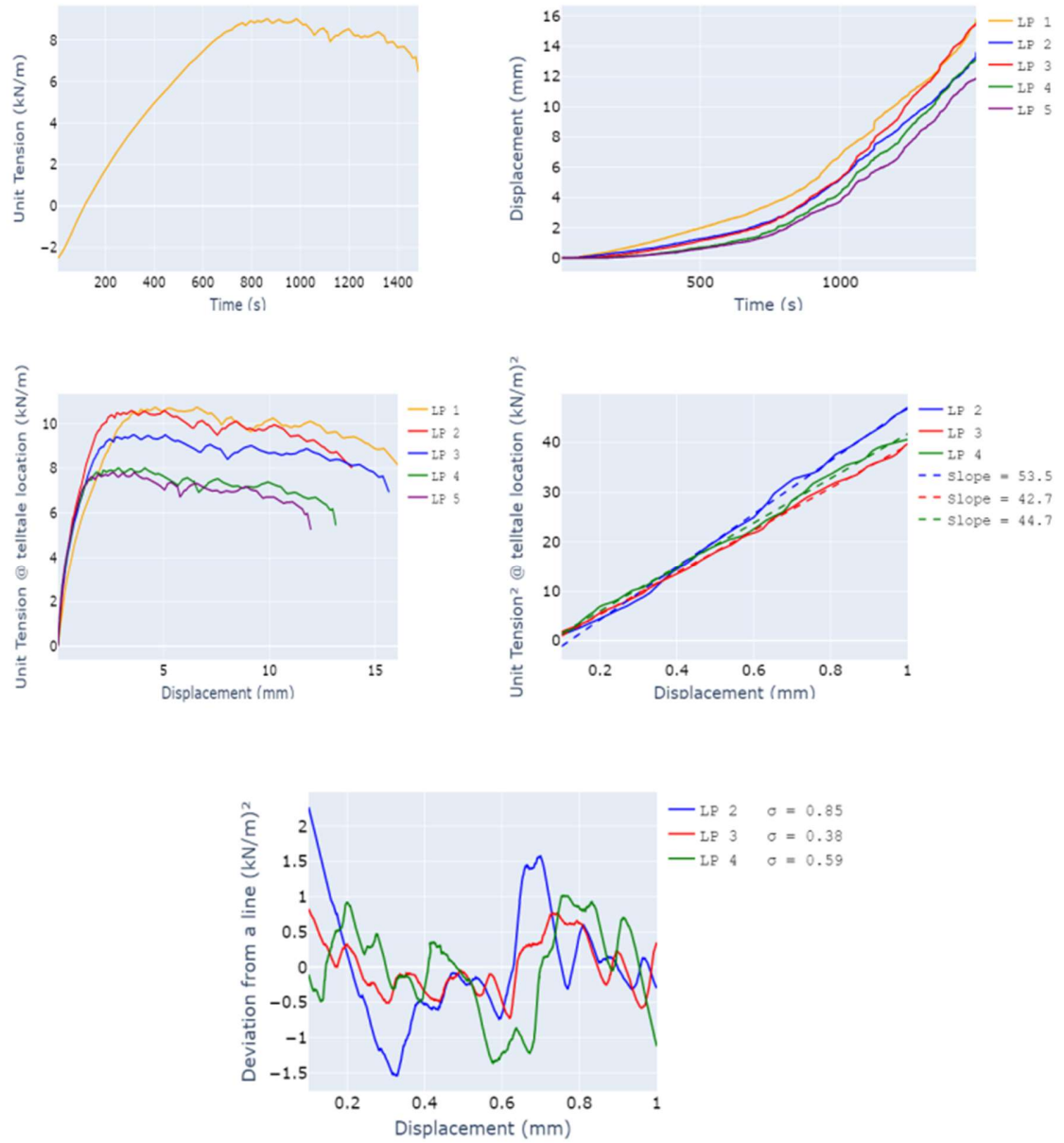


Figure A.5 - Results from fifth test of configuration involving GG1 and Round SAggr2

LP 1: Trigger Time (sec): 45.2 - T0 (kN/m): -1.71

LP 2: Trigger Time (sec): 51.0 - T0 (kN/m): -1.56

LP 3: Trigger Time (sec): 93.0 - T0 (kN/m): -0.48

LP 4: Trigger Time (sec): 162.6 - T0 (kN/m): 1.0

LP 5: Trigger Time (sec): 172.0 - T0 (kN/m): 1.2

Deviation from a line:

LP 2 - $sd = 0.9 \text{ (kN/m)}^2$ - Outlier: False

LP 3 - $sd = 0.4 \text{ (kN/m)}^2$ - Outlier: False

LP 4 - $sd = 0.6 \text{ (kN/m)}^2$ - Outlier: False

K_{SGC} values:

LP2: 53.5 - Outlier = False

LP3: 42.7 - Outlier = False

LP4: 44.7 - Outlier = False

Final results:

$K_{SGC} = 50.03$ - $P_{max} = 9.01$

A.1.6 Summary of results from configuration involving GG1 and Round SAggr2

N° of tests: 5

$$K_{SGC,MAD} = 6.46 - P_{MAX,MAD} = 0.76$$

$$K_{SGC,median} = 40.3 - P_{max median} = 12.21$$

If $((K_{SGC,i} - K_{SGC,median}) / K_{SGC,MAD}) > 2$: outlier

If $((P_{MAX,i} - P_{MAX,median}) / P_{MAX,MAD}) > 2.5$: outlier

Test 1

Pmax = 12.7 - Outlier: False - $K_{SGC} = 44.7$ - Outlier: False

Test 2

Pmax = 12.5 - Outlier: False - $K_{SGC} = 40.3$ - Outlier: False

Test 3

Pmax = 12.2 - Outlier: False - $K_{SGC} = 40.1$ - Outlier: False

Test 4

Pmax = 4.2 - Outlier: True - $K_{SGC} = N/A$ - Outlier: True

Test 5

Pmax = 9.0 - Outlier: True - $K_{SGC} = 50.0$ - Outlier: False

Final results for this configuration:

Average $K_{SGC} = 41.68$ - $K_{SGC} COV = 5.1\%$

Average Pmax = 12.47 - Pmax COV = 1.7%

A.2 CONFIGURATION INVOLVING GG1 AND ANGULAR SAGGR2

A.2.1 Test 1

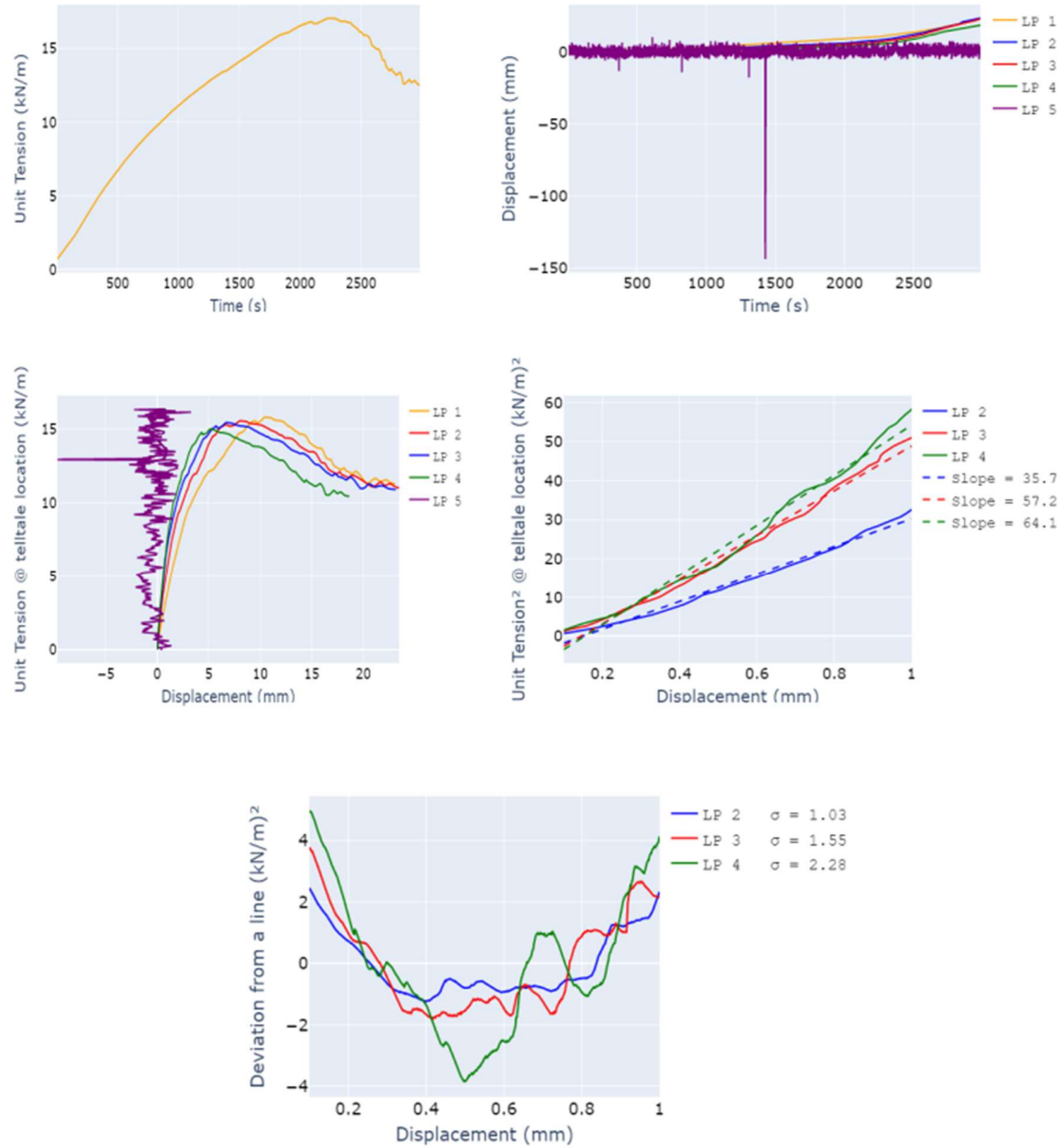


Figure A.6 - Results from the first test of configuration involving GG1 and Angular SAGgr2

LP 1: Trigger Time (sec): 51.0 - T0 (kN/m): 1.24
LP 2: Trigger Time (sec): 75.8 - T0 (kN/m): 1.5
LP 3: Trigger Time (sec): 87.0 - T0 (kN/m): 1.62
LP 4: Trigger Time (sec): 128.4 - T0 (kN/m): 2.06

Deviation from a line:

LP 2 - $sd = 1.0 \text{ (kN/m)}^2$ - Outlier: False
LP 3 - $sd = 1.5 \text{ (kN/m)}^2$ - Outlier: True
LP 4 - $sd = 2.3 \text{ (kN/m)}^2$ - Outlier: True

K_{SGC} values:

LP2: 35.7 - Outlier = True
LP3: 57.2 - Outlier = False
LP4: 64.1 - Outlier = False

Final results:

$K_{SGC} = 0$ - Pmax = 17.05

A.2.2 Test 2

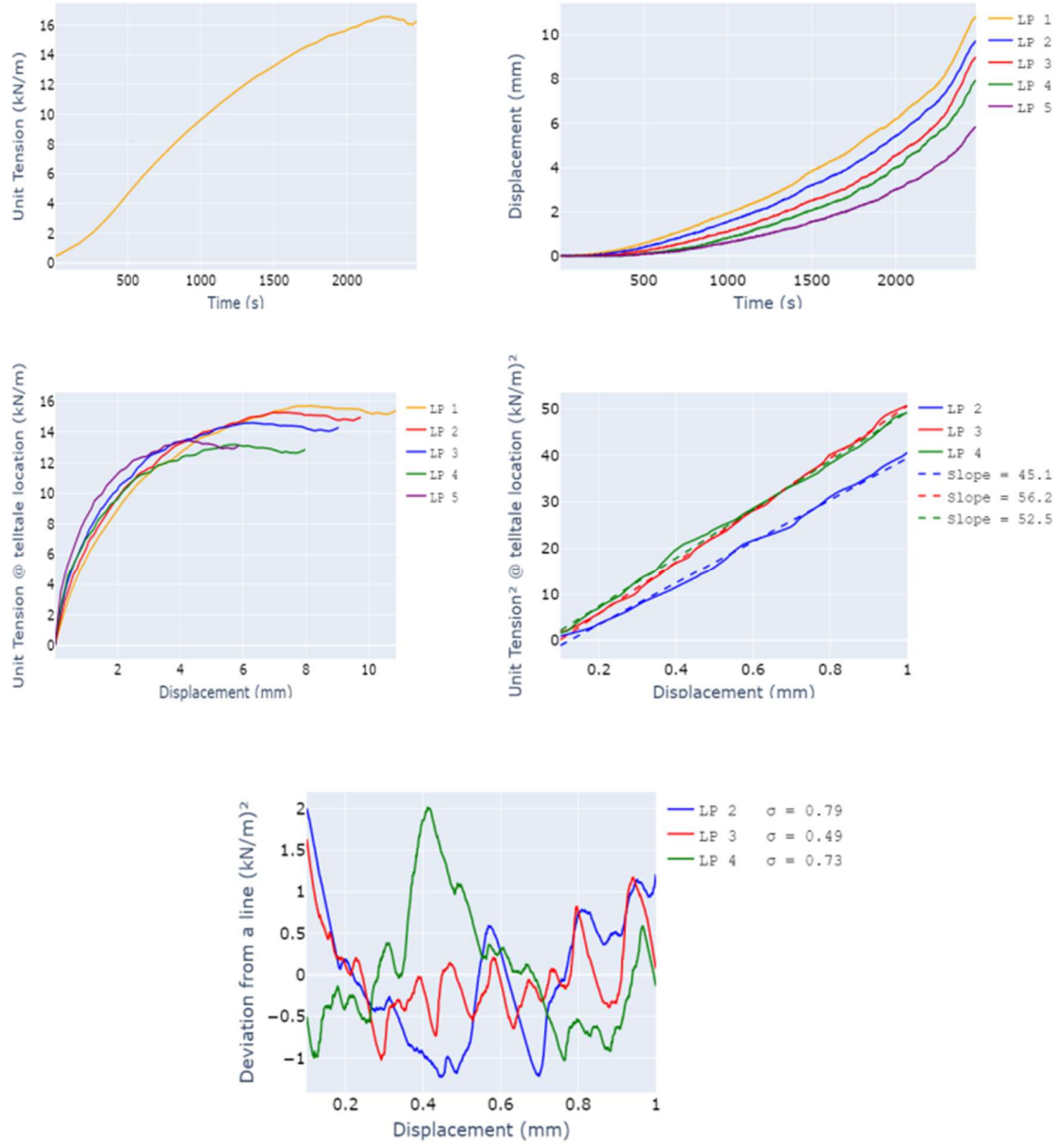


Figure A.7 - Results from the second test of configuration involving GG1 and Angular SAggr2

LP 1: Trigger Time (sec): 88.6 - T0 (kN/m): 0.9

LP 2: Trigger Time (sec): 161.6 - T0 (kN/m): 1.3

LP 3: Trigger Time (sec): 253.8 - T0 (kN/m): 2.0

LP 4: Trigger Time (sec): 394.6 - T0 (kN/m): 3.4

LP 5: Trigger Time (sec): 371.2 - T0 (kN/m): 3.1

Deviation from a line:

LP 2 - $sd = 0.8 \text{ (kN/m)}^2$ - Outlier: False

LP 3 - $sd = 0.5 \text{ (kN/m)}^2$ - Outlier: False

LP 4 - $sd = 0.7 \text{ (kN/m)}^2$ - Outlier: False

K_{SGC} values:

LP2: 45.1 - Outlier = False

LP3: 56.2 - Outlier = False

LP4: 52.5 - Outlier = False

Final results:

$K_{SGC} = 50.6$ - $P_{max} = 16.6$

A.2.3 Test 3

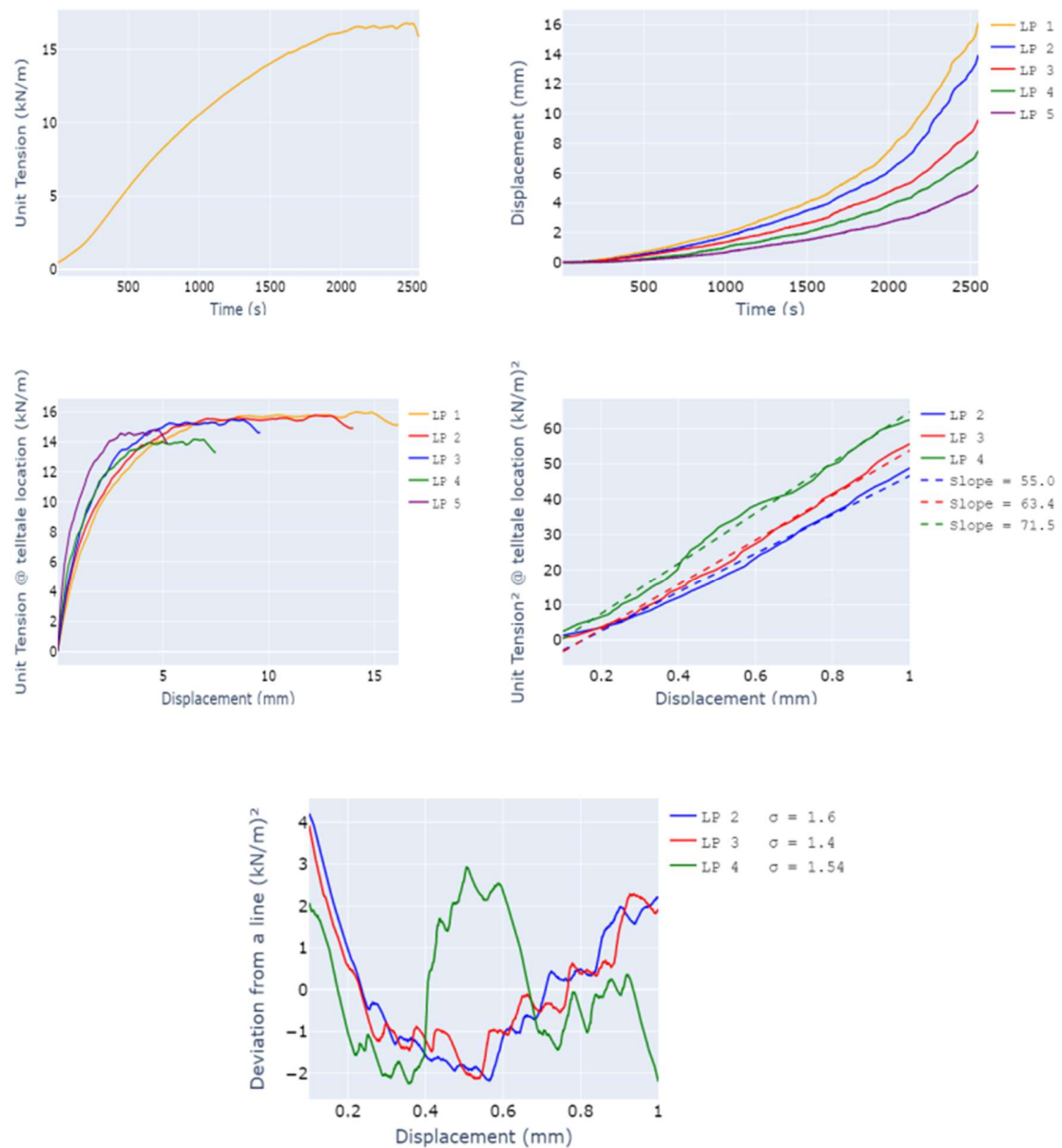


Figure A.8 - Results from the third test of configuration involving GG1 and Angular SAggr2

LP 1: Trigger Time (sec): 63.0 - T0 (kN/m): 0.8

LP 2: Trigger Time (sec): 94.0 - T0 (kN/m): 1.0

LP 3: Trigger Time (sec): 136.4 - T0 (kN/m): 1.3

LP 4: Trigger Time (sec): 267.4 - T0 (kN/m): 2.6

LP 5: Trigger Time (sec): 213.4 - T0 (kN/m): 2.0

Deviation from a line:

LP 2 - $sd = 1.6 \text{ (kN/m)}^2$ - Outlier: True

LP 3 - $sd = 1.4 \text{ (kN/m)}^2$ - Outlier: False

LP 4 - $sd = 1.5 \text{ (kN/m)}^2$ - Outlier: True

K_{SGC} values:

LP2: 55.0 - Outlier = False

LP3: 63.4 - Outlier = False

LP4: 71.5 - Outlier = False

Final results:

$K_{SGC} = 63.4$ - $P_{max} = 16.8$

A.2.4 Test 4

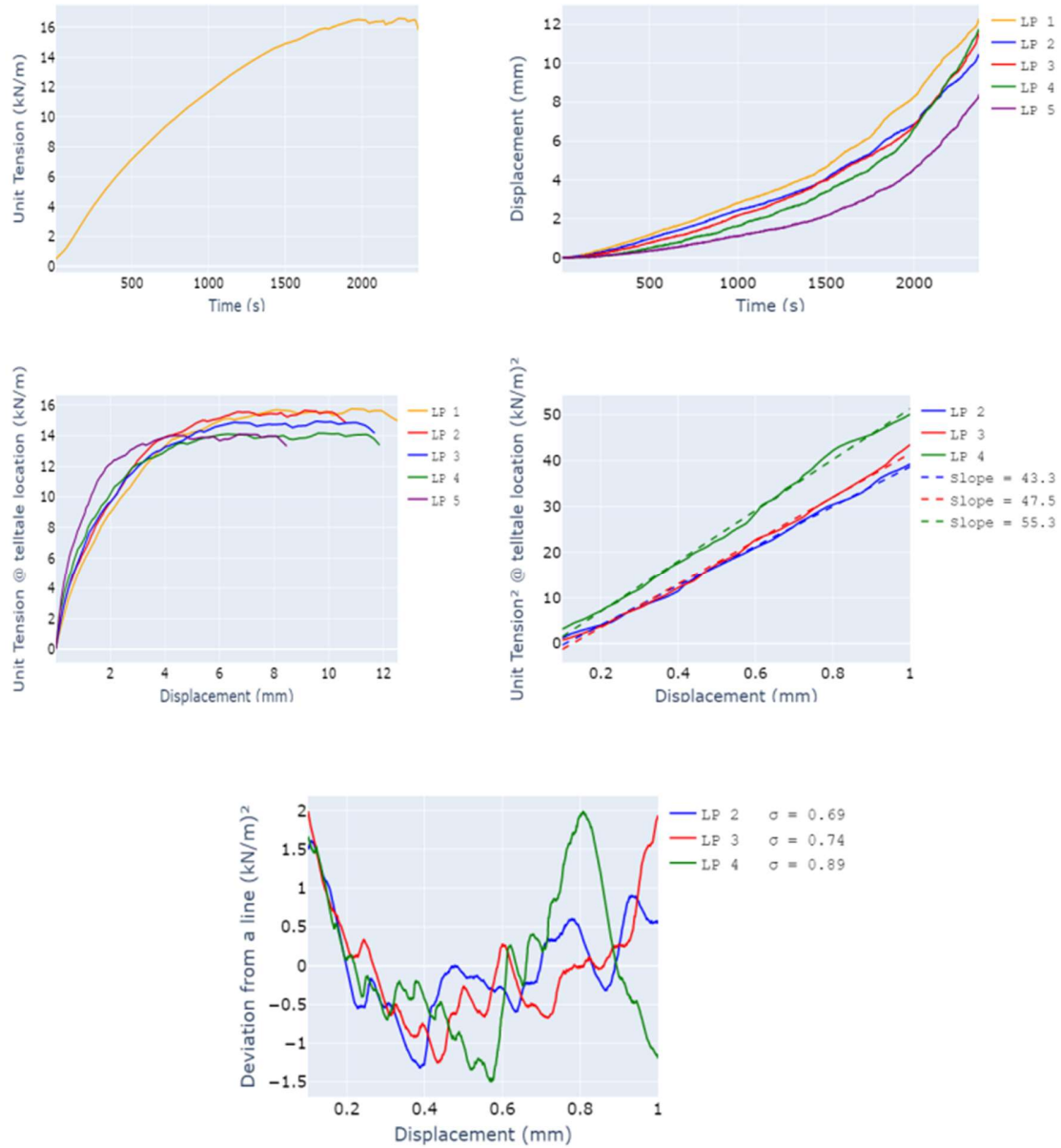


Figure A.9 - Results from the fourth test of configuration involving GG1 and Angular SAggr2

LP 1: Trigger Time (sec): 39.2 - T0 (kN/m): 0.8
LP 2: Trigger Time (sec): 49.2 - T0 (kN/m): 0.9
LP 3: Trigger Time (sec): 99.2 - T0 (kN/m): 1.6
LP 4: Trigger Time (sec): 147.0 - T0 (kN/m): 2.4
LP 5: Trigger Time (sec): 150.8 - T0 (kN/m): 2.5

Deviation from a line:

LP 2 - sd = 0.7 (kN/m)² - Outlier: False
LP 3 - sd = 0.7 (kN/m)² - Outlier: False
LP 4 - sd = 0.9 (kN/m)² - Outlier: False

K_{SGC} values:

LP2: 43.3 - Outlier = False
LP3: 47.5 - Outlier = False
LP4: 55.3 - Outlier = True

Final results:

$K_{SGC} = 48.3$ - Pmax = 16.6

A.2.5 Test 5

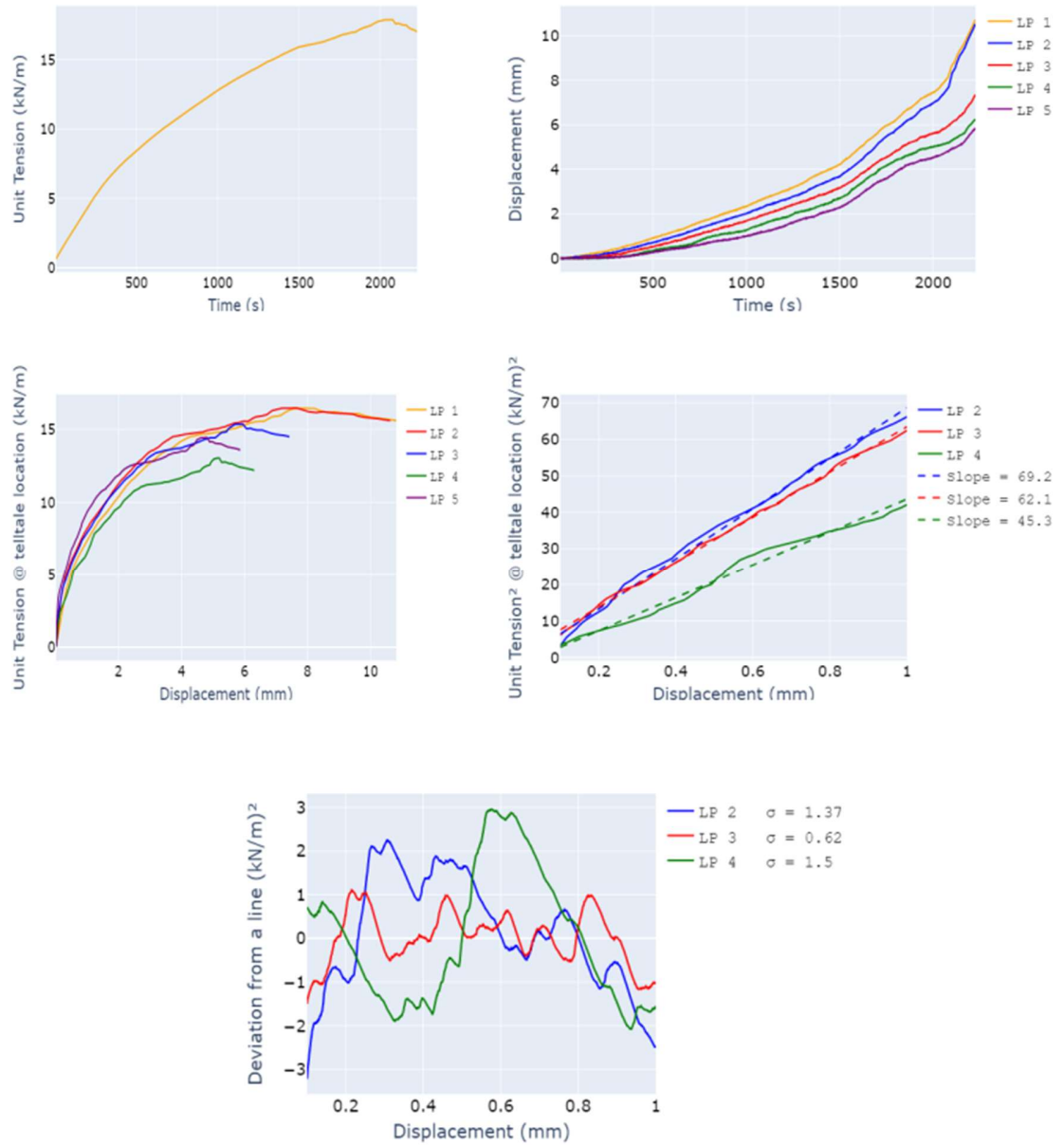


Figure A.10 - Results from the fifth test of configuration involving GG1 and Angular SAggr2

LP 1: Trigger Time (sec): 42.4 - T0 (kN/m): 1.4

LP 2: Trigger Time (sec): 42.6 - T0 (kN/m): 1.4

LP 3: Trigger Time (sec): 100.4 - T0 (kN/m): 2.5

LP 4: Trigger Time (sec): 225.4 - T0 (kN/m): 4.8

LP 5: Trigger Time (sec): 149.2 - T0 (kN/m): 3.4

Deviation from a line:

LP 2 - $sd = 1.4 \text{ (kN/m)}^2$ - Outlier: False

LP 3 - $sd = 0.6 \text{ (kN/m)}^2$ - Outlier: False

LP 4 - $sd = 1.5 \text{ (kN/m)}^2$ - Outlier: False

K_{SGC} values:

LP2: 69.2 - Outlier = False

LP3: 62.1 - Outlier = False

LP4: 45.3 - Outlier = True

Final results:

$K_{SGC} = 61.3$ - $P_{max} = 17.9$

A.2.6 Summary of results from configuration involving GG1 and Angular SAggr2

K_{SGC} MAD = 15.85 - Pmax MAD = 0.3

Ksgc meadin = 50.61 - Pmax median = 16.78

If $((K_{sgc_i} - K_{sgc_meadian})/MAD) > 2$: outlier

If $((P_{max_i} - P_{max_meadian})/MAD) > 2.5$: outlier

Test 1

Pmax = 17.1 - Outlier: False - K_{SGC} = N/A - Outlier : True

Test 2

Pmax = 16.6 - Outlier: False - K_{SGC} = 50.6 - Outlier : False

Test 3

Pmax = 16.8 - Outlier: False - K_{SGC} = 63.4 - Outlier : False

Test 4

Pmax = 16.6 - Outlier: False - K_{SGC} = 48.3 - Outlier : False

Test 5

Pmax = 17.9 - Outlier: True - K_{SGC} = 61.3 - Outlier : False

Final results for this configuration:

Average K_{SGC} = 54.1 - K_{SGC} COV = 12.3%

Average Pmax = 16.7 - Pmax COV = 0.6%

A.3 CONFIGURATION INVOLVING GG1 AND ANGULAR SAGGR3

A.3.1 Test 1

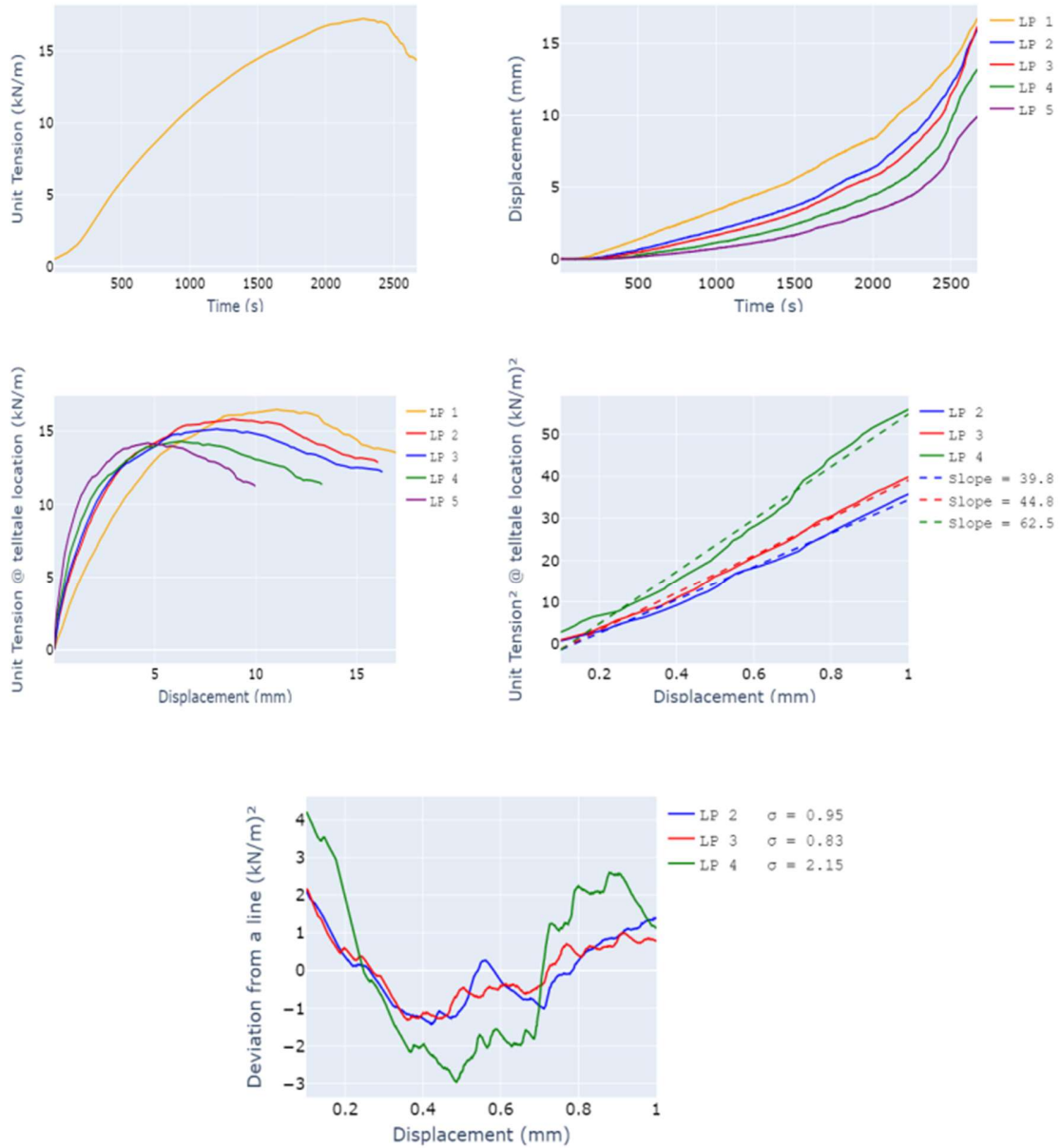


Figure A.11 - Results from the first test of configuration involving GG1 and Angular SAGGR3

LP 1: Trigger Time (sec): 67.8 - T0 (kN/m): 0.8

LP 2: Trigger Time (sec): 166.2 - T0 (kN/m): 1.5

LP 3: Trigger Time (sec): 223.0 - T0 (kN/m): 2.1

LP 4: Trigger Time (sec): 280.8 - T0 (kN/m): 3.0

LP 5: Trigger Time (sec): 289.2 - T0 (kN/m): 3.1

Deviation from a line:

LP 2 - $sd = 0.9 \text{ (kN/m)}^2$ - Outlier: False

LP 3 - $sd = 0.8 \text{ (kN/m)}^2$ - Outlier: False

LP 4 - $sd = 2.2 \text{ (kN/m)}^2$ - Outlier: True

K_{SGC} values:

LP2: 39.8 - Outlier = False

LP3: 44.8 - Outlier = False

LP4: 62.5 - Outlier = True

Final results:

$K_{SGC} = 45.83$ - $P_{max} = 17.27$

A.3.2 Test 2

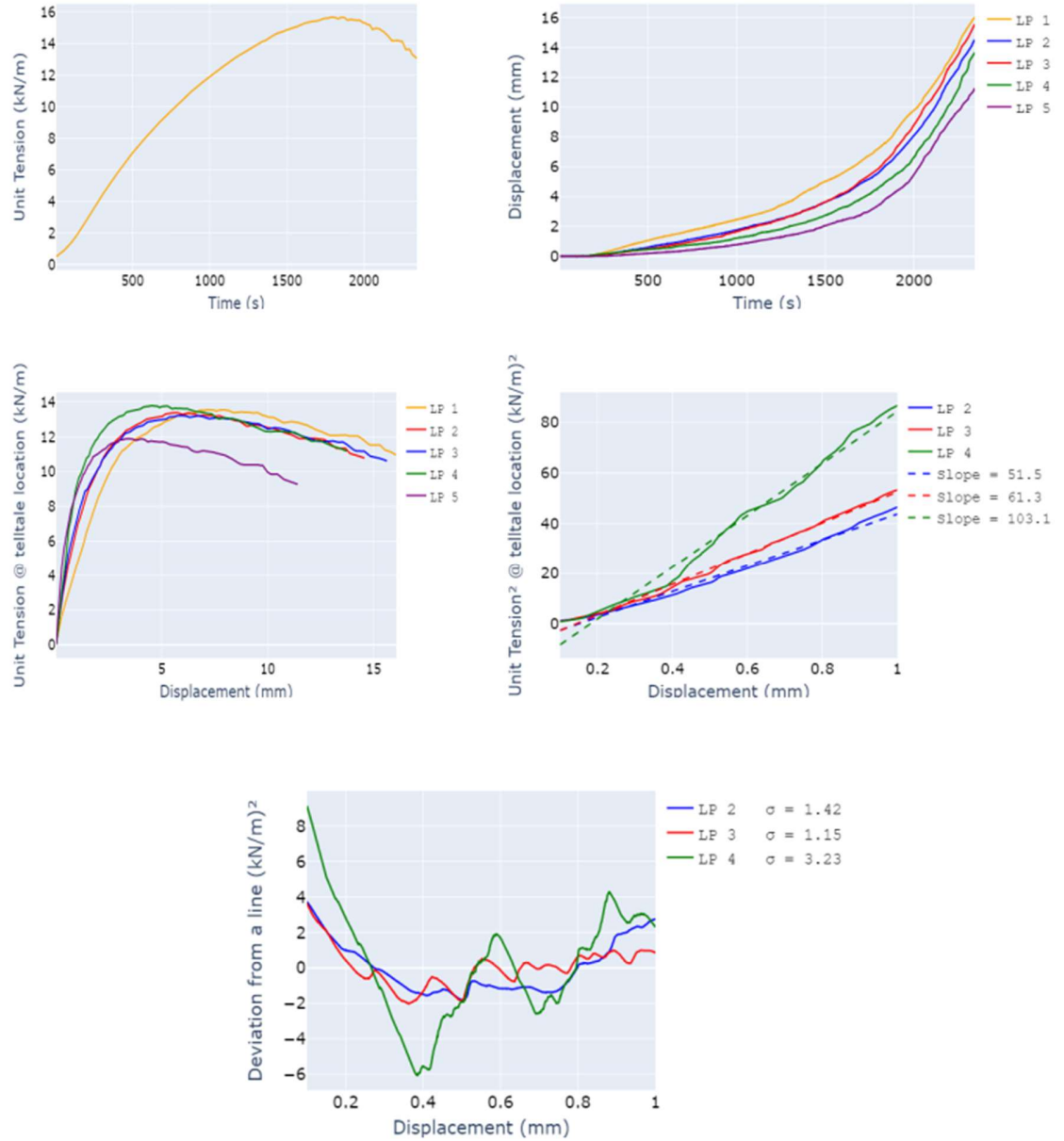


Figure A.12 - Results from the second test of configuration involving GG1 and Angular SAgg3

LP 1: Trigger Time (sec): 154.0 - T0 (kN/m): 2.1

LP 2: Trigger Time (sec): 166.8 - T0 (kN/m): 2.3

LP 3: Trigger Time (sec): 177.2 - T0 (kN/m): 2.4

LP 4: Trigger Time (sec): 138.8 - T0 (kN/m): 1.9

LP 5: Trigger Time (sec): 261.4 - T0 (kN/m): 3.8

Deviation from a line:

LP 2 - $sd = 1. (kN/m)^2$ - Outlier: False

LP 3 - $sd = 1.1 (kN/m)^2$ - Outlier: False

LP 4 - $sd = 3.2 (kN/m)^2$ - Outlier: True

K_{SGC} values:

LP2: 51.5 - Outlier = False

LP3: 61.3 - Outlier = False

LP4: 103.1 - Outlier = True

Final results:

$K_{SGC} = 65.36$ - $P_{max} = 15.65$

A.3.3 Test 3

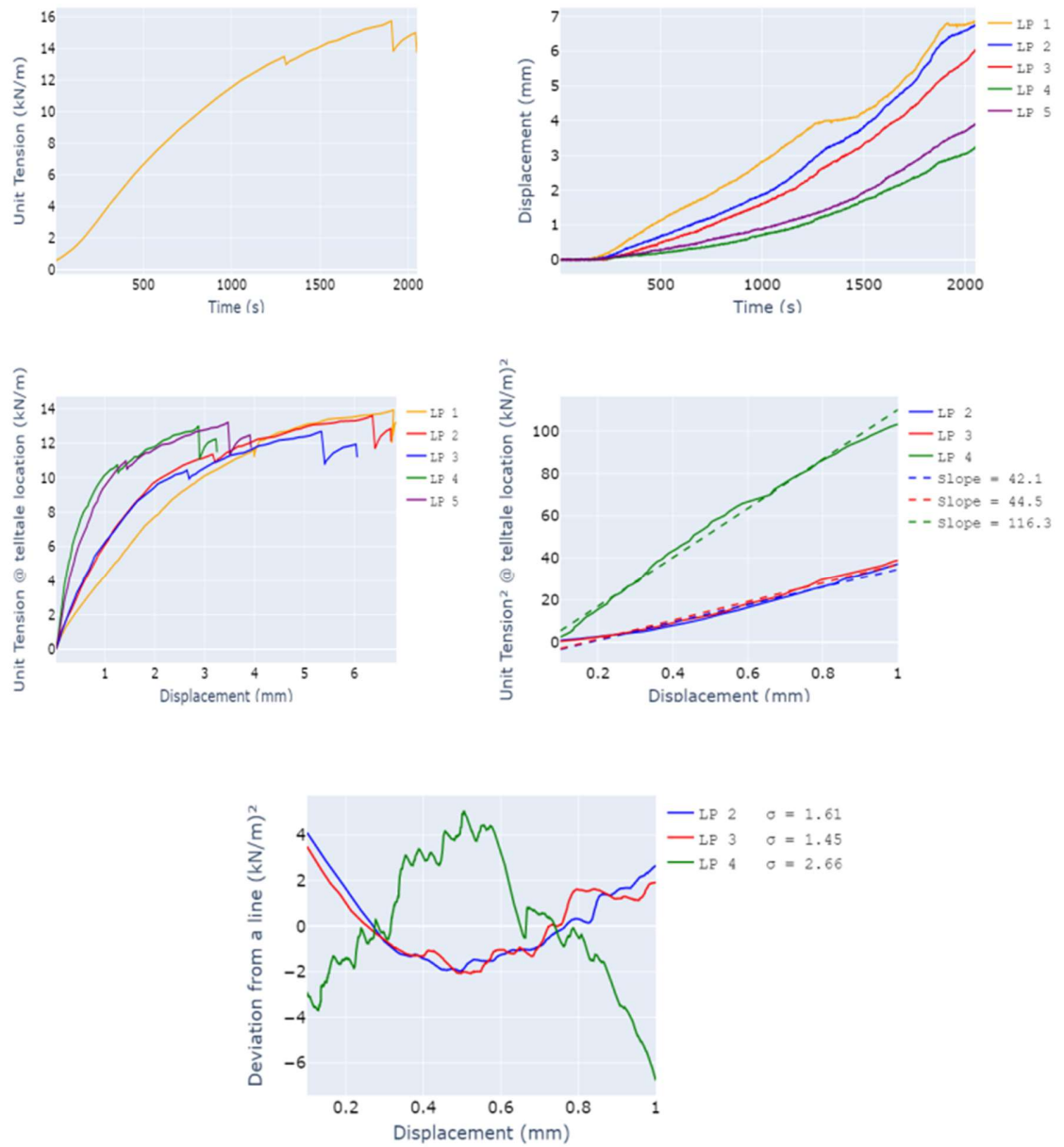


Figure A.13 - Results from the third test of configuration involving GG1 and Angular SAgg3

LP 1: Trigger Time (sec): 144.0 - T0 (kN/m): 1.8
LP 2: Trigger Time (sec): 170.8 - T0 (kN/m): 2.1
LP 3: Trigger Time (sec): 237.0 - T0 (kN/m): 3.0
LP 4: Trigger Time (sec): 215.8 - T0 (kN/m): 2.7
LP 5: Trigger Time (sec): 200.0 - T0 (kN/m): 2.51

Deviation from a line:

LP 2 - $sd = 1.6 \text{ (kN/m)}^2$ - Outlier: True
LP 3 - $sd = 1.5 \text{ (kN/m)}^2$ - Outlier: False
LP 4 - $sd = 2.7 \text{ (kN/m)}^2$ - Outlier: True

K_{SGC} values:

LP2: 42.1 - Outlier = False
LP3: 44.5 - Outlier = False
LP4: 116.3 - Outlier = True

Final results:

$K_{SGC} = 44.5$ - $P_{max} = 15.7$

A.3.4 Test 4

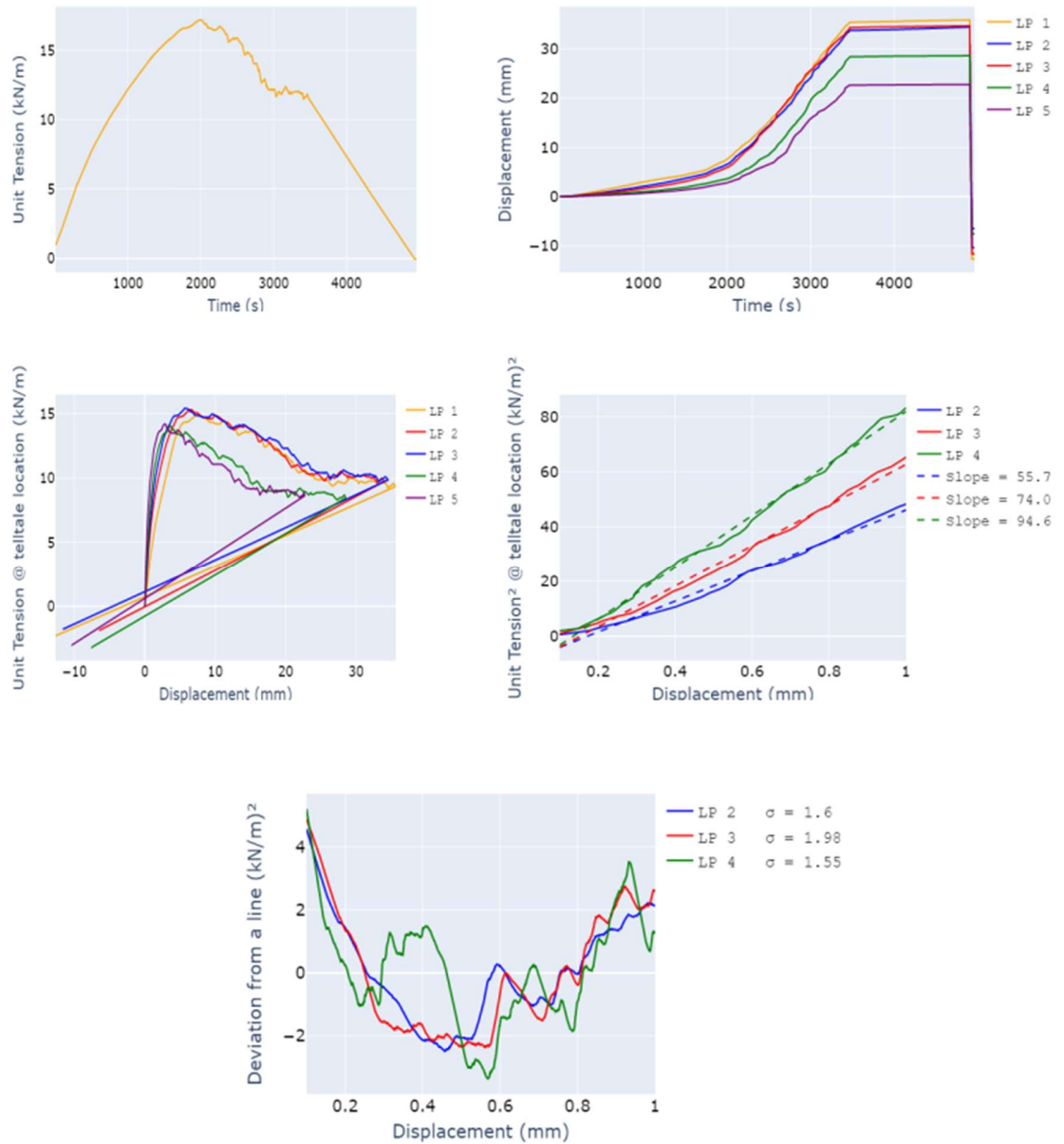


Figure A.14 - Results from the fourth test of configuration involving GG1 and Angular SAgg3

LP 1: Trigger Time (sec): 99.0 - T0 (kN/m): 2.2

LP 2: Trigger Time (sec): 72.8 - T0 (kN/m): 1.8

LP 3: Trigger Time (sec): 66.4 - T0 (kN/m): 1.7

LP 4: Trigger Time (sec): 153.6 - T0 (kN/m): 3.1

LP 5: Trigger Time (sec): 142.8 - T0 (kN/m): 3.0

Deviation from a line:

LP 2 - $sd = 1.6 \text{ (kN/m)}^2$ - Outlier: True

LP 3 - $sd = 2.0 \text{ (kN/m)}^2$ - Outlier: True

LP 4 - $sd = 1.6 \text{ (kN/m)}^2$ - Outlier: True

K_{SGC} values:

LP2: 55.7 - Outlier = False

LP3: 74.0 - Outlier = False

LP4: 94.6 - Outlier = True

Final results:

$K_{SGC} = \text{N/A}$ - $P_{\max} = 17.2$

A.3.5 Test 5

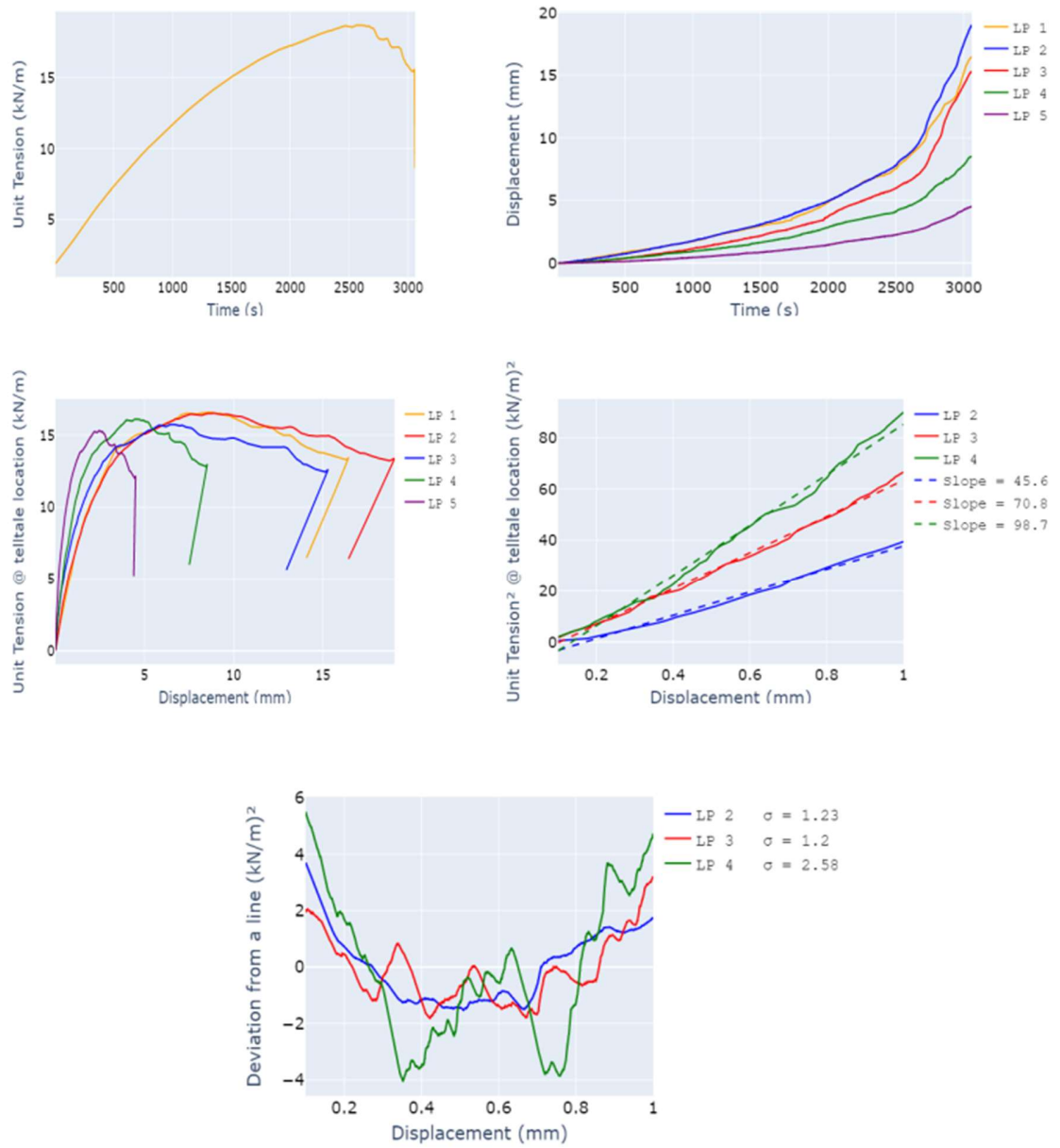


Figure 15 - Results from the fourth test of configuration involving GG1 and Angular SAgg3

LP 1: Trigger Time (sec): 29.2 - T0 (kN/m): 2.2

LP 2: Trigger Time (sec): 34.6 - T0 (kN/m): 2.2

LP 3: Trigger Time (sec): 107.4 - T0 (kN/m): 3.0

LP 4: Trigger Time (sec): 73.8 - T0 (kN/m): 2.6

LP 5: Trigger Time (sec): 146.8 - T0 (kN/m): 3.4

Deviation from a line:

LP 2 - $sd = 1.2 \text{ (kN/m)}^2$ - Outlier: False

LP 3 - $sd = 1.2 \text{ (kN/m)}^2$ - Outlier: False

LP 4 - $sd = 2.6 \text{ (kN/m)}^2$ - Outlier: True

K_{SGC} values:

LP2: 45.6 - Outlier = False

LP3: 70.8 - Outlier = False

LP4: 98.7 - Outlier = True

Final results:

$K_{SGC} = 72.8$ - $P_{max} = 18.7$

A.3.6 Summary of results from configuration involving GG1 and Angular SAggr3

Ksgc MAD = 15.4 - Pmax MAD = 1.2

Ksgc median = 55.6 - Pmax median = 16.5

If $((K_{sgc_i} - K_{sgc_median})/MAD) > 2$: outlier

If $((P_{max_i} - P_{max_median})/MAD) > 2.5$: outlier

Test 1

Pmax = 17.3 - Outlier: False - $K_{SGC} = 45.8$ - Outlier: False

Test 2

Pmax = 15.6 - Outlier: False - $K_{SGC} = 65.4$ - Outlier: False

Test 3

Pmax = 15.7 - Outlier: False - Ksgc = 44.5 - Outlier: False

Test 4

Pmax = 17.2 - Outlier: False - Ksgc = N/A - Outlier: True

Test 5

Pmax = 18.7 - Outlier: False - Ksgc = 72.8 - Outlier: False

Final results for this configuration:

Average Ksgc = 57.1 - Ksgc COV = 21.4%

Average Pmax = 16.8 - Pmax COV = 7.5%

A.4 CONFIGURATION INVOLVING GG1 AND ANGULAR WG

A.4.1 Test 1

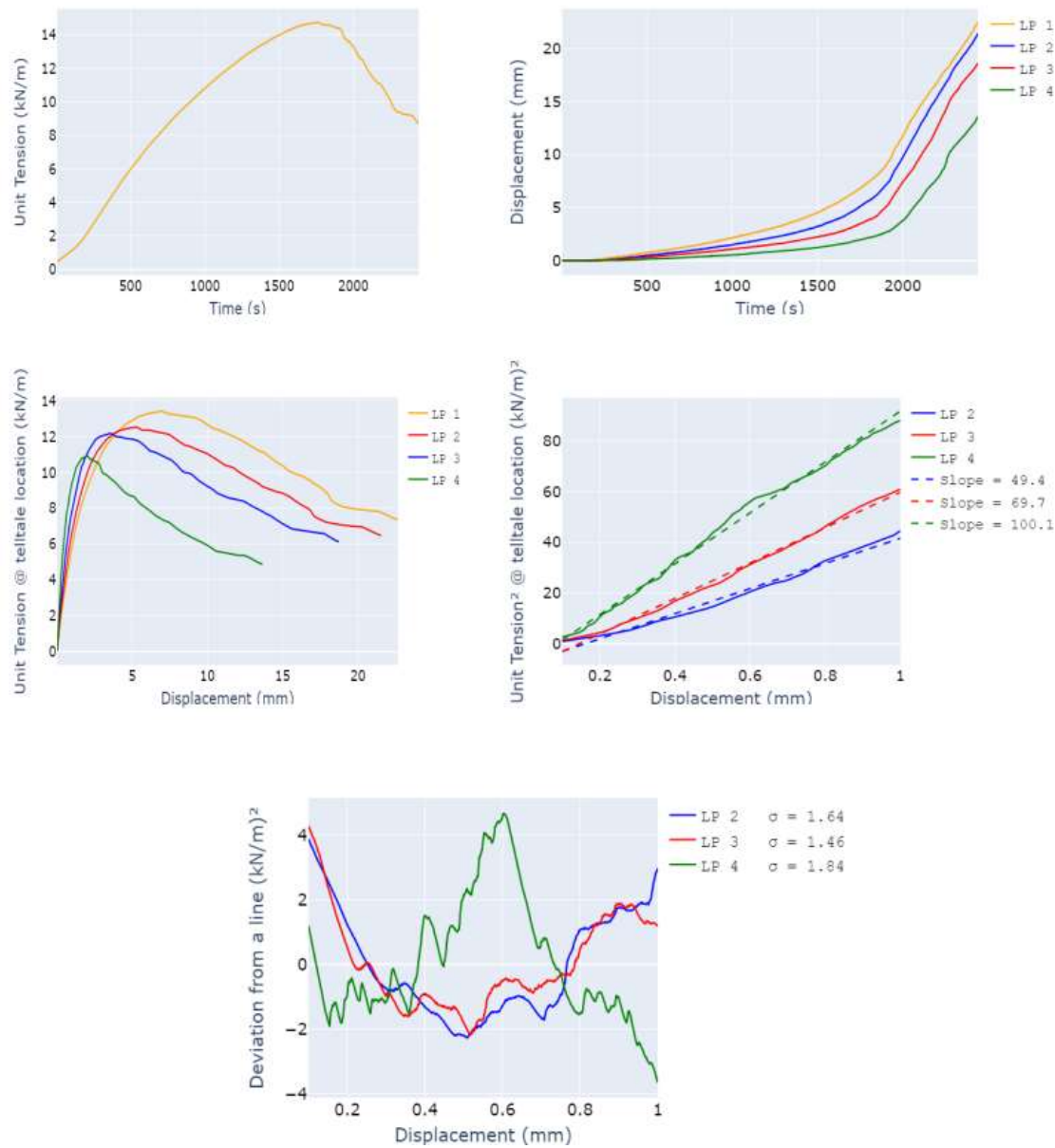


Figure A.16 - Results from the first test of configuration involving GG1 and Angular WG

LP 1: Trigger Time (sec): 133.0 - T0 (kN/m): 1.34

LP 2: Trigger Time (sec): 213.4 - T0 (kN/m): 2.23

LP 3: Trigger Time (sec): 240.0 - T0 (kN/m): 2.58

LP 4: Trigger Time (sec): 331.2 - T0 (kN/m): 3.84

Deviation from a line:

LP 2 - $sd = 1.6 \text{ (kN/m)}^2$ - Outlier: True

LP 3 - $sd = 1.4 \text{ (kN/m)}^2$ - Outlier: False

LP 4 - $sd = 1.8 \text{ (kN/m)}^2$ - Outlier: True

Ksgc values:

LP2: 49.4 - Outlier = False

LP3: 69.7 - Outlier = False

LP4: 100.1 - Outlier = True

Final results:

Ksgc = 69.7 - Pmax = 14.8

A.4.2 Test 2

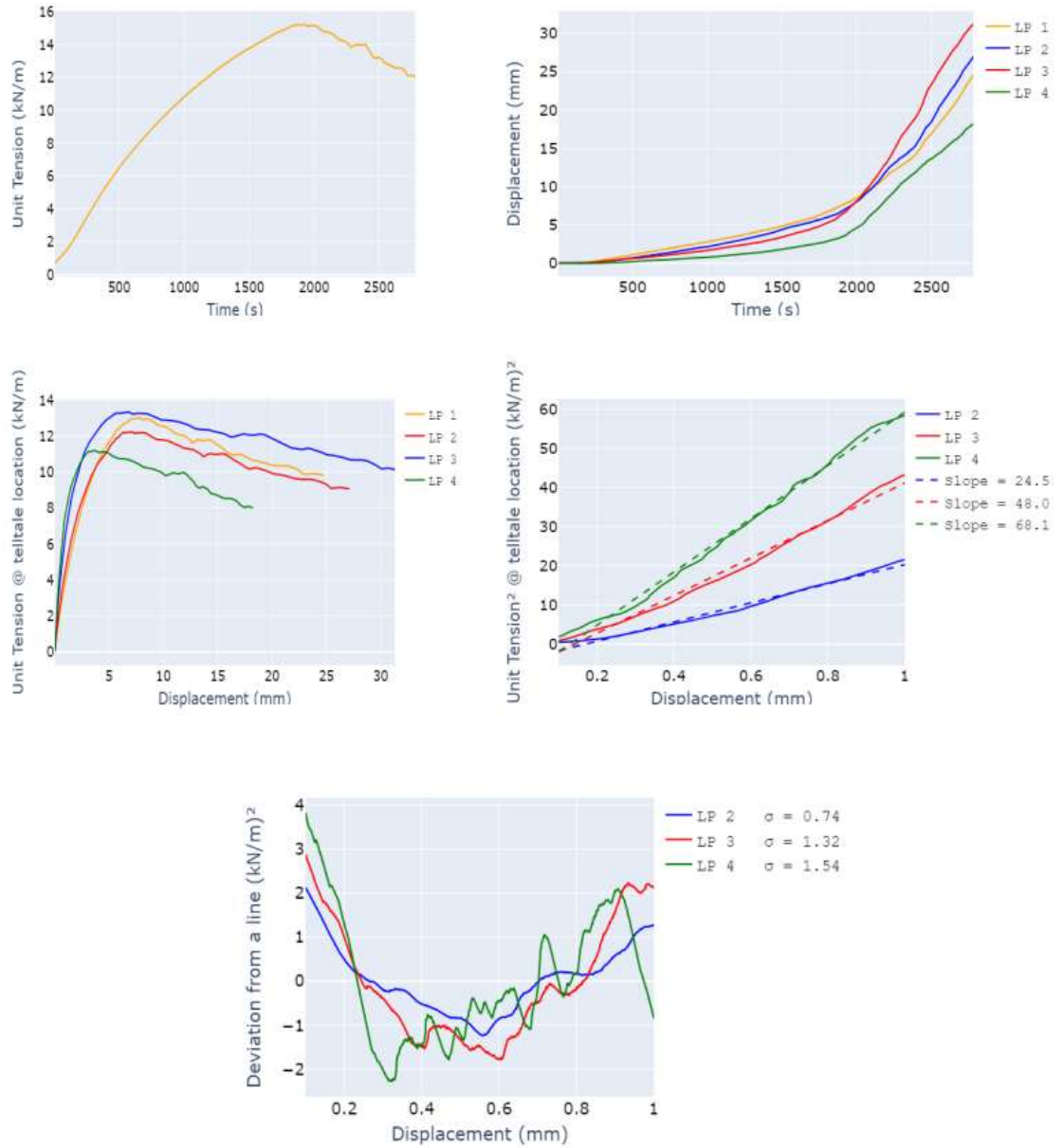


Figure A.17 - Results from the second test of configuration involving GG1 and Angular WG

LP 1: Trigger Time (sec): 157.6 - T0 (kN/m): 2.2

LP 2: Trigger Time (sec): 215.6 - T0 (kN/m): 2.9

LP 3: Trigger Time (sec): 132.6 - T0 (kN/m): 1.9

LP 4: Trigger Time (sec): 292.2 - T0 (kN/m): 4.0

Deviation from a line:

LP 2 - $sd = 0.7 \text{ (kN/m)}^2$ - Outlier: False

LP 3 - $sd = 1.3 \text{ (kN/m)}^2$ - Outlier: False

LP 4 - $sd = 1.6 \text{ (kN/m)}^2$ - Outlier: True

Ksgc values:

LP2: 24.5 - Outlier = True

LP3: 48.0 - Outlier = False

LP4: 68.1 - Outlier = False

Final results:

Ksgc = 48.0 - Pmax = 15.2

A.4.3 Test 3

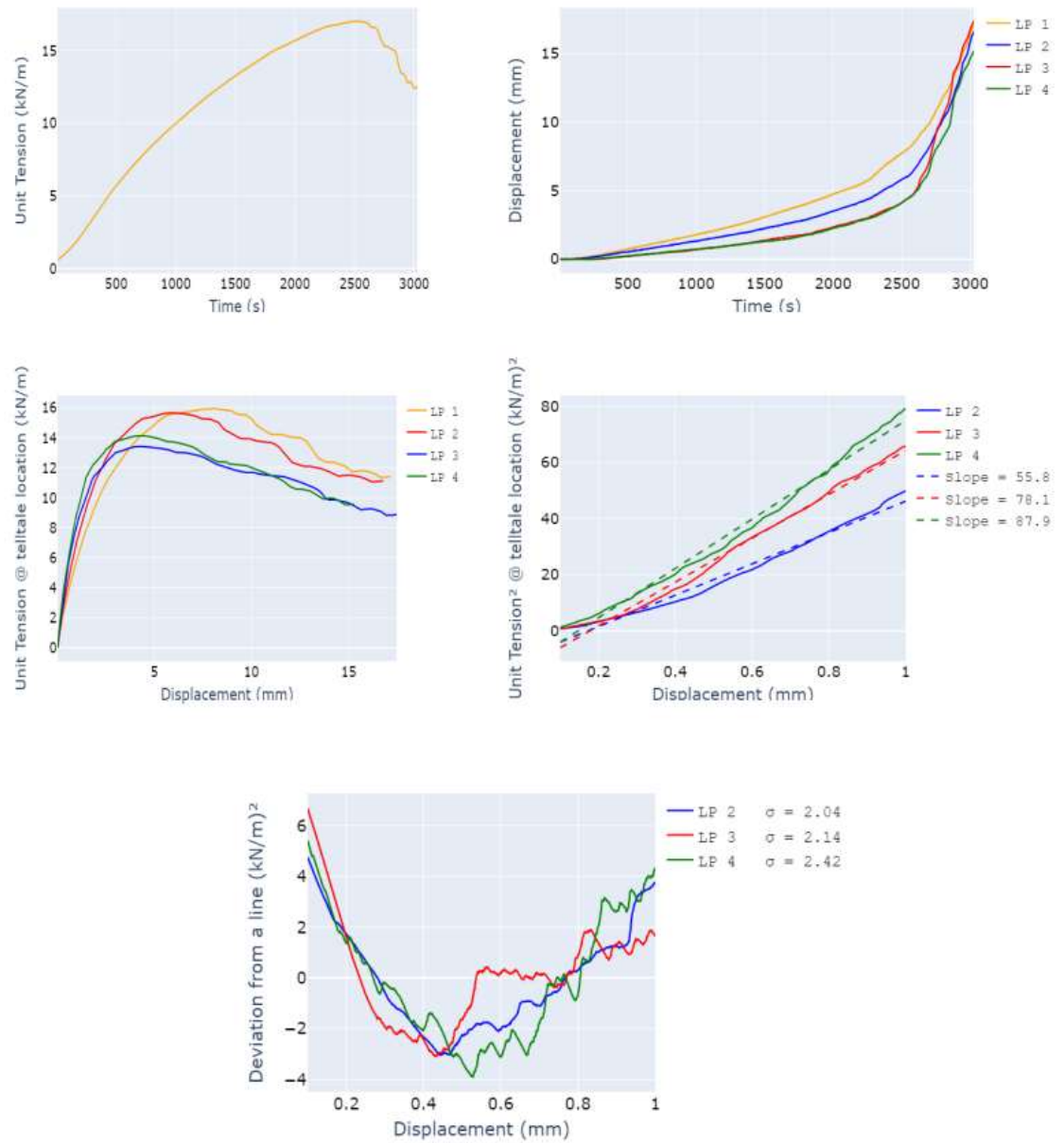


Figure A.18 - Results from the third test of configuration involving GG1 and Angular WG

LP 1: Trigger Time (sec): 75.4 - T0 (kN/m): 1.1
LP 2: Trigger Time (sec): 112.2 - T0 (kN/m): 1.3
LP 3: Trigger Time (sec): 313.0 - T0 (kN/m): 3.6
LP 4: Trigger Time (sec): 256.6 - T0 (kN/m): 2.9

Deviation from a line:

LP 2 - $sd = 2.0 \text{ (kN/m)}^2$ - Outlier: True
LP 3 - $sd = 2.1 \text{ (kN/m)}^2$ - Outlier: True
LP 4 - $sd = 2.4 \text{ (kN/m)}^2$ - Outlier: True

Ksgc values:

LP2: 55.8 - Outlier = True
LP3: 78.1 - Outlier = False
LP4: 87.9 - Outlier = False

Final results:

$Ksgc = 0$ - $Pmax = 17.0$

A.4.4 Test 4

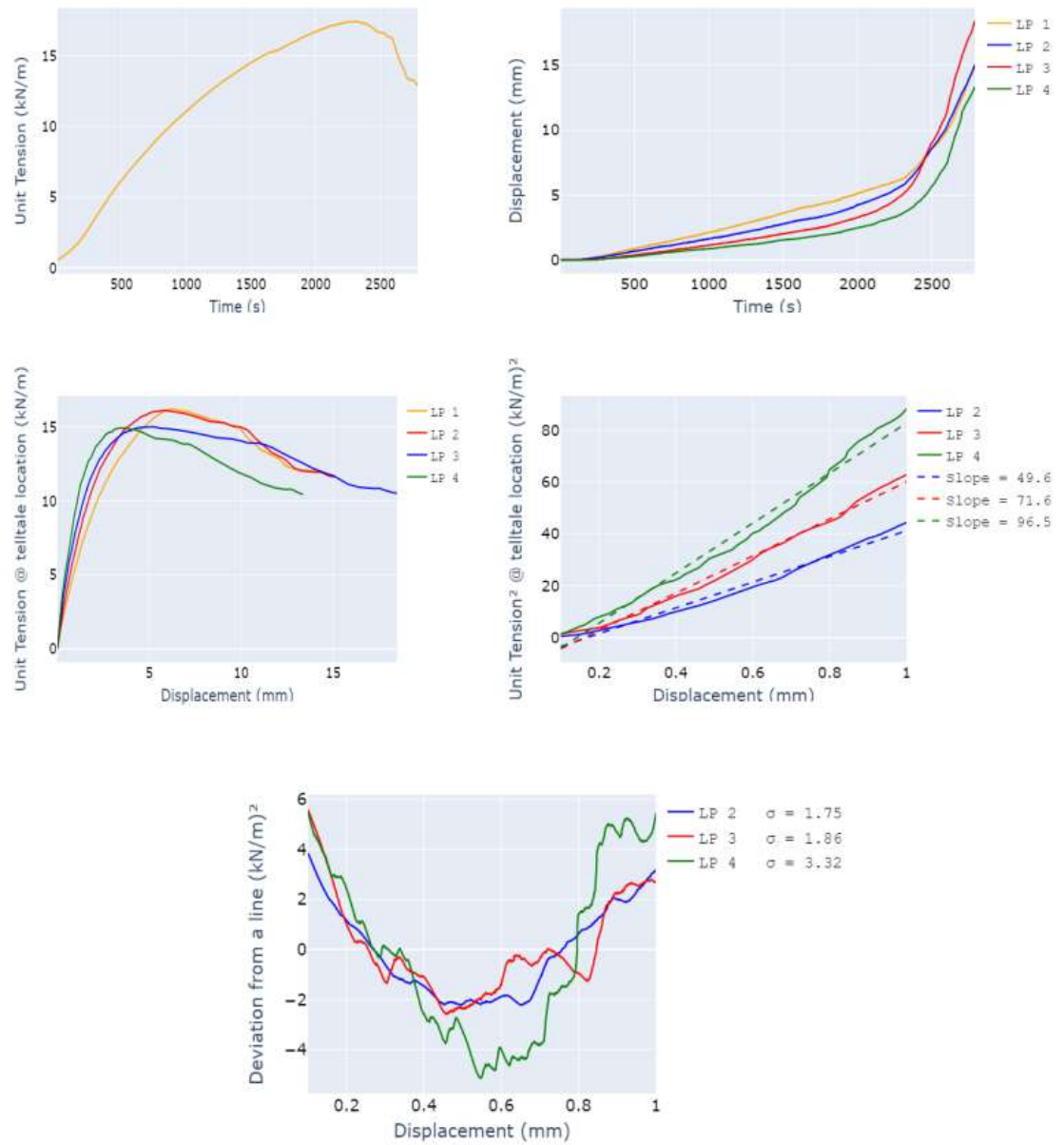


Figure A.19 - Results from the fourth test of configuration involving GG1 and Angular WG

LP 1: Trigger Time (sec): 106.6 - T0 (kN/m): 1.2

LP 2: Trigger Time (sec): 118.0 - T0 (kN/m): 1.3

LP 3: Trigger Time (sec): 219.4 - T0 (kN/m): 2.4

LP 4: Trigger Time (sec): 224.0 - T0 (kN/m): 2.5

Deviation from a line:

LP 2 - sd = 1.75 - Outlier: True

LP 3 - sd = 1.86 - Outlier: True

LP 4 - sd = 3.32 - Outlier: True

Ksgc values:

LP2: 49.6 - Outlier = False

LP3: 71.6 - Outlier = False

LP4: 96.5 - Outlier = True

Final results:

Ksgc = 0 - Pmax = 17.44

A.4.5 Test 5

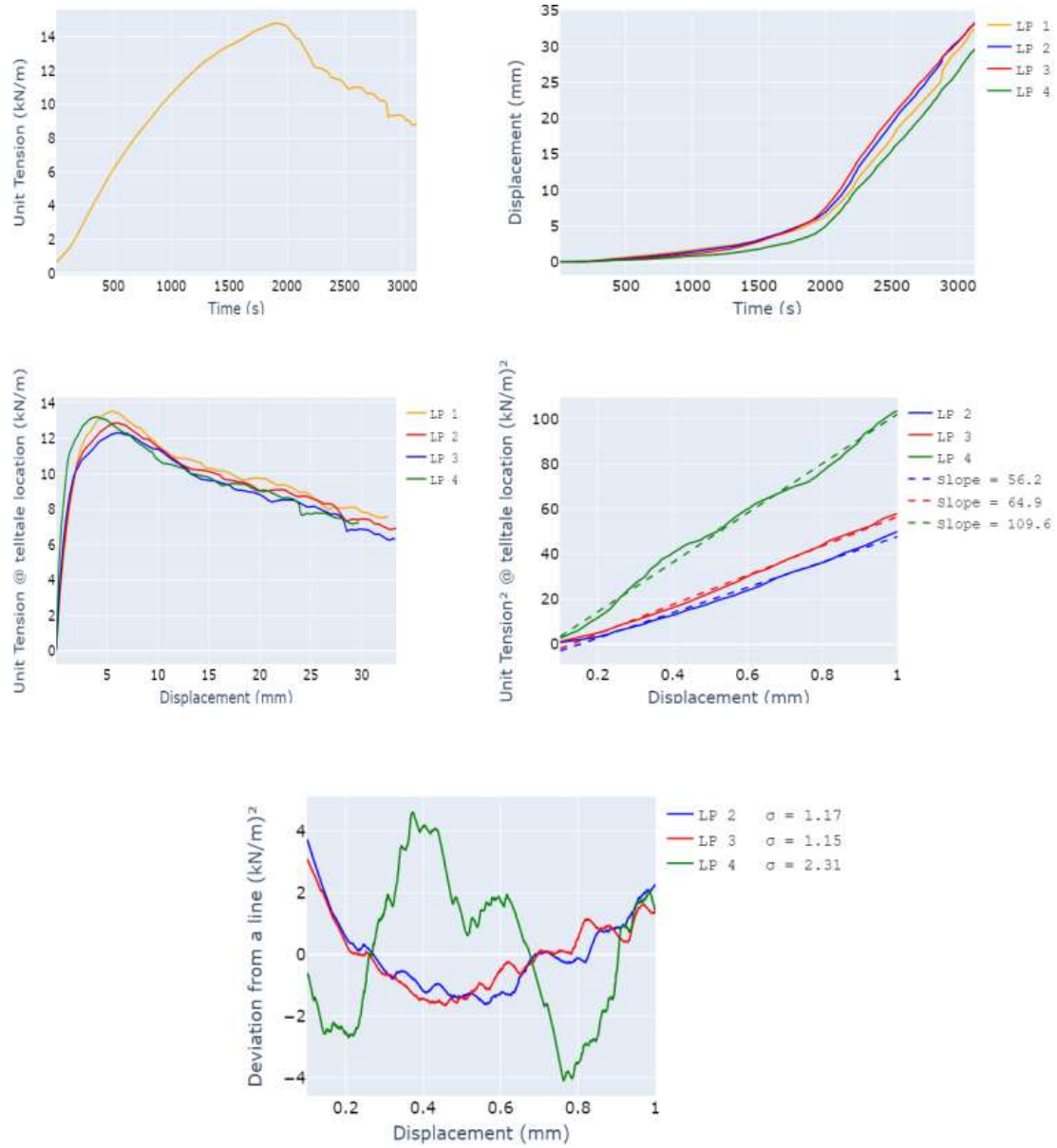


Figure A.20 - Results from the fifth test of configuration involving GG1 and Angular WG

LP 1: Trigger Time (sec): 92.6 - T0 (kN/m): 1.3
LP 2: Trigger Time (sec): 159.0 - T0 (kN/m): 1.9
LP 3: Trigger Time (sec): 205.8 - T0 (kN/m): 2.5
LP 4: Trigger Time (sec): 128.2 - T0 (kN/m): 1.59

Deviation from a line:

LP 2 - sd = 1.17 - Outlier: False
LP 3 - sd = 1.15 - Outlier: False
LP 4 - sd = 2.31 - Outlier: True

Ksgc values:

LP2: 56.2 - Outlier = False
LP3: 64.9 - Outlier = False
LP4: 109.6 - Outlier = True

Final results:

Ksgc = 64.64 - Pmax = 14.82

A.4.6 Summary of results from configuration involving GG1 and Angular SAggr3

Ksgc MAD = 7.5 - Pmax MAD = 0.1

Ksgc median = 64.6 - Pmax median = 14.8

If $((Ksgc_i - Ksgc_median)/MAD) > 2$: outlier

If $((Pmax_i - Pmax_median)/MAD) > 2.5$: outlier

Test 1

Pmax = 14.8 - Outlier: False - Ksgc = 69.7 - Outlier : False

Test 2

Pmax = 15.2 - Outlier: True - Ksgc = 48.0 - Outlier : True

Test 3

Pmax = 17.0 - Outlier: True - Ksgc = N/A - Outlier : True

Test 4

Pmax = 17.4 - Outlier: True - Ksgc = N/A - Outlier : True

Test 5

Pmax = 14.8 - Outlier: False - Ksgc = 64.6 - Outlier : False

Final results for this configuration:

Average Ksgc = 67.18 - Ksgc COV = 3.8%

Average Pmax = 14.78 - Pmax COV = 0.2%

A.5 CONFIGURATION INVOLVING GG1 AND 50-50 SAGGR2

A.5.1 Test 1

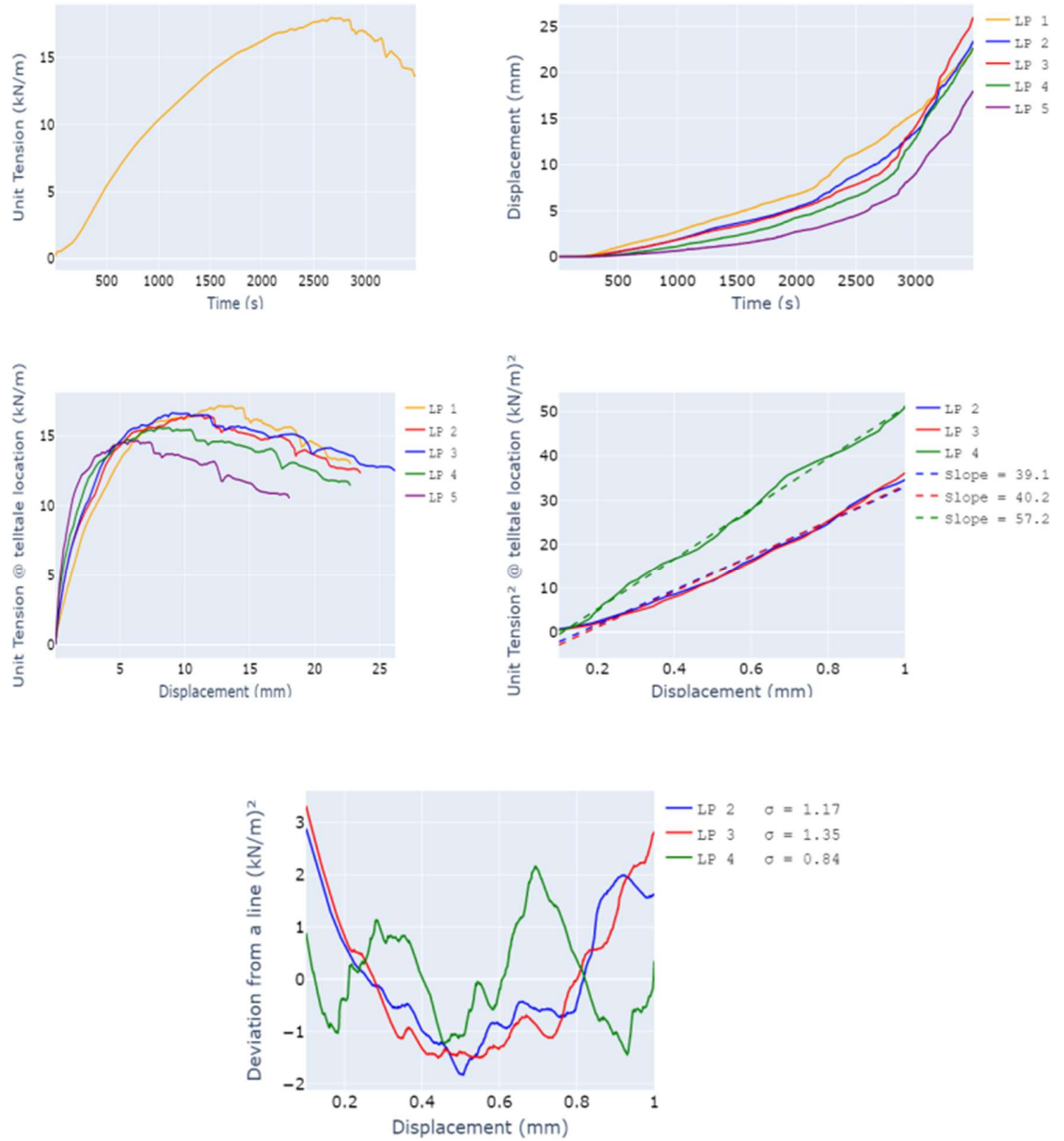


Figure A.21 - Results from the first test of configuration involving GG1 and 50-50 SAGgr2

LP 1: Trigger Time (sec): 110.2 - T0 (kN/m): 0.8

LP 2: Trigger Time (sec): 200.6 - T0 (kN/m): 1.5

LP 3: Trigger Time (sec): 184.6 - T0 (kN/m): 1.3

LP 4: Trigger Time (sec): 276.0 - T0 (kN/m): 2.4

LP 5: Trigger Time (sec): 340.4 - T0 (kN/m): 3.3

Deviation from a line:

LP 2 - sd = 1.2 - Outlier: False

LP 3 - sd = 1.4 - Outlier: False

LP 4 - sd = 0.8 - Outlier: False

Ksgc values:

LP2: 39.1 - Outlier = False

LP3: 40.2 - Outlier = False

LP4: 57.2 - Outlier = True

Final results:

Ksgc = 40.4 - Pmax = 17.9

A.5.2 Test 2

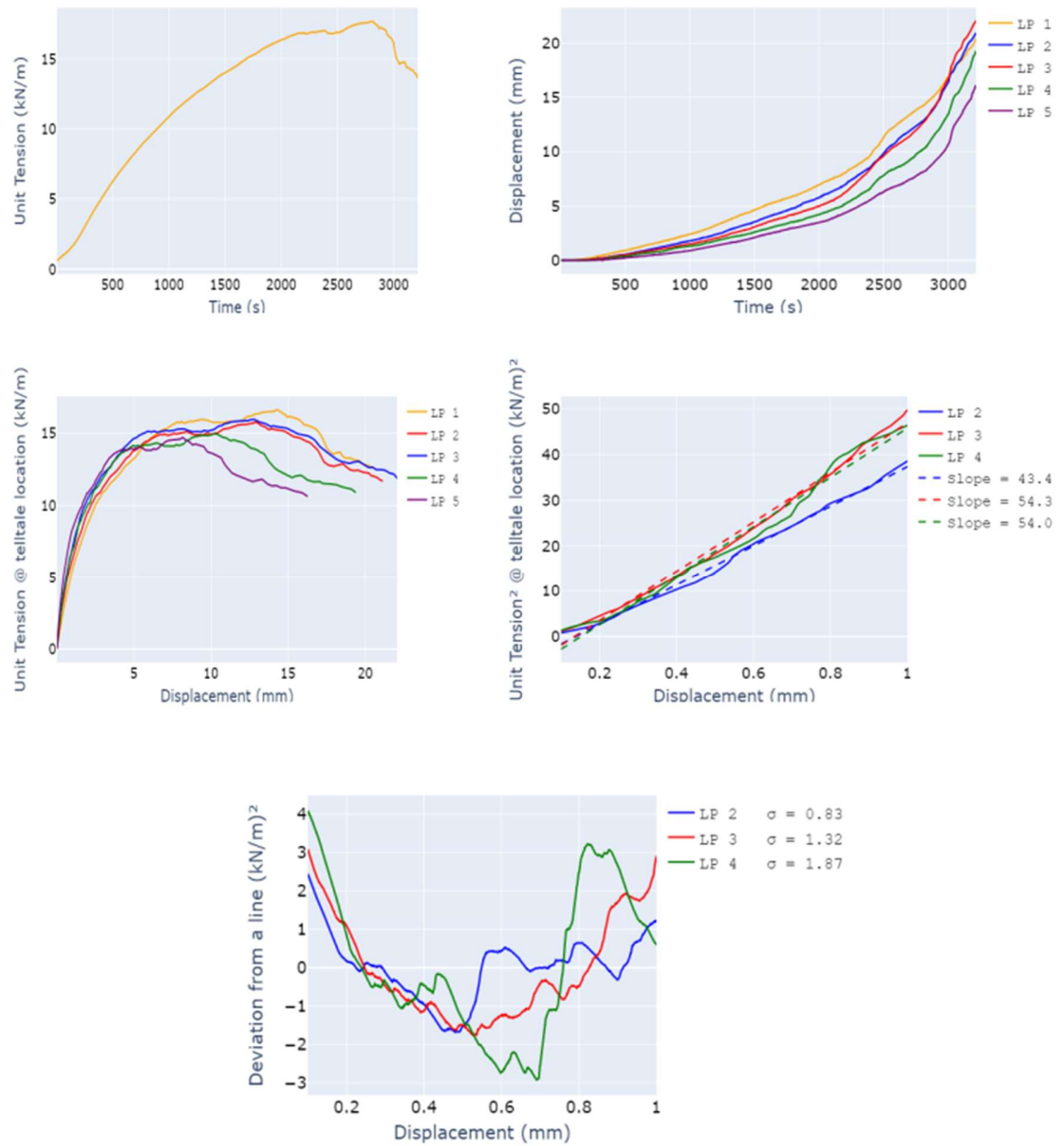


Figure A.22 - Results from the second test of configuration involving GG1 and 50-50 SAggr2

LP 1: Trigger Time (sec): 80.2 - T0 (kN/m): 1.1
LP 2: Trigger Time (sec): 173.8 - T0 (kN/m): 2.0
LP 3: Trigger Time (sec): 156.2 - T0 (kN/m): 1.8
LP 4: Trigger Time (sec): 232.2 - T0 (kN/m): 2.7
LP 5: Trigger Time (sec): 251.4 - T0 (kN/m): 3.0

Deviation from a line:

LP 2 - sd = 0.83 - Outlier: False
LP 3 - sd = 1.32 - Outlier: False
LP 4 - sd = 1.87 - Outlier: True

Ksgc values:

LP2: 43.4 - Outlier = False
LP3: 54.3 - Outlier = False
LP4: 54.0 - Outlier = False

Final results:

Ksgc = 54.93 - Pmax = 17.71

A.5.3 Test 3

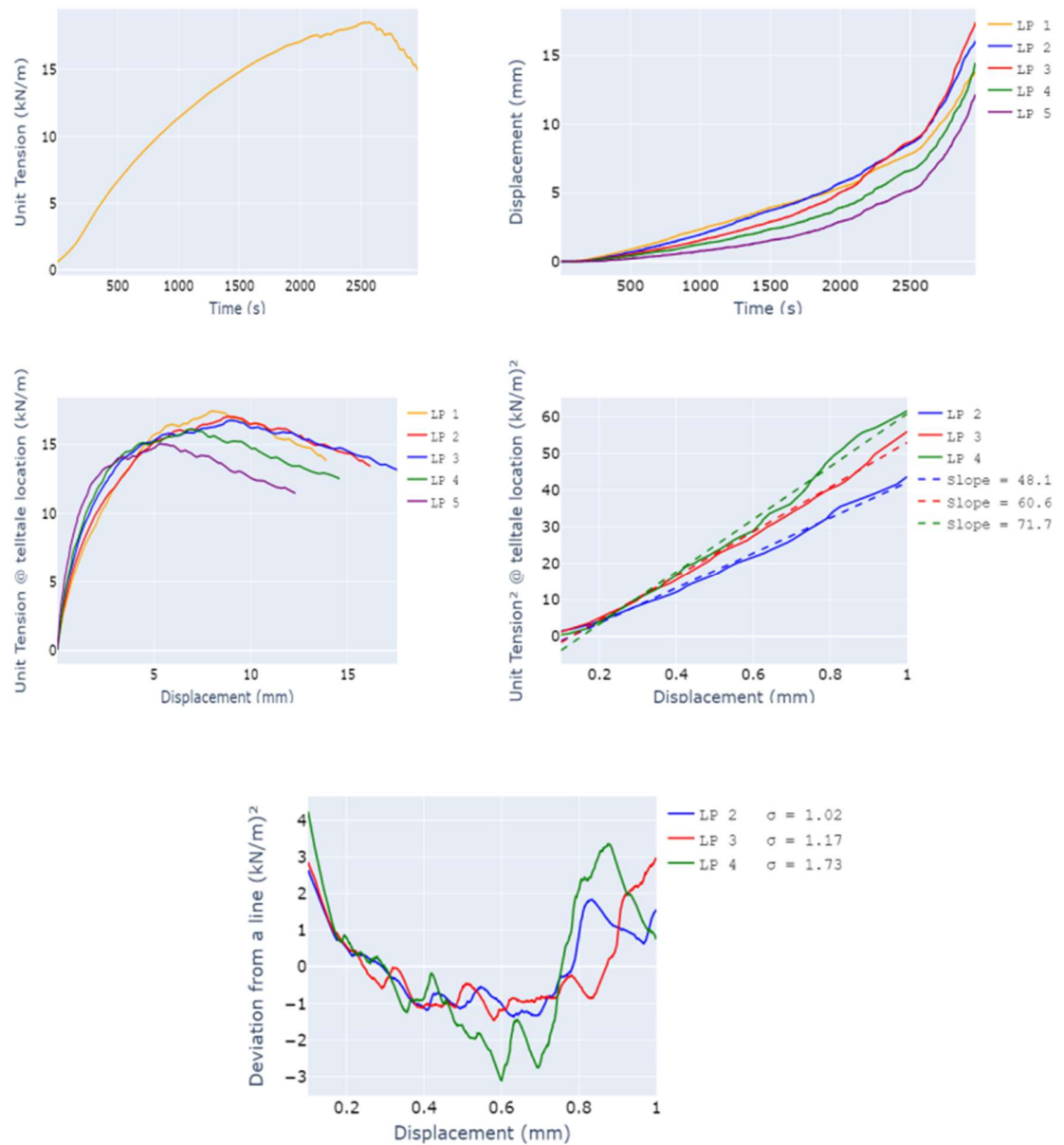


Figure A.23 - Results from the third test of configuration involving GG1 and 50-50 SAggr2

LP 1: Trigger Time (sec): 71.4 - T0 (kN/m): 1.1
LP 2: Trigger Time (sec): 114.6 - T0 (kN/m): 1.5
LP 3: Trigger Time (sec): 140.0 - T0 (kN/m): 1.8
LP 4: Trigger Time (sec): 191.0 - T0 (kN/m): 2.4
LP 5: Trigger Time (sec): 259.2 - T0 (kN/m): 3.5

Deviation from a line:

LP 2 - sd = 1.0 - Outlier: False
LP 3 - sd = 1.2 - Outlier: False
LP 4 - sd = 1.7 - Outlier: True

Ksgc values:

LP2: 48.1 - Outlier = False
LP3: 60.6 - Outlier = False
LP4: 71.7 - Outlier = False

Final results:

Ksgc = 61.8 - Pmax = 18.5

A.5.4 Test 4

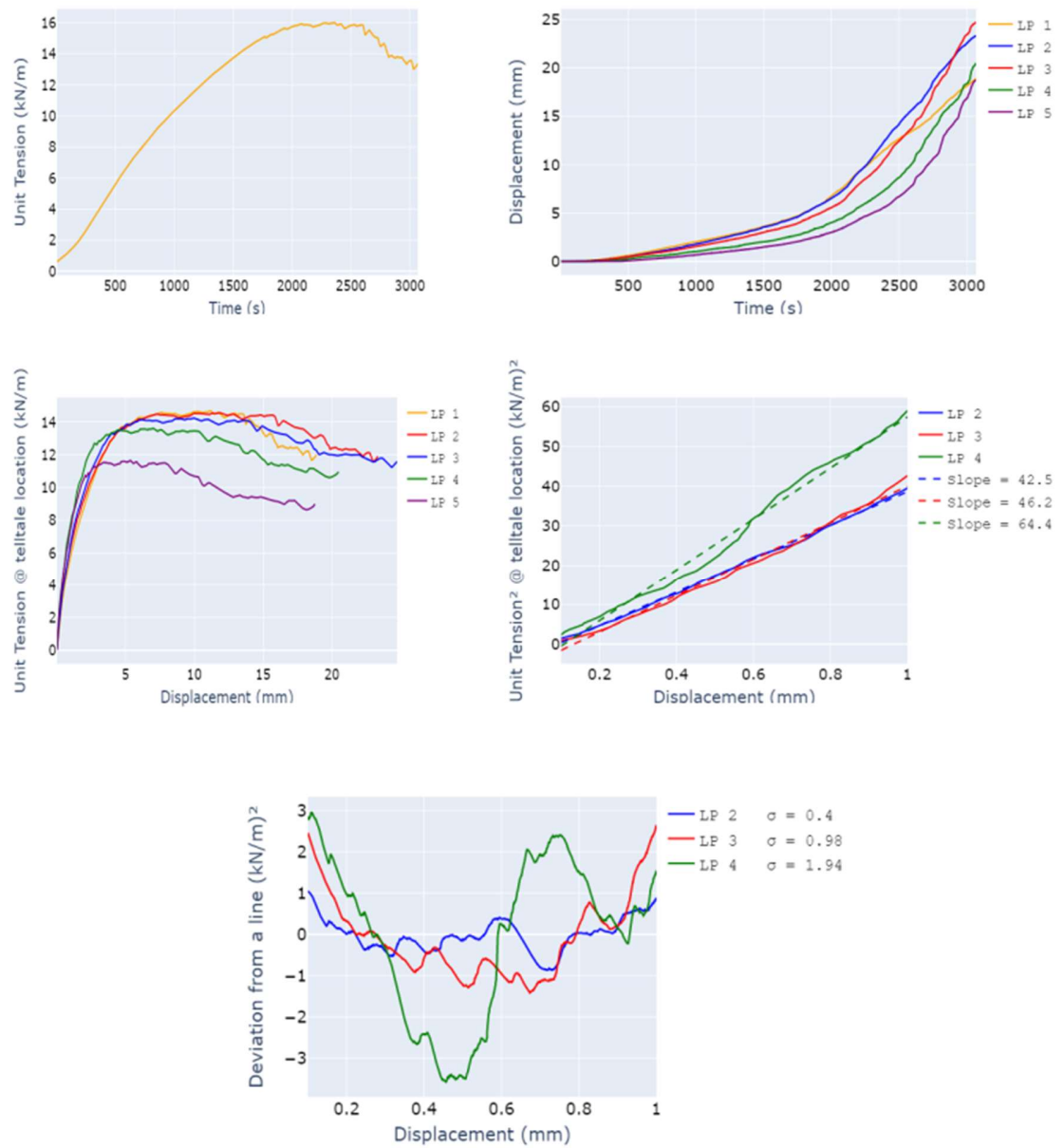


Figure A.24 - Results from the fourth test of configuration involving GG1 and 50-50 SAggr2

LP 1: Trigger Time (sec): 117.6 - T0 (kN/m): 1.3

LP 2: Trigger Time (sec): 130.4 - T0 (kN/m): 1.4

LP 3: Trigger Time (sec): 170.4 - T0 (kN/m): 1.8

LP 4: Trigger Time (sec): 231.8 - T0 (kN/m): 2.4

LP 5: Trigger Time (sec): 395.4 - T0 (kN/m): 4.4

Deviation from a line:

LP 2 - sd = 0.4 - Outlier: False

LP 3 - sd = 0.98 - Outlier: False

LP 4 - sd = 1.94 - Outlier: True

Ksgc values:

LP2: 42.5 - Outlier = False

LP3: 46.2 - Outlier = False

LP4: 64.4 - Outlier = True

Final results:

Ksgc = 46.11 - Pmax = 16.03

A.5.5 Test 5

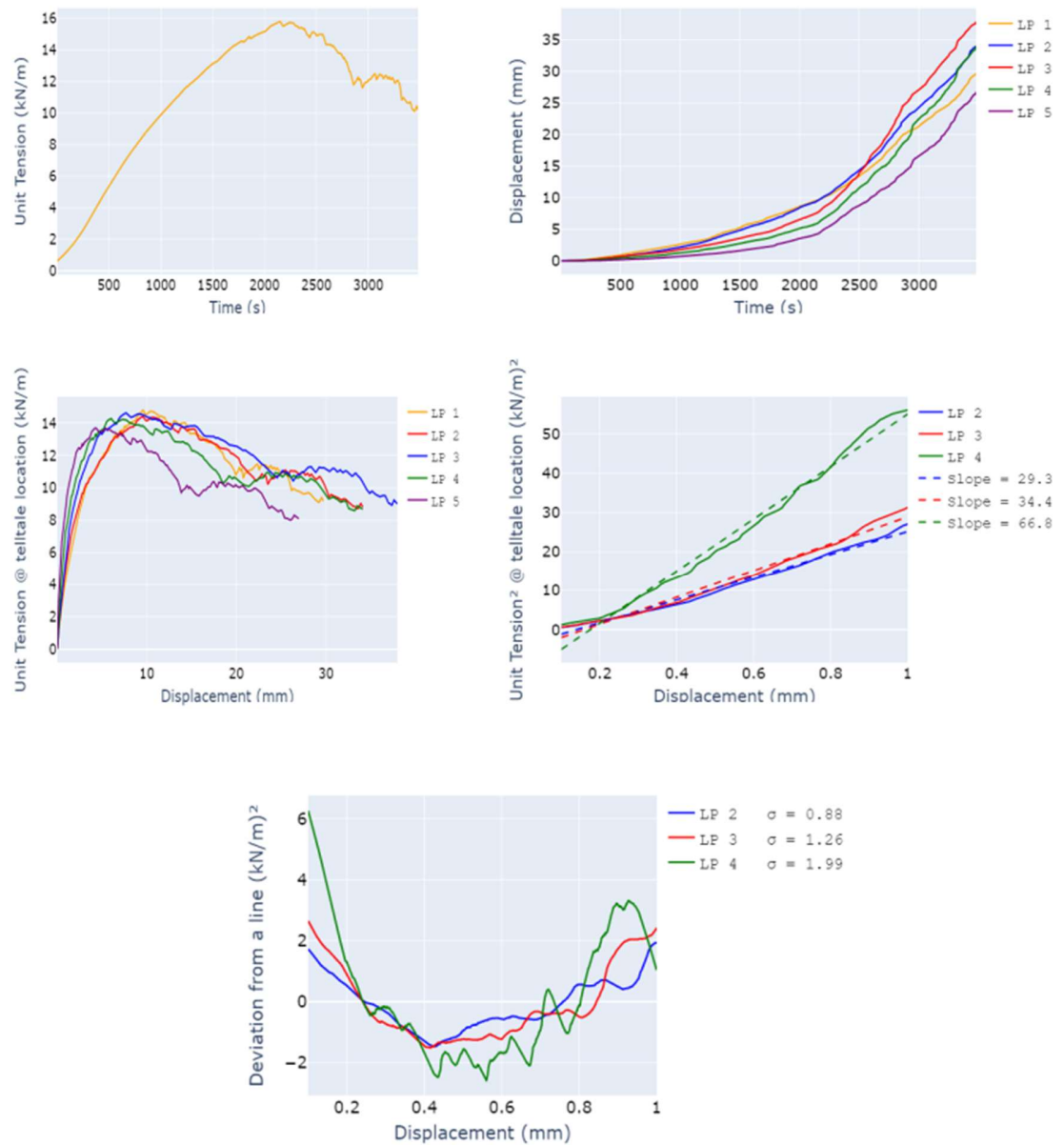


Figure A.25 - Results from the fifth test of configuration involving GG1 and 50-50 SAggr2

LP 1: Trigger Time (sec): 66.2 - T0 (kN/m): 1.0

LP 2: Trigger Time (sec): 120.6 - T0 (kN/m): 1.3

LP 3: Trigger Time (sec): 91.8 - T0 (kN/m): 1.2

LP 4: Trigger Time (sec): 137.4 - T0 (kN/m): 1.5

LP 5: Trigger Time (sec): 203.2 - T0 (kN/m): 2.1

Deviation from a line:

LP 2 - sd = 0.9 - Outlier: False

LP 3 - sd = 1.3 - Outlier: False

LP 4 - sd = 2.0 - Outlier: True

Ksgc values:

LP2: 29.3 - Outlier = False

LP3: 34.4 - Outlier = False

LP4: 66.8 - Outlier = True

Final results:

Ksgc = 36.9 - Pmax = 15.8

A.5.6 Summary of results from configuration involving GG1 and 50-50 SAggr2

Ksgc MAD = 13.1 - Pmax MAD = 1.2

Ksgc meadin = 46.1 - Pmax median = 17.7

If $((Ksgc_i - Ksgc_meadian)/MAD) > 2$: outlier

If $((Pmax_i - Pmax_meadian)/MAD) > 2.5$: outlier

Test 1

Pmax = 17.9 - Outlier: False - Ksgc = 40.4 - Outlier : False

Test 2

Pmax = 17.7 - Outlier: False - Ksgc = 54.9 - Outlier : False

Test 3

Pmax = 18.5 - Outlier: False - Ksgc = 62.0 - Outlier : False

Test 4

Pmax = 16.0 - Outlier: False - Ksgc = 46.1 - Outlier : False

Test 5

Pmax = 15.8 - Outlier: False - Ksgc = 36.9 - Outlier : False

Final results for this configuration:

Average Ksgc = 48.1 - Ksgc COV = 19.2%

Average Pmax = 17.2 - Pmax COV = 6.3%

A.6 CONFIGURATION INVOLVING GG2 AND ROUND SAGGR2

A.6.1 Test 1

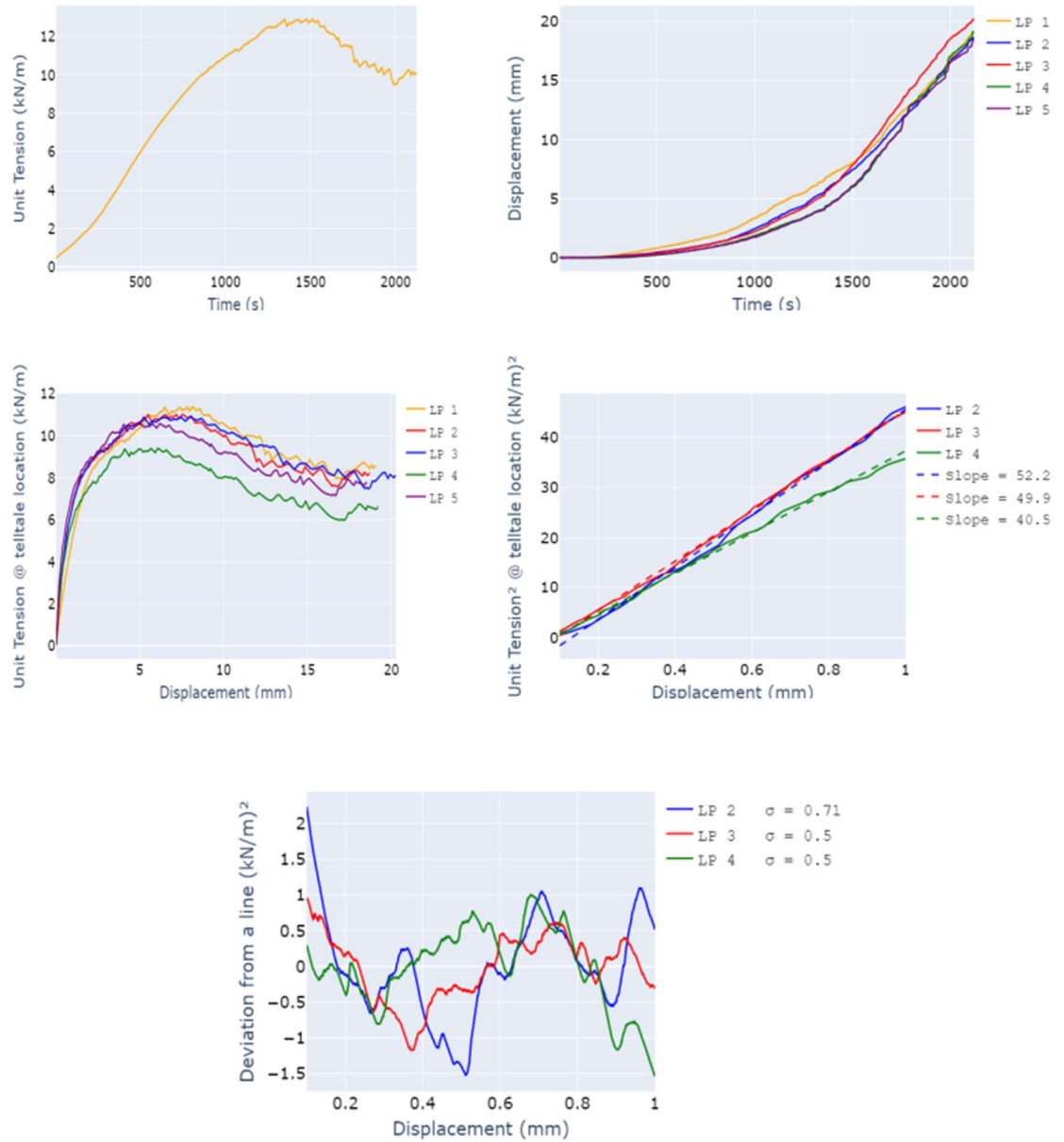


Figure A.26 - Results from the first test of configuration involving GG2 and Round SAggr2

LP 1: Trigger Time (sec): 146.2 - T0 (kN/m): 1.5

LP 2: Trigger Time (sec): 187.8 - T0 (kN/m): 1.9

LP 3: Trigger Time (sec): 199.4 - T0 (kN/m): 2.0

LP 4: Trigger Time (sec): 324.6 - T0 (kN/m): 3.5

LP 5: Trigger Time (sec): 229.8 - T0 (kN/m): 2.3

Deviation from a line:

LP 2 - sd = 0.71 - Outlier: False

LP 3 - sd = 0.5 - Outlier: False

LP 4 - sd = 0.5 - Outlier: False

Ksgc values:

LP2: 52.2 - Outlier = False

LP3: 49.9 - Outlier = False

LP4: 40.5 - Outlier = False

Final results:

Ksgc = 52.16 - Pmax = 12.9

A.6.2 Test 2

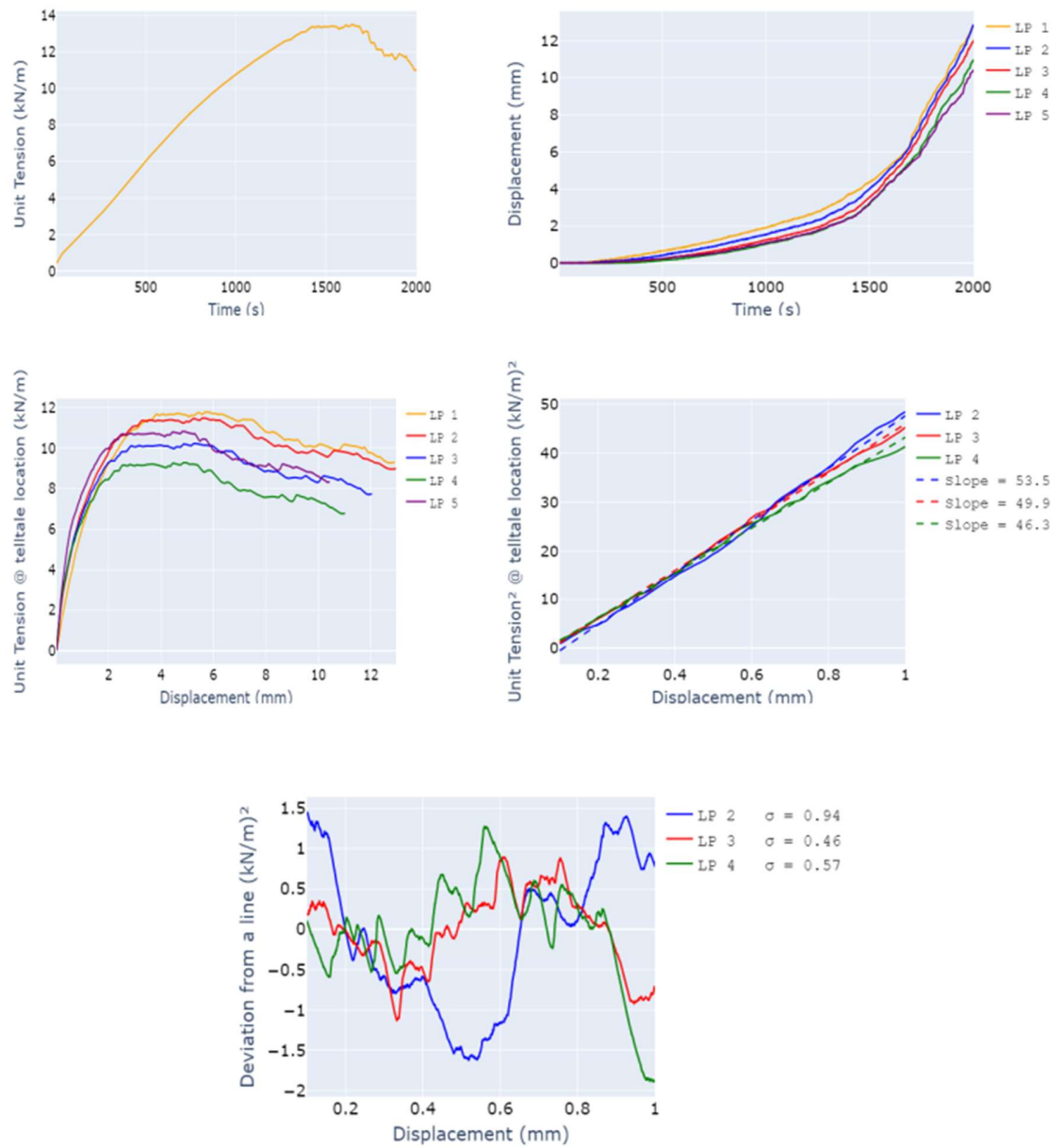


Figure A.27 - Results from the second test of configuration involving GG2 and Round SAggr2

LP 1: Trigger Time (sec): 113.8 - T0 (kN/m): 1.73

LP 2: Trigger Time (sec): 144.4 - T0 (kN/m): 2.03

LP 3: Trigger Time (sec): 265.6 - T0 (kN/m): 3.28

LP 4: Trigger Time (sec): 347.8 - T0 (kN/m): 4.22

LP 5: Trigger Time (sec): 209.0 - T0 (kN/m): 2.69

Deviation from a line:

LP 2 - sd = 0.94 - Outlier: False

LP 3 - sd = 0.46 - Outlier: False

LP 4 - sd = 0.57 - Outlier: False

Ksgc values:

LP2: 53.5 - Outlier = False

LP3: 49.9 - Outlier = False

LP4: 46.3 - Outlier = False

Final results:

Ksgc = 53.67 - Pmax = 13.5

A.6.3 Test 3

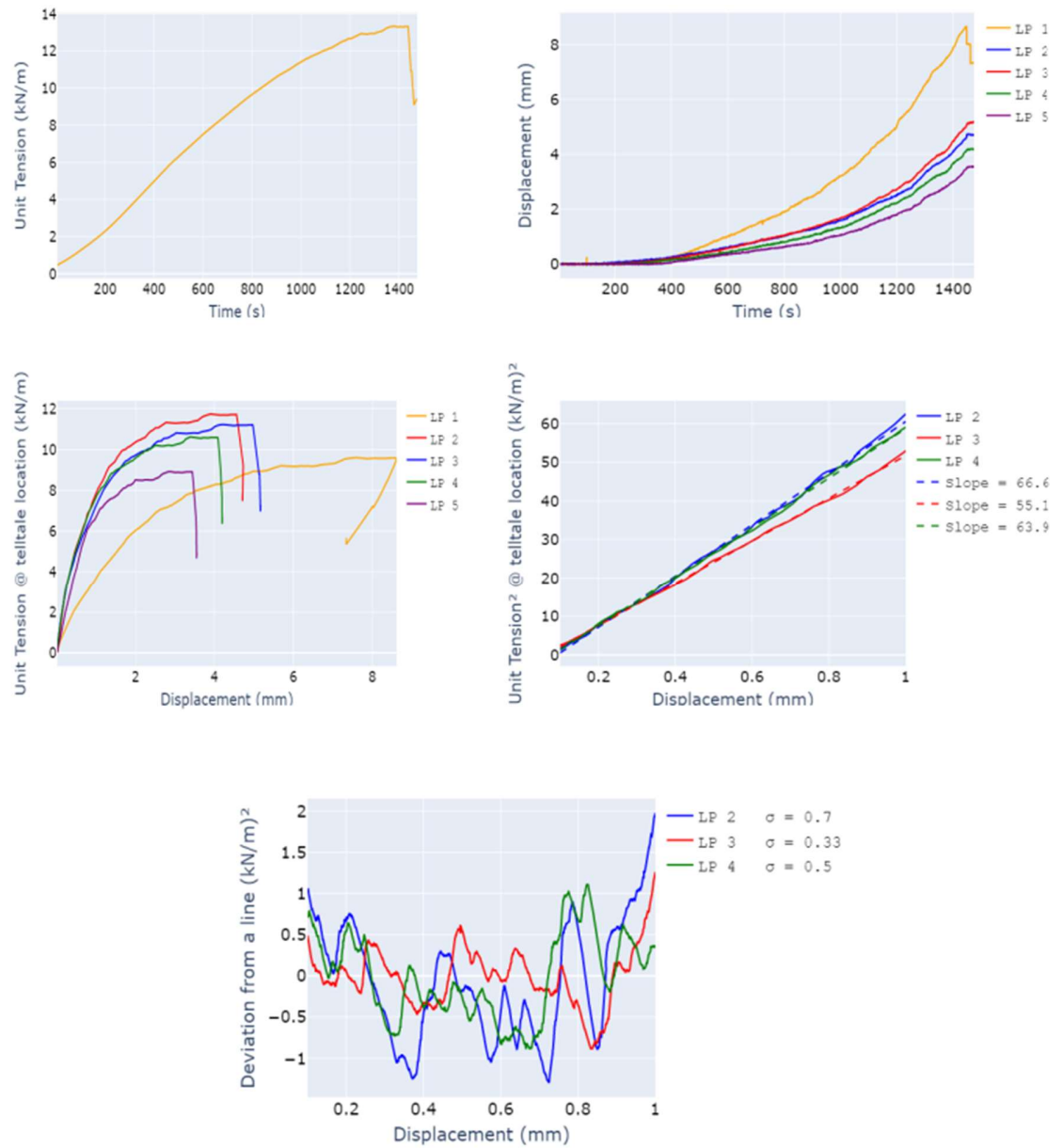


Figure A.28 - Results from the third test of configuration involving GG2 and Round SAggr2

LP 1: Trigger Time (sec): 310.6 - T0 (kN/m): 3.73

LP 2: Trigger Time (sec): 135.6 - T0 (kN/m): 1.61

LP 3: Trigger Time (sec): 185.6 - T0 (kN/m): 2.12

LP 4: Trigger Time (sec): 236.0 - T0 (kN/m): 2.73

LP 5: Trigger Time (sec): 359.6 - T0 (kN/m): 4.42

Deviation from a line:

LP 2 - sd = 0.7 - Outlier: False

LP 3 - sd = 0.33 - Outlier: False

LP 4 - sd = 0.5 - Outlier: False

Ksgc values:

LP2: 66.6 - Outlier = False

LP3: 55.1 - Outlier = False

LP4: 63.9 - Outlier = False

Final results:

Ksgc = 63.13 - Pmax = 13.35

A.6.4 Test 4

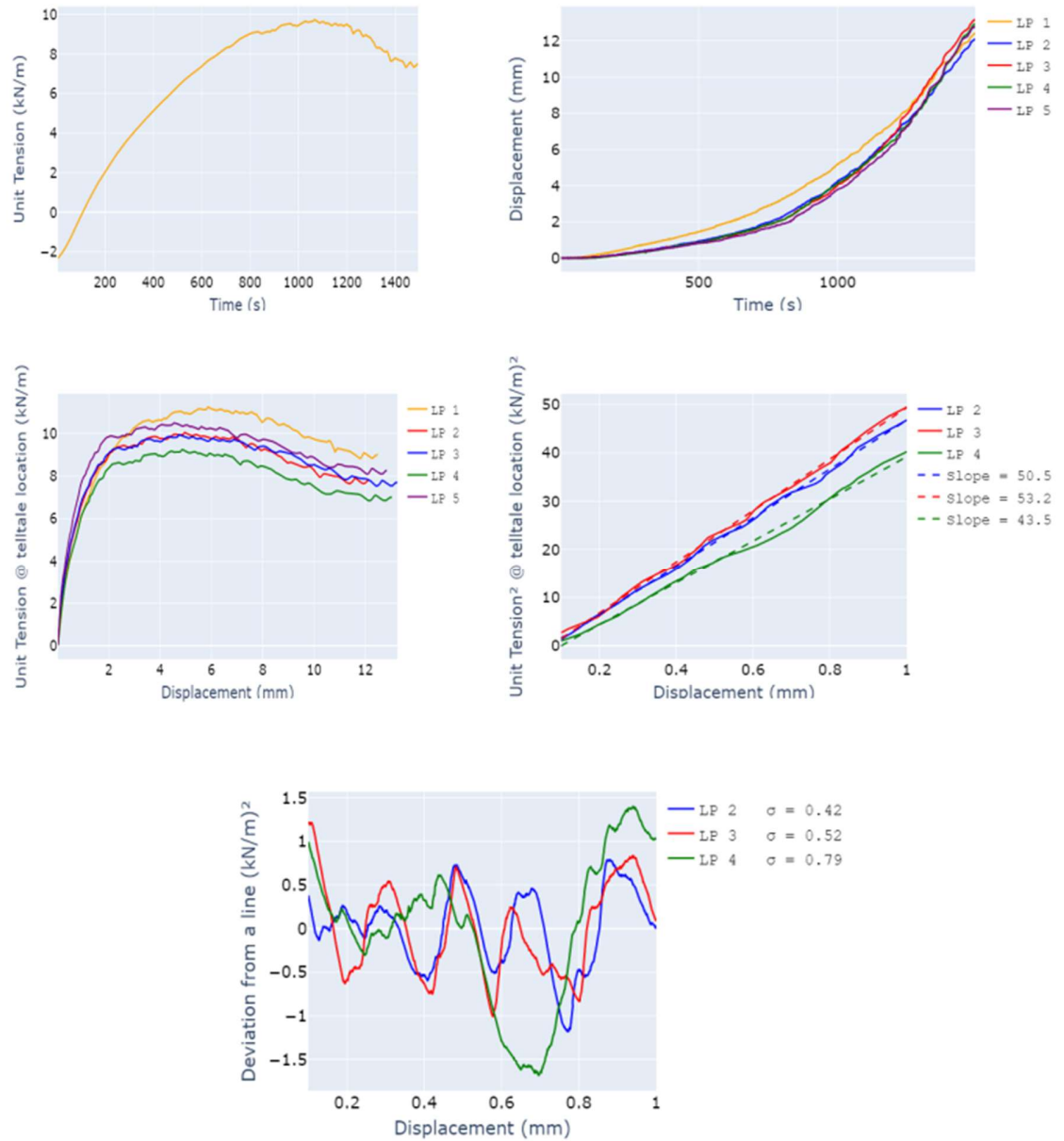


Figure 29 - Results from the fourth test of configuration involving GG2 and Round SAggr2

LP 1: Trigger Time (sec): 48.8 - T0 (kN/m): -1.51

LP 2: Trigger Time (sec): 95.4 - T0 (kN/m): -0.32

LP 3: Trigger Time (sec): 99.4 - T0 (kN/m): -0.21

LP 4: Trigger Time (sec): 127.2 - T0 (kN/m): 0.48

LP 5: Trigger Time (sec): 78.0 - T0 (kN/m): -0.77

Deviation from a line:

LP 2 - sd = 0.42 - Outlier: False

LP 3 - sd = 0.52 - Outlier: False

LP 4 - sd = 0.79 - Outlier: False

Ksgc values:

LP2: 50.5 - Outlier = False

LP3: 53.2 - Outlier = False

LP4: 43.5 - Outlier = False

Final results:

Ksgc = 52.23 - Pmax = 9.73

A.6.5 Test 5

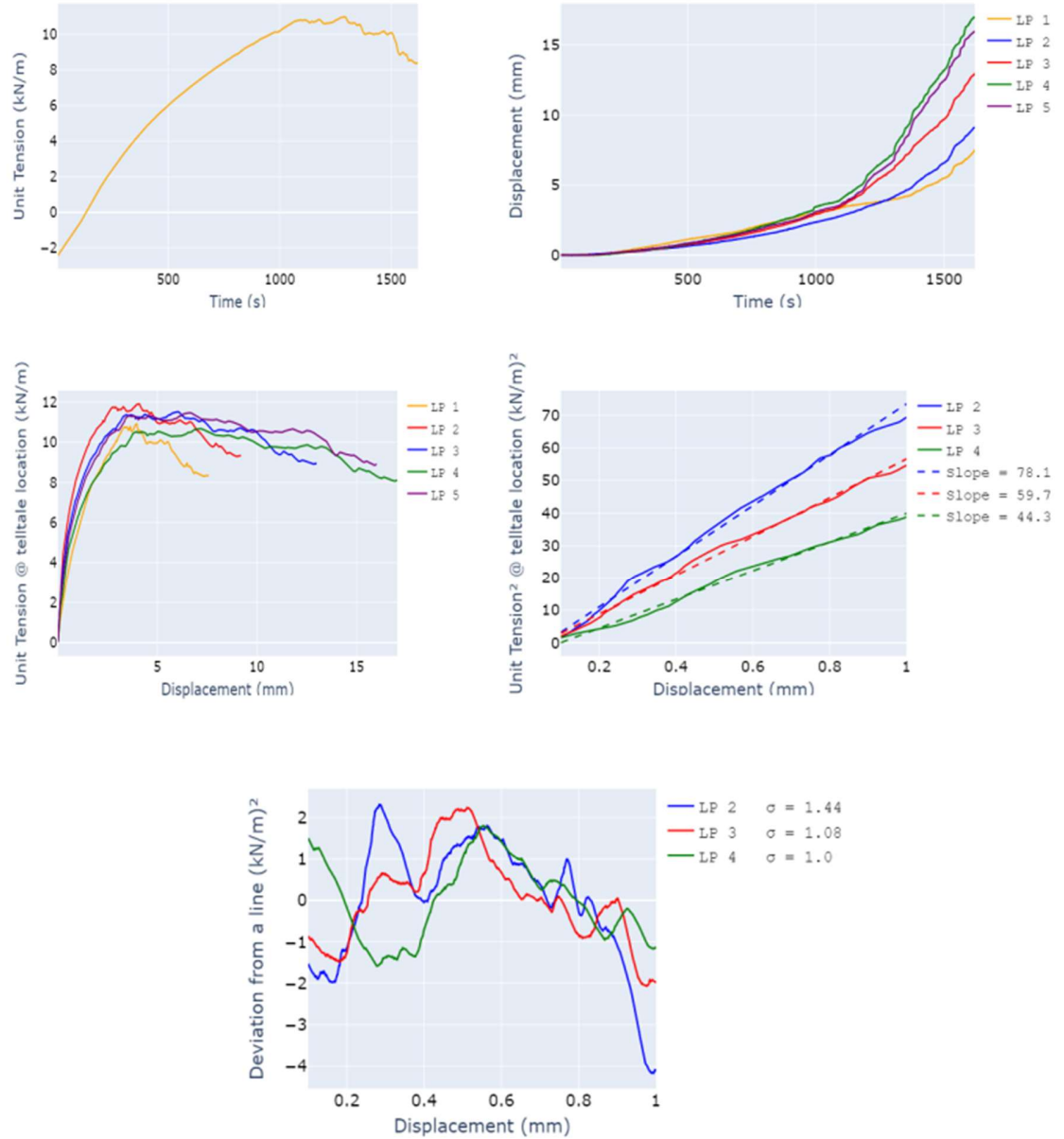


Figure A.30 - Results from the fifth test of configuration involving GG2 and Round SAggr2

LP 1: Trigger Time (sec): 134.4 - T0 (kN/m): 0.1
LP 2: Trigger Time (sec): 88.4 - T0 (kN/m): -0.9
LP 3: Trigger Time (sec): 108.0 - T0 (kN/m): -0.5
LP 4: Trigger Time (sec): 145.0 - T0 (kN/m): 0.31
LP 5: Trigger Time (sec): 110.2 - T0 (kN/m): -0.48

Deviation from a line:

LP 2 - sd = 1.44 - Outlier: False
LP 3 - sd = 1.08 - Outlier: False
LP 4 - sd = 1.0 - Outlier: False

Ksgc values:

LP2: 78.1 - Outlier = True
LP3: 59.7 - Outlier = False
LP4: 44.3 - Outlier = False

Final results:

Ksgc = 70.7 - Pmax = 10.98

A.6.6 Summary of results from configuration involving GG2 and Round SAggr2

Ksgc MAD = 2.2 - Pmax MAD = 0.9

Ksgc median = 53.7 - Pmax median = 12.9

If $((Ksgc_i - Ksgc_median)/MAD) > 2$: outlier

If $((Pmax_i - Pmax_median)/MAD) > 2.5$: outlier

Test 1

Pmax = 12.9 - Outlier: False - Ksgc = 52.16 - Outlier: False

Test 2

Pmax = 13.5 - Outlier: False - Ksgc = 53.67 - Outlier: False

Test 3

Pmax = 13.35 - Outlier: False - Ksgc = 63.13 - Outlier: True

Test 4

Pmax = 9.73 - Outlier: True - Ksgc = 52.23 - Outlier: False

Test 5

Pmax = 10.98 - Outlier: False - Ksgc = 70.7 - Outlier: True

Final results for this configuration:

Average Ksgc = 52.92 - Ksgc COV = 1.4%

Average Pmax = 13.2 - Pmax COV = 2.3%

A.7 CONFIGURATION INVOLVING GG2 AND ANGULAR SAGGR2

A.7.1 Test 1

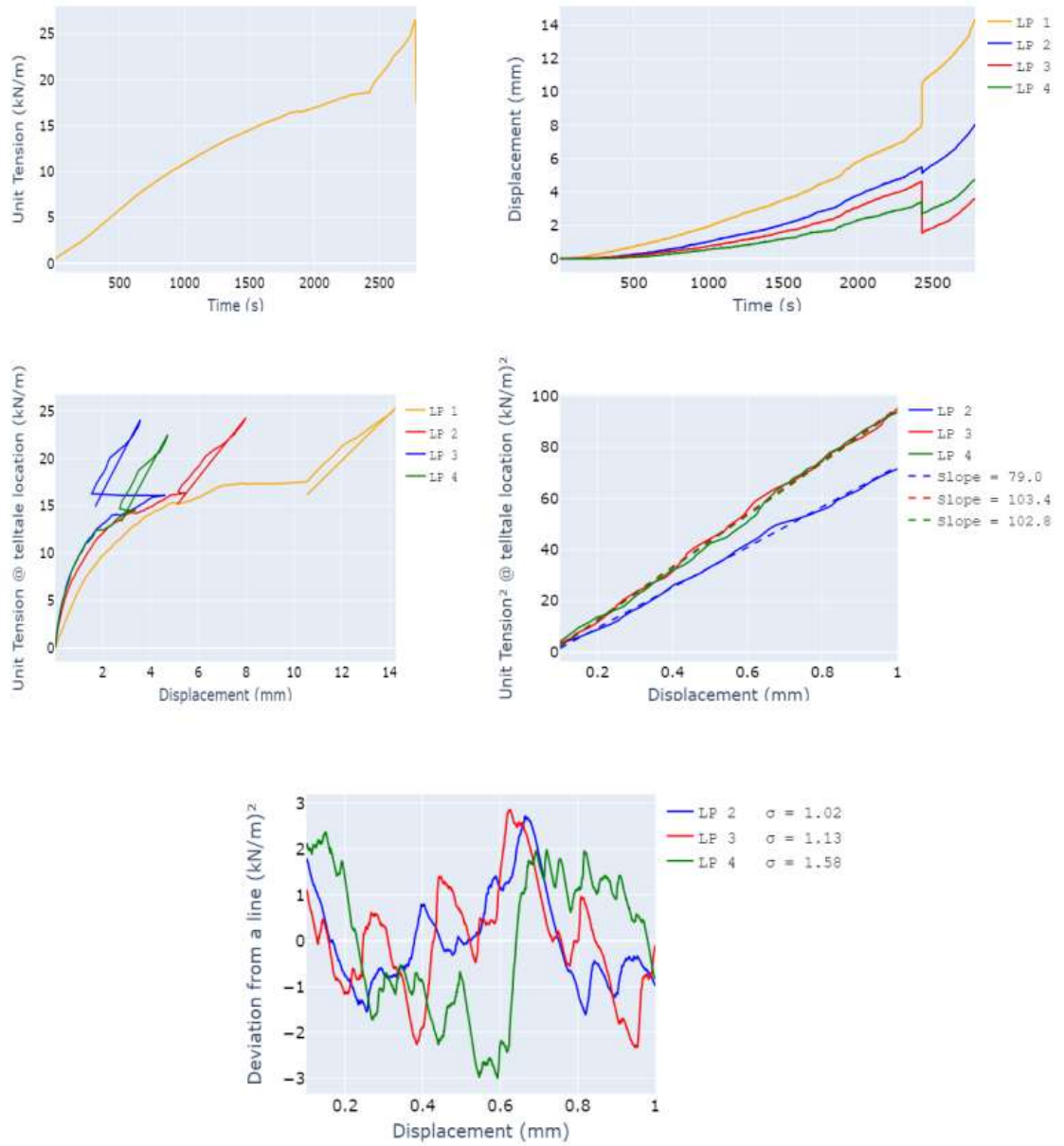


Figure A.31 - Results from the first test of configuration involving GG2 and Angular SAggr2

LP 1: Trigger Time (sec): 82.0 - T0 (kN/m): 1.26
LP 2: Trigger Time (sec): 195.4 - T0 (kN/m): 2.28
LP 3: Trigger Time (sec): 216.8 - T0 (kN/m): 2.5
LP 4: Trigger Time (sec): 350.4 - T0 (kN/m): 4.07
LP 5: Trigger Time (sec): 248.0 - T0 (kN/m): 2.84

Deviation from a line:

LP 2 - sd = 1.02 - Outlier: False
LP 3 - sd = 1.13 - Outlier: False
LP 4 - sd = 1.58 - Outlier: True

Ksgc values:

LP2: 79.0 - Outlier = False
LP3: 103.4 - Outlier = False
LP4: 102.8 - Outlier = False

Final results:

Ksgc = 73.56 - Pmax = 26.55

A.7.2 Test 2

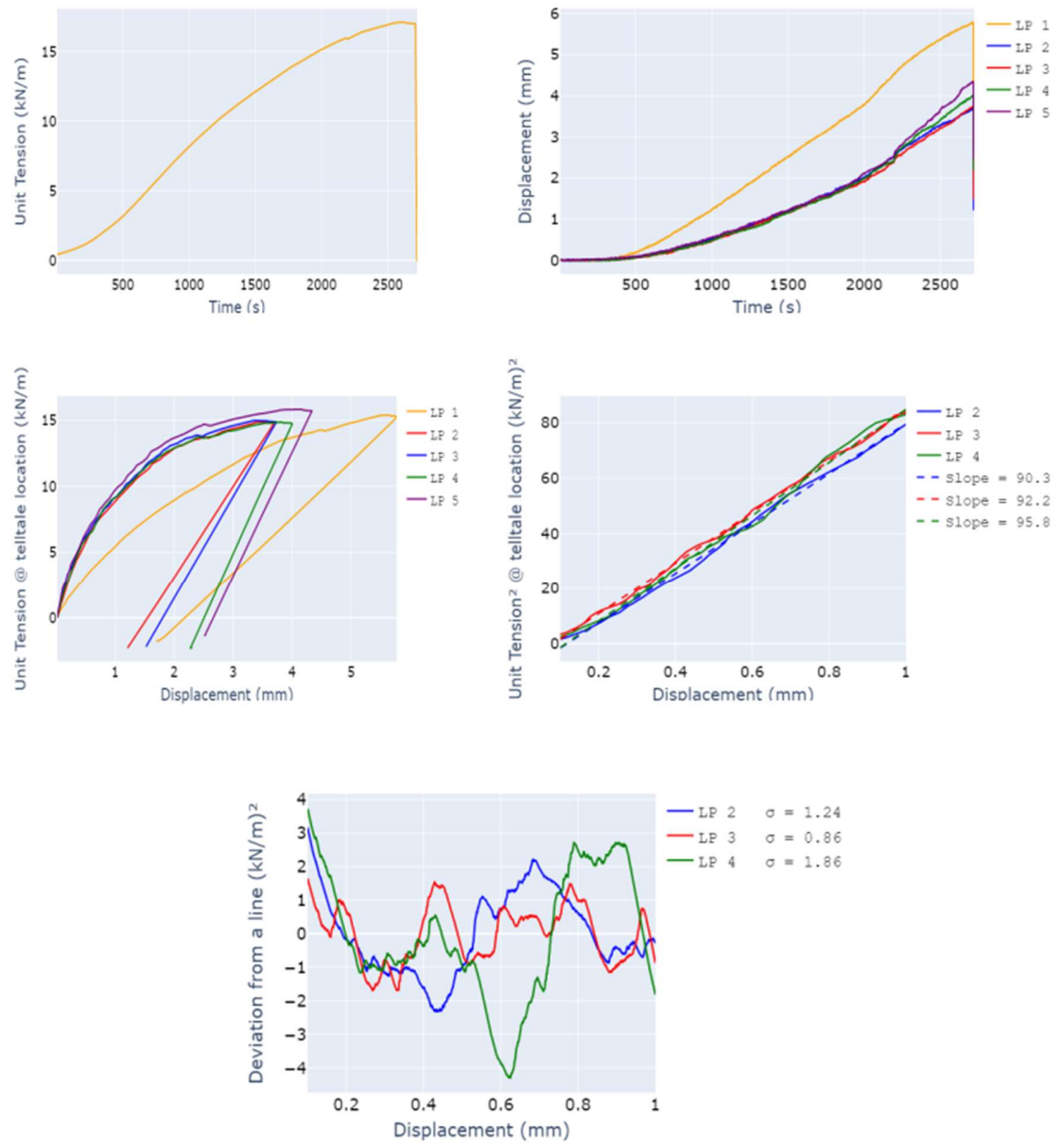


Figure A.32 - Results from the second test of configuration involving GG2 and Angular SAggr2

LP 1: Trigger Time (sec): 310.0 - T0 (kN/m): 1.72

LP 2: Trigger Time (sec): 381.8 - T0 (kN/m): 2.24

LP 3: Trigger Time (sec): 363.6 - T0 (kN/m): 2.12

LP 4: Trigger Time (sec): 384.0 - T0 (kN/m): 2.25

LP 5: Trigger Time (sec): 243.2 - T0 (kN/m): 1.3

Deviation from a line:

LP 2 - sd = 1.24 - Outlier: False

LP 3 - sd = 0.86 - Outlier: False

LP 4 - sd = 1.86 - Outlier: True

Ksgc values:

LP2: 90.3 - Outlier = False

LP3: 92.2 - Outlier = False

LP4: 95.8 - Outlier = False

Final results:

Ksgc = 90.7 - Pmax = 17.11

A.7.3 Test 3

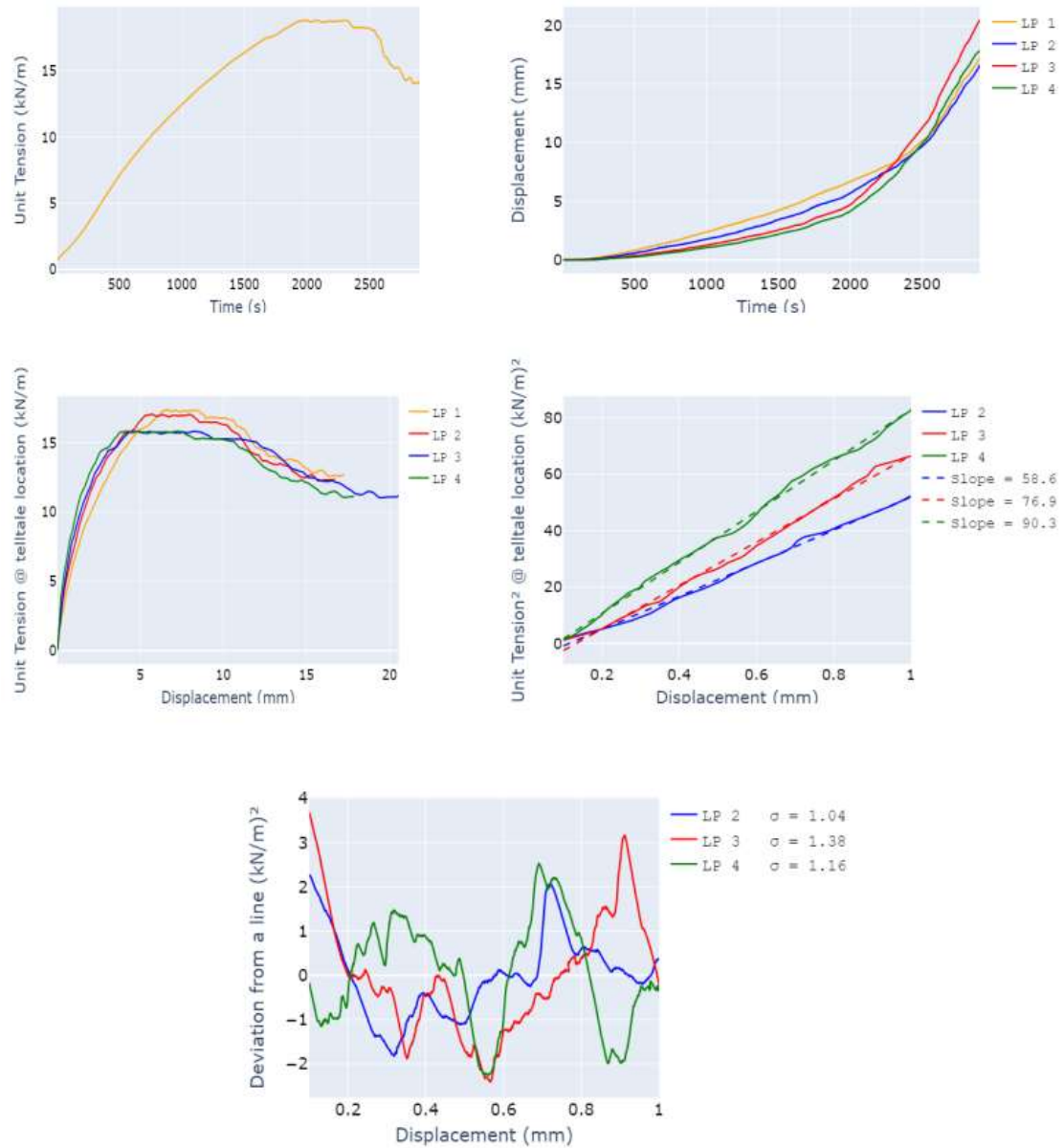


Figure A.33 - Results from the third test of configuration involving GG2 and Angular SAggr2

LP 1: Trigger Time (sec): 80.6 - T0 (kN/m): 1.46
LP 2: Trigger Time (sec): 113.8 - T0 (kN/m): 1.79
LP 3: Trigger Time (sec): 220.6 - T0 (kN/m): 3.01
LP 4: Trigger Time (sec): 218.6 - T0 (kN/m): 2.99
LP 5: Trigger Time (sec): 535.2 - T0 (kN/m): 7.54

Deviation from a line:

LP 2 - sd = 1.0 - Outlier: False
LP 3 - sd = 1.4 - Outlier: False
LP 4 - sd = 1.2 - Outlier: False

Ksgc values:

LP2: 58.6 - Outlier = False
LP3: 76.9 - Outlier = False
LP4: 90.3 - Outlier = False

Final results:

Ksgc = 75.6 - Pmax = 18.8

A.7.4 Test 4

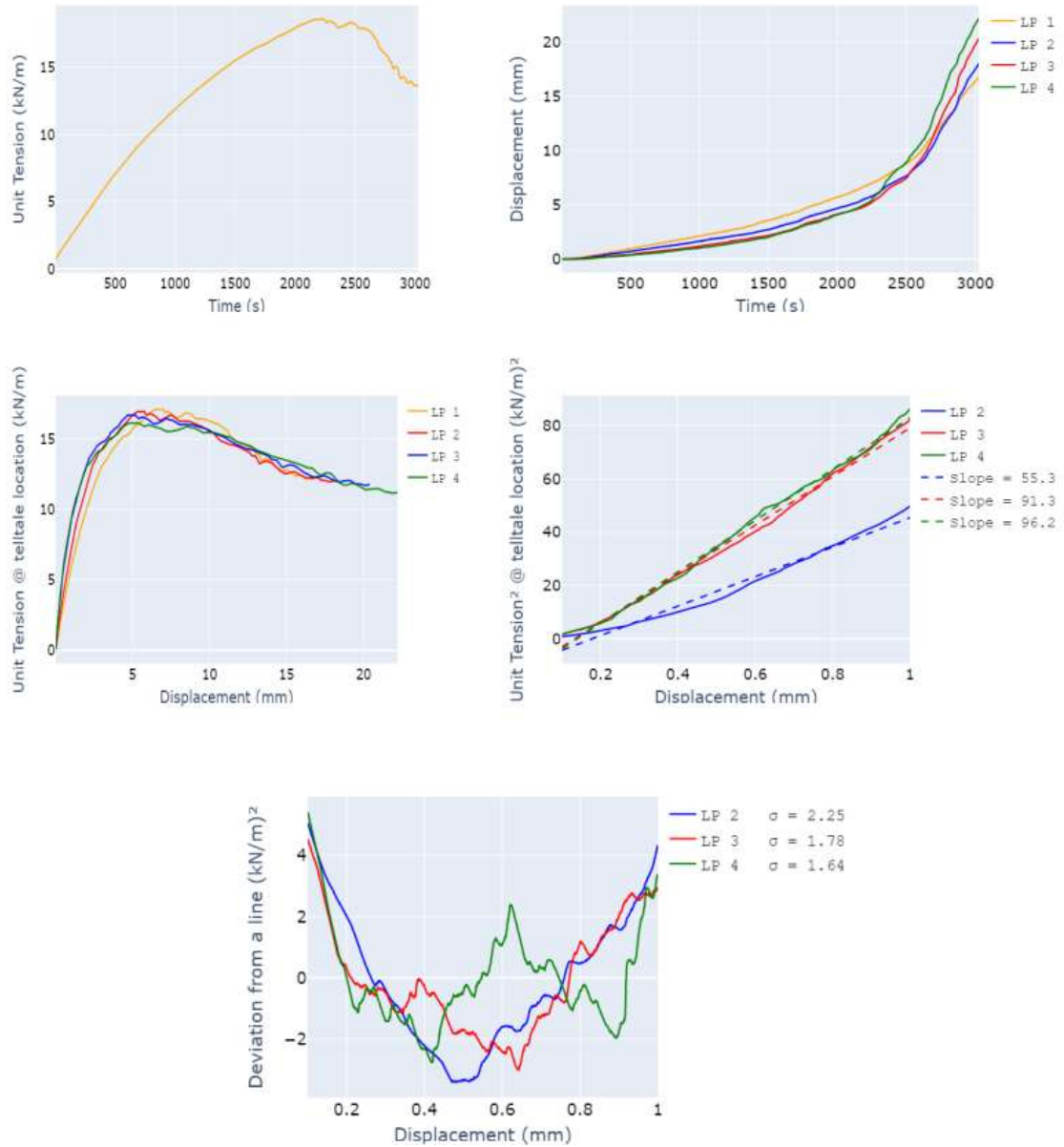


Figure A.34 - Results from the fourth test of configuration involving GG2 and Angular SAggr2

LP 1: Trigger Time (sec): 59.8 - T0 (kN/m): 1.5

LP 2: Trigger Time (sec): 72.2 - T0 (kN/m): 1.7

LP 3: Trigger Time (sec): 94.4 - T0 (kN/m): 1.9

LP 4: Trigger Time (sec): 139.2 - T0 (kN/m): 2.5

LP 5: Trigger Time (sec): 84.8 - T0 (kN/m): 1.8

Deviation from a line:

LP 2 - sd = 2.25 - Outlier: True

LP 3 - sd = 1.78 - Outlier: True

LP 4 - sd = 1.64 - Outlier: True

Ksgc values:

LP2: 55.3 - Outlier = True

LP3: 91.3 - Outlier = False

LP4: 96.2 - Outlier = False

Final results:

Ksgc = N/A - Pmax = 18.6

A.7.5 Test 5

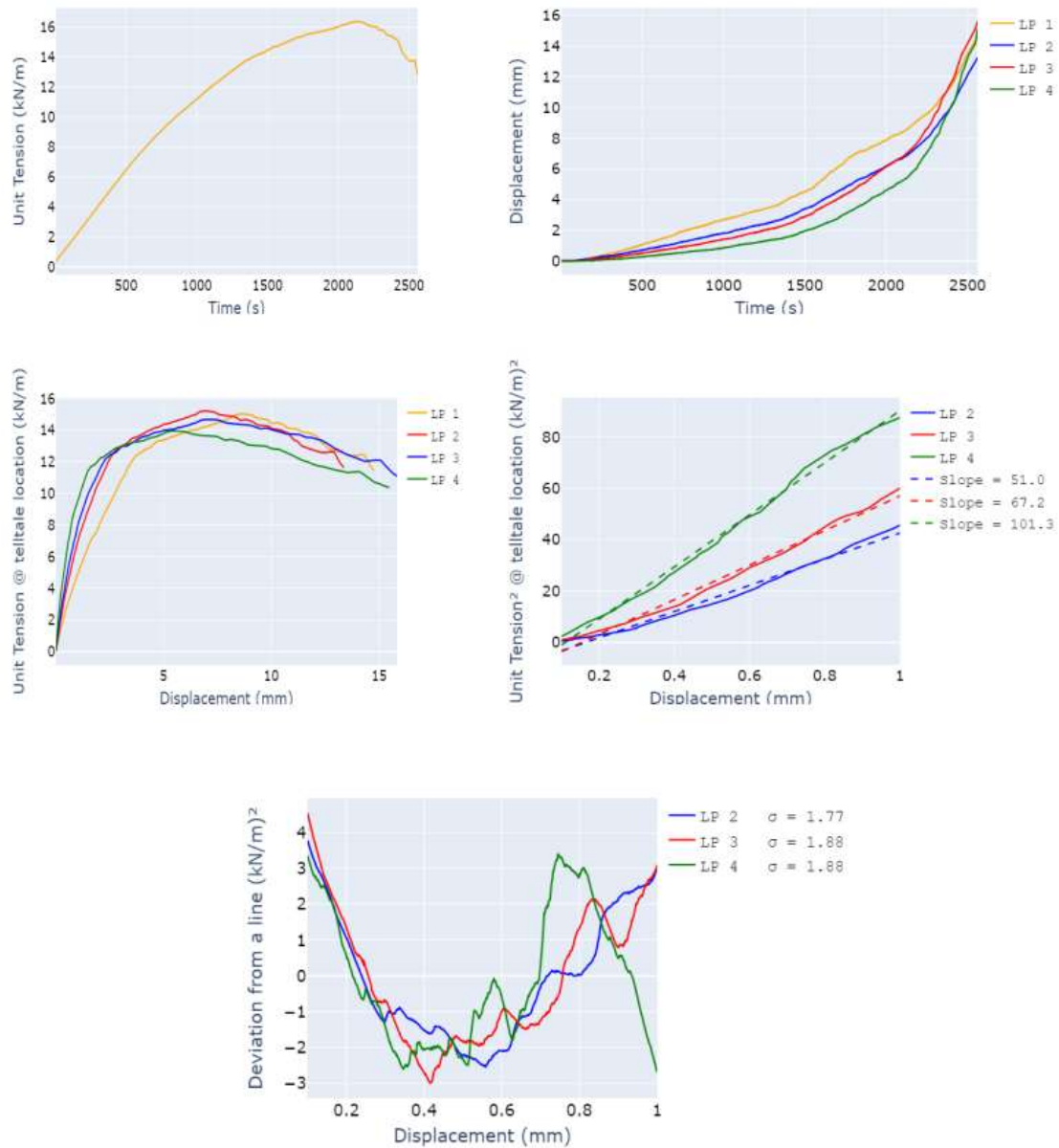


Figure A.35 - Results from the fifth test of configuration involving GG2 and Angular SAggr2

LP 1: Trigger Time (sec): 86.2 - T0 (kN/m): 1.4

LP 2: Trigger Time (sec): 70.2 - T0 (kN/m): 1.2

LP 3: Trigger Time (sec): 113.6 - T0 (kN/m): 1.7

LP 4: Trigger Time (sec): 174.0 - T0 (kN/m): 2.4

LP 5: Trigger Time (sec): 19.6 - T0 (kN/m): 0.6

Deviation from a line:

LP 2 - sd = 1.8 - Outlier: True

LP 3 - sd = 1.9 - Outlier: True

LP 4 - sd = 1.9 - Outlier: True

Ksgc values:

LP2: 51.0 - Outlier = False

LP3: 67.2 - Outlier = False

LP4: 101.3 - Outlier = True

Final results:

Ksgc = N/A - Pmax = 16.39

A.7.6 Summary of results from configuration involving GG2 and Angular SAggr2

Ksgc MAD = 3.05 - Pmax MAD = 2.55 Ksgc

median = 75.62 - Pmax median = 18.83

If $((Ksgc_i - Ksgc_median)/MAD) > 2$: outlier

If $((Pmax_i - Pmax_median)/MAD) > 2.5$: outlier

Test 1

Pmax = 26.55 - Outlier: True - Ksgc = 73.56 - Outlier : False

Test 2

Pmax = 17.11 - Outlier: False - Ksgc = 90.7 - Outlier : True

Test 3

Pmax = 18.83 - Outlier: False - Ksgc = 75.62 - Outlier : False

Test 4

Pmax = 18.62 - Outlier: False - Ksgc = 0 - Outlier : True

Test 5

Pmax = 16.39 - Outlier: False - Ksgc = 0 - Outlier : True

Final results for this configuration:

Average Ksgc = 75.62 - Ksgc COV = 0.0%

Average Pmax = 18.83 - Pmax COV = 0.0%

A.8 CONFIGURATION INVOLVING GT1 AND ROUND SAGGR2

A.8.1 Test 1

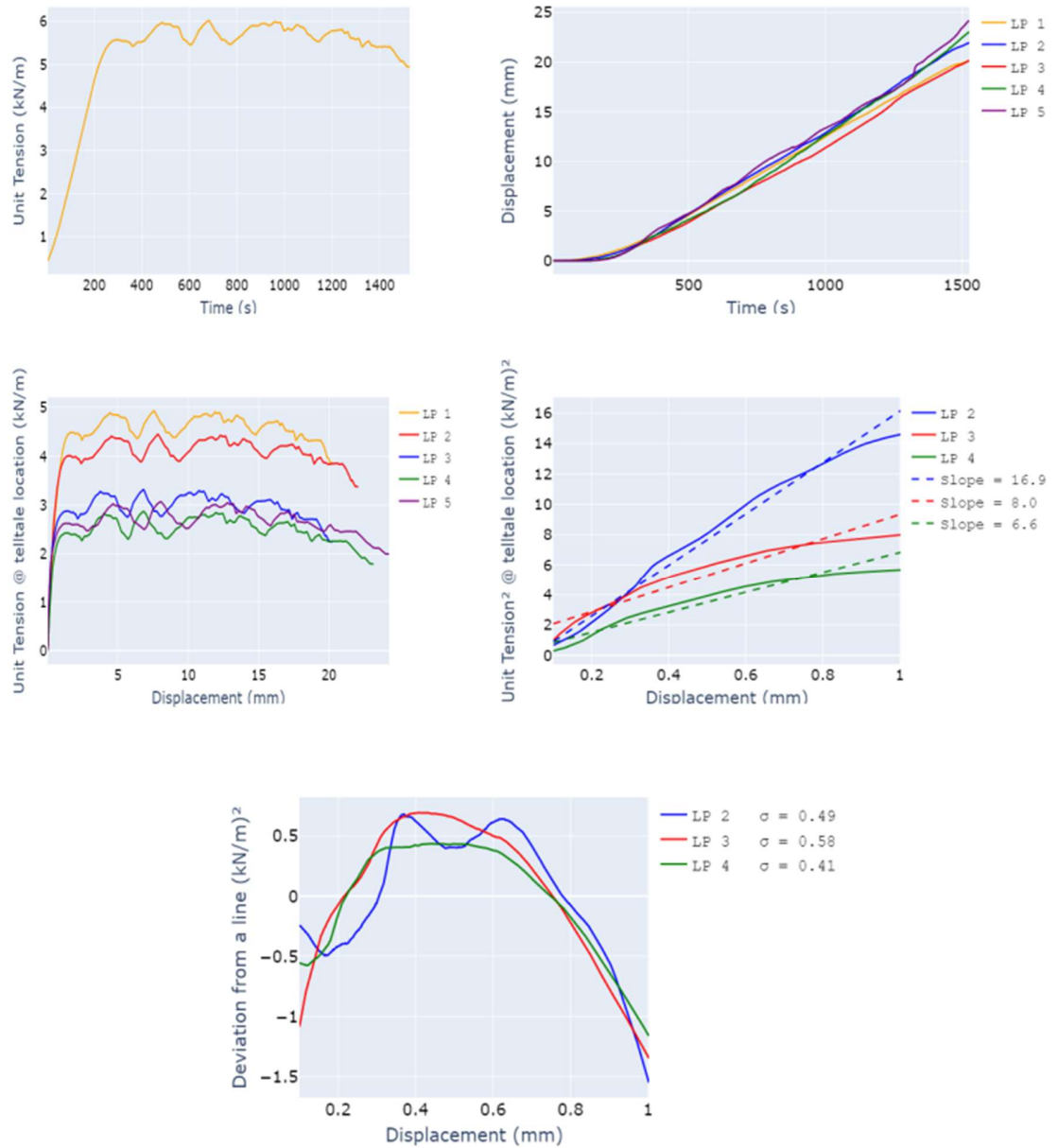


Figure A.36 - Results from the first test of configuration involving GT1 and Round SAGgr2

LP 1: Trigger Time (sec): 44.8 - T0 (kN/m): 1.1
LP 2: Trigger Time (sec): 68.6 - T0 (kN/m): 1.57
LP 3: Trigger Time (sec): 117.8 - T0 (kN/m): 2.7
LP 4: Trigger Time (sec): 136.2 - T0 (kN/m): 3.2
LP 5: Trigger Time (sec): 128.2 - T0 (kN/m): 2.9

Deviation from a line:

LP 2 - sd = 0.49 - Outlier: False
LP 3 - sd = 0.58 - Outlier: False
LP 4 - sd = 0.41 - Outlier: False

Ksgc values:

LP2: 16.9 - Outlier = True
LP3: 8.0 - Outlier = False
LP4: 6.6 - Outlier = False

Final results:

Ksgc = 7.41 - Pmax = 6.02

A.8.2 Test 2

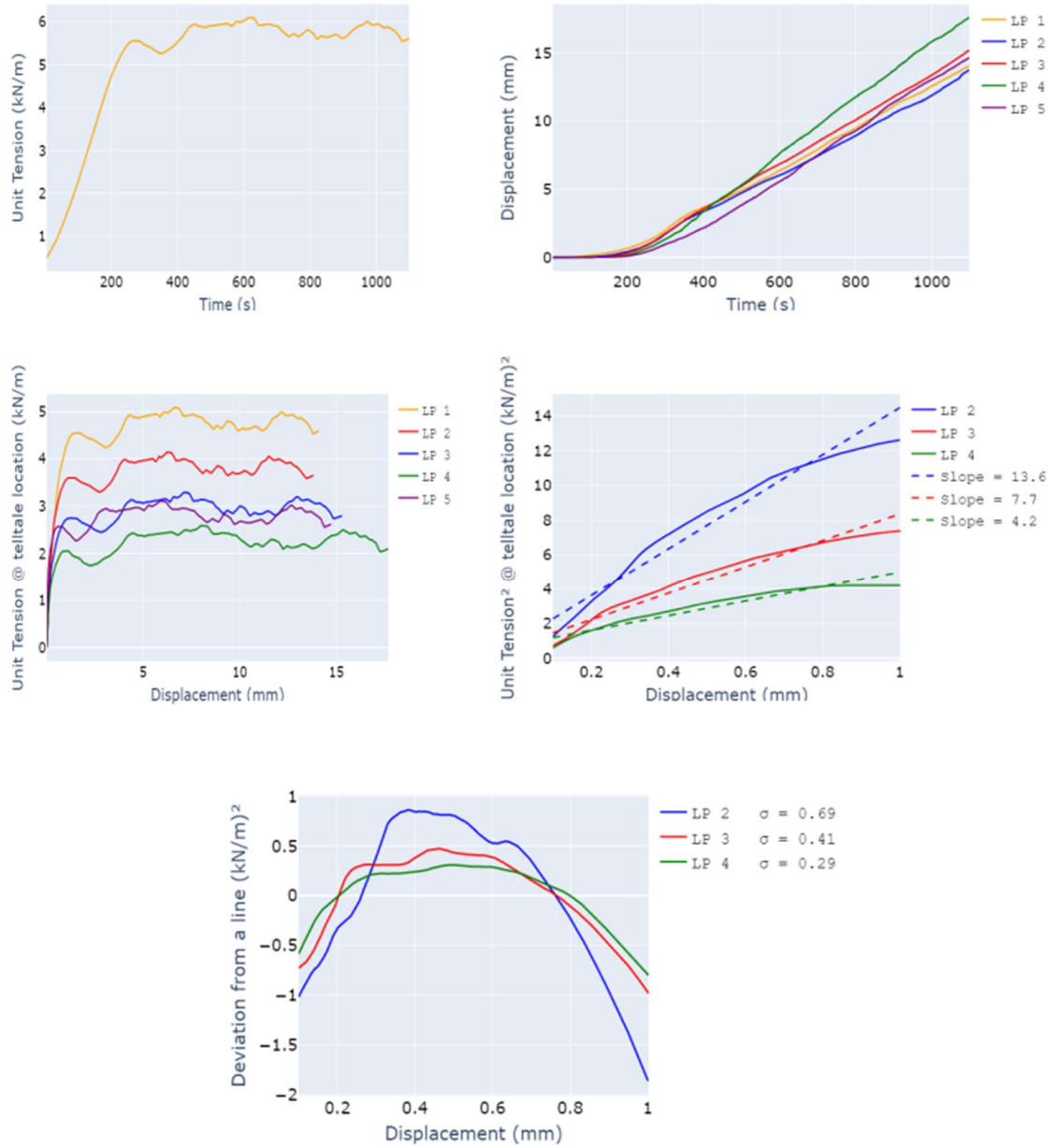


Figure A.37 - Results from the second test of configuration involving GT1 and Round SAggr2

LP 1: Trigger Time (sec): 40.2 - T0 (kN/m): 1.02
LP 2: Trigger Time (sec): 86.0 - T0 (kN/m): 1.96
LP 3: Trigger Time (sec): 121.6 - T0 (kN/m): 2.81
LP 4: Trigger Time (sec): 149.0 - T0 (kN/m): 3.51
LP 5: Trigger Time (sec): 128.8 - T0 (kN/m): 2.99

Deviation from a line:

LP 2 - sd = 0.69 - Outlier: False
LP 3 - sd = 0.41 - Outlier: False
LP 4 - sd = 0.29 - Outlier: False

Ksgc values:

LP2: 13.6 - Outlier = True
LP3: 7.7 - Outlier = False
LP4: 4.2 - Outlier = False

Final results:

Ksgc = 6.03 - Pmax = 6.1

A.8.3 Test 3

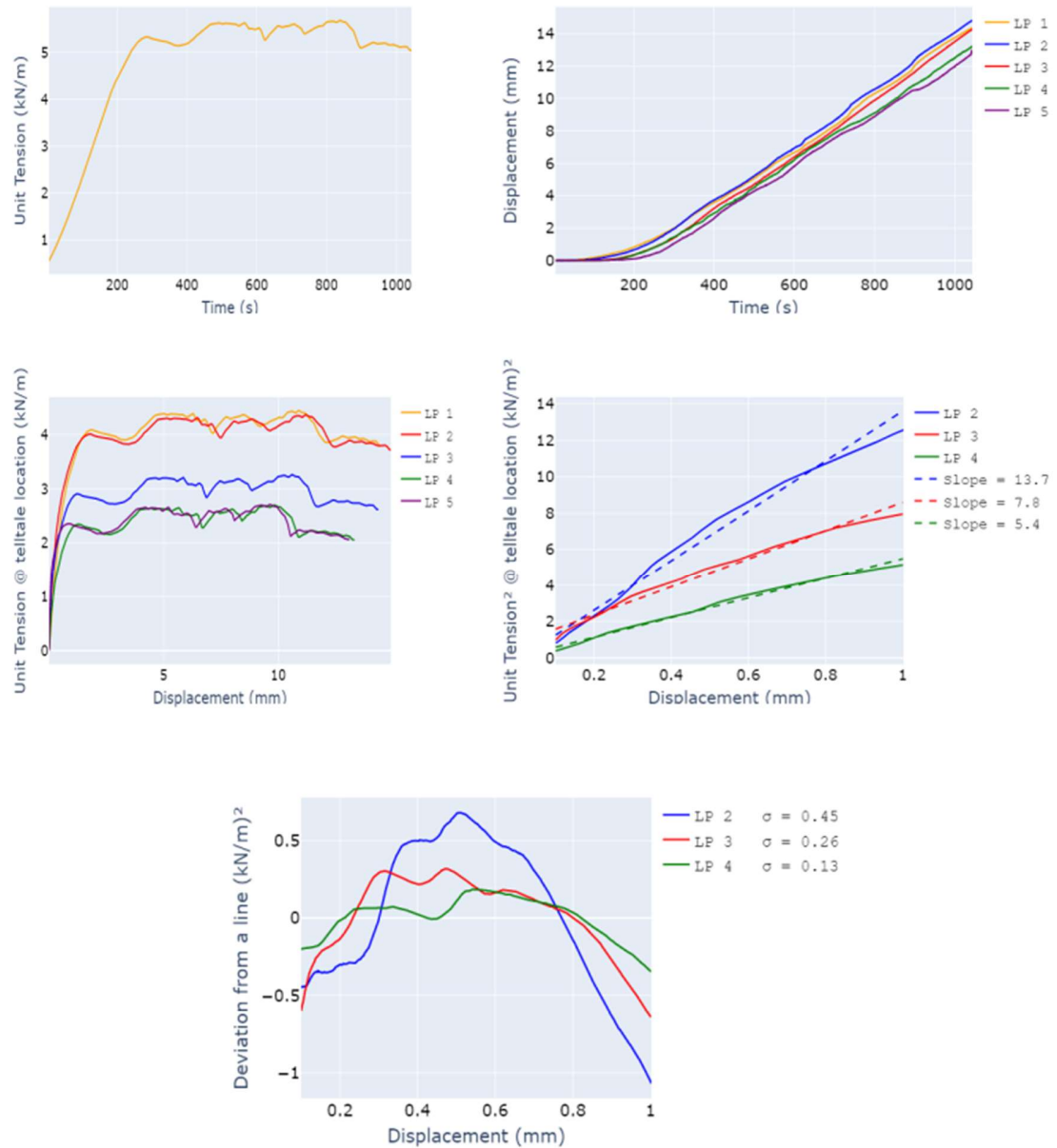


Figure A.38 - Results from the third test of configuration involving GT1 and Round SAggr2

LP 1: Trigger Time (sec): 46.0 - T0 (kN/m): 1.2

LP 2: Trigger Time (sec): 50.8 - T0 (kN/m): 1.3

LP 3: Trigger Time (sec): 104.0 - T0 (kN/m): 2.4

LP 4: Trigger Time (sec): 129.4 - T0 (kN/m): 3.0

LP 5: Trigger Time (sec): 128.6 - T0 (kN/m): 3.0

Deviation from a line:

LP 2 - sd = 0.4 - Outlier: False

LP 3 - sd = 0.3 - Outlier: False

LP 4 - sd = 0.1 - Outlier: False

Ksgc values:

LP2: 13.7 - Outlier = True

LP3: 7.8 - Outlier = False

LP4: 5.4 - Outlier = False

Final results:

Ksgc = 6.8 - Pmax = 5.7

A.8.4 Test 4

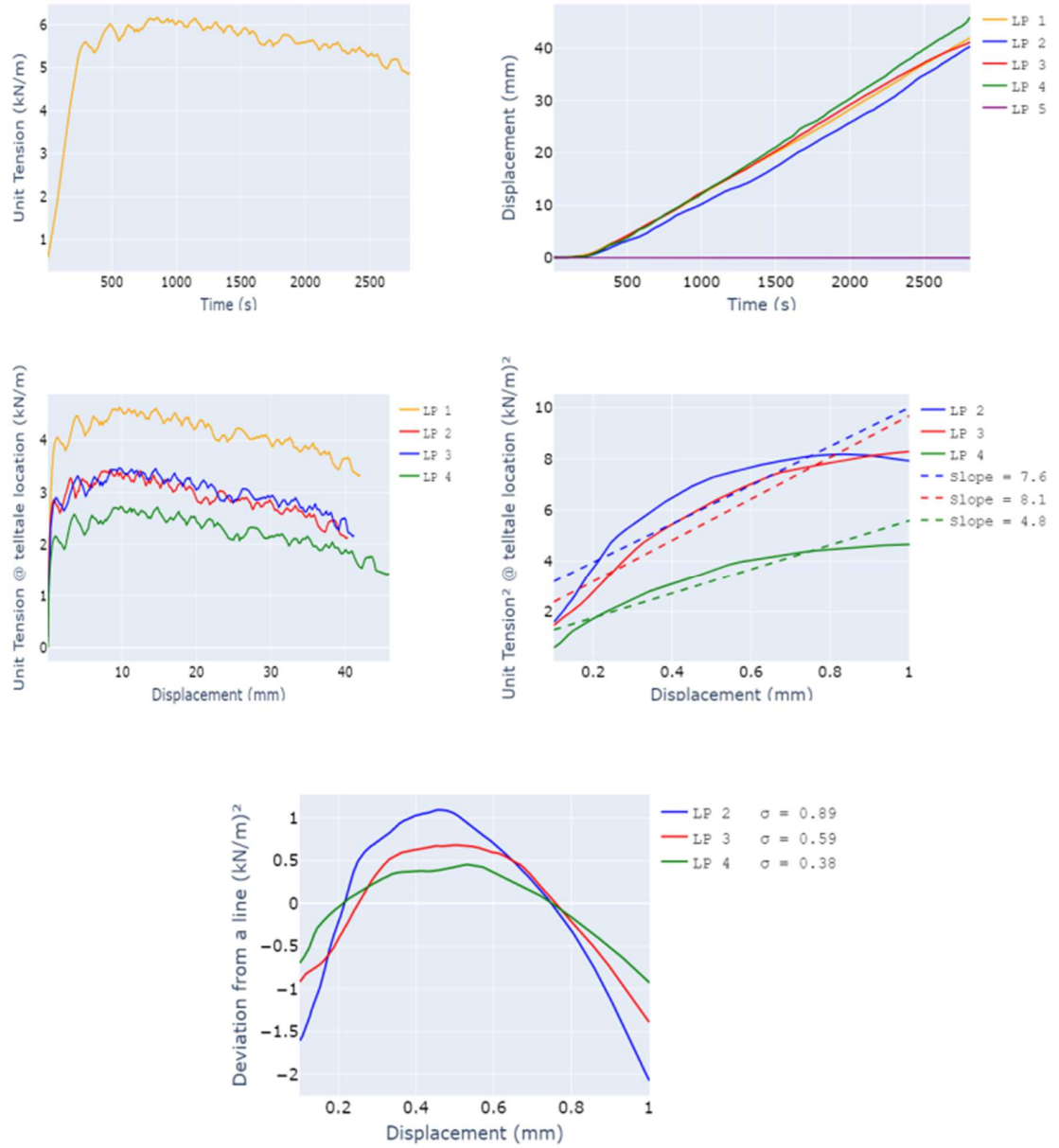


Figure A.39 - Results from the fourth test of configuration involving GT1 and Round SAggr2

LP 1: Trigger Time (sec): 61.4 - T0 (kN/m): 1.5

LP 2: Trigger Time (sec): 116.2 - T0 (kN/m): 2.7

LP 3: Trigger Time (sec): 114.2 - T0 (kN/m): 2.7

LP 4: Trigger Time (sec): 146.8 - T0 (kN/m): 3.4

LP 5: Trigger Time (sec): 0.0 - T0 (kN/m): 0.0

Deviation from a line:

LP 2 - sd = 0.89 - Outlier: False

LP 3 - sd = 0.59 - Outlier: False

LP 4 - sd = 0.38 - Outlier: False

Ksgc values:

LP2: 7.6 - Outlier = False

LP3: 8.1 - Outlier = False

LP4: 4.8 - Outlier = True

Final results:

Ksgc = 8.34 - Pmax = 6.17

A.8.5 Test 5

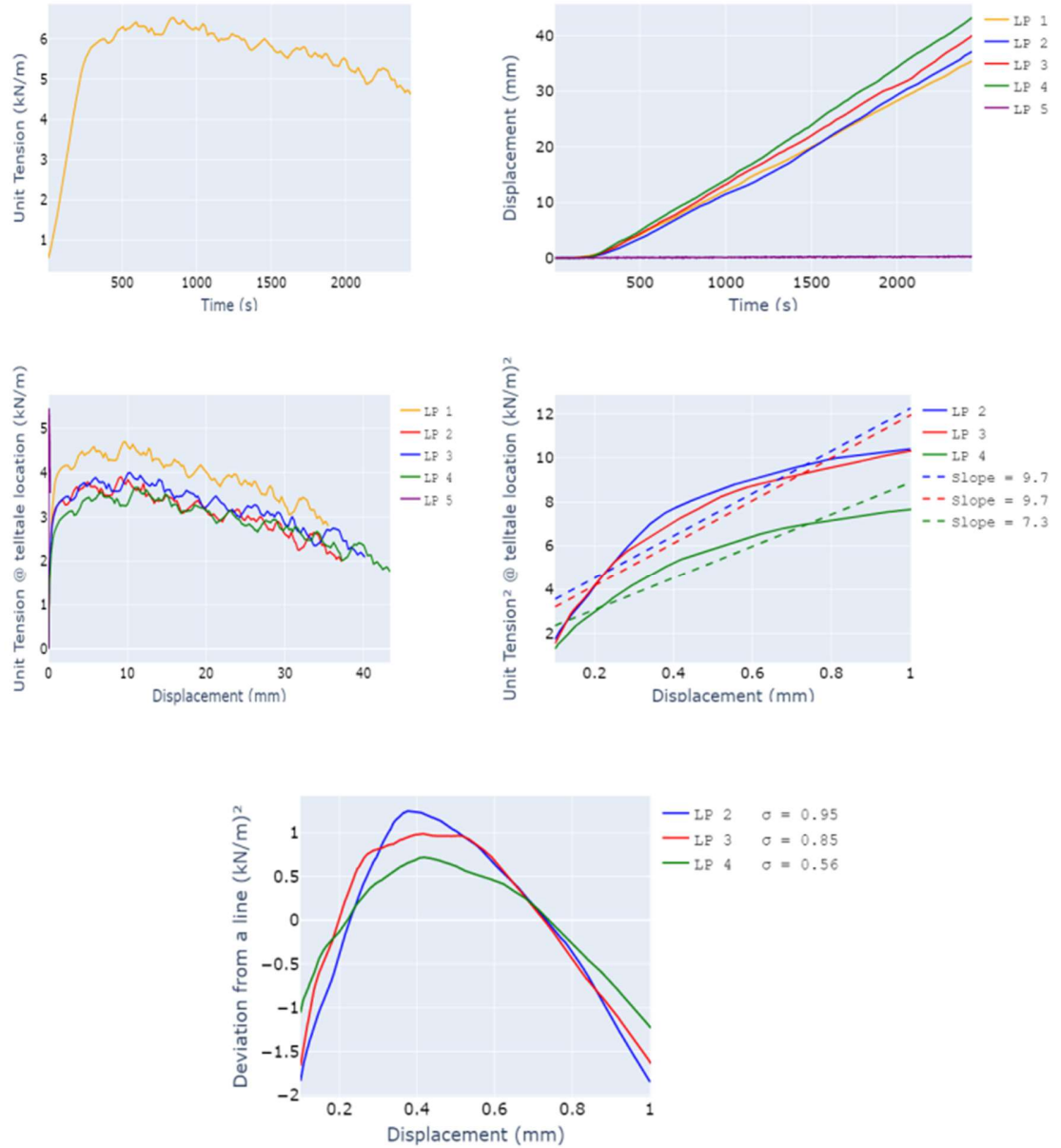


Figure A.40 - Results from the fifth test of configuration involving GT1 and Round SAggr2

LP 1: Trigger Time (sec): 75.6 - T0 (kN/m): 1.8

LP 2: Trigger Time (sec): 111.0 - T0 (kN/m): 2.6

LP 3: Trigger Time (sec): 107.0 - T0 (kN/m): 2.5

LP 4: Trigger Time (sec): 121.2 - T0 (kN/m): 2.9

LP 5: Trigger Time (sec): 37.4 - T0 (kN/m): 1.1

Deviation from a line:

LP 2 - sd = 0.9 - Outlier: False

LP 3 - sd = 0.9 - Outlier: False

LP 4 - sd = 0.6 - Outlier: False

Ksgc values:

LP2: 9.7 - Outlier = False

LP3: 9.7 - Outlier = False

LP4: 7.3 - Outlier = False

Final results:

Ksgc = 8.75 - Pmax = 6.53

A.8.6 Summary of results from configuration involving GT1 and Round SAggr2

Ksgc MAD = 1.38 - Pmax MAD = 0.12

Ksgc median = 7.41 - Pmax median = 6.1

If $((Ksgc_i - Ksgc_median)/MAD) > 2$: outlier

If $((Pmax_i - Pmax_median)/MAD) > 2.5$: outlier

Test 1

Pmax = 6.02 - Outlier: False - Ksgc = 7.41 - Outlier: False

Test 2

Pmax = 6.1 - Outlier: False - Ksgc = 6.03 - Outlier: False

Test 3

Pmax = 5.68 - Outlier: True - Ksgc = 6.76 - Outlier: False

Test 4

Pmax = 6.17 - Outlier: False - Ksgc = 8.34 - Outlier: False

Test 5

Pmax = 6.53 - Outlier: True - Ksgc = 8.75 - Outlier: False

Final results for this configuration:

Average Ksgc = 7.26 - Ksgc COV = 13.1%

Average Pmax = 6.1 - Pmax COV = 1.0%

A.9 CONFIGURATION INVOLVING GT1 AND ANGULAR SAGGR2

A.9.1 Test 1

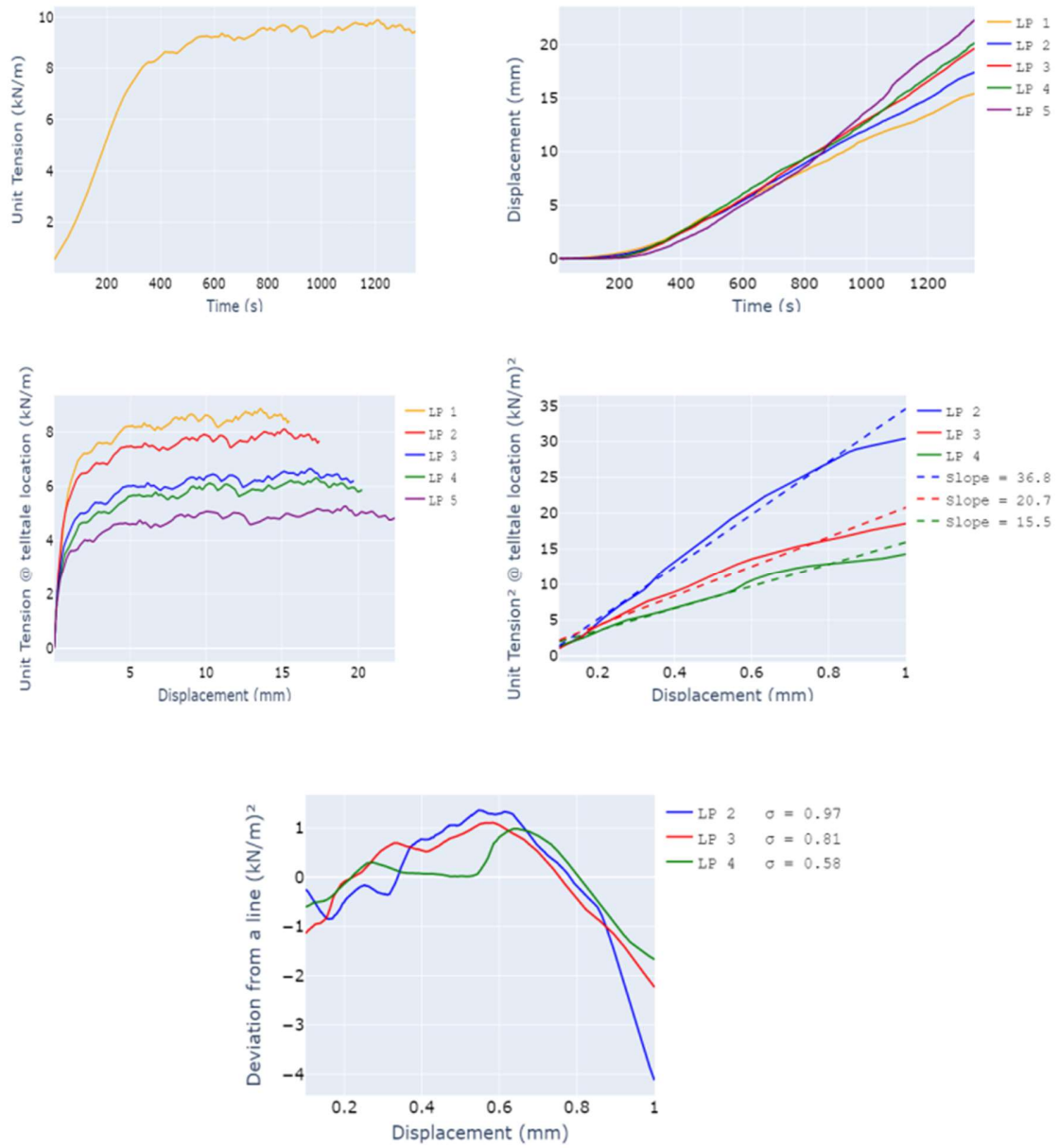


Figure A.41 - Results from the first test of configuration involving GT1 and Angular SAGgr2

LP 1: Trigger Time (sec): 34.8 - T0 (kN/m): 1.0

LP 2: Trigger Time (sec): 72.6 - T0 (kN/m): 1.8

LP 3: Trigger Time (sec): 131.2 - T0 (kN/m): 3.2

LP 4: Trigger Time (sec): 143.4 - T0 (kN/m): 3.6

LP 5: Trigger Time (sec): 178.8 - T0 (kN/m): 4.6

Deviation from a line:

LP 2 - sd = 0.97 - Outlier: False

LP 3 - sd = 0.81 - Outlier: False

LP 4 - sd = 0.58 - Outlier: False

Ksgc values:

LP2: 36.8 - Outlier = True

LP3: 20.7 - Outlier = False

LP4: 15.5 - Outlier = False

Final results:

Ksgc = 18.39 - Pmax = 9.88

A.9.2 Test 2

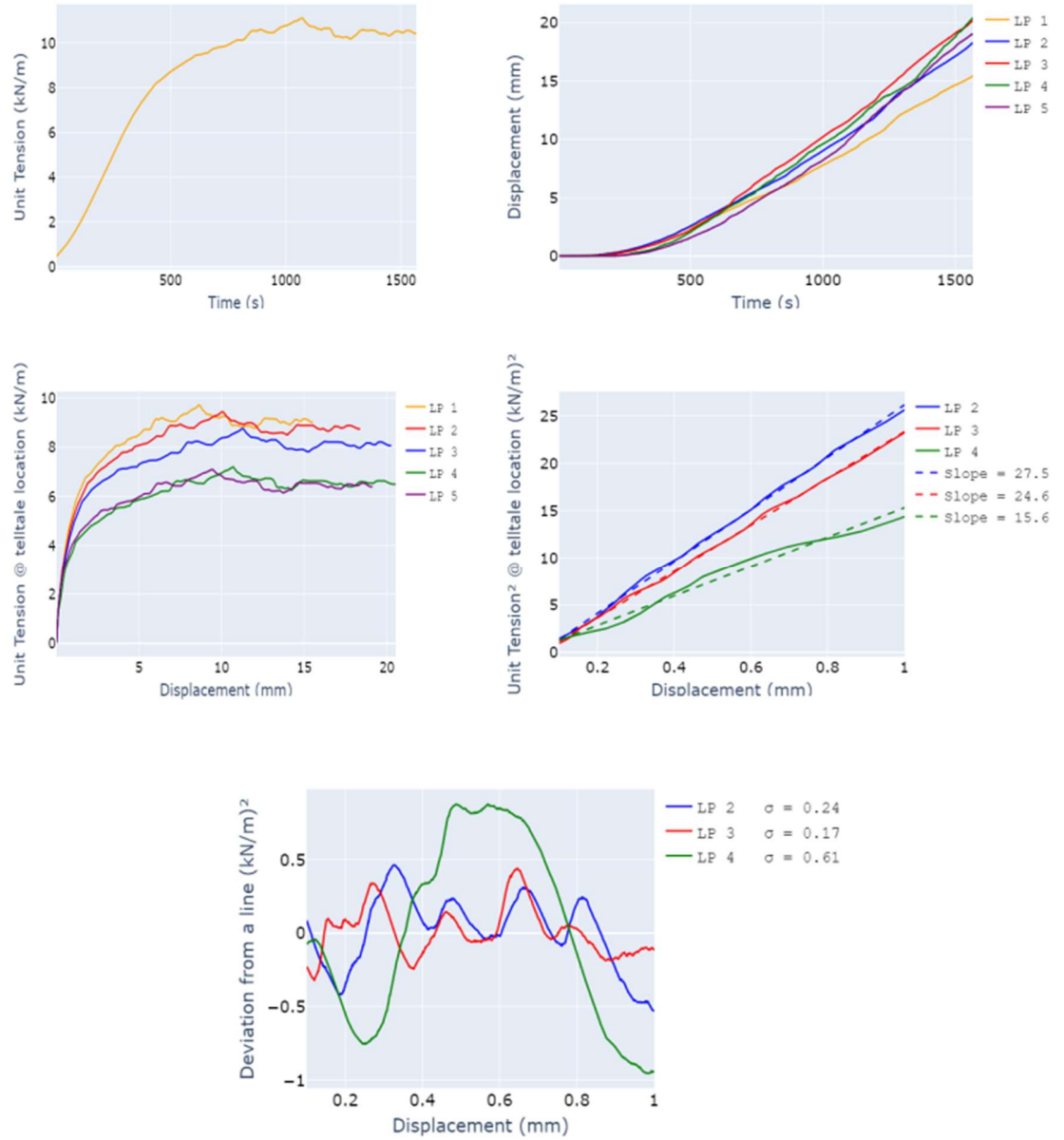


Figure A.42 - Results from the second test of configuration involving GT1 and Angular SAggr2

LP 1: Trigger Time (sec): 75.6 - T0 (kN/m): 1.4

LP 2: Trigger Time (sec): 91.6 - T0 (kN/m): 1.9

LP 3: Trigger Time (sec): 127.8 - T0 (kN/m): 2.4

LP 4: Trigger Time (sec): 200.6 - T0 (kN/m): 3.9

LP 5: Trigger Time (sec): 205.0 - T0 (kN/m): 4.0

Deviation from a line:

LP 2 - sd = 0.2 - Outlier: False

LP 3 - sd = 0.2 - Outlier: False

LP 4 - sd = 0.6 - Outlier: False

Ksgc values:

LP2: 27.5 - Outlier = False

LP3: 24.6 - Outlier = False

LP4: 15.6 - Outlier = True

Final results:

Ksgc = 24.87 - Pmax = 11.13

A.9.3 Test 3

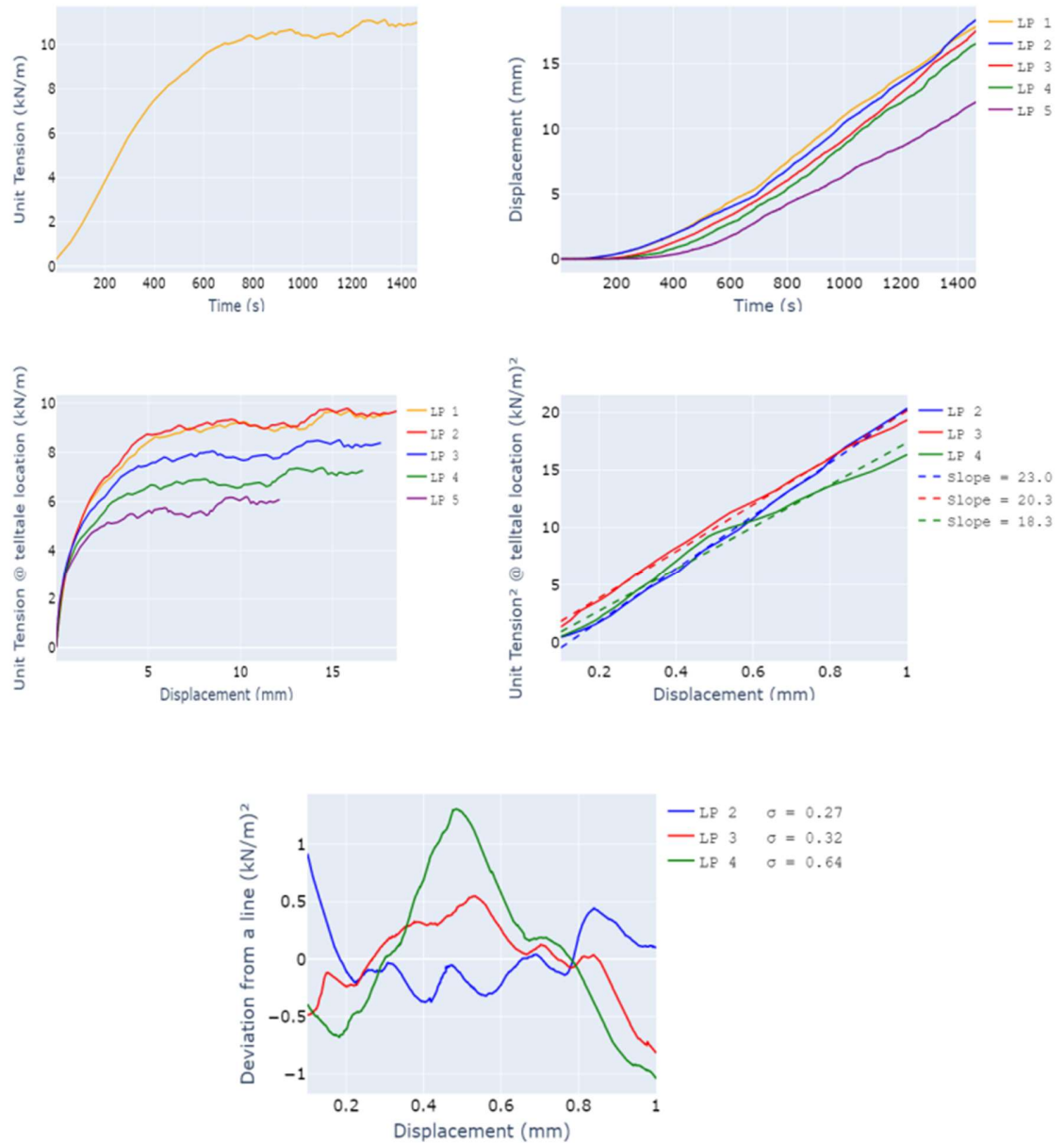


Figure A.43 - Results from the third test of configuration involving GT1 and Angular SAggr2

LP 1: Trigger Time (sec): 81.4 - T0 (kN/m): 1.4

LP 2: Trigger Time (sec): 75.6 - T0 (kN/m): 1.3

LP 3: Trigger Time (sec): 143.4 - T0 (kN/m): 2.6

LP 4: Trigger Time (sec): 195.8 - T0 (kN/m): 3.7

LP 5: Trigger Time (sec): 250.2 - T0 (kN/m): 4.9

Deviation from a line:

LP 2 - sd = 0.3 - Outlier: False

LP 3 - sd = 0.3 - Outlier: False

LP 4 - sd = 0.6 - Outlier: False

Ksgc values:

LP2: 23.0 - Outlier = False

LP3: 20.3 - Outlier = False

LP4: 18.3 - Outlier = False

Final results:

Ksgc = 20.6 - Pmax = 11.

A.9.4 Test 4

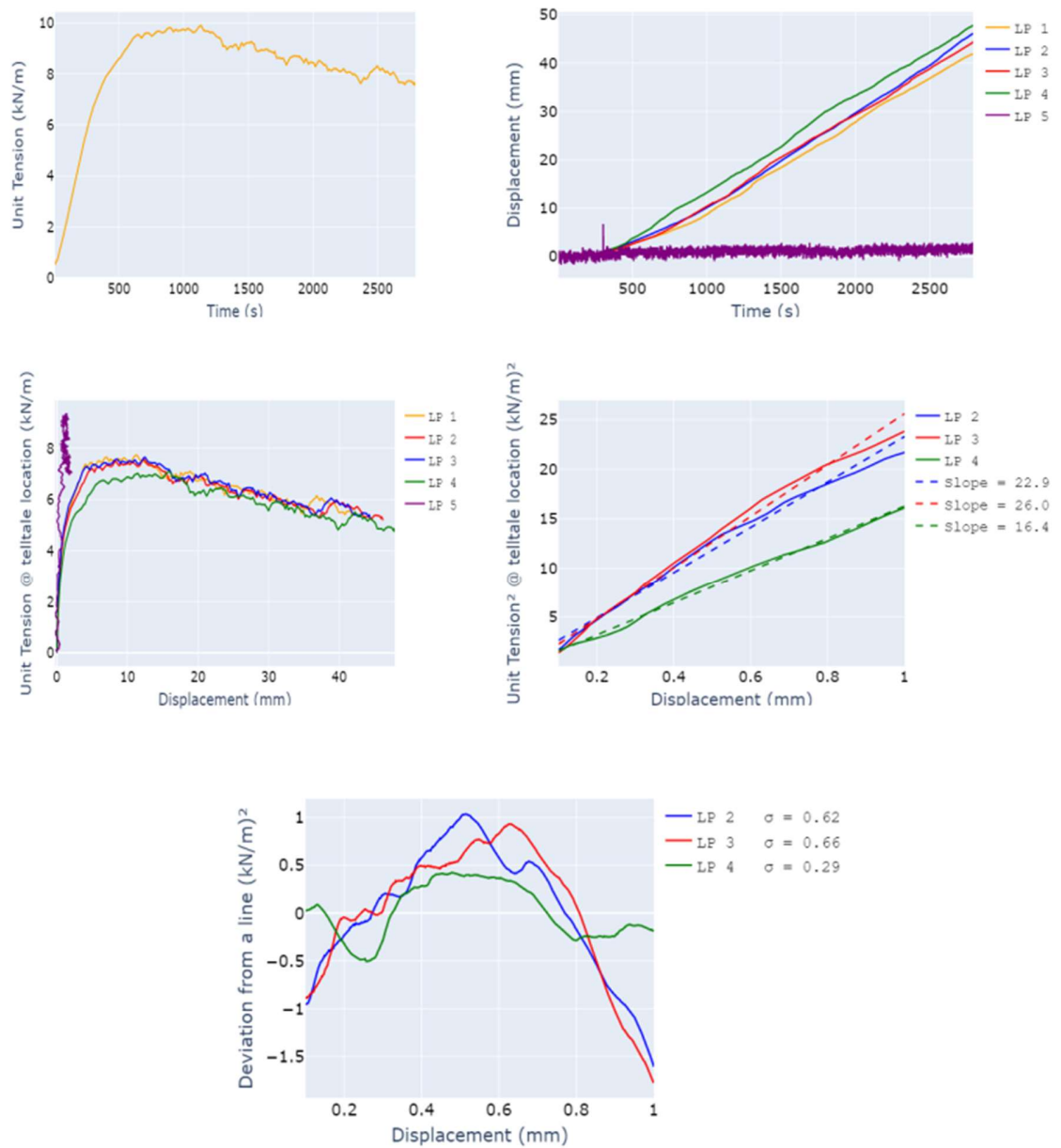


Figure 44 - Results from the fourth test of configuration involving GT1 and Angular SAggr2

LP 1: Trigger Time (sec): 93.4 - T0 (kN/m): 2.8

LP 2: Trigger Time (sec): 101.2 - T0 (kN/m): 2.3

LP 3: Trigger Time (sec): 97.0 - T0 (kN/m): 2.3

LP 4: Trigger Time (sec): 120.6 - T0 (kN/m): 2.8

LP 5: Trigger Time (sec): 7.4 - T0 (kN/m): 0.6

Deviation from a line:

LP 2 - sd = 0.6 - Outlier: False

LP 3 - sd = 0.7 - Outlier: False

LP 4 - sd = 0.3 - Outlier: False

Ksgc values:

LP2: 22.9 - Outlier = False

LP3: 26.0 - Outlier = False

LP4: 16.4 - Outlier = True

Final results:

Ksgc = 26.9 - Pmax = 9.9

A.9.5 Test 5

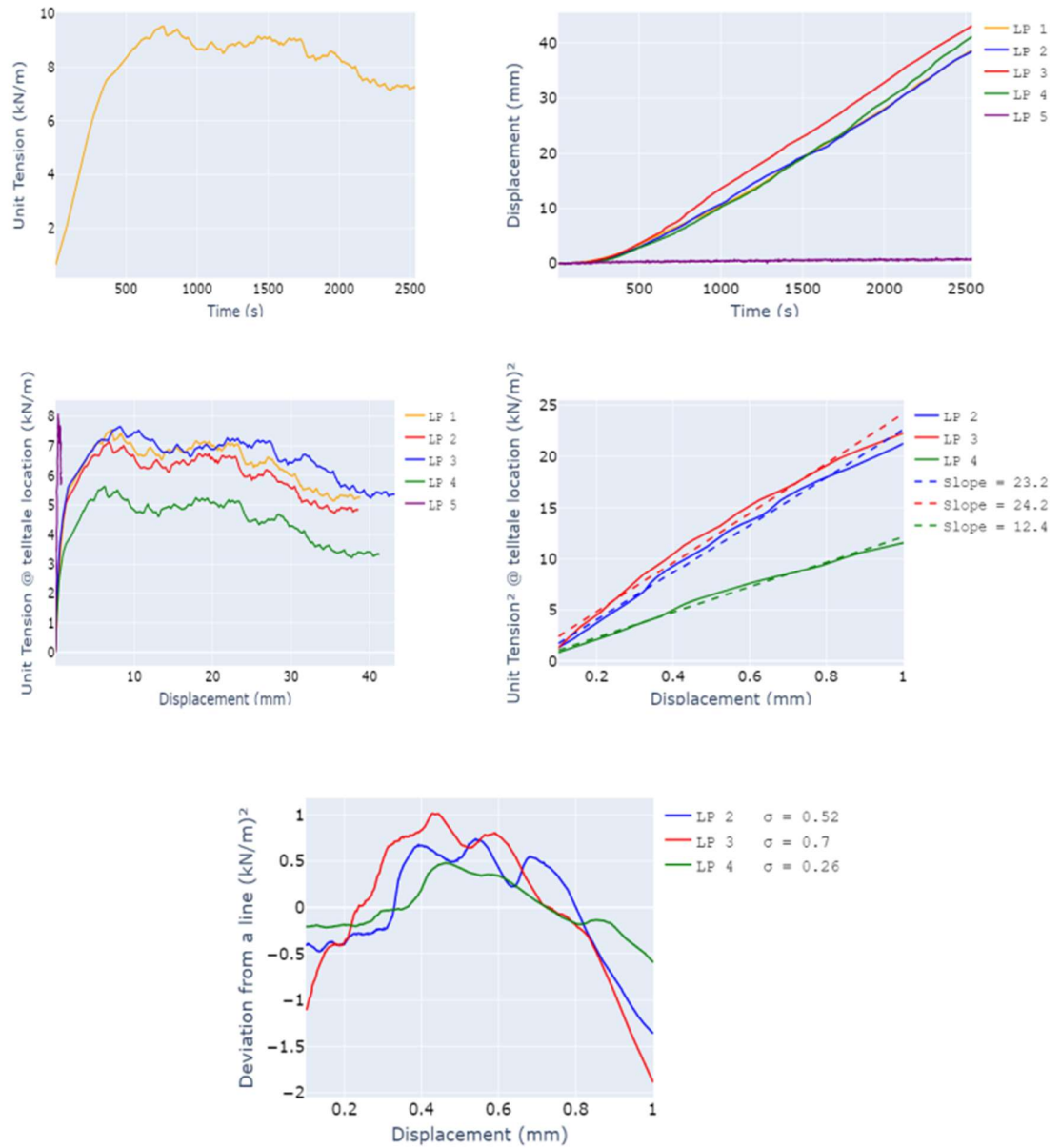


Figure A.45 - Results from the fifth test of configuration involving GT1 and Angular SAggr2

LP 1: Trigger Time (sec): 79.4 - T0 (kN/m): 2.0

LP 2: Trigger Time (sec): 99.0 - T0 (kN/m): 2.4

LP 3: Trigger Time (sec): 74.8 - T0 (kN/m): 1.9

LP 4: Trigger Time (sec): 164.4 - T0 (kN/m): 3.9

LP 5: Trigger Time (sec): 52.2 - T0 (kN/m): 1.5

Deviation from a line:

LP 2 - sd = 0.5 - Outlier: False

LP 3 - sd = 0.7 - Outlier: False

LP 4 - sd = 0.3 - Outlier: False

Ksgc values:

LP2: 23.2 - Outlier = False

LP3: 24.2 - Outlier = False

LP4: 12.4 - Outlier = True

Final results:

Ksgc = 24.2 - Pmax = 9.5

A.9.6 Summary of results from configuration involving GT1 and Angular SAggr2

Ksgc MAD = 3.93 - Pmax MAD = 0.55

Ksgc median = 24.24 - Pmax median = 9.91

If $((Ksgc_i - Ksgc_median)/MAD) > 2$: outlier

If $((Pmax_i - Pmax_median)/MAD) > 2.5$: outlier

Test 1

Pmax = 9.88 - Outlier: False - Ksgc = 18.39 - Outlier : False

Test 2

Pmax = 11.13 - Outlier: False - Ksgc = 24.87 - Outlier : False

Test 3

Pmax = 11.1 - Outlier: False - Ksgc = 20.6 - Outlier : False

Test 4

Pmax = 9.91 - Outlier: False - Ksgc = 26.89 - Outlier : False

Test 5

Pmax = 9.54 - Outlier: False - Ksgc = 24.24 - Outlier : False

Final results for this configuration:

Average Ksgc = 23.0 - Ksgc COV = 13.4%

Average Pmax = 10.31 - Pmax COV = 6.5%

A.10 CONFIGURATION INVOLVING GT1 AND ANGULAR SAGGR3

A.10.1 Test 1

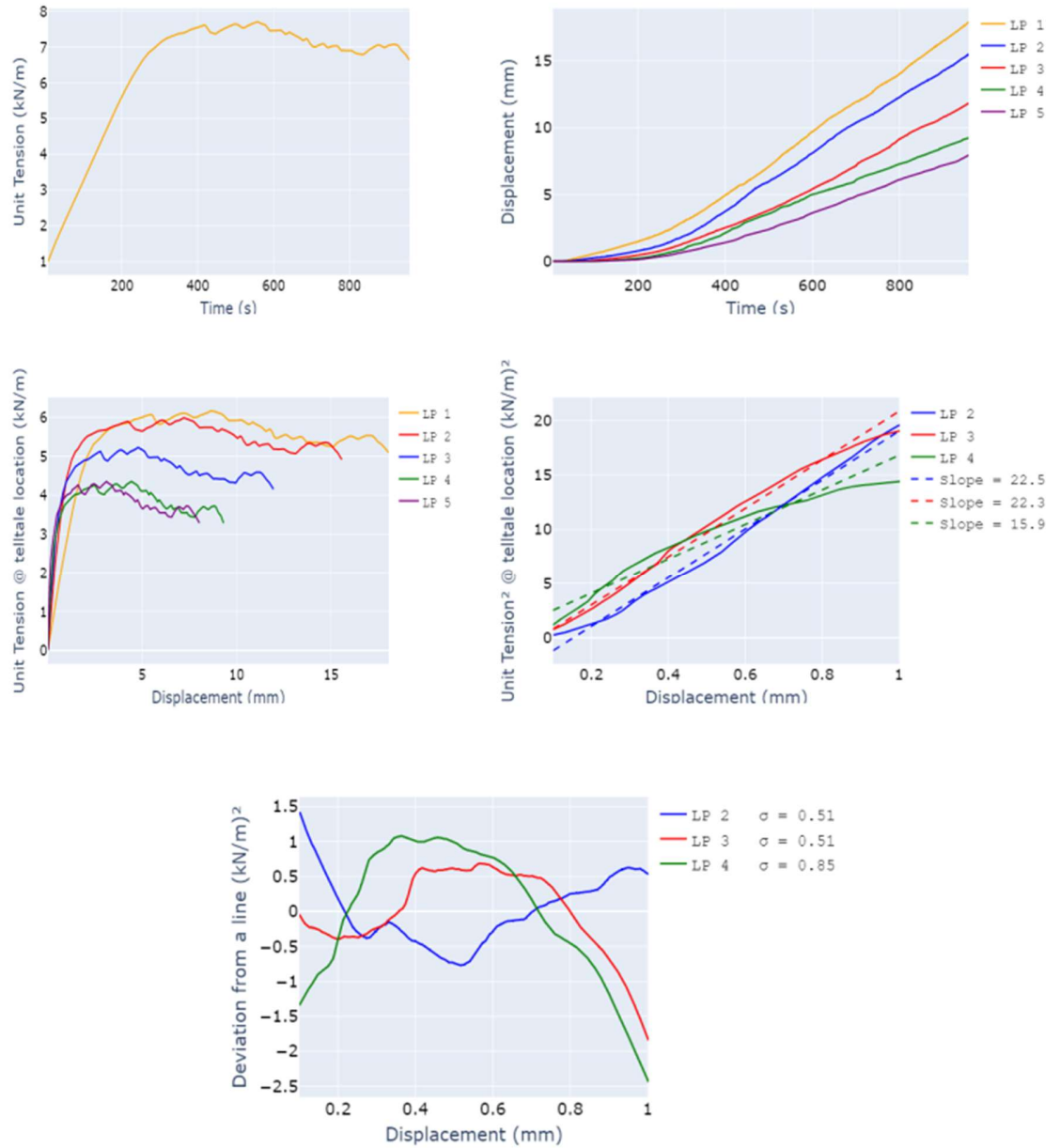


Figure A.46 - Results from the first test of configuration involving GT1 and Angular SAggr3

LP 1: Trigger Time (sec): 24.8 - T0 (kN/m): 1.5

LP 2: Trigger Time (sec): 32.2 - T0 (kN/m): 1.7

LP 3: Trigger Time (sec): 64.8 - T0 (kN/m): 2.5

LP 4: Trigger Time (sec): 102.4 - T0 (kN/m): 3.4

LP 5: Trigger Time (sec): 102.4 - T0 (kN/m): 3.4

Deviation from a line:

LP 2 - sd = 0.5 - Outlier: False

LP 3 - sd = 0.5 - Outlier: False

LP 4 - sd = 0.9 - Outlier: False

Ksgc values:

LP2: 22.5 - Outlier = False

LP3: 22.3 - Outlier = False

LP4: 15.9 - Outlier = True

Final results:

Ksgc = 22.2 - Pmax = 7.7

A.10.2 Test 2

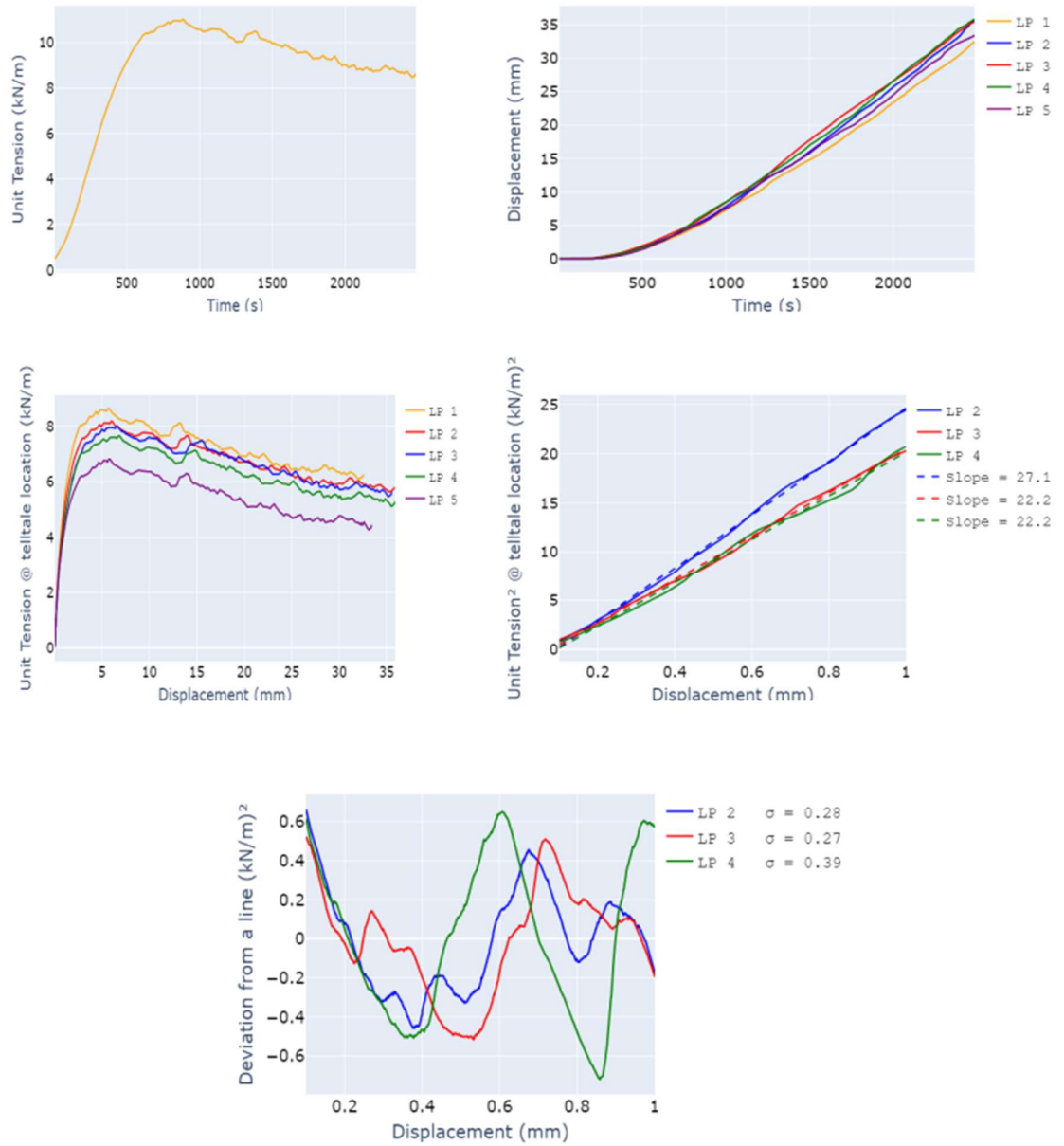


Figure A.47 - Results from the second test of configuration involving GT1 and Angular SAggr3

LP 1: Trigger Time (sec): 138.4 - T0 (kN/m): 2.37

LP 2: Trigger Time (sec): 160.6 - T0 (kN/m): 2.83

LP 3: Trigger Time (sec): 168.6 - T0 (kN/m): 3.0

LP 4: Trigger Time (sec): 184.4 - T0 (kN/m): 3.35

LP 5: Trigger Time (sec): 222.4 - T0 (kN/m): 4.19

Deviation from a line:

LP 2 - sd = 0.28 - Outlier: False

LP 3 - sd = 0.27 - Outlier: False

LP 4 - sd = 0.39 - Outlier: False

Ksgc values:

LP2: 27.1 - Outlier = False

LP3: 22.2 - Outlier = False

LP4: 22.2 - Outlier = False

Final results:

Ksgc = 22.92 - Pmax = 11.02

A.10.3 Test 3

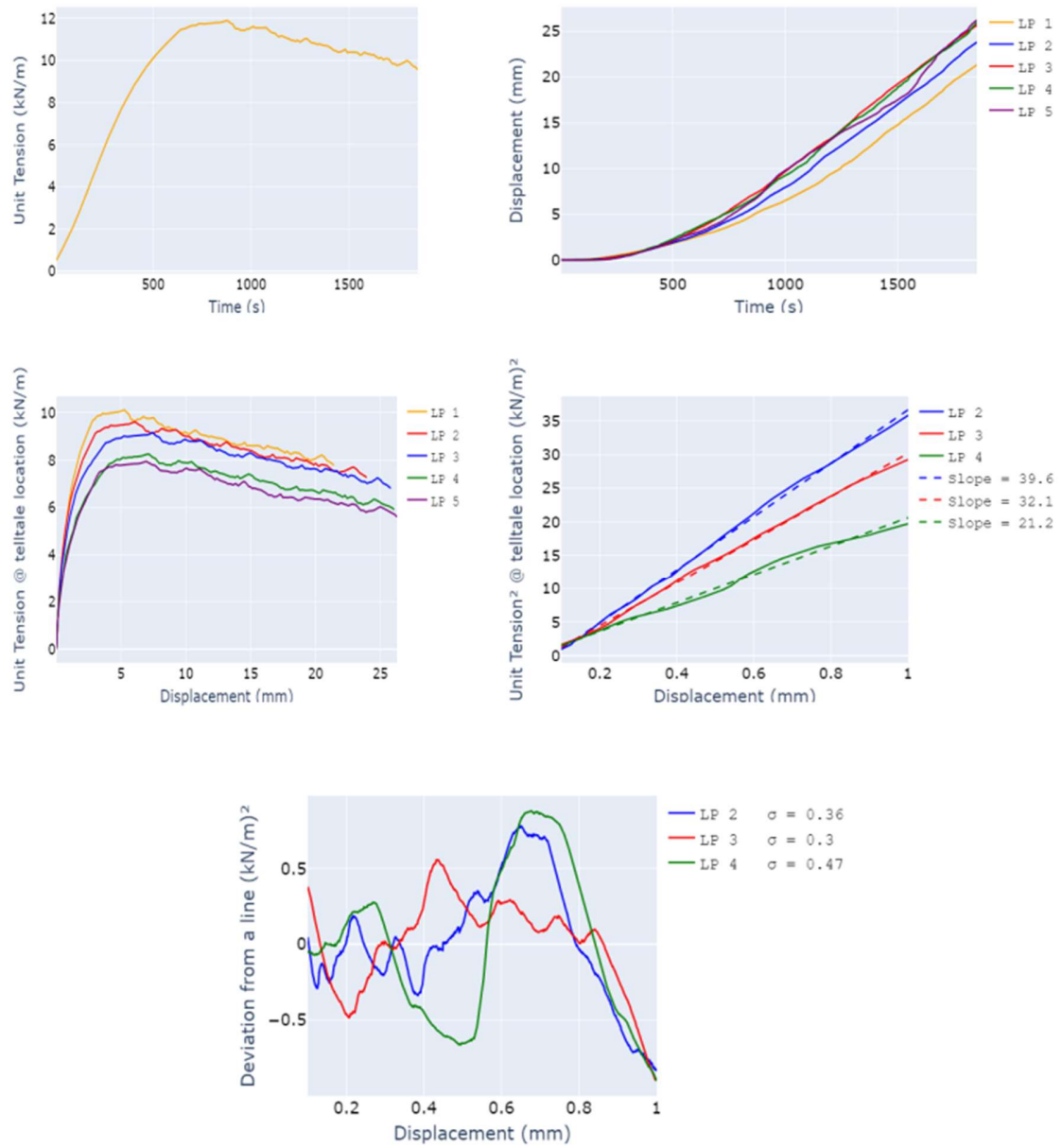


Figure A.48 - Results from the third test of configuration involving GT1 and Angular SAggr3

LP 1: Trigger Time (sec): 73.8 - T0 (kN/m): 1.8

LP 2: Trigger Time (sec): 98.2 - T0 (kN/m): 2.3

LP 3: Trigger Time (sec): 119.0 - T0 (kN/m): 2.7

LP 4: Trigger Time (sec): 157.0 - T0 (kN/m): 3.6

LP 5: Trigger Time (sec): 169.4 - T0 (kN/m): 3.9

Deviation from a line:

LP 2 - sd = 0.4 - Outlier: False

LP 3 - sd = 0.3 - Outlier: False

LP 4 - sd = 0.5 - Outlier: False

Ksgc values:

LP2: 39.6 - Outlier = False

LP3: 32.1 - Outlier = False

LP4: 21.2 - Outlier = True

Final results:

Ksgc = 32.9 - Pmax = 11.9

A.10.4 Test 4

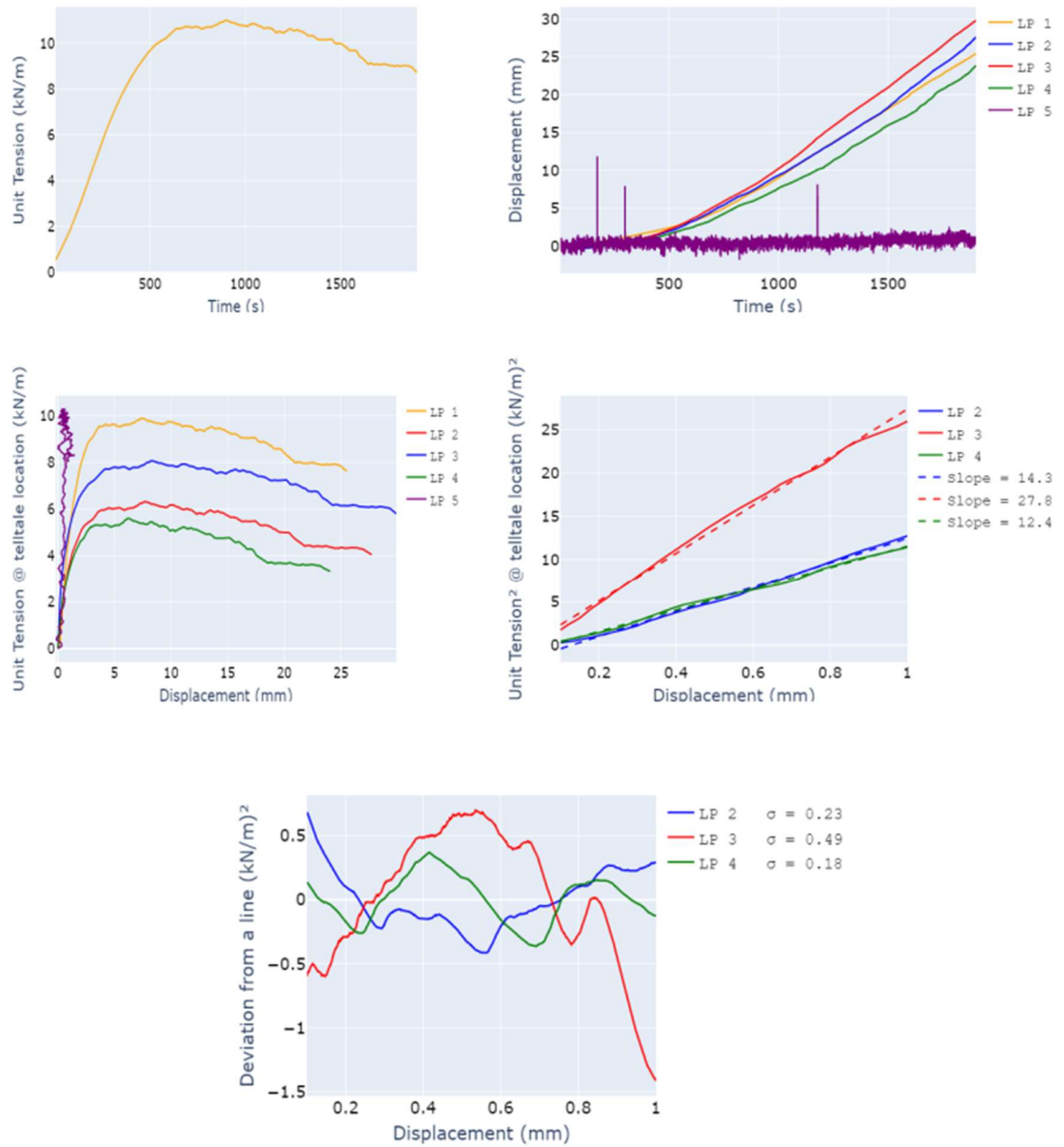


Figure A.49 - Results from the fourth test of configuration involving GT1 and Angular SAggr3

LP 1: Trigger Time (sec): 39.8 - T0 (kN/m): 1.1

LP 2: Trigger Time (sec): 204.4 - T0 (kN/m): 4.7

LP 3: Trigger Time (sec): 130.8 - T0 (kN/m): 2.9

LP 4: Trigger Time (sec): 235.0 - T0 (kN/m): 5.4

LP 5: Trigger Time (sec): 15.8 - T0 (kN/m): 0.7

Deviation from a line:

LP 2 - sd = 0.2 - Outlier: False

LP 3 - sd = 0.5 - Outlier: False

LP 4 - sd = 0.2 - Outlier: False

Ksgc values:

LP2: 14.3 - Outlier = False

LP3: 27.8 - Outlier = True

LP4: 12.4 - Outlier = False

Final results:

Ksgc = 13.1 - Pmax = 11.0

A.10.5 Test 5

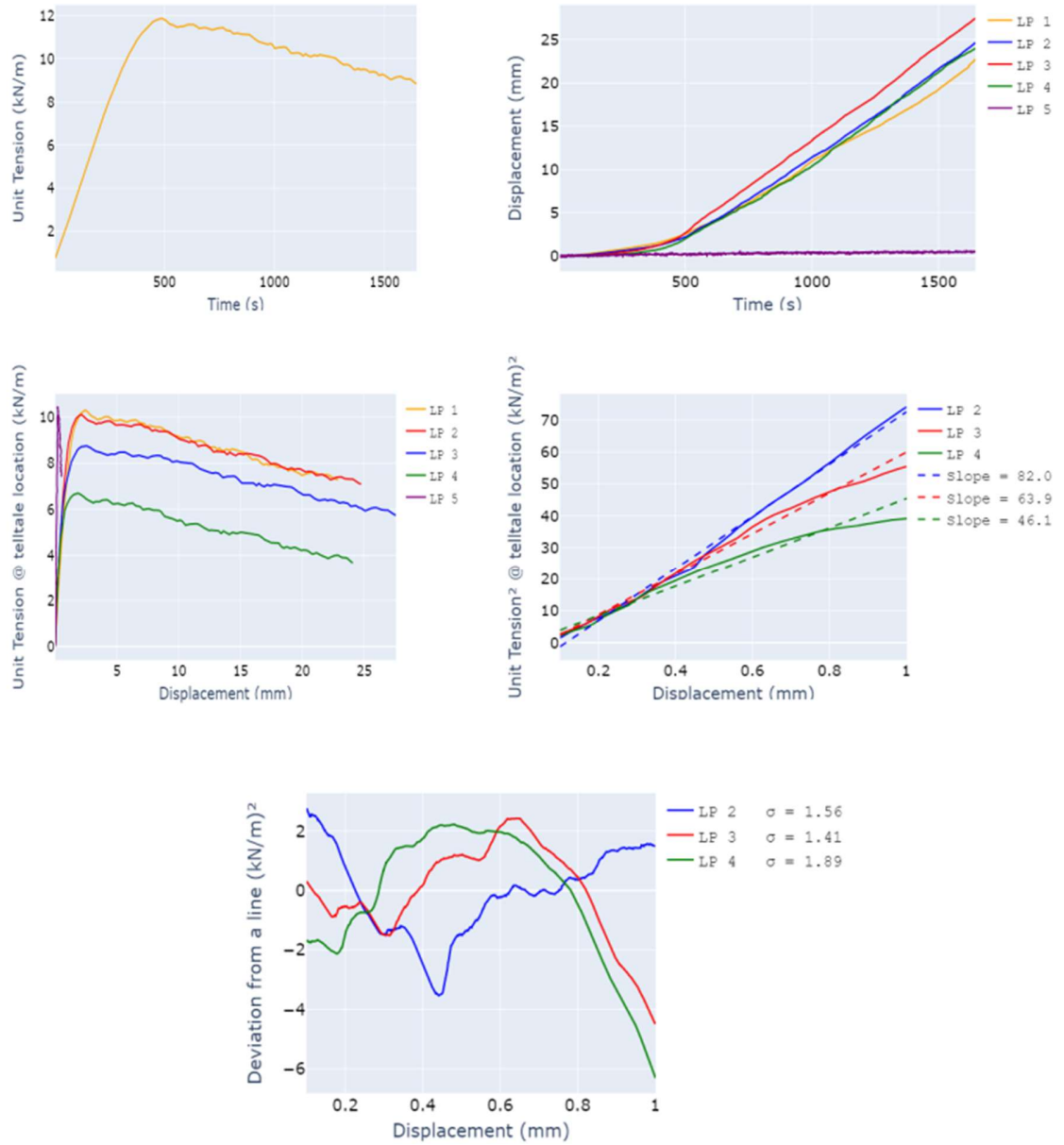


Figure A.50 - Results from the fifth test of configuration involving GT1 and Angular SAggr3

LP 1: Trigger Time (sec): 32.4 - T0 (kN/m): 1.6

LP 2: Trigger Time (sec): 39.4 - T0 (kN/m): 1.8

LP 3: Trigger Time (sec): 84.8 - T0 (kN/m): 3.1

LP 4: Trigger Time (sec): 151.0 - T0 (kN/m): 5.2

LP 5: Trigger Time (sec): 28.0 - T0 (kN/m): 1.4

Deviation from a line:

LP 2 - sd = 1.6 - Outlier: True

LP 3 - sd = 1.4 - Outlier: False

LP 4 - sd = 1.9 - Outlier: True

Ksgc values:

LP2: 82.0 - Outlier = True

LP3: 63.9 - Outlier = False

LP4: 46.1 - Outlier = False

Final results:

Ksgc = 63.9 - Pmax = 11.9

A.10.6 Summary of results from configuration involving GT1 and Angular SAggr3

Ksgc MAD = 14.6 - Pmax MAD = 1.3

Ksgc median = 22.9 - Pmax median = 11.1

If $((Ksgc_i - Ksgc_median)/MAD) > 2$: outlier

If $((Pmax_i - Pmax_median)/MAD) > 2.5$: outlier

Test 1

Pmax = 7.71 - Outlier: True - Ksgc = 22.18 - Outlier: False

Test 2

Pmax = 11.02 - Outlier: False - Ksgc = 22.92 - Outlier: False

Test 3

Pmax = 11.9 - Outlier: False - Ksgc = 32.85 - Outlier: False

Test 4

Pmax = 10.99 - Outlier: False - Ksgc = 13.07 - Outlier: False

Test 5

Pmax = 11.87 - Outlier: False - Ksgc = 63.87 - Outlier: True

Final results for this configuration:

Average Ksgc = 22.95 - Ksgc COV = 35.2%

Average Pmax = 11.3 - Pmax COV = 3.7%

A.11 CONFIGURATION INVOLVING GT1 AND ANGULAR WG

A.11.1 Test 1

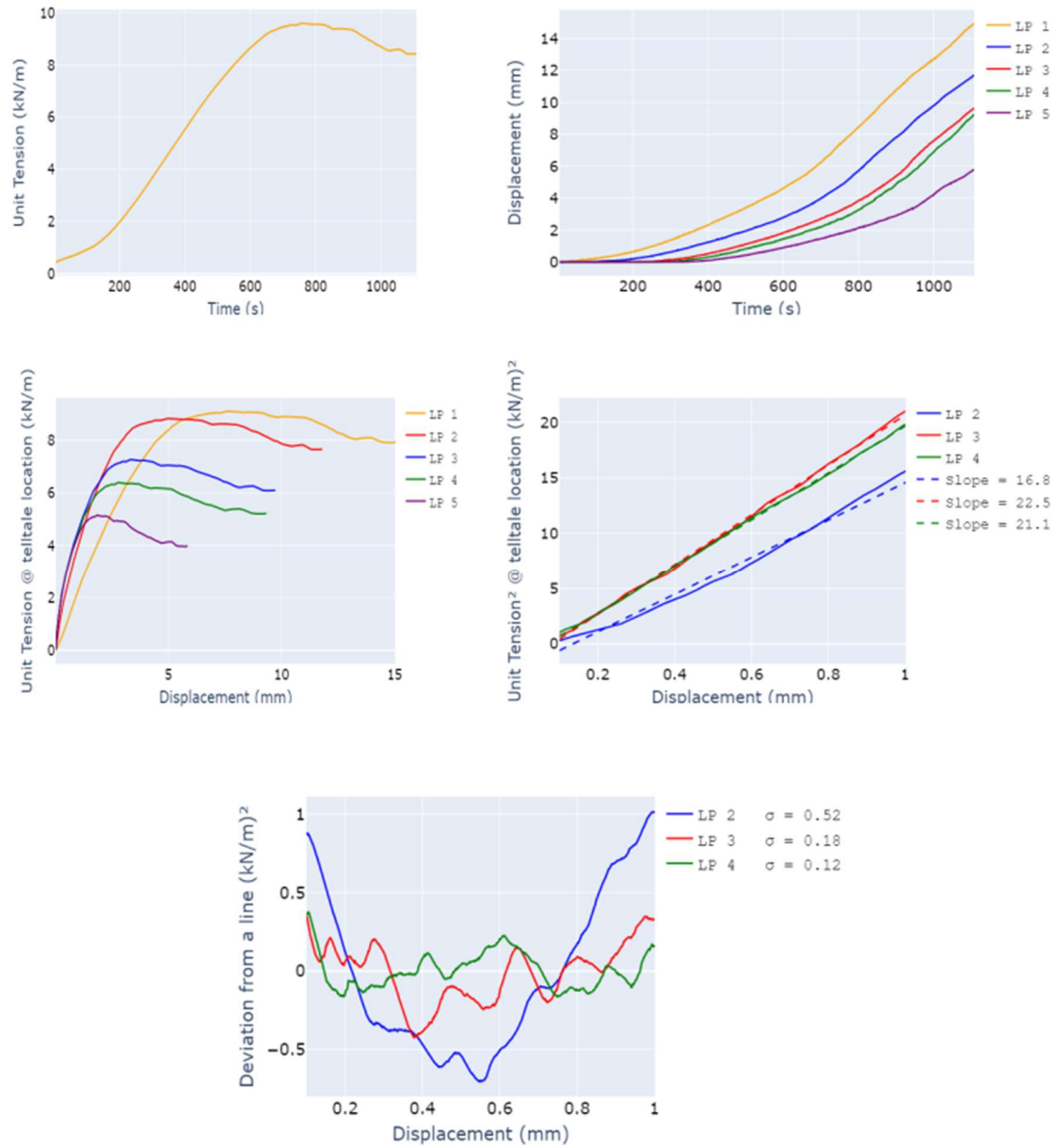


Figure A.51 - Results from the first test of configuration involving GT1 and Angular WG

A.11.2 Test 2

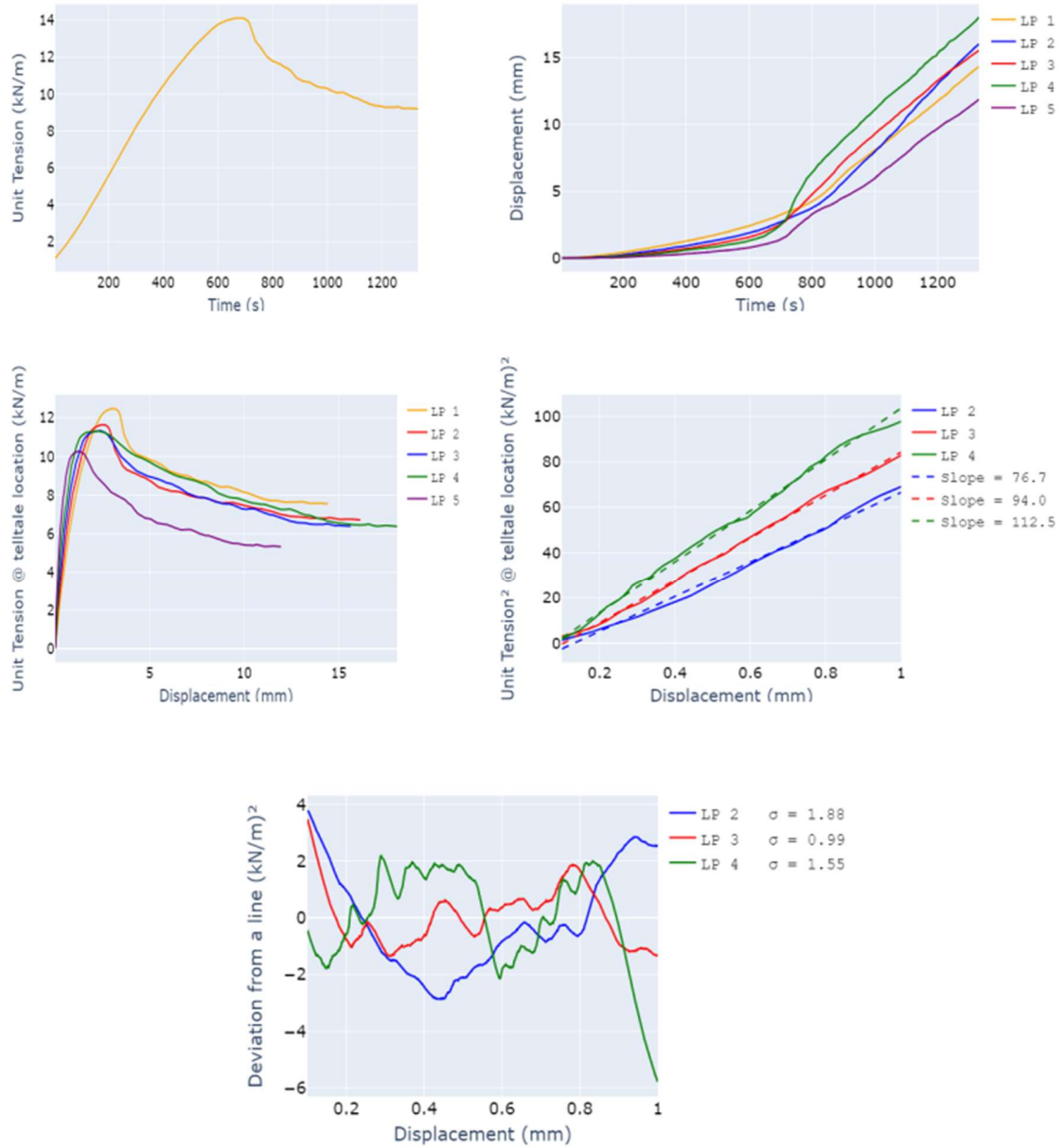


Figure A.52 - Results from the second test of configuration involving GT1 and Angular WG

LP 1: Trigger Time (sec): 35.4 - T0 (kN/m): 1.65

LP 2: Trigger Time (sec): 75.2 - T0 (kN/m): 2.48

LP 3: Trigger Time (sec): 89.8 - T0 (kN/m): 2.8

LP 4: Trigger Time (sec): 90.6 - T0 (kN/m): 2.82

LP 5: Trigger Time (sec): 134.6 - T0 (kN/m): 3.9

Deviation from a line:

LP 2 - sd = 1.88 - Outlier: True

LP 3 - sd = 0.99 - Outlier: False

LP 4 - sd = 1.55 - Outlier: True

Ksgc values:

LP2: 76.7 - Outlier = False

LP3: 94.0 - Outlier = False

LP4: 112.5 - Outlier = True

Final results:

Ksgc = 94.0- Pmax = 14.1

A.11.3 Test 3

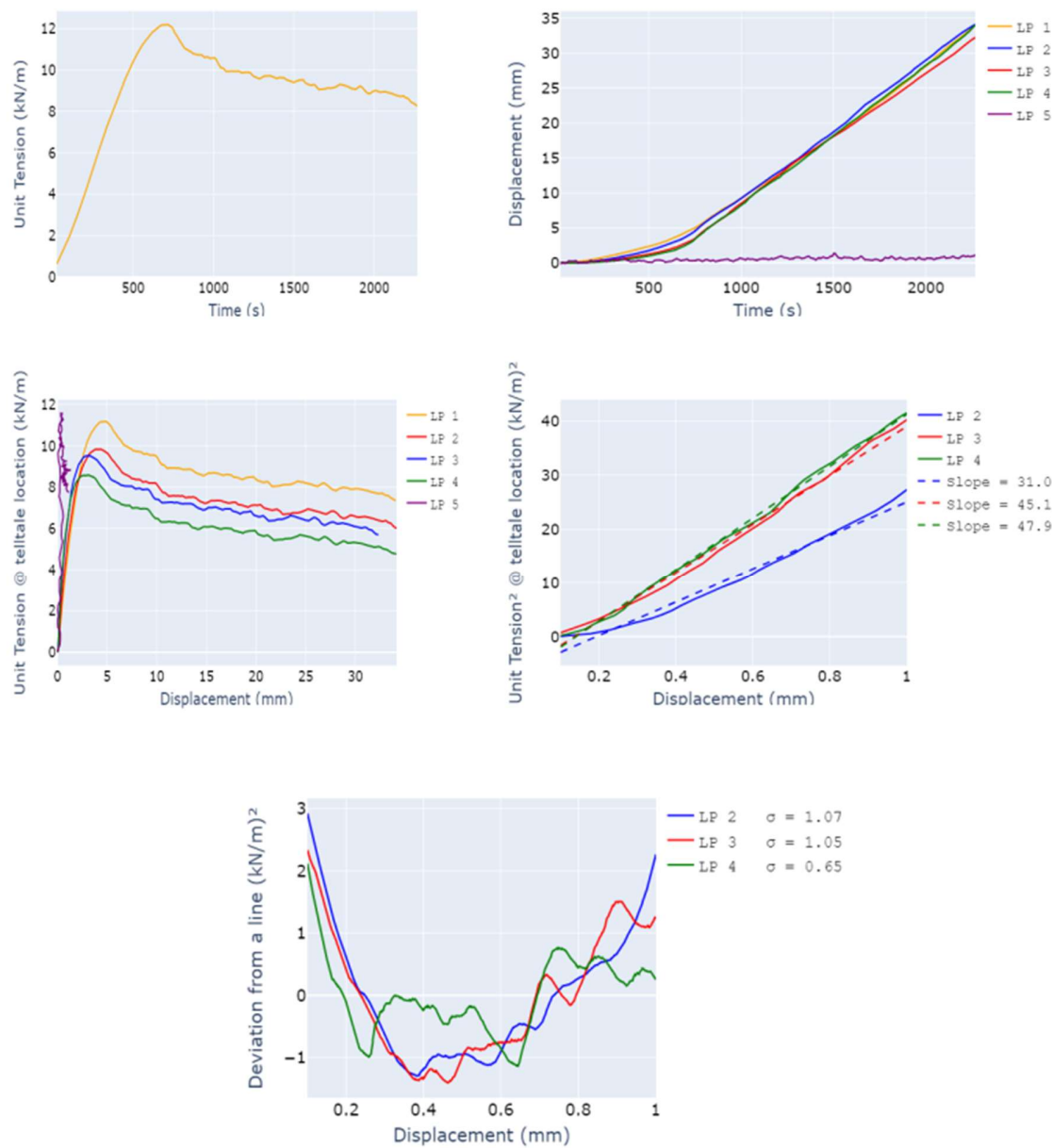


Figure A.53 - Results from the third test of configuration involving GT1 and Angular WG

LP 1: Trigger Time (sec): 50.0 - T0 (kN/m): 1.03

LP 2: Trigger Time (sec): 124.4 - T0 (kN/m): 2.4

LP 3: Trigger Time (sec): 139.8 - T0 (kN/m): 2.7

LP 4: Trigger Time (sec): 181.8 - T0 (kN/m): 3.6

LP 5: Trigger Time (sec): 23.8 - T0 (kN/m): 0.6

Deviation from a line:

LP 2 - sd = 1.1 - Outlier: False

LP 3 - sd = 1.1 - Outlier: False

LP 4 - sd = 0.7 - Outlier: False

Ksgc values:

LP2: 31.0 - Outlier = True

LP3: 45.1 - Outlier = False

LP4: 47.9 - Outlier = False

Final results:

Ksgc = 45.7 - Pmax = 12.2

A.11.4 Test 4

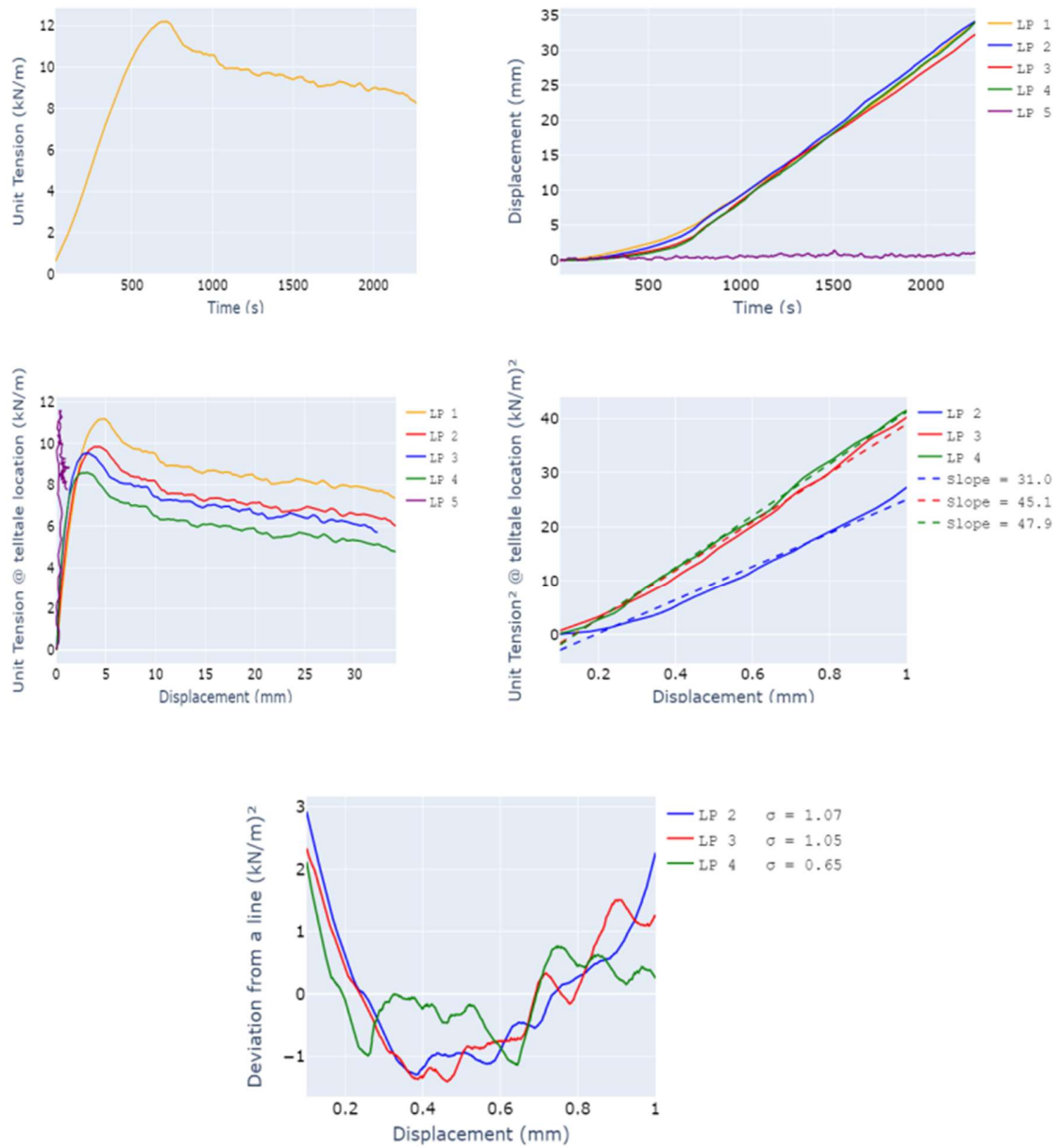


Figure A.54 - Results from the fourth test of configuration involving GT1 and Angular WG

LP 1: Trigger Time (sec): 34.2 - T0 (kN/m): 1.0

LP 2: Trigger Time (sec): 77.6 - T0 (kN/m): 1.8

LP 3: Trigger Time (sec): 136.4 - T0 (kN/m): 3.1

LP 4: Trigger Time (sec): 126.0 - T0 (kN/m): 2.9

LP 5: Trigger Time (sec): 181.6 - T0 (kN/m): 4.3

Deviation from a line:

LP 2 - sd = 1.4 - Outlier: False

LP 3 - sd = 1.1 - Outlier: False

LP 4 - sd = 0.8 - Outlier: False

Ksgc values:

LP2: 57.8 - Outlier = False

LP3: 54.4 - Outlier = False

LP4: 87.6 - Outlier = True

Final results:

Ksgc = 54.4 - Pmax = 13.3

A.11.5 Test 5

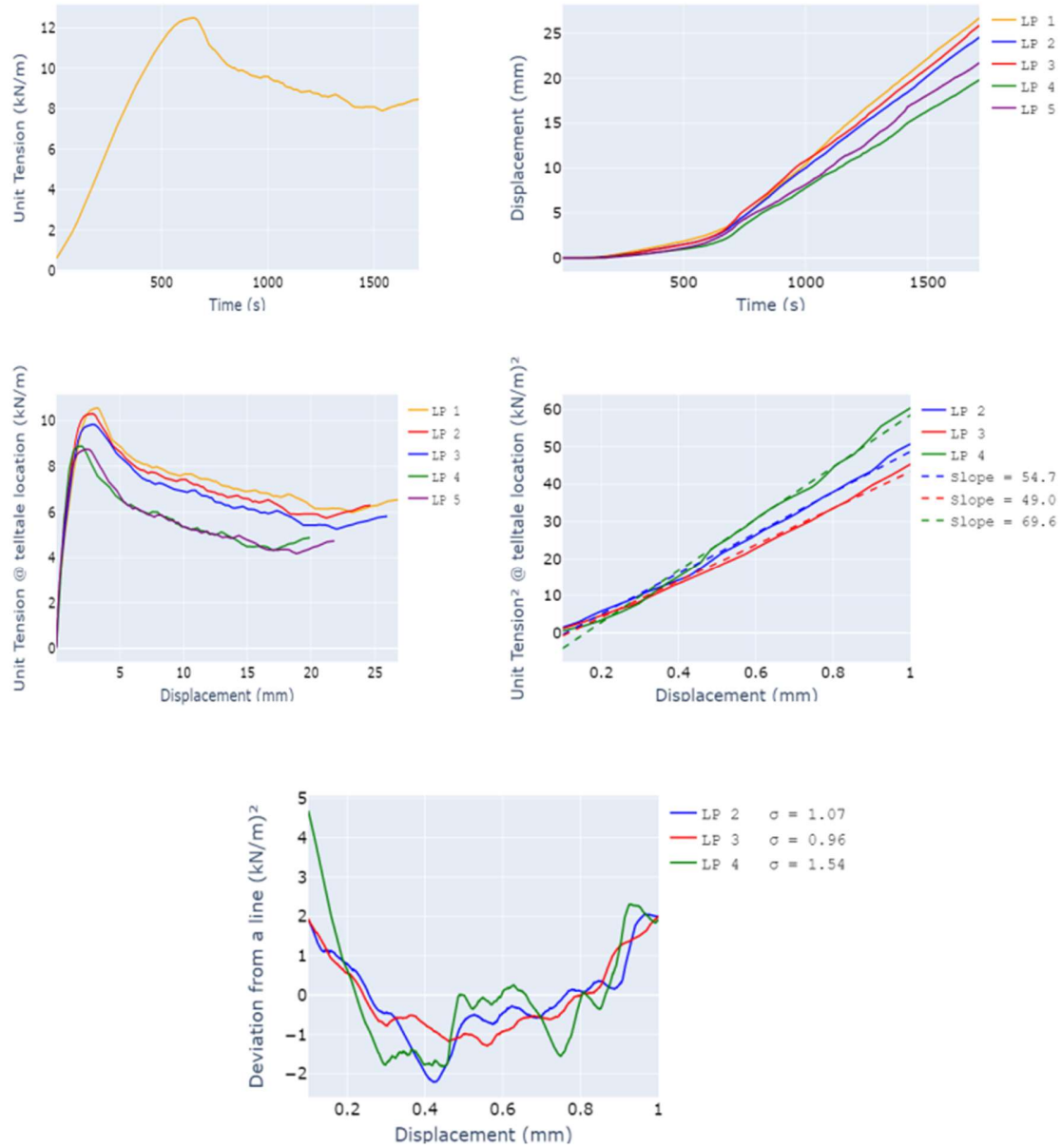


Figure A.55 - Results from the fifth test of configuration involving GT1 and Angular WG

LP 1: Trigger Time (sec): 81.4 - T0 (kN/m): 1.9

LP 2: Trigger Time (sec): 92.6 - T0 (kN/m): 2.2

LP 3: Trigger Time (sec): 114.0 - T0 (kN/m): 2.7

LP 4: Trigger Time (sec): 152.2 - T0 (kN/m): 3.6

LP 5: Trigger Time (sec): 157.8 - T0 (kN/m): 3.7

Deviation from a line:

LP 2 - sd = 1.07 - Outlier: False

LP 3 - sd = 0.96 - Outlier: False

LP 4 - sd = 1.54 - Outlier: True

Ksgc values:

LP2: 54.7 - Outlier = False

LP3: 49.0 - Outlier = False

LP4: 69.6 - Outlier = True

Final results:

Ksgc = 48.53 - Pmax = 12.48

A.11.6 Summary of results from configuration involving GT1 and Angular WG

Ksgc MAD = 8.6 - Pmax MAD = 1.2

Ksgc median = 48.5 - Pmax median = 12.5

If $((Ksgc_i - Ksgc_median)/MAD) > 2$: outlier

If $((Pmax_i - Pmax_median)/MAD) > 2.5$: outlier

Test 1

Pmax = 9.6 - Outlier: False - Ksgc = 22.05 - Outlier : True

Test 2

Pmax = 14.13 - Outlier: False - Ksgc = 93.99 - Outlier : True

Test 3

Pmax = 12.21 - Outlier: False - Ksgc = 45.68 - Outlier : False

Test 4

Pmax = 13.27 - Outlier: False - Ksgc = 54.36 - Outlier : False

Test 5

Pmax = 12.48 - Outlier: False - Ksgc = 48.53 - Outlier : False

Final results for this configuration:

Average Ksgc = 49.52 - Ksgc COV = 7.3%

Average Pmax = 12.65 - Pmax COV = 3.6%

A.12 CONFIGURATION INVOLVING GT1 AND 50-50 SAGGR2

A.12.1 Test 1

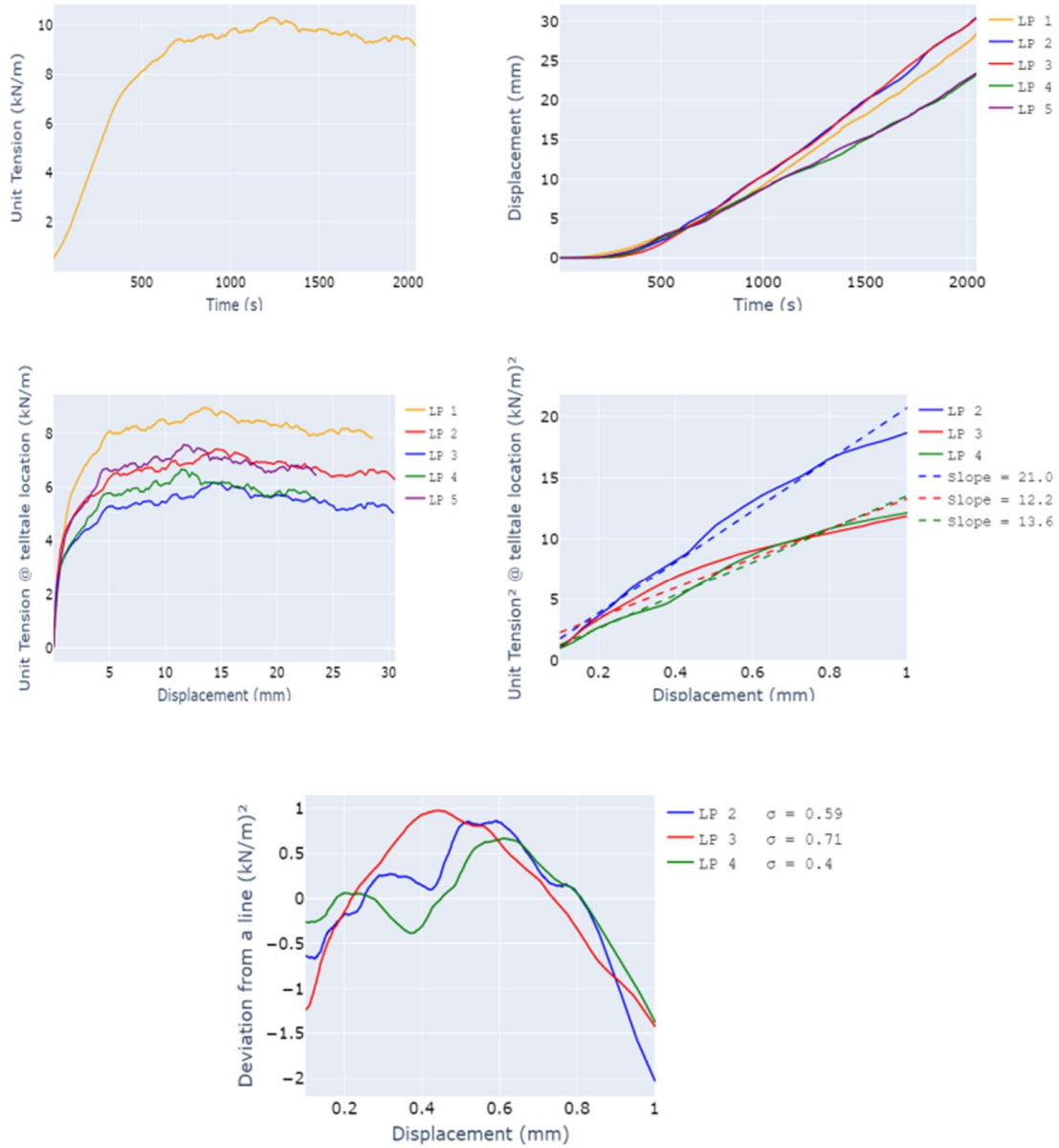


Figure A.56 - Results from the first test of configuration involving GT1 and 50-50 SAggr2

LP 1: Trigger Time (sec): 70.4 - T0 (kN/m): 1.4

LP 2: Trigger Time (sec): 154.4 - T0 (kN/m): 2.9

LP 3: Trigger Time (sec): 214.4 - T0 (kN/m): 4.1

LP 4: Trigger Time (sec): 190.4 - T0 (kN/m): 3.6

LP 5: Trigger Time (sec): 146.8 - T0 (kN/m): 2.7

Deviation from a line:

LP 2 - sd = 0.6 - Outlier: False

LP 3 - sd = 0.7 - Outlier: False

LP 4 - sd = 0.4 - Outlier: False

Ksgc values:

LP2: 21.0 - Outlier = True

LP3: 12.2 - Outlier = False

LP4: 13.6 - Outlier = False

Final results:

Ksgc = 13.0 - Pmax = 10.3

A.12.2 Test 2

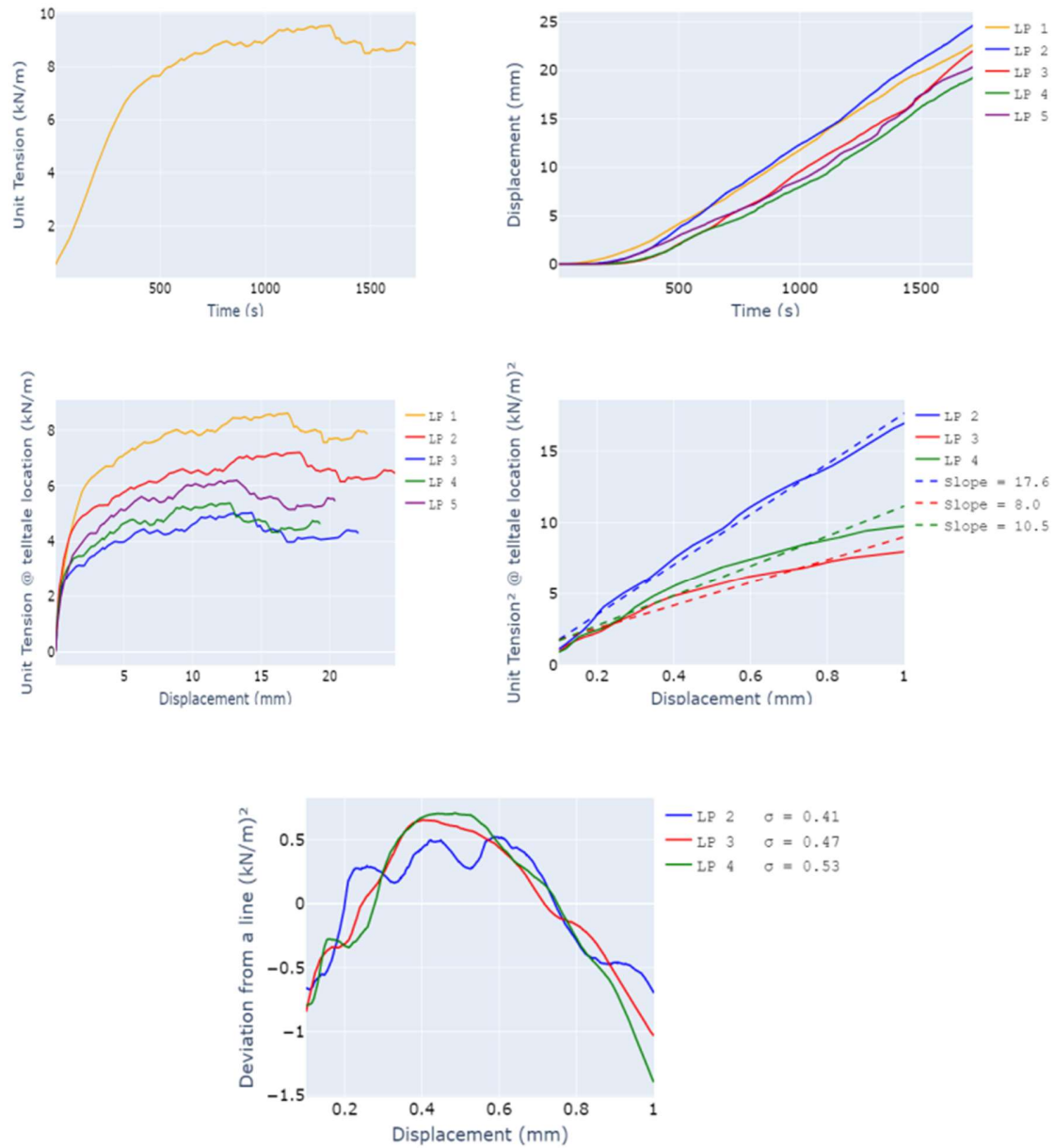


Figure A.57 - Results from the second test of configuration involving GT1 and 50-50 SAggr2

LP 1: Trigger Time (sec): 32.0 - T0 (kN/m): 0.9
LP 2: Trigger Time (sec): 113.0 - T0 (kN/m): 2.4
LP 3: Trigger Time (sec): 212.2 - T0 (kN/m): 4.5
LP 4: Trigger Time (sec): 195.8 - T0 (kN/m): 4.2
LP 5: Trigger Time (sec): 158.6 - T0 (kN/m): 3.36

Deviation from a line:

LP 2 - sd = 0.41 - Outlier: False
LP 3 - sd = 0.47 - Outlier: False
LP 4 - sd = 0.53 - Outlier: False

Ksgc values:

LP2: 17.6 - Outlier = True
LP3: 8.0 - Outlier = False
LP4: 10.5 - Outlier = False

Final results:

Ksgc = 8.17 - Pmax = 9.56

A.12.3 Test 3

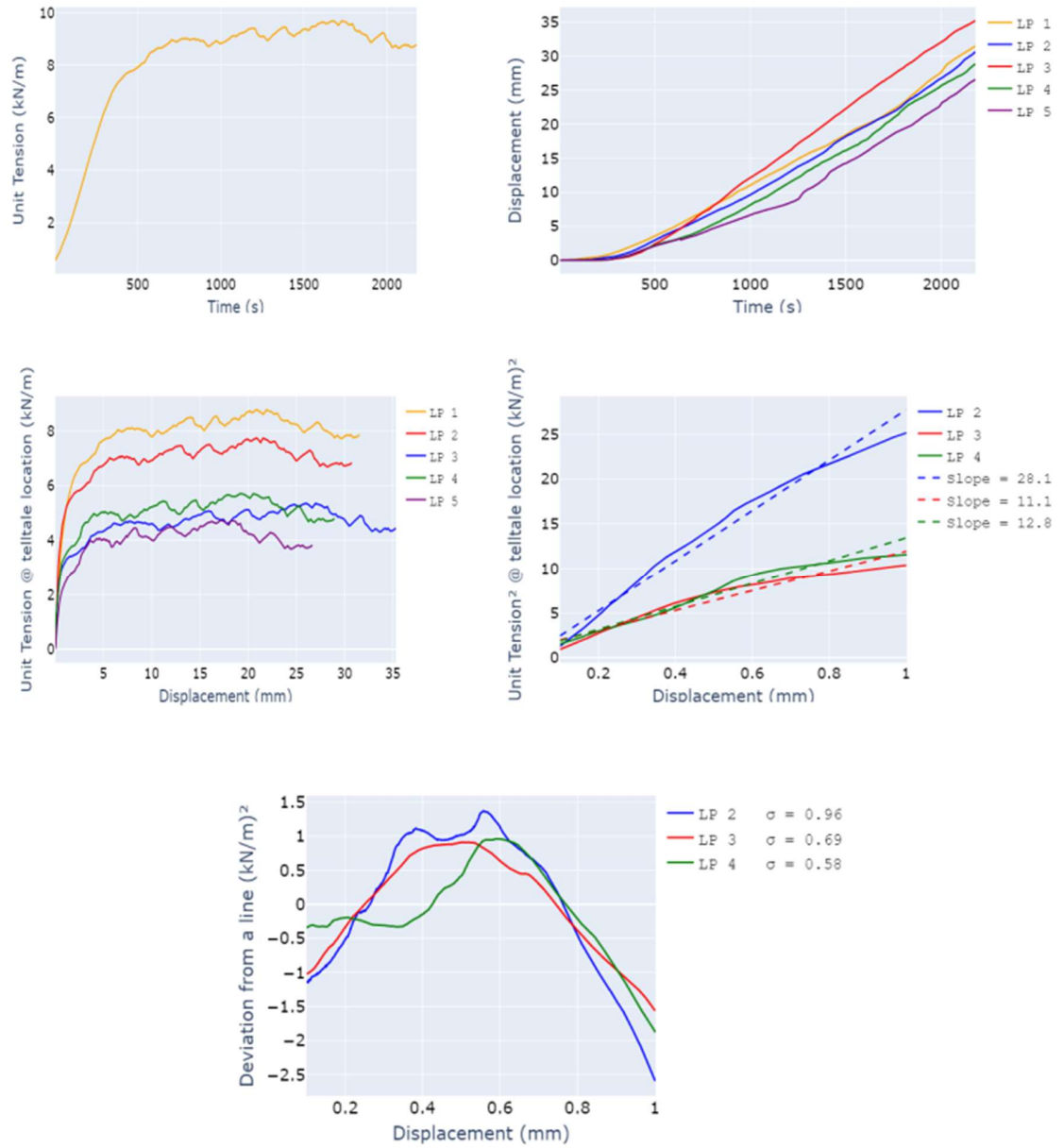


Figure A.58 - Results from the third test of configuration involving GT1 and 50-50 SAggr2

LP 1: Trigger Time (sec): 34.6 - T0 (kN/m): 0.9

LP 2: Trigger Time (sec): 94.8 - T0 (kN/m): 2.0

LP 3: Trigger Time (sec): 204.6 - T0 (kN/m): 4.3

LP 4: Trigger Time (sec): 189.2 - T0 (kN/m): 4.0

LP 5: Trigger Time (sec): 233.4 - T0 (kN/m): 5.0

Deviation from a line:

LP 2 - sd = 1.0 - Outlier: False

LP 3 - sd = 0.7 - Outlier: False

LP 4 - sd = 0.6 - Outlier: False

Ksgc values:

LP2: 28.1 - Outlier = True

LP3: 11.1 - Outlier = False

LP4: 12.8 - Outlier = False

Final results:

Ksgc = 11.2 - Pmax = 9.7

A.12.4 Test 4

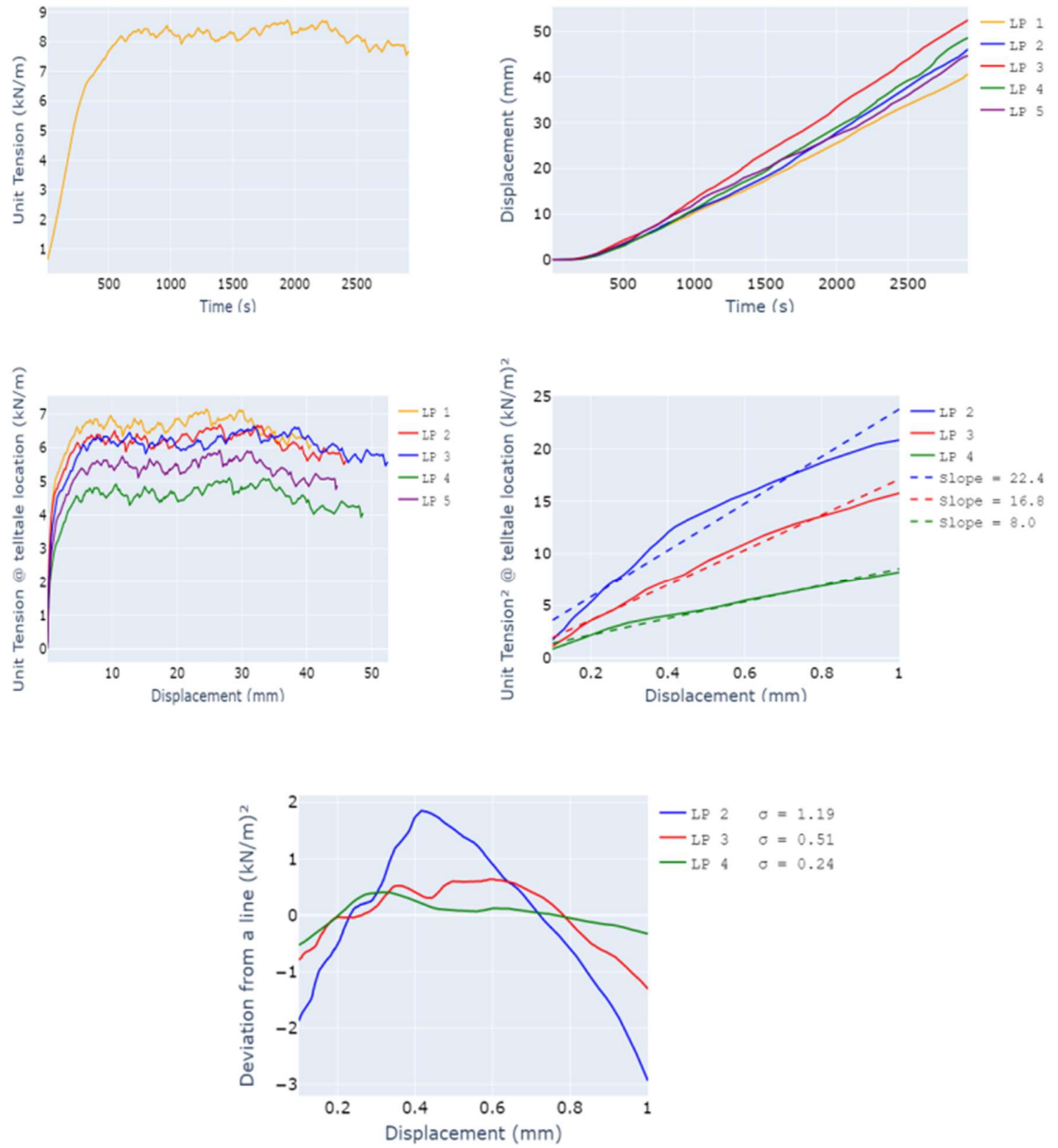


Figure A.59 - Results from the fourth test of configuration involving GT1 and 50-50 SAggr2

LP 1: Trigger Time (sec): 58.2 - T0 (kN/m): 1.6

LP 2: Trigger Time (sec): 81.0 - T0 (kN/m): 2.1

LP 3: Trigger Time (sec): 83.2 - T0 (kN/m): 2.1

LP 4: Trigger Time (sec): 150.0 - T0 (kN/m): 3.6

LP 5: Trigger Time (sec): 115.2 - T0 (kN/m): 2.8

Deviation from a line:

LP 2 - sd = 1.19 - Outlier: False

LP 3 - sd = 0.51 - Outlier: False

LP 4 - sd = 0.24 - Outlier: False

Ksgc values:

LP2: 22.4 - Outlier = False

LP3: 16.8 - Outlier = False

LP4: 8.0 - Outlier = True

Final results:

Ksgc = 17.01 - Pmax = 8.73

A.12.5 Test 5

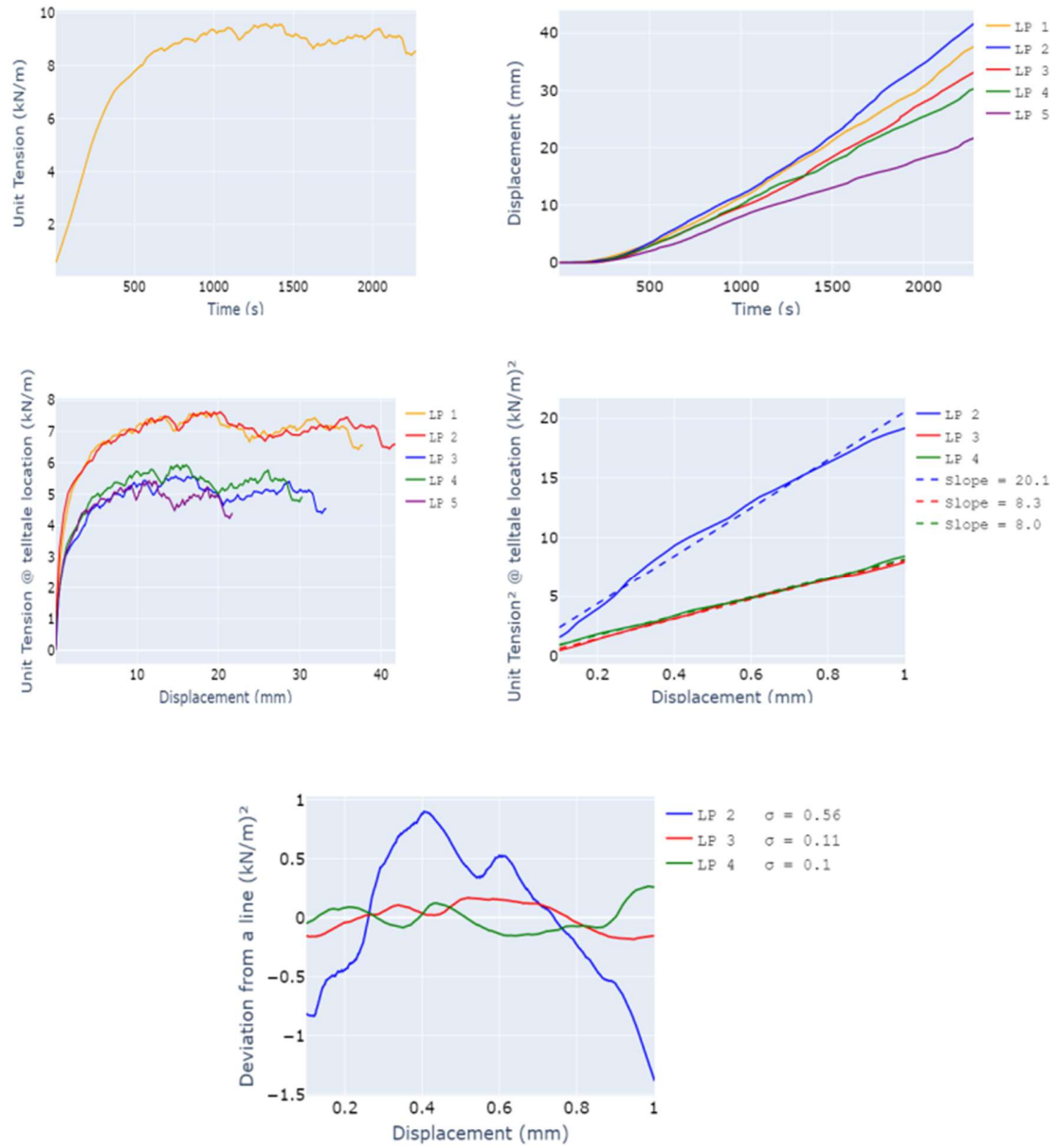


Figure A.60 - Results from the fifth test of configuration involving GT1 and 50-50 SAggr2

LP 1: Trigger Time (sec): 84.2 - T0 (kN/m): 2.0

LP 2: Trigger Time (sec): 83.6 - T0 (kN/m): 1.9

LP 3: Trigger Time (sec): 178.8 - T0 (kN/m): 4.0

LP 4: Trigger Time (sec): 162.6 - T0 (kN/m): 3.6

LP 5: Trigger Time (sec): 186.6 - T0 (kN/m): 4.2

Deviation from a line:

LP 2 - sd = 0.7 - Outlier: False

LP 3 - sd = 0.1 - Outlier: False

LP 4 - sd = 0.1 - Outlier: False

Ksgc values:

LP2: 20.1 - Outlier = True

LP3: 8.3 - Outlier = False

LP4: 8.0 - Outlier = False

Final results:

Ksgc = 8.3 - Pmax = 9.6

A.12.6 Summary of results from configuration involving GT1 and 50-50 SAggr2

Ksgc MAD = 4.28 - Pmax MAD = 0.18

Ksgc median = 11.21 - Pmax median = 9.58

If $((Ksgc_i - Ksgc_median)/MAD) > 2$: outlier

If $((Pmax_i - Pmax_median)/MAD) > 2.5$: outlier

Test 1

Pmax = 10.31 - Outlier: True - Ksgc = 13.04 - Outlier : False

Test 2

Pmax = 9.56 - Outlier: False - Ksgc = 8.17 - Outlier : False

Test 3

Pmax = 9.7 - Outlier: False - Ksgc = 11.21 - Outlier : False

Test 4

Pmax = 8.73 - Outlier: True - Ksgc = 17.01 - Outlier : False

Test 5

Pmax = 9.58 - Outlier: False - Ksgc = 8.32 - Outlier : False

Final results for this configuration:

Average Ksgc = 9.23 - Ksgc COV = 15.2%

Average Pmax = 9.61 - Pmax COV = 0.6%

A.13 CONFIGURATION INVOLVING GT1 AND MONTEREY SAND

A.13.1 Test 1

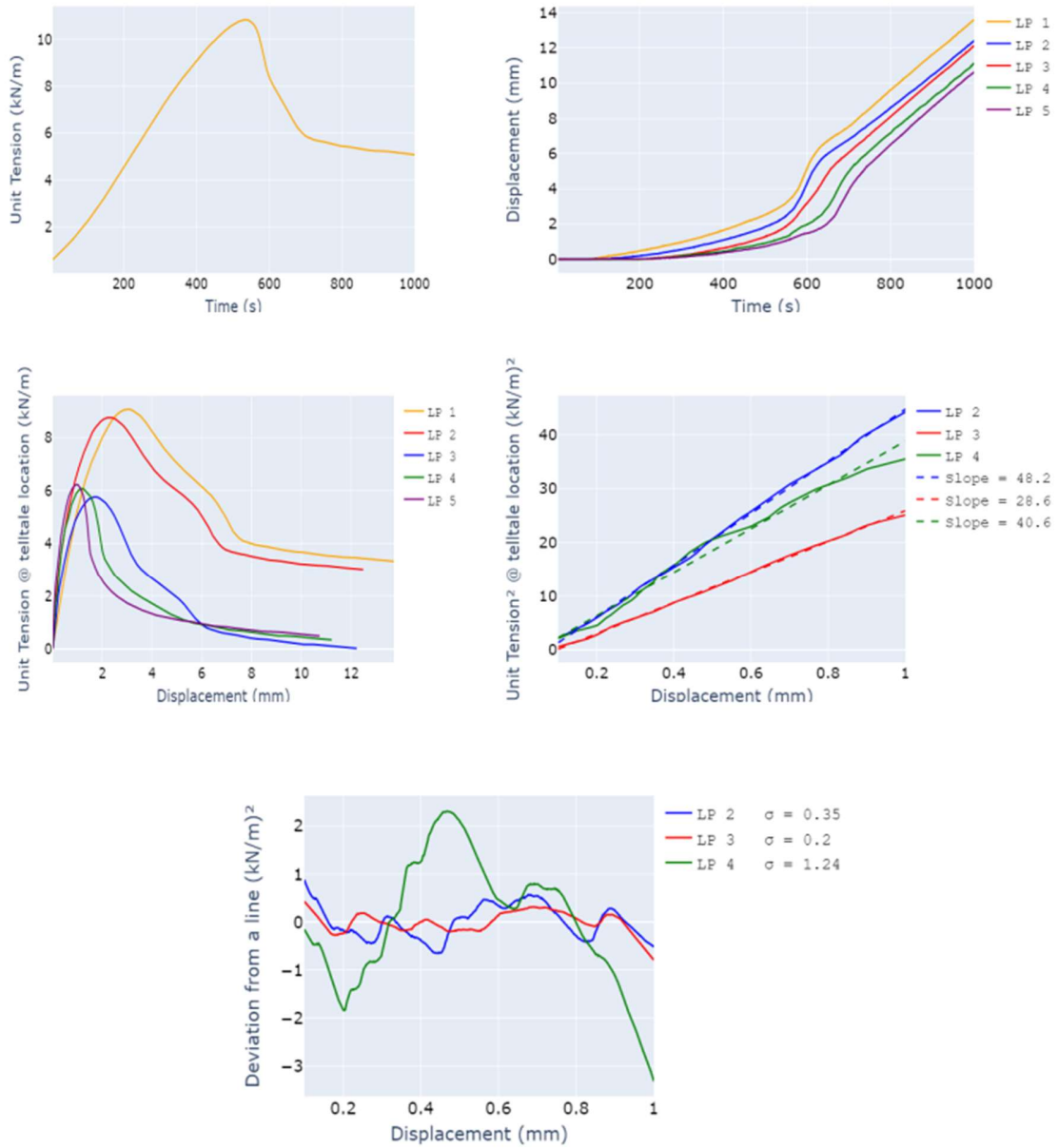


Figure A.61 - Results from the first test of configuration involving GT1 and Monterey Sand

LP 1: Trigger Time (sec): 75.0 - T0 (kN/m): 1.75
LP 2: Trigger Time (sec): 91.4 - T0 (kN/m): 2.06
LP 3: Trigger Time (sec): 220.6 - T0 (kN/m): 5.06
LP 4: Trigger Time (sec): 208.0 - T0 (kN/m): 4.74
LP 5: Trigger Time (sec): 201.8 - T0 (kN/m): 4.59

Deviation from a line:

LP 2 - sd = 0.3 - Outlier: False
LP 3 - sd = 0.2 - Outlier: False
LP 4 - sd = 1.2 - Outlier: False

Ksgc values:

LP2: 48.2 - Outlier = False
LP3: 28.6 - Outlier = True
LP4: 40.6 - Outlier = False

Final results:

Ksgc = 44.6 - Pmax = 10.8

A.13.2 Test 2

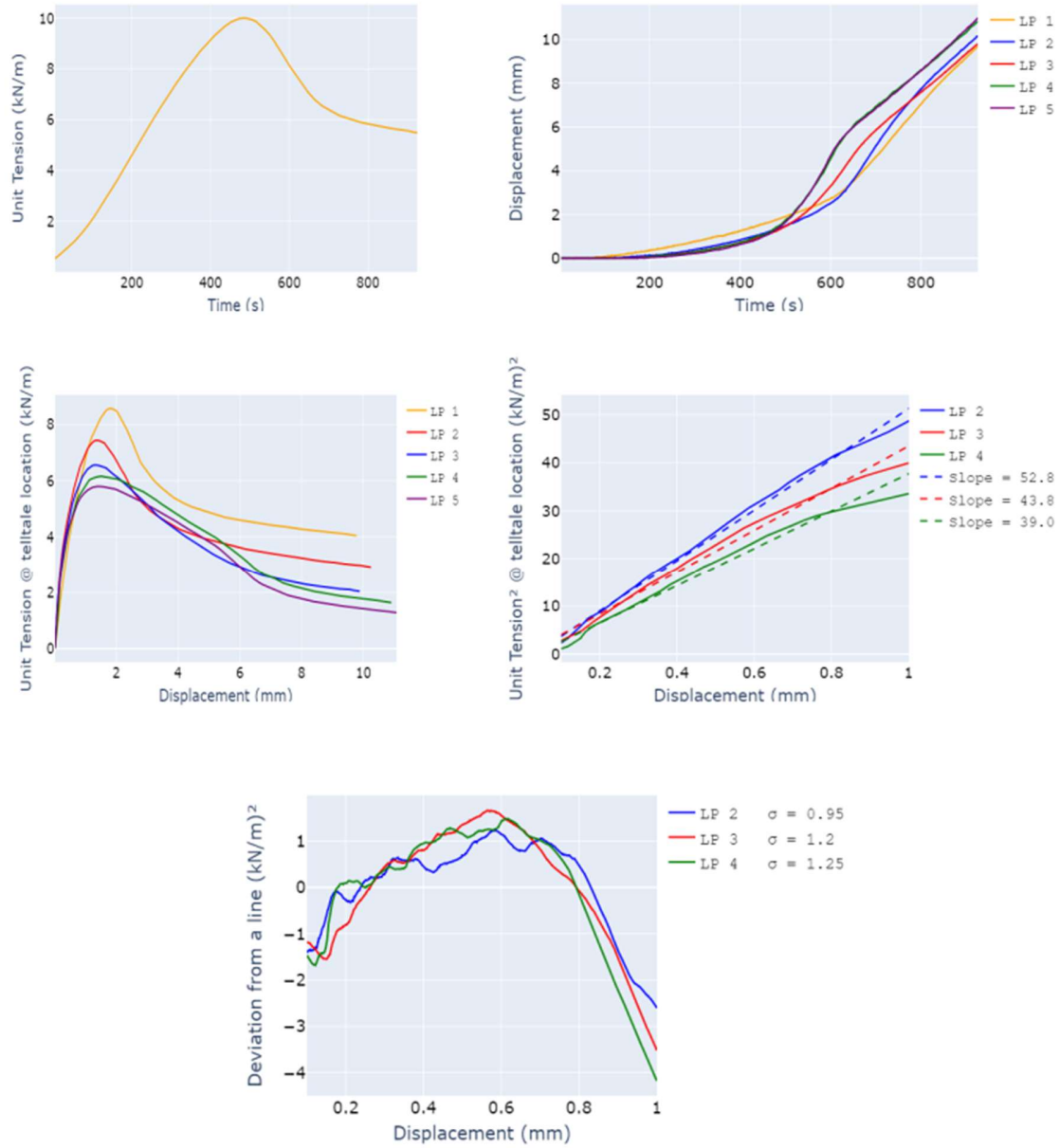


Figure A.62 - Results from the first test of configuration involving GT1 and Monterey Sand

LP 1: Trigger Time (sec): 68.2 - T0 (kN/m): 1.4

LP 2: Trigger Time (sec): 121.0 - T0 (kN/m): 2.6

LP 3: Trigger Time (sec): 156.6 - T0 (kN/m): 3.5

LP 4: Trigger Time (sec): 172.0 - T0 (kN/m): 3.9

LP 5: Trigger Time (sec): 185.6 - T0 (kN/m): 4.2

Deviation from a line:

LP 2 - sd = 1.0 - Outlier: False

LP 3 - sd = 1.2 - Outlier: False

LP 4 - sd = 1.3 - Outlier: False

Ksgc values:

LP2: 52.8 - Outlier = False

LP3: 43.8 - Outlier = False

LP4: 39.0 - Outlier = False

Final results:

Ksgc = 43.8 - Pmax = 10.0

A.13.3 Test 3

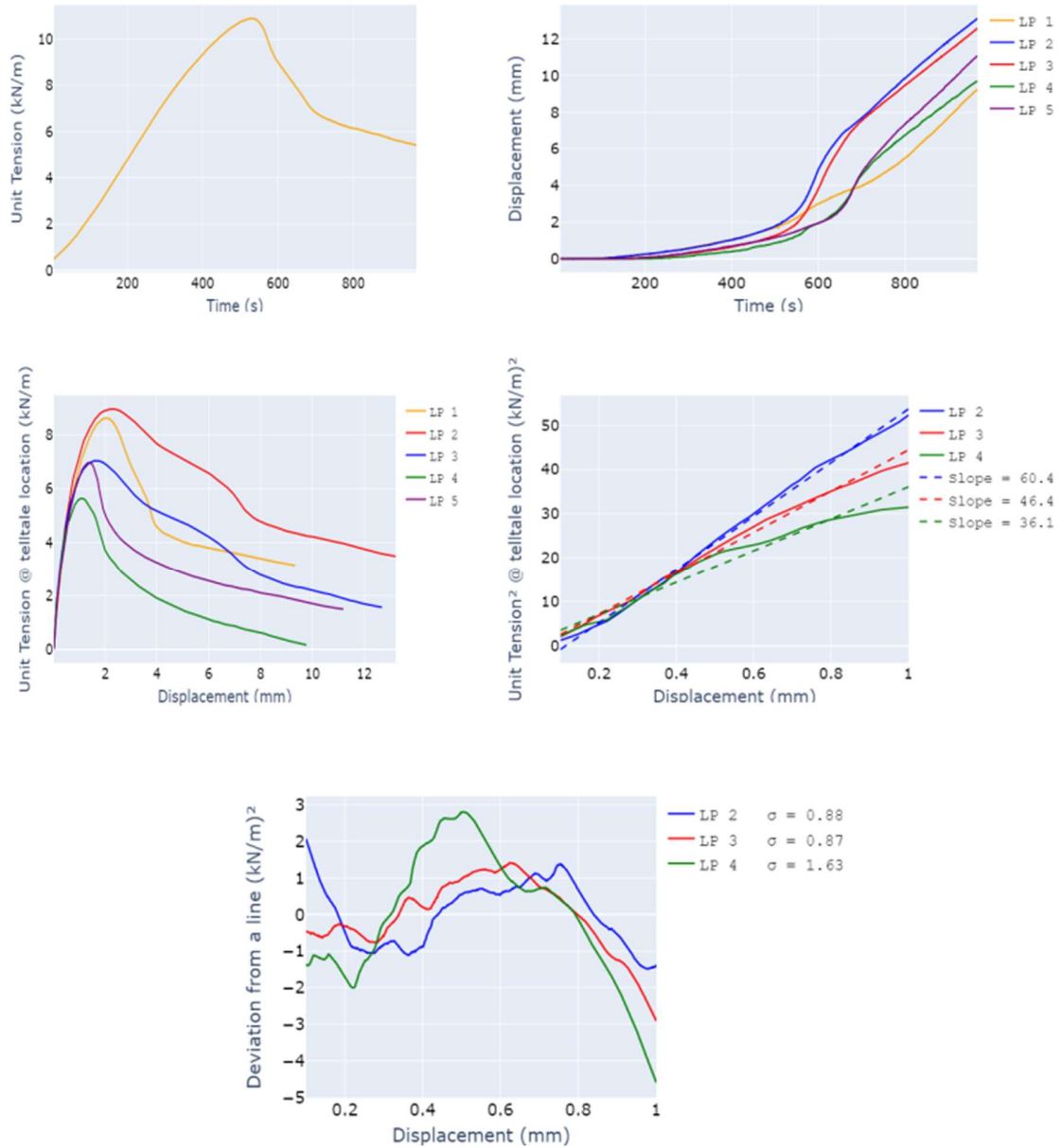


Figure A.63 - Results from the third test of configuration involving GT1 and Monterey Sand

LP 1: Trigger Time (sec): 100.2 - T0 (kN/m): 2.3

LP 2: Trigger Time (sec): 85.0 - T0 (kN/m): 1.9

LP 3: Trigger Time (sec): 164.2 - T0 (kN/m): 3.9

LP 4: Trigger Time (sec): 217.4 - T0 (kN/m): 5.3

LP 5: Trigger Time (sec): 167.0 - T0 (kN/m): 3.9

Deviation from a line:

LP 2 - sd = 0.88 - Outlier: False

LP 3 - sd = 0.87 - Outlier: False

LP 4 - sd = 1.63 - Outlier: True

Ksgc values:

LP2: 60.4 - Outlier = True

LP3: 46.4 - Outlier = False

LP4: 36.1 - Outlier = False

Final results:

Ksgc = 46.44 - Pmax = 10.89

A.13.4 Summary of results from configuration involving GT1 and Monterey Sand

Ksgc MAD = 1.16 - Pmax MAD = 0.1

Ksgc median = 44.61 - Pmax median = 10.8

If $((Ksgc_i - Ksgc_median)/MAD) > 2$: outlier

If $((Pmax_i - Pmax_median)/MAD) > 2.5$: outlier

Test 1

Pmax = 10.82 - Outlier: False - Ksgc = 44.61 - Outlier: False

Test 2

Pmax = 10.01 - Outlier: True - Ksgc = 43.83 - Outlier: False

Test 3

Pmax = 10.89 - Outlier: False - Ksgc = 46.44 - Outlier: False

Final results for this configuration:

Average Ksgc = 45.52 - Ksgc COV = 2.0%

Average Pmax = 10.86 - Pmax COV = 0.3%

A.14 CONFIGURATION INVOLVING GT2 AND ROUND SAGGR2

A.14.1 Test 1

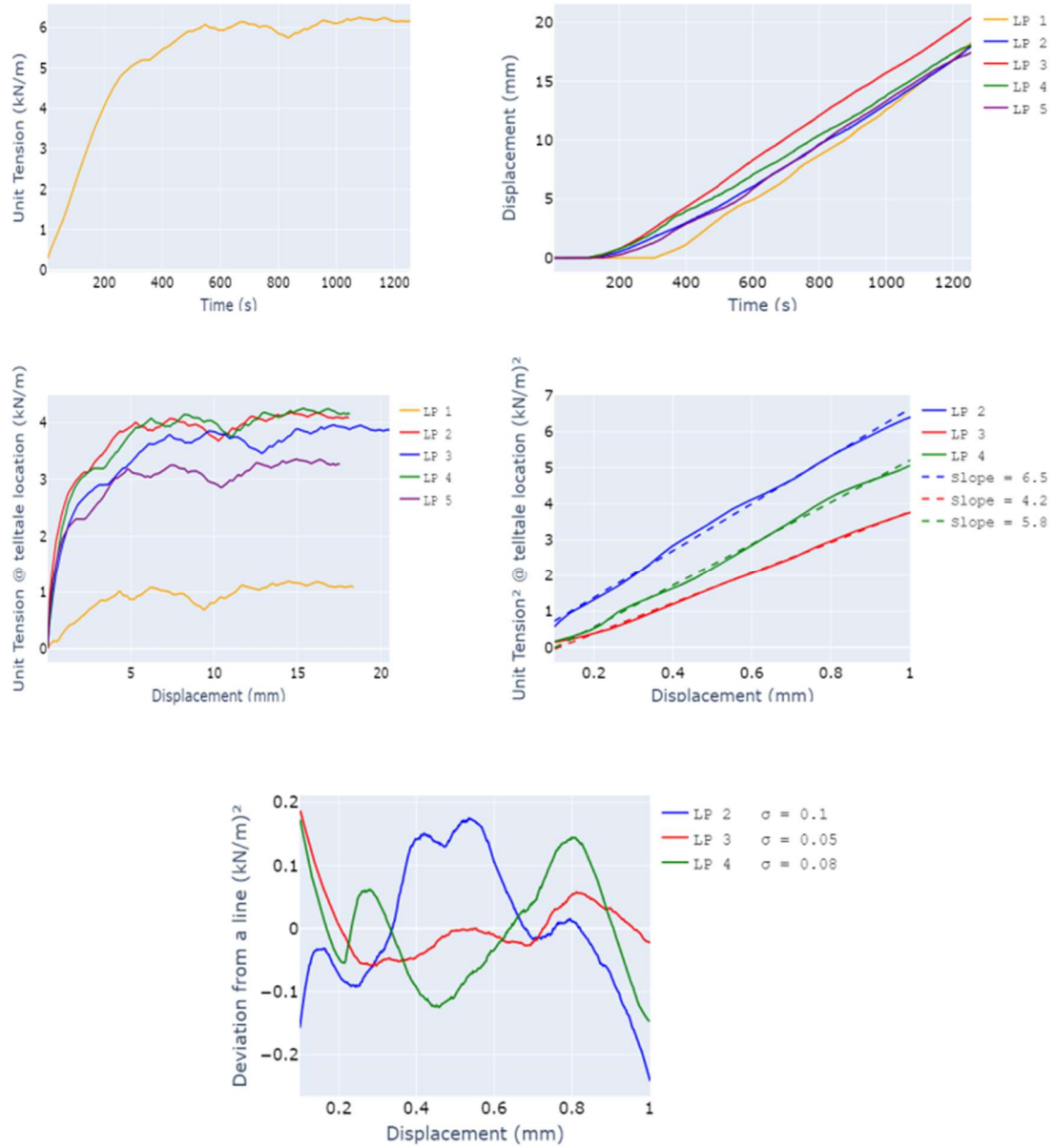


Figure A.64 - Results from the first test of configuration involving GT2 and Round SAggr2

LP 1: Trigger Time (sec): 298.4 - T0 (kN/m): 5.1

LP 2: Trigger Time (sec): 96.6 - T0 (kN/m): 2.1

LP 3: Trigger Time (sec): 106.6 - T0 (kN/m): 2.3

LP 4: Trigger Time (sec): 93.6 - T0 (kN/m): 2.0

LP 5: Trigger Time (sec): 135.0 - T0 (kN/m): 2.9

Deviation from a line:

LP 2 - sd = 0.1 - Outlier: False

LP 3 - sd = 0.1 - Outlier: False

LP 4 - sd = 0.1 - Outlier: False

Ksgc values:

LP2: 6.5 - Outlier = False

LP3: 4.2 - Outlier = True

LP4: 5.8 - Outlier = False

Final results:

Ksgc = 6.19 - Pmax = 6.25

A.14.2 Test 2

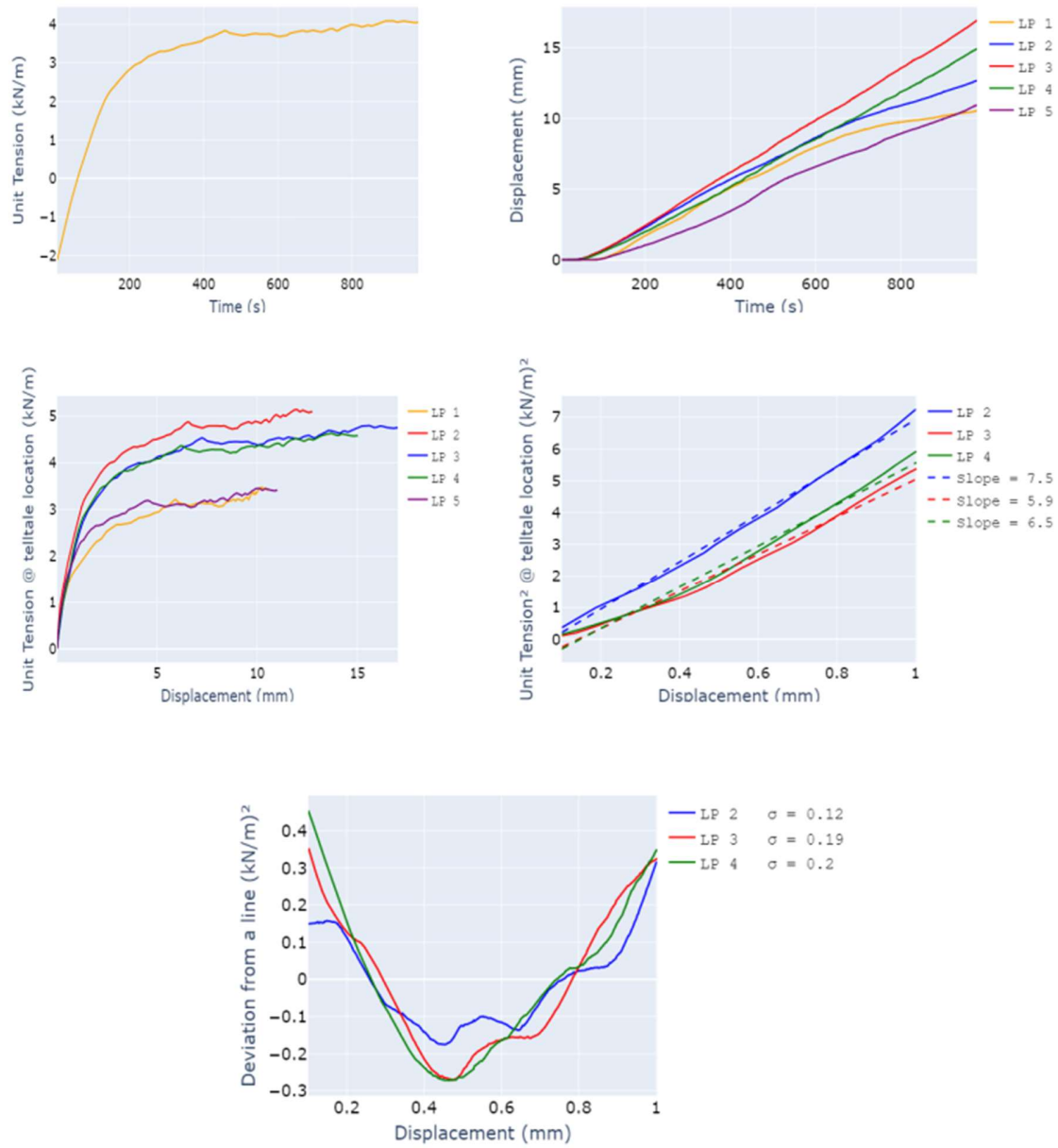


Figure A.65 - Results from the second test of configuration involving GT2 and Round SAggr2

LP 1: Trigger Time (sec): 80.4 - T0 (kN/m): 0.6

LP 2: Trigger Time (sec): 31.2 - T0 (kN/m): -1.0

LP 3: Trigger Time (sec): 39.4 - T0 (kN/m): -0.7

LP 4: Trigger Time (sec): 44.2 - T0 (kN/m): -0.5

LP 5: Trigger Time (sec): 81.0 - T0 (kN/m): 0.6

Deviation from a line:

LP 2 - sd = 0.12 - Outlier: False

LP 3 - sd = 0.19 - Outlier: False

LP 4 - sd = 0.2 - Outlier: False

Ksgc values:

LP2: 7.5 - Outlier = True

LP3: 5.9 - Outlier = False

LP4: 6.5 - Outlier = False

Final results:

Ksgc = 5.85 - Pmax = 4.1

A.14.3 Test 3

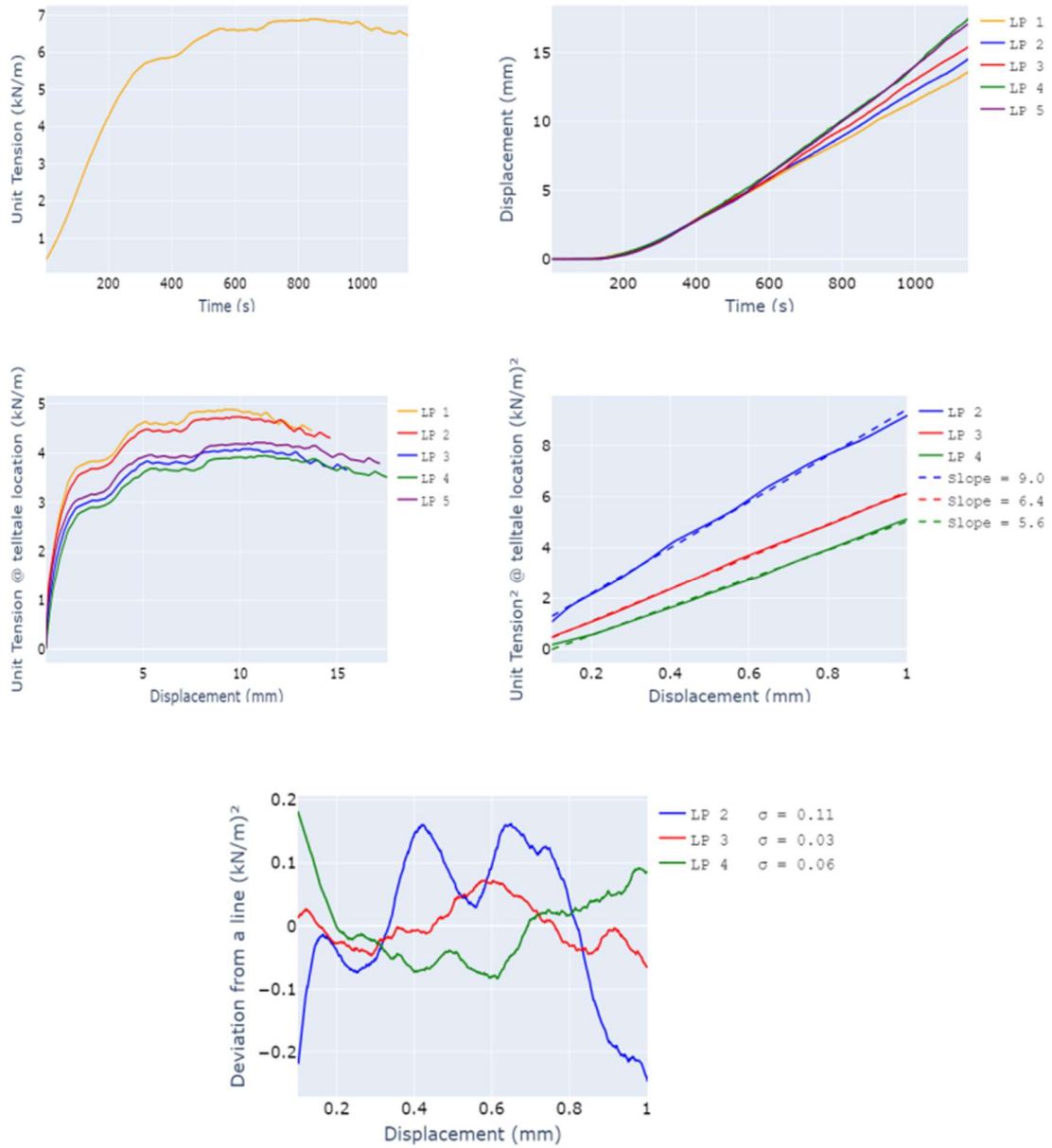


Figure A.66 - Results from the third test of configuration involving GT2 and Round SAggr2

LP 1: Trigger Time (sec): 90.6 - T0 (kN/m): 2.0

LP 2: Trigger Time (sec): 97.6 - T0 (kN/m): 2.2

LP 3: Trigger Time (sec): 126.0 - T0 (kN/m): 2.8

LP 4: Trigger Time (sec): 132.4 - T0 (kN/m): 2.9

LP 5: Trigger Time (sec): 120.2 - T0 (kN/m): 2.7

Deviation from a line:

LP 2 - sd = 0.1 - Outlier: False

LP 3 - sd = 0.0 - Outlier: False

LP 4 - sd = 0.1 - Outlier: False

Ksgc values:

LP2: 9.0 - Outlier = True

LP3: 6.4 - Outlier = False

LP4: 5.6 - Outlier = False

Final results:

Ksgc = 6.6 - Pmax = 6.9

A.14.4 Test 4

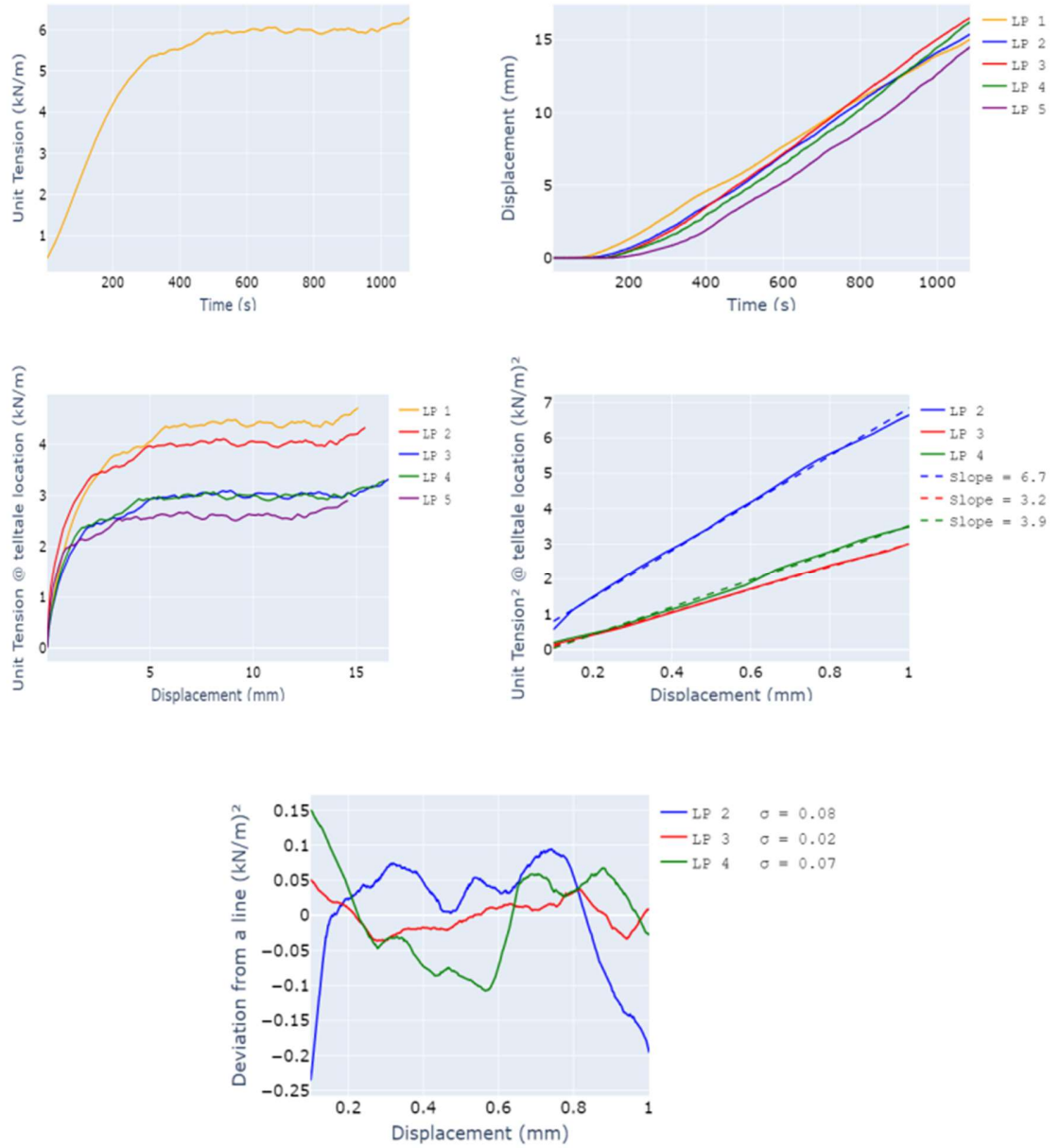


Figure A.67 - Results from the fourth test of configuration involving GT2 and Round SAggr2

LP 1: Trigger Time (sec): 66.0 - T0 (kN/m): 1.6

LP 2: Trigger Time (sec): 83.6 - T0 (kN/m): 2.0

LP 3: Trigger Time (sec): 130.8 - T0 (kN/m): 3.0

LP 4: Trigger Time (sec): 132.2 - T0 (kN/m): 3.0

LP 5: Trigger Time (sec): 152.4 - T0 (kN/m): 3.4

Deviation from a line:

LP 2 - sd = 0.1 - Outlier: False

LP 3 - sd = 0.0 - Outlier: False

LP 4 - sd = 0.1 - Outlier: False

Ksgc values:

LP2: 6.7 - Outlier = True

LP3: 3.2 - Outlier = False

LP4: 3.9 - Outlier = False

Final results:

Ksgc = 3.2 - Pmax = 6.3

A.14.5 Test 5

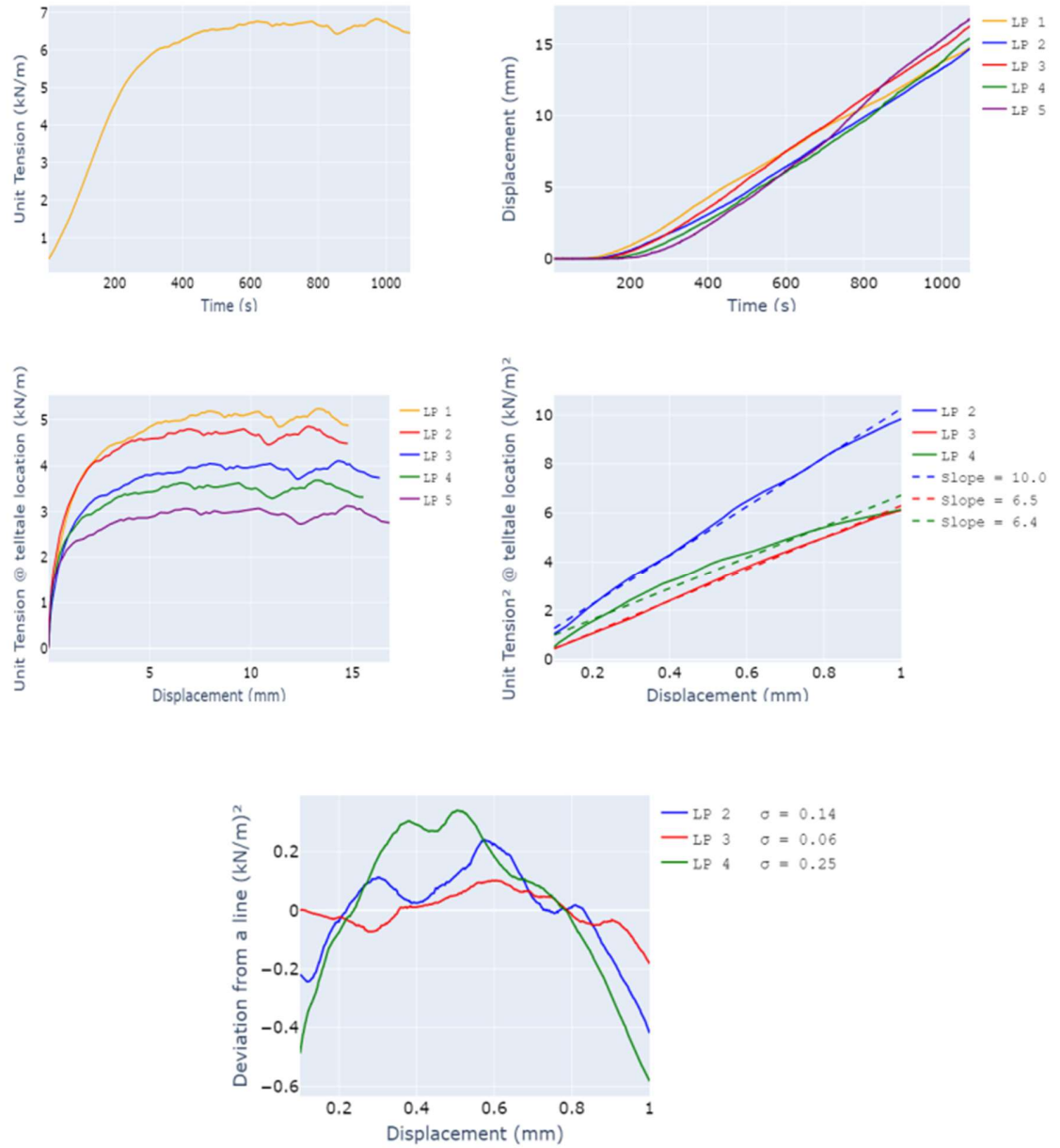


Figure A.68 - Results from the fourth test of configuration involving GT2 and Round SAggr2

LP 1: Trigger Time (sec): 69.8 - T0 (kN/m): 1.6

LP 2: Trigger Time (sec): 87.2 - T0 (kN/m): 2.0

LP 3: Trigger Time (sec): 118.4 - T0 (kN/m): 2.7

LP 4: Trigger Time (sec): 135.4 - T0 (kN/m): 3.1

LP 5: Trigger Time (sec): 159.0 - T0 (kN/m): 3.7

Deviation from a line:

LP 2 - sd = 0.1 - Outlier: False

LP 3 - sd = 0.1 - Outlier: False

LP 4 - sd = 0.3 - Outlier: False

Ksgc values:

LP2: 10.0 - Outlier = True

LP3: 6.5 - Outlier = False

LP4: 6.4 - Outlier = False

Final results:

Ksgc = 6.5 - Pmax = 6.83

A.14.6 Summary of results from configuration involving GT2 and Round SAggr2

Ksgc MAD = 0.5 - Pmax MAD = 0.8

Ksgc median = 6.19 - Pmax median = 6.29

If $((Ksgc_i - Ksgc_median)/MAD) > 2$: outlier

If $((Pmax_i - Pmax_median)/MAD) > 2.5$: outlier

Test 1

Pmax = 6.25 - Outlier: False - Ksgc = 6.19 - Outlier: False

Test 2

Pmax = 4.1 - Outlier: True - Ksgc = 5.85 - Outlier: False

Test 3

Pmax = 6.9 - Outlier: False - Ksgc = 6.58 - Outlier: False

Test 4

Pmax = 6.29 - Outlier: False - Ksgc = 3.17 - Outlier: True

Test 5

Pmax = 6.83 - Outlier: False - Ksgc = 6.5 - Outlier: False

Final results for this configuration:

Average Ksgc = 6.42 - Ksgc COV = 2.6%

Average Pmax = 6.66 - Pmax COV = 4.4%.

A.15 CONFIGURATION INVOLVING GT2 AND ANGULAR SAGGR2

A.15.1 Test 1

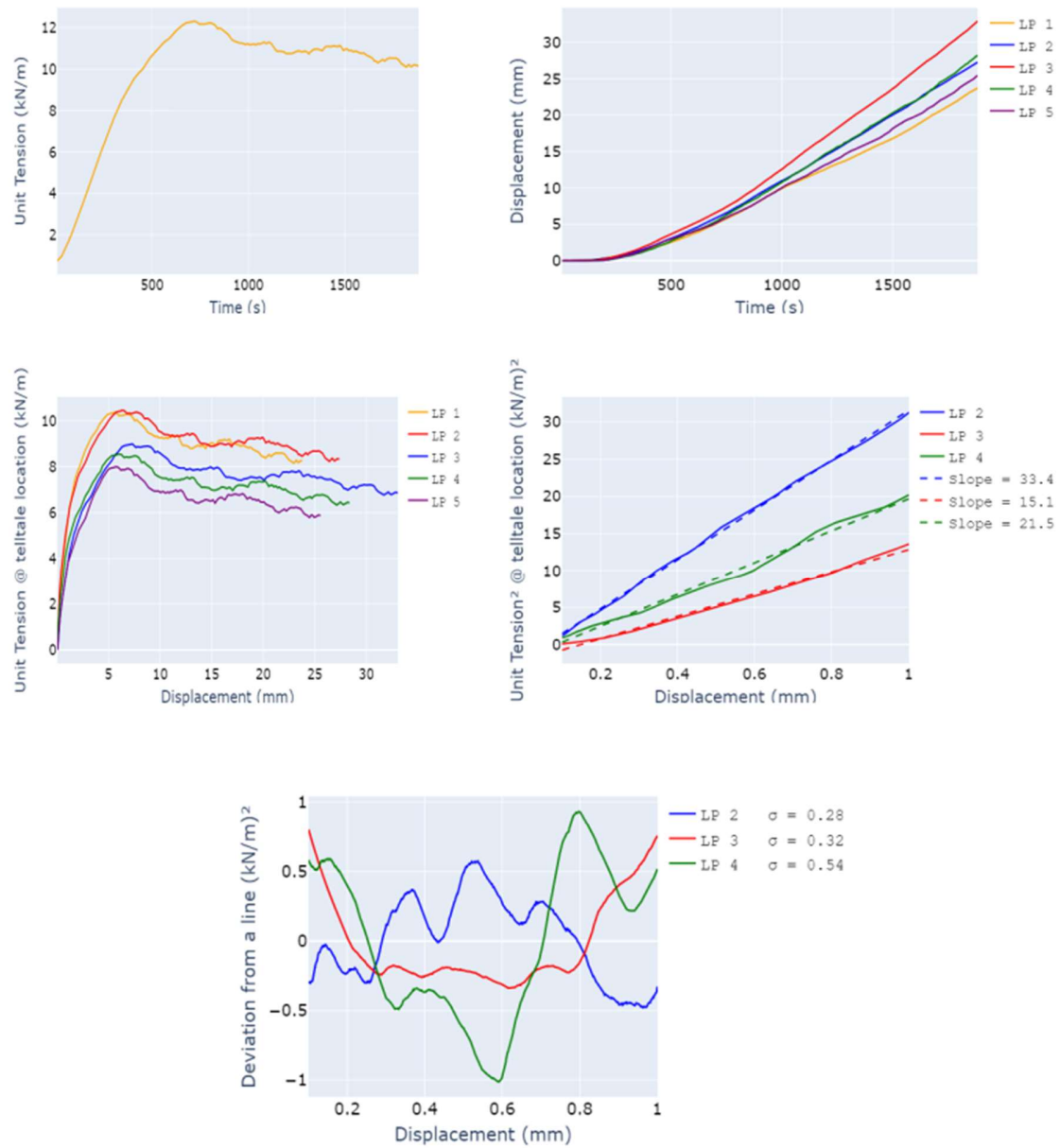


Figure A.69 - Results from the first test of configuration involving GT2 and Angular SAggr2

LP 1: Trigger Time (sec): 77.6 - T0 (kN/m): 1.9

LP 2: Trigger Time (sec): 74.2 - T0 (kN/m): 1.9

LP 3: Trigger Time (sec): 133.8 - T0 (kN/m): 3.3

LP 4: Trigger Time (sec): 150.2 - T0 (kN/m): 3.8

LP 5: Trigger Time (sec): 170.8 - T0 (kN/m): 4.3

Deviation from a line:

LP 2 - sd = 0.3 - Outlier: False

LP 3 - sd = 0.3 - Outlier: False

LP 4 - sd = 0.5 - Outlier: False

Ksgc values:

LP2: 33.4 - Outlier = True

LP3: 15.1 - Outlier = False

LP4: 21.5 - Outlier = False

Final results:

Ksgc = 14.5 - Pmax = 12.3

A.15.2 Test 2

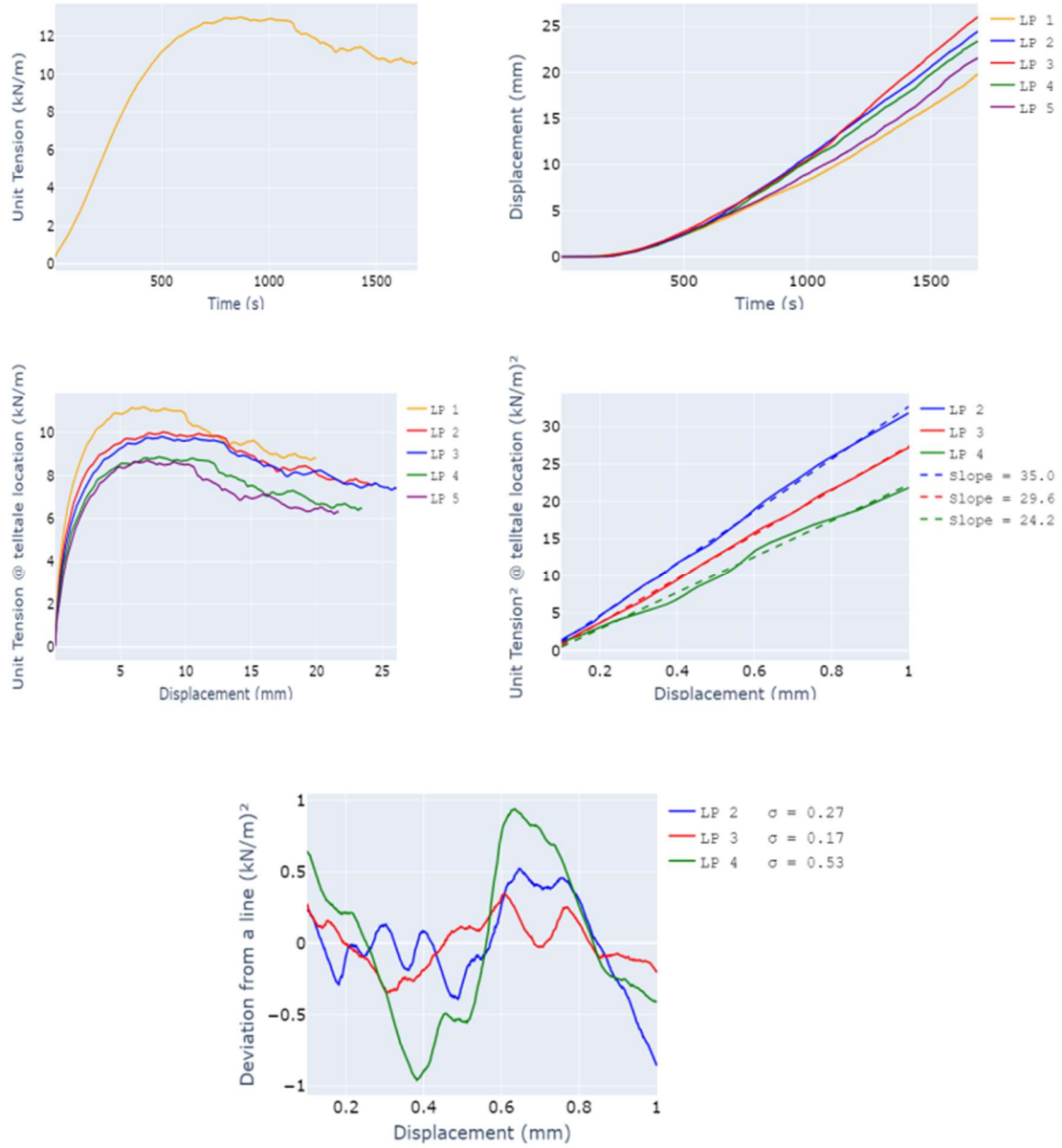


Figure A.70 - Results from the second test of configuration involving GT2 and Angular SAggr2

LP 1: Trigger Time (sec): 78.6 - T0 (kN/m): 1.8

LP 2: Trigger Time (sec): 129.4 - T0 (kN/m): 3.0

LP 3: Trigger Time (sec): 137.8 - T0 (kN/m): 3.2

LP 4: Trigger Time (sec): 172.6 - T0 (kN/m): 4.1

LP 5: Trigger Time (sec): 178.6 - T0 (kN/m): 4.3

Deviation from a line:

LP 2 - sd = 0.3 - Outlier: False

LP 3 - sd = 0.2 - Outlier: False

LP 4 - sd = 0.5 - Outlier: False

Ksgc values:

LP2: 35.0 - Outlier = False

LP3: 29.6 - Outlier = False

LP4: 24.2 - Outlier = True

Final results:

Ksgc = 30.9 - Pmax = 13.0

A.15.3 Test 3

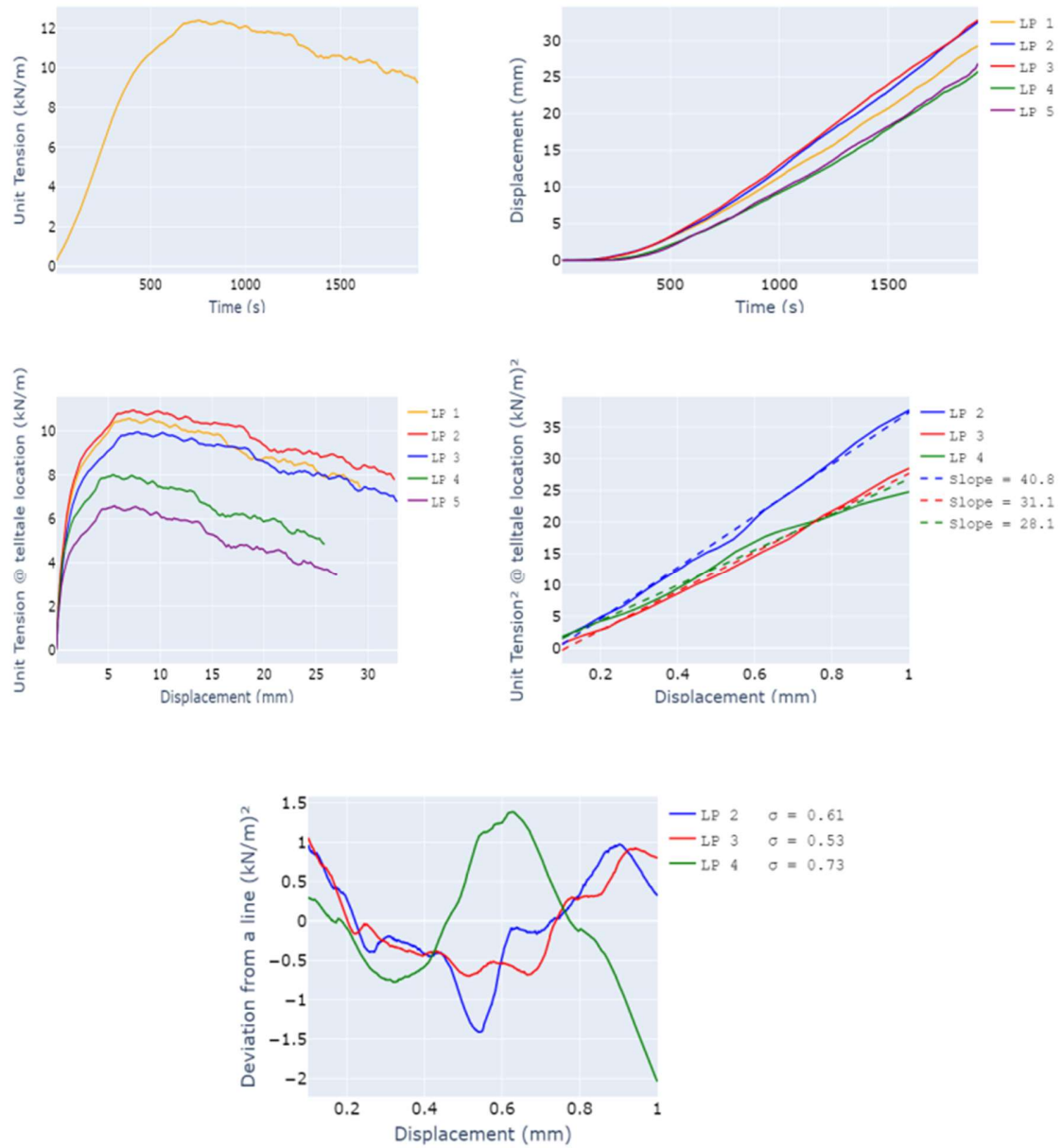


Figure A.71 - Results from the third test of configuration involving GT2 and Angular SAggr2

LP 1: Trigger Time (sec): 85.6 - T0 (kN/m): 1.8

LP 2: Trigger Time (sec): 67.8 - T0 (kN/m): 1.5

LP 3: Trigger Time (sec): 113.4 - T0 (kN/m): 2.5

LP 4: Trigger Time (sec): 187.6 - T0 (kN/m): 4.4

LP 5: Trigger Time (sec): 237.8 - T0 (kN/m): 5.8

Deviation from a line:

LP 2 - sd = 0.61 - Outlier: False

LP 3 - sd = 0.53 - Outlier: False

LP 4 - sd = 0.73 - Outlier: False

Ksgc values:

LP2: 40.8 - Outlier = True

LP3: 31.1 - Outlier = False

LP4: 28.1 - Outlier = False

Final results:

Ksgc = 31.84 - Pmax = 12.39

A.15.4 Test 4

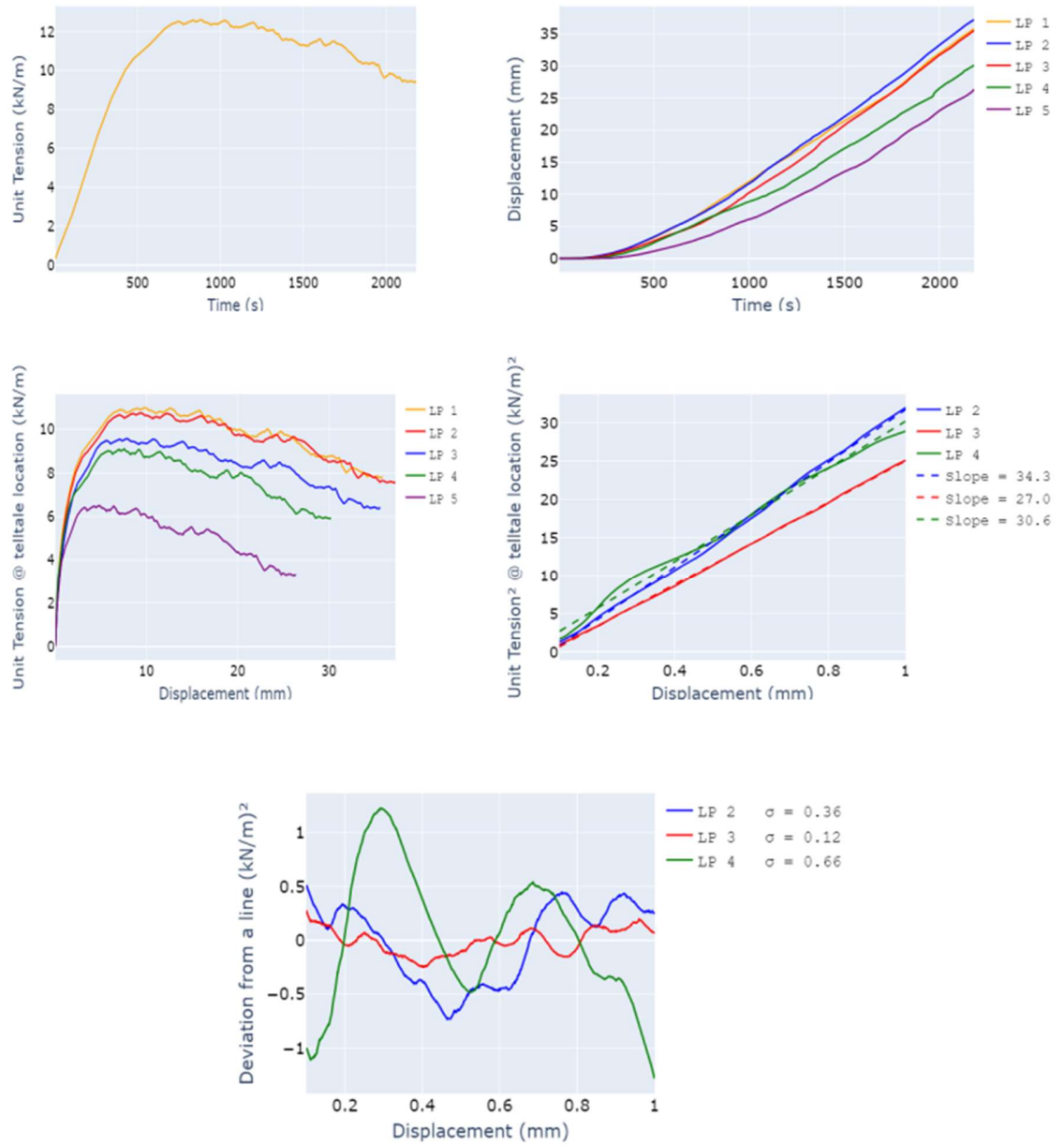


Figure A.72 - Results from the fourth test of configuration involving GT2 and Angular SAggr2

LP 1: Trigger Time (sec): 62.8 - T0 (kN/m): 1.6

LP 2: Trigger Time (sec): 73.4 - T0 (kN/m): 1.9

LP 3: Trigger Time (sec): 122.8 - T0 (kN/m): 3.0

LP 4: Trigger Time (sec): 140.6 - T0 (kN/m): 3.5

LP 5: Trigger Time (sec): 237.0 - T0 (kN/m): 6.1

Deviation from a line:

LP 2 - sd = 0.36 - Outlier: False

LP 3 - sd = 0.12 - Outlier: False

LP 4 - sd = 0.66 - Outlier: False

Ksgc values:

LP2: 34.3 - Outlier = True

LP3: 27.0 - Outlier = False

LP4: 30.6 - Outlier = False

Final results:

Ksgc = 26.15 - Pmax = 12.61

A.15.5 Test 5

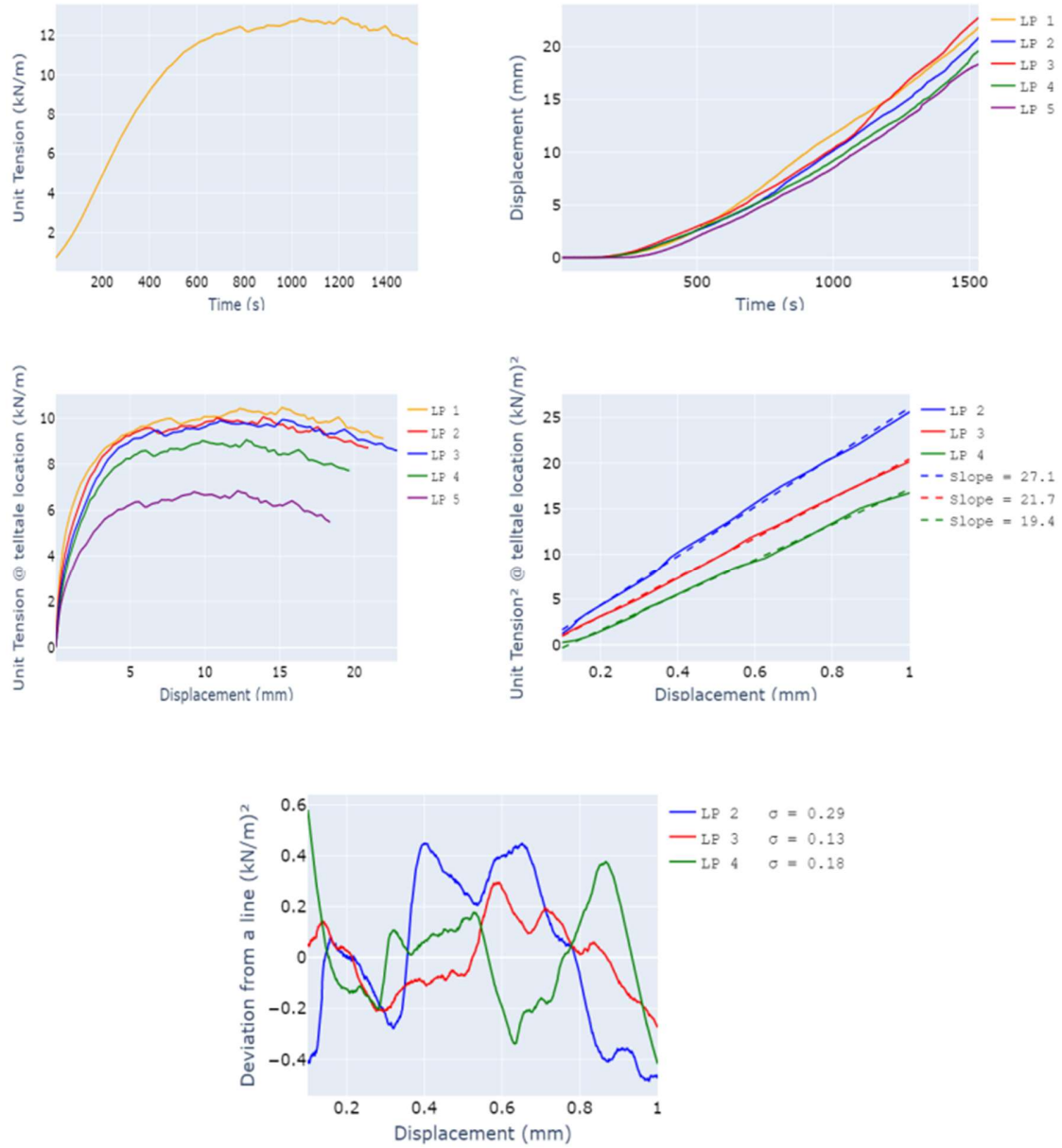


Figure A.73 - Results from the fifth test of configuration involving GT2 and Angular SAggr2

References

- AASHTO M 145-91 (12) (2012). "Standard Specification for Classification of Soils and Soil-Aggregate Mixtures for Highway Construction Purposes." *American Association of State Highway and Transportation Officials*, Washington, D.C., USA, 9p.
- ASTM. (2007a). "Standard test method for measuring geosynthetic pullout resistance in soil." ASTM D6706-01(07), West Conshohocken, PA.
- ASTM D2487-17 (20) (2020). "Standard Practice for Classification of Soils for Engineering Purposes (Unified Soil Classification System)." American Society for Testing and Materials, West Conshohocken, PA, USA, 10p.
- ASTM D4595-11 (2011). "Standard Test Method for Tensile Properties of Geotextiles by the Wide-Width Strip Method." American Society for Testing and Materials, West Conshohocken, PA, USA, 13p.
- ASTM D5617-04 (15) (2015). "Standard Test Method for Multi-Axial Tension Test for Geosynthetics." American Society for Testing and Materials, West Conshohocken, PA, USA, 5p.
- ASTM E11-20 (22) (2022). "Standard Specification for Woven Wire Test Sieve Cloth and Test Sieves." American Society for Testing and Materials, West Conshohocken, PA, USA, 12p.
- Fuller, W.B. and Thompson, S.E. (1907), "The Laws of Proportioning Concrete," *Transactions of the American Society of Civil Engineers*, V. 59, pp. 67-143
- Funk, J.E. and Dinger, D.R., Predictive Process Control of Crowded Particulate Suspensions Applied to Ceramic Manufacturing, *Kluwer Academic Publishers*, Boston, MA, 1994, 786 pp.
- Gupta, R., (2009). *A Study of Geosynthetic-Reinforced Flexible Pavement System*. PhD Dissertation, The University of Texas, Austin, Texas, USA, 318p.
- Peve, L. (2018). Sources of Variability in Small-Scale Soil-Geosynthetic Interaction Testing. MSc. dissertation, The University of Texas, Austin, Texas, August 2018, 196 p., Advisor: Jorge G. Zornberg.
- Roodi, G. H. (2016). *Analytical, Experimental, and Field Evaluations of Soil-geosynthetic Interaction under Small Displacements*. Ph.D. dissertation, The University of Texas, Austin, Texas, August 2016, 623 p., Advisor: Jorge G. Zornberg.

Roodi, G. H., Zornberg, J. G., Aboelwafa, M. M., Phillips, J. R., Zheng, L., and Martinez, J. (2018). “*Soil-geosynthetic Interaction Test to Develop Specifications for Geosynthetic-stabilized Roadways*” Center for Transportation Research (CTR), Report No. FHWA/TX-17/5-4829-03-R1, Austin, Texas, 100 p.

Rousseeuw, P.J. and Hubert, M. (2011), Robust statistics for outlier detection. *WIREs Data Mining Knowl Discov*, 1: 73-79. <https://doi.org/10.1002/widm.2>

Tutumluer, E., & Pan, T. (2008). Aggregate Morphology Affecting Strength and Permanent Deformation Behavior of Unbound Aggregate Materials. *Journal of Materials in Civil Engineering*, ASCE, Vol. 20, No. 9. doi: 10.1061/(ASCE)0899-1561(2008)20:9(617)

Zornberg, J. G., Roodi, G. H., & Gupta, R. (2017). Stiffness of Soil–Geosynthetic Composite under Small Displacements: I. Model Development. *Journal of Geotechnical and Geoenvironmental Engineering*, ASCE, Vol. 143, No. 10. doi: 10.1061/(asce)gt.1943-5606.0001768